Projections of hydrometeorological processes in Southern Ontario: Uncertainties due to internal variability of climate

By Olivier Champagne, M.A.Sc.

A Thesis

Submitted to the School of Geography and Earth Sciences

and the School of Graduate Studies

in Partial Fulfillment of the Requirements for the Degree of

DOCTOR OF PHILOSOPHY

DOCTOR OF PHILOSOPHY (2020) McMaster University

School of Geography and earth Sciences Hamilton, Ontario, Canada

TITLE: Projections of hydrometeorological processes in Southern Ontario: Uncertainties due to internal variability of climate.

AUTHOR: Olivier Champagne

M. Sc. (Université de Bourgogne)

B. Sc. (Université de Lorraine)

SUPERVISOR: Dr. Altaf Arain

NUMBER OF PAGES: xx, 185

Abstract

Flooding is a major concern for Canadian society as it is the costliest natural disaster type in Canada. Southern Ontario, which houses one-third of the Canadian population, is particularly affected by early spring floods following snowmelt. During the last three decades, there has been a shift in flooding events from March-April to earlier months due to earlier snowmelt coupled with extreme rain events. Hydrological models run with different scenarios of climate change suggest further enhancement of this shift in the future. These projections of streamflow are associated with a cascade of uncertainties due to the choice of Global Climate Models (GCM's), climate change scenarios, downscaling methods or hydrological models. A large part of the uncertainty is also associated with internal variability of climate due to the chaotic nature of the climate system. Despite these uncertainties, little is known about the impact of atmospheric circulation on past streamflow in southern Ontario and how the internal variability of climate is expected to impact the overall uncertainties in the projections of the future hydrological processes.

In this thesis, the Precipitation Runoff Modelling System (PRMS), a semi-distributed conceptual hydrological model, was established in four watersheds in southern Ontario to assess the impact of atmospheric circulation on the modulation of streamflow and number of high flows. Recurrent meteorological patterns (Or Weather regimes), based on 500hPa geopotential height (Z500), have been first identified in Northeastern North America using the k-means algorithm. The occurrences of these weather regimes patterns were used to create a regime-normalized hypothetical temperature and precipitation dataset that have been used as input in PRMS. Then, to investigate

the future evolution of the hydrological processes, PRMS was forced with temperature and precipitation from the 50-members Canadian Regional Climate Model Large Ensemble (CRCM5-LE), a dynamically downscaled version of CanESM2-LE. The 50-members were classified into different classes of similar change in average temperature, precipitation and streamflow to identify the corresponding large-scale patterns. The specific focus of this analysis was on winter high flows, with the identification of a heavy rain and warm index, that can help to explain the generation of winter high flows in southern Ontario. The future evolution of these hydrometeorological extreme events, calculated for each member of CRCM5-LE, was analyzed with respect to the corresponding k-means weather regimes calculated for each member of CanESM2-LE. Finally, the uncertainties in the projections of the hydrometeorological extremes from the 50-members ensemble were compared to other sources of uncertainties using an analysis of variance applied to 504 simulations in the Big creek watershed. The high flows were projected using seven sets of PRMS parameters, 11 CMIP5 climate models forced with 2 scenarios of climate change and the 50 members of CRCM5-LE.

The results, focusing on the winter season, showed that weather regimes High-Pressure (HP) and southerly winds (South) are associated with a higher average streamflow volume and high-flows frequency in the historical period. Regime HP is characterized by high geopotential height anomalies on top of the Great Lakes region together with higher temperature and precipitation amounts. Regime South is characterized by high Z500 anomalies in the Atlantic east coast and is associated with stronger southerly winds and higher precipitation amount in southern Ontario. The temporal increase in HP in the past contributed more than 40% of the increase in average

streamflow in winter. In the future, all 50 members of CRCM5-LE ensemble produce an increase in January-February streamflow. 14% of the ensemble depict a larger streamflow increase due to increase in Z500 anomalies in the east coast. This pattern, well defined by the regimes South, is expected to become a major contributor in the generation of hydrometeorological extreme events in Southern Ontario in the future. Regime HP is expected to contribute less to the high-flows due to the disappearance of snow. Overall, the contribution of internal variability of climate to high flows will be stable through the 21st century, primarily due to an increase in rainfall as generators of high flow events. The results suggest that the regional representation of rainfall in the GCMs-RCMs chains will be a critical area to improve with great societal implications for floods.

Acknowledgements

This research has been done on the traditional territory of the Haudensaunee and Anishnaabeg. This territory is covered by the Upper Canada Treaties and directly adjacent to Haldiman Treaty territory. I am grateful for the opportunity to conduct research on this land and I thank all the generations of people who have taken care of this area for thousands of years.

I would like to express my gratitude toward my supervisor Dr. Altaf Arain and toward the members of the supervisory committee Dr. Paulin Coulibaly and Dr. Sean Carey for their constructive feedbacks to constantly improve this research. I would like to also thank the members of my comprehensive examination committee Dr. Jim Smith and Dr. Yiping Guo and the external examiner Bryan Tolson for their insights. I am also grateful to the Hydromet Lab for their daily support and particularly Shawn McKenzie for his reviews on English language.

This work would not have been possible without the support of Martin Leduc from the Consortium Ouranos. I warmly thank him and Ouranos for allowing me to use the Climex data, for giving me useful feedbacks and for inviting me to present my research in Montréal. I could not be grateful enough for all his help.

My thoughts are also toward all the professionals giving me advices throughout my PhD. I am particularly grateful to Mason Marchildon from Oak Ridges Morain Groundwater Program, Lauren Somers from Mc Gill university and Robert Reagan from USGS for their precious advices on hydrological modelling. I am not forgetting the FloodNet community who boosted me after each General meeting.

I am also acknowledging the Province of Ontario, Natural Science and Engineering Research Council (NSERC), Environment and Climate Change Canada (ECCC), Water Survey of Canada (WSC), The Ontario Ministry of Northern development, Mines and Forestry, the Long Point Region Conservation Authority (LPRCA), the Upper Thames River Conservation Authority (UTRCA) and the Grand River Conservation Authority (GRCA), the school of graduate studies, the department of Geography and Earth Sciences and the McMaster Centre for Climate Change.

I am finally grateful for my partner in crime Uttra who gave me all the love and support that I can hope for. I also thank my Mom Bernadette, my brother Thibaut and my sister Hélène back in Europe who gave me incredible support during this journey. My Niece Nina and my Nephew Marc were also particularly supportive in their own way.

I dedicate this thesis to my Dad, Jacques Champagne. His legacy gave me the faith to go through all this hard work.

Table of Contents

List of Figures

List of Tables

Declaration of Academic Achievement

This thesis is comprised of four published papers or manuscripts. It is written in accordance with the regulations provided by the School of Graduate Studies at McMaster University. Details of the published and submitted manuscripts to peer-reviewed journals is given below:

Chapter 2: Atmospheric circulation amplifies shift of winter streamflow in Southern Ontario. O. Champagne, M.A. Arain and P. Coulibaly, Journal of Hydrology, 124051. Doi: 10.1016/j.jhydrol.2019.124051, 2019. (With permission from publisher)

Chapter 3: Future shift in winter streamflow modulated by internal variability of climate in southern Ontario. O. Champagne, A. Arain, M. Leduc, P. Coulibaly, S. McKenzie, Hydrology and Earth System Sciences Discussions, 1–30. Doi: 10.5194/hess-2019-204, in review 2019. (With permission from publisher)

Chapter 4: Winter hydrometeorological extreme events modulated by large scale atmospheric circulation in southern Ontario. O. Champagne, M. Leduc, P. Coulibaly, M.A. Arain, Earth System Dynamics Discussion., Doi: 10.5194/esd-2019-56**,** accepted for publication, 2019. (With permission from publisher).

Chapter 5: Sources of uncertainties in the projections of streamflow in a Great Lakes watershed. O. Champagne, M. Leduc, P. Coulibaly, M.A. Arain, Journal of Hydrology: Regional studies. In Review (EJRH_2019_371), 2019.

For all of these four manuscripts I conducted the computational and data analysis work and wrote the first draft of manuscripts. M. Altaf Arain reviewed and edited the papers. Paulin Coulibaly gave feedbacks on various aspects. Martin Leduc provided detailed comments and advices for the chapter 3 to 5 and Shawn McKenzie provided feedback and English editorial support for the chapter 3. The manuscript for the chapter 2 was published in Journal of Hydrology in August 2019. The manuscript for the chapter 3 has been first submitted to Hydrological and Earth System Sciences in April 2019, revised according to the reviews made public in September 2019 and was resubmitted in December 2019. The manuscript for the chapter 4 has been accepted for publication in Earth System Dynamics in February 2020. The manuscript for the chapter 5 has been submitted to Journal of Hydrology: Regional Studies in December 2019. Because of the nature of the thesis, there is some overlap in the text among these chapters mostly while describing study methods and model details.

Chapter 1. Introduction

1.1 Background

In February 2018, a major flooding event affected many rivers in southern Ontario due to multi-day rainfall and quick snowmelt. In London, Ontario, the Thames river reached its third highest level in record and the highest level ever recorded in February (Historical Hydrometric Data - Water Level and Flow - Environment Canada,, 2018). This event costed 43 Millions Canadian Dollars in insurance across the southern part of the province (Insurance Bureau of Canada, 2018).

This event was a consequence of a shift from spring melt peak flows to earlier high flows observed recently in southern-Ontario (Cunderlik & Ouarda, 2009, Adamowski et al., 2013, Burn and Whitfield, 2016). A similar shift was observed worldwide in many snow dominated catchments (Barnett et al., 2005). This shift is attributed to global warming that accelerates snowmelt and enhance the rain to snow ratio in winter (Burn et al., 2016). The warming also plays a role in increasing precipitation due to increase in water holding capacity of the air (Pall et al., 2007; Trenberth et al., 2003). In this context, hydrological models forced with climate projections are being widely used to predict the future evolution of hydrological processes (Mendoza et al., 2016). This modelling chain is associated with a cascade of uncertainties due to methodological choices including the greenhouse gases emissions pathway scenario, the global climate model (GCM), the downscaling technique or the hydrological model used for the study (Clark et al., 2016). Some of these uncertainties can be reduced by improving simulation of the climatic processes in the GCMs and the downscaling methods used for local or watershed scales studies. The ability of the hydrological models to simulate the hydrological processes can also be improved. For other

uncertainties, the prospect of potential improvements is much smaller. The future pathways of greenhouse gases emissions that human activities will achieve is unknown despite the recent polices that attempt to stabilize and reduce these emissions. Another critical challenge in the projections of hydrological processes originates from the inherently chaotic nature of the climate system (Lorenz, 1963) also referred to internal variability of climate. The first Intergovernmental Panel on Climate Change assessments (IPCC) predicted a linear increase in global temperature (Intergovernmental Panel on Climate Change, 1992). Recent observations have shown a more chaotic evolution of global temperature than suggested in these first reports. A dramatic warming at the end of 1990's was following by a long hiatus terminated by a sharp increase in global temperature around 2015 (Watanabe et al., 2014). This global hiatus has been attributed to a decadal cooling in the eastern equatorial Pacific associated with internal variability of climate (Dai et al., 2015; Watanabe et al., 2014) and the decadal variability of climate will continue to play a great role in the evolution of future global and regional climates (Deser et al., 2012; Thompson et al., 2015). This decadal modulation of temperature and precipitation by internal variability of climate will also play a significant role in the future evolution of streamflow and other hydrological processes in southern Ontario.

1.2 Hydrological processes modulated by internal variability of climate

In the literature, a few studies have focused on the high-frequency linkages (synoptic and interannual variability) between atmospheric circulation and hydro-meteorological events in the Great Lakes region using large-scale modes of variability (Stone et al., 2000; Mallakpour & Villarini, 2016; Ning & Bradley, 2015; Zhao et al., 2013; Thiombiano et al., 2017). In winter, the negative phase of the Pacific North American pattern (PNA^-), high pressure anomalies in eastern

North America and low pressure anomalies in the west, generally induce warm events (Ning & Bradley, 2015), precipitation extremes (Stone et al., 2000,Thiombiano et al., 2017) and more high-flows in the Great lakes region (Mallakpour and Villarini, 2016). The positive phase of North Atlantic Oscillation (NAO^+), characterized by a strong gradient between low pressure in Iceland and high pressure in the Azores, is associated with warmer winter temperature in the Great Lakes region (Ning & Bradley, 2015) but its association with streamflow is inconclusive (Nalley et al., 2016). These large scale modes of atmospheric variability explain only a small portion of the large scale flow variability compared to synoptic climatology that is widely studied and used in North America (Papritz & Grams, 2018; Grotjahn et al., 2016). Rohli et al., (2001) used an eigenvector-based surface pattern classification scheme and showed higher monthly discharge in the Great Lakes region is associated to high pressure anomalies over the northeast North American coast. Kunkel et al., (2012) showed that the generation of extreme precipitation in the Great lakes is almost exclusively associated to frontal systems, generally formed between a trough on the west and high pressure in the east (Mallakpour & Villarini, 2016).

Other studies have been linking trends in hydrometeorological processes with change in atmospheric circulation patterns in the Great Lakes region. Winter NAO^+ and PNA^+ have been following a positive trend throughout the 20th century (Liu et al., 2017; Vincent et al., 2015) but the increase of winter streamflow in the Great lakes region have been mostly attributed to anthropogenic warming (Ahn et al., 2016). The future trend in variability modes and atmospheric circulation are unknown but are expected to greatly modulate the occurrence of hydrometeorological events in the region (Shepherd, 2014). The uncertainties of projected

temperature and precipitation due to internal variability of climate have been investigated recently using GCM ensembles (Deser et al., 2014, Kumar et al., 2015, Kay et al., 2015). Each member of the ensemble has a different initial condition and provides different evolution of climate because of the atmospheric circulation trajectories. These ensemble have been used as input in hydrological models to assess how these uncertainties are transferred to hydrological processes (Gelfan ,2015, Gusev et al., 2017; Troin et al., 2015). A local scale internal variability of climate due to similar atmospheric patterns leading to very different local conditions was also identified by Lafaysse et al., (2014) and is generally identified in the downscaling method by investigating the range of output produced by different regional climate model or the different replicated produced by a stochastic statistical method (Lafaysse et al., 2014). This internal variability has been studied in several watersheds worldwide (Coulibaly, 2009, Teutschbein et al., 2011, Braun et al., 2012; Music & Caya, 2009; Steinschneider et al., 2015). In Southern Ontario a future shift in streamflow from early Spring to winter is well documented (Erler et al., 2018; Grillakis et al., 2011; Kuo et al., 2017; Rahman et al., 2012; Sultana & Coulibaly, 2011) but the contribution of internal variability of climate to the past and future shift in hydrometeorological processes has not been yet investigated in the literature.

1.3 Objectives

The aim of this thesis is to assess the impacts of internal variability of climate on winter hydrometeorological processes in southern Ontario. To achieve these objectives, the Precipitation Runoff Modeling System (PRMS), a semi distributed conceptual hydrological model, was applied to four watersheds in southern Ontario (Markstrom et al., 2015). Study results have been summarized in the form of four articles published or submitted in the peer-reviewed journals. Each

article is presented in a separate chapter in this thesis: In **Chapter 2** the goal is to analyse the trends in past streamflow, and their linkages to the evolution of recurrent regional atmospheric circulation patterns using a hydrological model PRMS. A sensitivity analysis of PRMS was conducted over the historical period (1957-2012) using climate hypothetical datasets. These hypothetical datasets have already been used in the past, but without a sufficient temporal resolution for hydrological models at daily steps. In this chapter a new algorithm was developed to create these hypothetical dataset that removed the trend in recurrent synoptic patterns frequencies. These datasets can be used as input in any hydrological model. In **Chapter 3** PRMS was used to simulate the future evolution of streamflow and hydrological processes in the four watersheds and asses the uncertainties due to internal variability of climate. This study took advantage of the newly created Canadian Regional Climate Model Large Ensemble (CRCM5-LE) dataset, which is a downscaled version of the 50 members Canadian global climate model large ensemble (CanESM2-LE). Use of such a large and fine resolution regional ensemble dataset has the advantage of being compatible with the spatial resolution of a hydrological model. It also has potential to associate each member of the ensemble to large scale circulation components from CanESM2-LE. The uncertainties in the streamflow projections associated to internal variability of climate were assessed by identifying classes of similar changes in temperature, precipitation and streamflow and by relating these classes to the average change in large-scale circulation from CanESM2-LE. In **Chapter 4** the goal was to assess how the hydrometeorological extreme events are modulated by internal variability of climate in the past and future. To study the impact of internal variability of climate on high flows the average change in large-scale circulation is not pertinent. To overcome this shortcoming, use of future recurrent synoptic patterns estimated for each member of CanESM2-LE is a novel

technique presented in this chapter. A new weather extreme index, pertinent to explain the generation of winter high flows, was also introduced. Finally, in **Chapter 5,** the uncertainties in the future evolution of the hydrometeorological extreme events due to internal variability of climate were compared to other sources of uncertainty using an analysis of variance.

The results of this study will have important societal implications for floods mitigation and adaptation in southern Ontario. A better knowledge in the relationships between atmospheric circulation and local hydrometeorological extremes will help improve the predictions of high-flow events at weekly or seasonal timescale. The range of possible future streamflow projected in our study will be an asset to help the planning decisions. The change in streamflow regime that will be investigated in this study have also implications for industries or hydroelectricity companies that depend highly on streamflow level. Finally, the investigation of the rivers adjacent to the Great Lakes is fundamental to understand Great Lakes pollution that depend greatly on streamflow regimes.

1.4 References

Adamowski, J., Adamowski, K. and Prokoph, A.: Quantifying the spatial temporal variability of annual streamflow and meteorological changes in eastern Ontario and southwestern Quebec using wavelet analysis and GIS, Journal of Hydrology, 499, 27–40, doi:10.1016/j.jhydrol.2013.06.029, 2013.

Ahn, K.-H., Merwade, V., Ojha, C. S. P. and Palmer, R. N.: Quantifying relative uncertainties in the detection and attribution of human-induced climate change on winter streamflow, Journal of Hydrology, doi:10.1016/j.jhydrol.2016.09.015, 2016.

Anon: Historical Hydrometric Data - Water Level and Flow - Environment Canada, [online] Available from: https://wateroffice.ec.gc.ca/mainmenu/historical_data_index_e.html (Accessed 13 June 2019), n.d.

Barnett, T. P., Adam, J. C. and Lettenmaier, D. P.: Potential impacts of a warming climate on water availability in snow-dominated regions, Nature, 438(7066), 303–309, doi:10.1038/nature04141, 2005.

Bliss, A., Hock, R. and Radić, V.: Global response of glacier runoff to twenty-first century climate change, Journal of Geophysical Research: Earth Surface, 119(4), 717–730, doi:10.1002/2013JF002931, 2014.

Braun, M., Caya, D., Frigon, A. and Slivitzky, M.: Internal Variability of the Canadian RCM's Hydrological Variables at the Basin Scale in Quebec and Labrador, Journal of Hydrometeorology, 13(2), 443–462, doi:10.1175/JHM-D-11-051.1, 2012.

Burn, D. H., Whitfield, P. H. and Sharif, M.: Identification of changes in floods and flood regimes in Canada using a peaks over threshold approach: Changes in Floods and Flood Regimes in Canada Based on a POT Approach, Hydrological Processes, 30(18), 3303–3314, doi:10.1002/hyp.10861, 2016.

Clark, M. P., Wilby, R. L., Gutmann, E. D., Vano, J. A., Gangopadhyay, S., Wood, A. W., Fowler, H. J., Prudhomme, C., Arnold, J. R. and Brekke, L. D.: Characterizing Uncertainty of the Hydrologic Impacts of Climate Change, Current Climate Change Reports, 2(2), 55–64, doi:10.1007/s40641-016-0034-x, 2016.

Coulibaly, P.: Multi-model approach to hydrologic impact of climate change, in From Headwaters to the Ocean: Hydrological changes and watershed management, pp. 249–255, CRC Press, Leiden, Netherlands., 2009.

Cunderlik, J. M. and Ouarda, T. B. M. J.: Trends in the timing and magnitude of floods in Canada, Journal of Hydrology, 375(3–4), 471–480, doi:10.1016/j.jhydrol.2009.06.050, 2009.

Dai, A., Fyfe, J. C., Xie, S.-P. and Dai, X.: Decadal modulation of global surface temperature by internal climate variability, Nature Climate Change, 5(6), 555–559, doi:10.1038/nclimate2605, 2015.

Deser, C., Knutti, R., Solomon, S. and Phillips, A. S.: Communication of the role of natural variability in future North American climate, Nature Climate Change, 2(11), 775–779, doi:10.1038/nclimate1562, 2012.

Deser, C., Phillips, A. S., Alexander, M. A. and Smoliak, B. V.: Projecting North American climate over the next 50 years: uncertainty due to internal variability*, Journal of Climate, 27(6), 2271–2296, 2014.

Erler, A. R., Frey, S. K., Khader, O., d'Orgeville, M., Park, Y.-J., Hwang, H.-T., Lapen, D., Peltier, W. R. and Sudicky, E. A.: Simulating Climate Change Impacts on Surface Water Resources within a Lake Affected Region using Regional Climate Projections, Water Resources Research, doi:10.1029/2018WR024381, 2018.

Gelfan, A., Semenov, V. A., Gusev, E., Motovilov, Y., Nasonova, O., Krylenko, I. and Kovalev, E.: Large-basin hydrological response to climate model outputs: uncertainty caused by internal atmospheric variability, Hydrology and Earth System Sciences, 19(6), 2737–2754, doi:10.5194/hess-19-2737-2015, 2015.

Grillakis, M. G., Koutroulis, A. G. and Tsanis, I. K.: Climate change impact on the hydrology of Spencer Creek watershed in Southern Ontario, Canada, Journal of Hydrology, 409(1–2), 1–19, doi:10.1016/j.jhydrol.2011.06.018, 2011.

Grotjahn, R., Black, R., Leung, R., Wehner, M. F., Barlow, M., Bosilovich, M., Gershunov, A., Gutowski, W. J., Gyakum, J. R., Katz, R. W., Lee, Y.-Y., Lim, Y.-K. and Prabhat: North American extreme temperature events and related large scale meteorological patterns: a review of statistical methods, dynamics, modeling, and trends, Climate Dynamics, 46(3–4), 1151–1184, doi:10.1007/s00382-015-2638-6, 2016.

Gusev, Y. M., Semenov, V. A., Nasonova, O. N. and Kovalev, E. E.: Weather noise impact on the uncertainty of simulated water balance components of river basins, Hydrological Sciences Journal, 62(8), 1181–1199, doi:10.1080/02626667.2017.1319064, 2017.

Insurance Bureau of Canada: February storms, floods caused more than $57 million in insured damage across Southern Ontario and Quebec, [online] Available from: https://www.newswire.ca/news-releases/february-storms-floods-caused-more-than-57-million-in-insured-damage-across-southern-ontario-and-quebec-677383083.html (Accessed 13 June 2019), 2018.

Intergovernmental Panel on Climate Change: Climate change: the IPCC 1990 and 1992 assessments., The Panel, Geneva., 1992.

Kay, J. E., Deser, C., Phillips, A., Mai, A., Hannay, C., Strand, G., Arblaster, J. M., Bates, S. C., Danabasoglu, G., Edwards, J., Holland, M., Kushner, P., Lamarque, J.-F., Lawrence, D., Lindsay, K., Middleton, A., Munoz, E., Neale, R., Oleson, K., Polvani, L. and Vertenstein, M.: The Community Earth System Model (CESM) Large Ensemble Project: A Community Resource for Studying Climate Change in the Presence of Internal Climate Variability, Bulletin of the American Meteorological Society, 96(8), 1333–1349, doi:10.1175/BAMS-D-13-00255.1, 2015.

Kunkel, K. E., Easterling, D. R., Kristovich, D. A. R., Gleason, B., Stoecker, L. and Smith, R.: Meteorological Causes of the Secular Variations in Observed Extreme Precipitation Events for the Conterminous United States, Journal of Hydrometeorology, 13(3), 1131–1141, doi:10.1175/JHM-D-11-0108.1, 2012.

Kuo, C. C., Gan, T. Y. and Higuchi, K.: Evaluation of Future Streamflow Patterns in Lake Simcoe Subbasins Based on Ensembles of Statistical Downscaling, Journal of Hydrologic Engineering, 22(9), 04017028, doi:10.1061/(ASCE)HE.1943-5584.0001548, 2017.

Lafaysse, M., Hingray, B., Mezghani, A., Gailhard, J. and Terray, L.: Internal variability and model uncertainty components in future hydrometeorological projections: The Alpine Durance basin, Water Resources Research, 50(4), 3317–3341, doi:10.1002/2013WR014897, 2014.

Liu, Z., Tang, Y., Jian, Z., Poulsen, C. J., Welker, J. M. and Bowen, G. J.: Pacific North American circulation pattern links external forcing and North American hydroclimatic change over the past millennium, Proceedings of the National Academy of Sciences, 114(13), 3340–3345, doi:10.1073/pnas.1618201114, 2017.

Lorenz, E. N.: Deterministic Nonperiodic Flow, Journal of the Atmospheric Sciences, 20(2), 130–141, doi:10.1175/1520-0469(1963)020<0130:DNF>2.0.CO;2, 1963.

Mallakpour, I. and Villarini, G.: Investigating the relationship between the frequency of flooding over the central United States and large-scale climate, Advances in Water Resources, 92, 159–171, doi:10.1016/j.advwatres.2016.04.008, 2016.

Markstrom, S. L., Regan, R. S., Hay, L. E., Viger, R. J., Payn, R. A. and LaFontaine, J. H.: precipitation-runoff modeling system, version 4: U.S. Geological Survey Techniques and Methods., 2015.

Mendoza, P. A., Clark, M. P., Mizukami, N., Gutmann, E. D., Arnold, J. R., Brekke, L. D. and Rajagopalan, B.: How do hydrologic modeling decisions affect the portrayal of climate change impacts?: Subjective Hydrologic Modelling Decisions in Climate Change Impacts, Hydrological Processes, 30(7), 1071–1095, doi:10.1002/hyp.10684, 2016.

Music, B. and Caya, D.: Investigation of the Sensitivity of Water Cycle Components Simulated by the Canadian Regional Climate Model to the Land Surface Parameterization, the Lateral Boundary Data, and the Internal Variability, Journal of Hydrometeorology, 10(1), 3–21, doi:10.1175/2008JHM979.1, 2009.

Nalley, D., Adamowski, J., Khalil, B. and Biswas, A.: Inter-annual to inter-decadal streamflow variability in Quebec and Ontario in relation to dominant large-scale climate indices, Journal of Hydrology, 536, 426–446, doi:10.1016/j.jhydrol.2016.02.049, 2016.

Ning, L. and Bradley, R. S.: Winter climate extremes over the northeastern United States and southeastern Canada and teleconnections with large-scale modes of climate variability*, Journal of Climate, 28(6), 2475–2493, 2015a.

Pall, P., Allen, M. R. and Stone, D. A.: Testing the Clausius–Clapeyron constraint on changes in extreme precipitation under CO2 warming, Climate Dynamics, 28(4), 351–363, doi:10.1007/s00382-006-0180-2, 2007.

Papritz, L. and Grams, C. M.: Linking Low-Frequency Large-Scale Circulation Patterns to Cold Air Outbreak Formation in the Northeastern North Atlantic, Geophysical Research Letters, 45(5), 2542–2553, doi:10.1002/2017GL076921, 2018.

Rahman, M., Bolisetti, T. and Balachandar, R.: Hydrologic modelling to assess the climate change impacts in a Southern Ontario watershed, Canadian Journal of Civil Engineering, 39(1), 91–103, doi:10.1139/l11-112, 2012.

Rohli, R. V., Vega, A. J., Binkley, M. R., Britton, S. D., Heckman, H. E., Jenkins, J. M., Ono, Y. and Sheeler, D. E.: Synoptic circulation and stream discharge in the Great Lakes basin, USA, Applied Geography, 21(4), 369–385, doi:10.1016/S0143-6228(01)00011-X, 2001.

Shepherd, T. G.: Atmospheric circulation as a source of uncertainty in climate change projections, Nature Geoscience, 7(10), 703–708, doi:10.1038/ngeo2253, 2014.

Steinschneider, S., Wi, S. and Brown, C.: The integrated effects of climate and hydrologic uncertainty on future flood risk assessments: FLOOD RISK UNDER HYDROLOGIC AND CLIMATE UNCERTAINTY, Hydrological Processes, 29(12), 2823–2839, doi:10.1002/hyp.10409, 2015.

Stone, D. A., Weaver, A. J. and Zwiers, F. W.: Trends in Canadian precipitation intensity, Atmosphere-ocean, 38(2), 321–347, 2000.

Sultana, Z. and Coulibaly, P.: Distributed modelling of future changes in hydrological processes of Spencer Creek watershed, Hydrological Processes, 25(8), 1254–1270, doi:10.1002/hyp.7891, 2011.

Teutschbein, C., Wetterhall, F. and Seibert, J.: Evaluation of different downscaling techniques for hydrological climate-change impact studies at the catchment scale, Climate Dynamics, 37(9–10), 2087–2105, doi:10.1007/s00382-010-0979-8, 2011.

Thiombiano, A. N., El Adlouni, S., St-Hilaire, A., Ouarda, T. B. M. J. and El-Jabi, N.: Nonstationary frequency analysis of extreme daily precipitation amounts in Southeastern Canada

using a peaks-over-threshold approach, Theoretical and Applied Climatology, 129(1–2), 413–426, doi:10.1007/s00704-016-1789-7, 2017.

Thompson, D. W. J., Barnes, E. A., Deser, C., Foust, W. E. and Phillips, A. S.: Quantifying the Role of Internal Climate Variability in Future Climate Trends, Journal of Climate, 28(16), 6443–6456, doi:10.1175/JCLI-D-14-00830.1, 2015.

Trenberth, K. E., Dai, A., Rasmussen, R. M. and Parsons, D. B.: The Changing Character of Precipitation, Bulletin of the American Meteorological Society, 84(9), 1205–1217, doi:10.1175/BAMS-84-9-1205, 2003.

Troin, M., Velázquez, J. A., Caya, D. and Brissette, F.: Comparing statistical post-processing of regional and global climate scenarios for hydrological impacts assessment: A case study of two Canadian catchments, Journal of Hydrology, 520, 268–288, doi:10.1016/j.jhydrol.2014.11.047, 2015.

Vincent, L. A., Zhang, X., Brown, R. D., Feng, Y., Mekis, E., Milewska, E. J., Wan, H. and Wang, X. L.: Observed Trends in Canada's Climate and Influence of Low-Frequency Variability Modes, Journal of Climate, 28(11), 4545–4560, doi:10.1175/JCLI-D-14-00697.1, 2015.

Watanabe, M., Shiogama, H., Tatebe, H., Hayashi, M., Ishii, M. and Kimoto, M.: Contribution of natural decadal variability to global warming acceleration and hiatus, Nature Climate Change, 4(10), 893–897, doi:10.1038/nclimate2355, 2014.

Zhao, H., Higuchi, K., Waller, J., Auld, H. and Mote, T.: The impacts of the PNA and NAO on annual maximum snowpack over southern Canada during 1979-2009, International Journal of Climatology, 33(2), 388–395, doi:10.1002/joc.3431, 2013.

Chapter 2. Atmospheric circulation amplifies shift of winter streamflow in Southern Ontario

Champagne Olivier, Arain M. Altaf, and Coulibaly Paulin 2019. Atmospheric circulation amplifies shift of winter streamflow in Southern Ontario. *Journal of Hydrology*, 124051. https://doi.org/10.1016/j.jhydrol.2019.124051

2.1 Abstract

Flooding is a major concern for Canadian society as it is the costliest natural disaster type in Canada. Southern Ontario, which houses one-third of the Canadian population, is located in an area of high vulnerability for floods. The most significant floods in the region have historically occurred during the months of March and April due to snowmelt coupled with extreme rain events. However, during the last three decades, there has been a shift of flooding events to earlier months. The aim of this study was to understand the impacts of atmospheric circulation on the temporal shift of streamflow and high flow events observed in Southern Ontario over 1957 to 2013 period. Predominant weather regimes over North America, corresponding to recurrent meteorological situations, were identified using a discretization of daily geopotential height at 500HpA level (Z500). A regime-normalized hypothetical temperature and precipitation dataset was constructed to quantify the contribution of atmospheric circulation on streamflow response. The hypothetical dataset was used as input in the Precipitation Runoff Modeling System (PRMS), a rainfall-runoff semi-distributed hydrological model, and applied to four watersheds in Southern Ontario. The results showed an increase in the temporal frequency of the regime identified here as High Pressure (HP) close to eight occurrences per decade. Regime HP, characterized by a northern position of the polar vortex, is correlated with a positive phase of the NAO and is associated with warm and

wet conditions over Southern Ontario during winter. The temporal increase in HP contributed more than 40% of the increase in streamflow in winter and 30 to 45% decrease in streamflow in April. This atmospheric situation also contributed to increase the number of high flows by 25 to 50% in January. These results are important to improve the seasonal forecasting of high flows and to assess the uncertainty in the temporal evolution of streamflow in the Great Lakes region.

2.2 Introduction

A shift to earlier streamflow has been commonly observed around the world in glaciated or snow-dominated watersheds (Barnett et al., 2005; Bliss et al., 2014). This shift, attributed to global warming, has a large impact in water resource stability (Wu et al., 2015b), water quality (Chen et al., 2016), or flood management (Hamlet and Lettenmaier, 2007). Canada is greatly affected by this shift because the country has a high snowmelt contribution to streamflow (Burn and Whitfield, 2016), and is highly dependent on fluvial resources. Southern Ontario is a densely populated region in Canada and is a critical area to produce high quality agriculture products (Pim et al., 2005). The heterogeneous combination of urban areas, industrial activity and agricultural lands makes this region particularly vulnerable to the change in water resources and flood events. Historically, the number of high flow events in Southern Ontario has peaked in March and April in correspondence with the snow melt period (Burn and Whitfield, 2016; Buttle et al., 2016). In recent decades, similarly to what was observed worldwide, there has been an observed decline in spring maximum peak flows and an increase in winter flows attributed to an increase in winter temperatures to promote an earlier snowmelt (Adamowski et al., 2013; Cunderlik and Ouarda, 2009).

Global warming, that increased winter snowmelt in numerous snow dominated catchments around the world (Barnett et al., 2005) is modulated regionally by atmospheric circulation in the mid-latitudes (Nilsen et al., 2017). Recent studies have attempted to identify the contribution of large scale climate variability to the local variability of climate or hydrological processes in Southern Ontario, but, the results are generally not promising (Tan and Gan, 2015; Vincent et al., 2015; Zhang et al., 2010; Zhao et al., 2013). Some of these studies consider monthly values of streamflow (Nalley et al., 2016) or used coarse hydrometric data from large areas in Canada (Coulibaly and Burn, 2005). A recent study found that Pacific North American pattern (PNA), characterized in it positive phase by low pressure anomalies in eastern North America, was negatively correlated to extreme precipitation in Southern Ontario (Thiombiano et al., 2017). Similar results were found in the region south of the Great Lakes where a negative phase of the PNA was associated with more extreme precipitations events and higher frequency peak streamflow (Mallakpour & Villarini, 2016). Meanwhile, the negative phase of PNA was associated with lower mean winter streamflow in the northeastern United States (Bradbury et al., 2002). The positive phase of the North Atlantic Oscillation (NAO^+), associated with a strong gradient between low pressure in Iceland and high pressure in the Azores, has also been found to increase mean winter streamflow in the northeastern United States (Bradbury et al., 2002), while it was found to delay winter peak flows in Québec (Beauchamp et al., 2015). Other methods, described by Jones (1994), examined forcing of atmospheric circulation onto local meteorological conditions in the region of Great Lakes. A manual circulation-to-environment synoptical classification shows that high flows in Pennsylvania (U.S.) were associated with intense, low level pressure cells in the region (Yarnal & Frakes, 1997). A manual environment-to-circulation method was used in Atlantic Canada to show that Great

Lakes low pressure cells were important processes to generate floods in this region (Collins et al., 2014). In Rohli et al., (2001) an eigenvector-based map pattern classification scheme shows high stream discharge in the U.S. Great Lakes basin associated to high pressure anomalies over the northeast North American coast. These studies show that the impact of atmospheric circulation on streamflow may vary among different regions of the Great Lakes basin. The lack of robust studies on the relationship between atmospheric circulation and streamflow in Southern Ontario suggest relevance on focusing further work in this populated region of Canada.

The objective of this study is to examine the impact of atmospheric circulation on the modulation of streamflow in four diverse watersheds (i.e Grand River, upper-Thames River, Credit River and Big Creek) in southern Ontario and to quantify its role in overall streamflow shifts. Temporal evolution of atmospheric circulation is assessed using classes of recurrent large-scale meteorological patterns, called weather regimes. Weather regimes calculation was developed by Michelangeli et al. (1995) and have been used in Europe to identify impacts of regional atmospheric circulation on local climate variability and particularly extreme temperatures (Cassou et al., 2005; Fernández-Montes et al., 2013), extreme rainfall (Pfahl, 2014; Ullmann et al., 2014) or flood events (Santos et al., 2015). The sensitivity of mean streamflow and high flows to temporal shifts of weather regime occurrence frequency is tested by replacing the original precipitation and temperatures datasets with hypothetical, regime-normalized climate datasets as input in the Precipitation Runoff Modeling System (PRMS). The use of hypothetical datasets to understand the role of atmospheric circulation on local or regional weather conditions have been used in the past (Fleig et al., 2015). This method has been previously applied in the Great Lakes region to

understand the impact of atmospheric circulation on the evolution of snowfall (Leathers and Ellis, 1996). In our study weather patterns driven hypothetical dataset is used for the first time as input in a hydrological model.

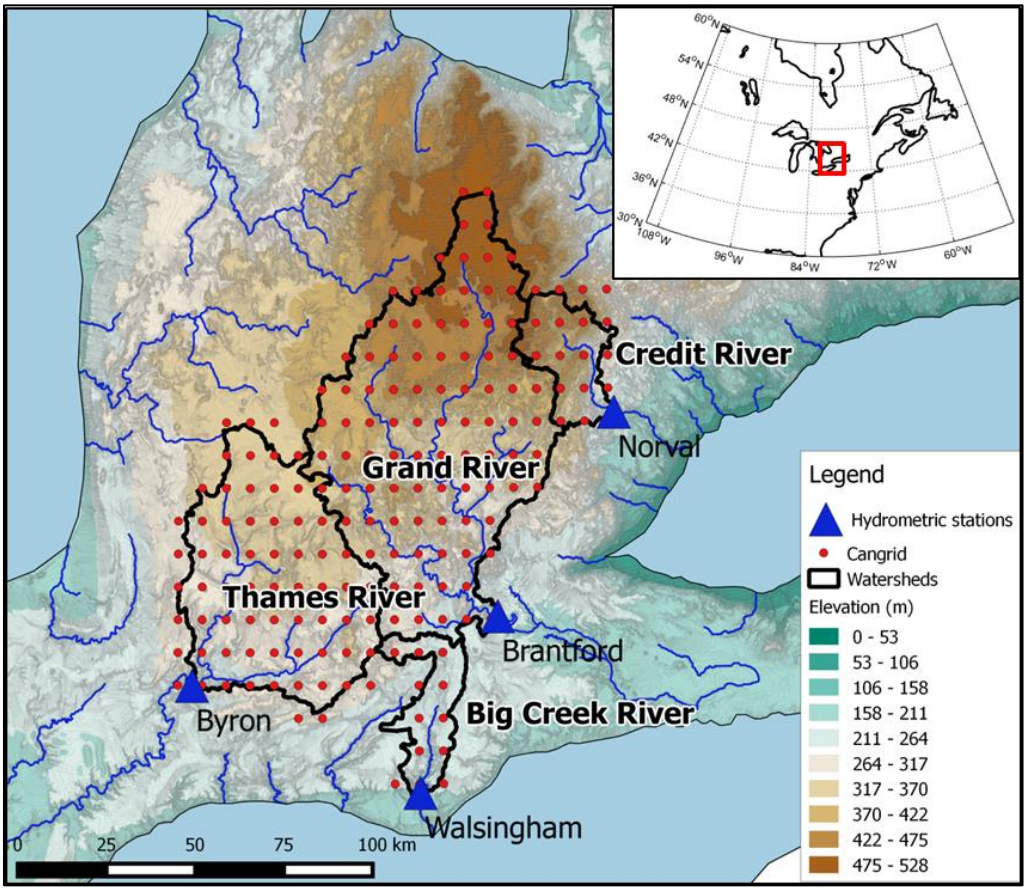

Figure 2-1 Location map of the four studied watersheds in southern Ontario

2.3 Methods

2.3.1 Study area

Four watersheds in southern Ontario were selected for their long hydrometric time series archives and represent well the diversity of scale, soil type, and land use in this region (Figure 2-1 and Table 2-1). Land use in all four watersheds is dominated by agricultural activity. Credit River has the highest proportion of forest cover. Two major cities, Brantford in Grand River, and London in

Thames River are present in the study area and additional urban areas are located in the Credit river watershed. The Big Creek watershed contains the lowest proportion of urbanization (2%). The watersheds also vary in soil type: sand predominates in Big Creek (79%) and Credit River (43%), but a large area of Credit is also covered by loamy soil (49%). Grand River has almost an equal proportion of sand (30%), loam (32%) and clay (38%) while Thames River contains more clay (39%). The elevation is also highly variable with the highest elevations in the North parts of Grand River (531 m) and Credit River (521 m) watersheds while the lowest areas are located in the sandplains further south in Grand River (178 m) and Big Creek (179 m).

Table 2-1 Geomorphic, land use, and soil characteristics of the four watersheds examined in this study

	Size (km^2)	**Elevation (m)**	**Land use (%)**				**Soil type (%)**		
			Barren	**Forest**	**Shrub**	**Crops/Grass**	**Sand**	**Loam**	**Clay**
Big Creek	571	179-336	1.9	17	0	81.1	78.6	6.4	15
Grand	5091	178-531	7.1	11.9	0	80.9	30.4	31.6	38
Thames	3061	215-423	6.9	5.4	0	87.7	14	46.7	39.4
Credit	646	190-521	6.6	31.7	0	61.8	42.5	49.1	8.4

2.3.2 Hydrological modelling

The Precipitation and Runoff Modeling System (PRMS), a semi-distributed conceptual hydrological model, was applied to all four watersheds. PRMS has been widely used in Snowmelt dominated regions in United States (Dressler et al., 2006; Mastin et al., 2011; Surfleet et al., 2012; Teng et al., 2018) and has been recently applied in China (Teng et al., 2017) and high latitude regions (Liao and Zhuang, 2017) with a good representation of the snowmelt processes. The hydrological calculations in PRMS is based on physical laws and empirical relations between

measured and estimated quantities (Markstrom et al., 2015). A series of hydrologic reservoirs is used (plant canopy interception, snowpack, soil zone, subsurface) and the water flowing between the reservoirs are computed for each hydrological response unit (HRU). In this study, HRUs consisted of surface grid cells of 200x200m for Big Creek and Credit River watersheds and 400mx400m for Grand River and Thames River. These two watersheds used coarser HRU's to reduce the parametrization calculations time. For each step of the model calculation PRMS allows to choose among different modules that are described in the supplementary materials (Section S1) and in Markstrom et al., (2015).

Parameter values used by PRMS were found in the literature and were spatialized for each HRU's (Table 2-3). These parameters were estimated according to land use, elevation, aspect, slope and soil type using Arcpy-GSFLOW under ArcGIS (Gardner et al., 2018). Arcpy-GSFLOW was also used to estimate the water cascade between the HRU's and the river segments. Some of these parameters were modified during calibration while keeping the relative spatial variability of the processes (Table 2-3).

Calibration was done by a trial and error approach and followed three-steps: (1) calibration of daily shortwave radiation using satellite data (2002-2008) furnished by Natural Resources Canada at 1/10 degree (almost 10km) resolution (Djebbar et al., 2012); (2) adjustment of potential evapotranspiration (PET) parameters with value of PET estimated using the Thornwaite method (Thornthwaite, 1948) and (3) calibration of 17 parameters by the Normal Root Mean Square Error (NRMSE) between daily and monthly mean streamflow. The Thornwaite method was used in this study because of readily available gridded temperature data. These steps were repeated until the

set of parameters produces satisfactory results. Parameter sources, spatial and temporal resolution and values after calibration are listed in Table 2-3.

Five years were used as the warm-up period (Oct 1984 to Sept 1989) to remove the errors due to initial conditions. Different simulations with a varying warm-up period length were tested in the Big Creek watershed and showed that five years were necessary to eliminate variability due to the initial conditions of the reservoirs. The calibration period was from 1989 to 2008 providing a 20-year calibration period and 2009 to 2013 period were used as the validation period. The input variables for PRMS were precipitation, minimum temperature and maximum temperature values. These variables were obtained from the gridded historical weather station data (CanGrid) produced by McKenney et al., (2011) using Natural Resources Canada and ECCC data archives at 10 km spatial resolution. 186 data points were needed to cover the area of the four watersheds (red markers on Figure 2-1). For model calculations, each HRU used climate data from the closest grid point.

2.3.3 Construction of North American temporal weather regimes

Temporal evolution of atmospheric circulation was assessed using discretization of daily geopotential height anomalies at 500 hPa level (Z500 hereafter) in recurrent weather regime patterns (Michelangeli et al., 1995). These maps documented the most robust location and intensity of anticyclone (positive geopotential height anomalies relative to the climatological mean) and depression (negative anomalies). Z500 fields were derived from the 20th Century Reanalysis version 2 available for all years since 1871 (Compo et al., 2011). The domain used was centered on the Great Lakes and extended into the eastern part of North America (30N-60N / 110W-50W).

The weather regimes were calculated for the period 1950 to 2014 by a K-means algorithm applied to the first principal components explaining 80% of the total Z500 daily variance. 100 K-means partitions were performed for each potential number of class (2 to 10) and the final number of classes were determined by a red noise test described in the supplementary materials (Section S3). A complete description of the use of the K-means algorithm to compute the weather regimes is described in Michelangeli et al., (1995). The relationship between weather regimes and large scale mode of variability (i.e. NAO and PNA) were also considered, as these modes are known for having impacts on local winter conditions in the region (Beauchamp et al., 2015; Bradbury et al., 2002; Thiombiano et al., 2017; Zhao et al., 2013). Monthly NAO indices were based on Iceland and Gibraltar sea level pressure furnished by the Climatic Research Unit (Jones, 1994). The PNA oscillation monthly indices were furnished by the National Oceanic and Atmospheric Administration (Barnston and Livezey, 1987).

2.3.4 Construction of original and experimental climate datasets

CanGrid temperature and precipitation data for the period 1957-2013 are taken as a control data set (CTL). CTL data are used to create experimental (EXP) climate data sets that represent climate variability that would occur without the influence of atmospheric circulation. In previous studies, experimental climate datasets were based on average conditions of each weather pattern (Fleig et al., 2015) but had limited application in hydrological models which require realistic daily data series. In this study, a new algorithm was developed under Matlab to create regime-normalized climate occurrence data sets to be used as input in hydrological models. Weather regimes occurrences were first modified to remove their 1957 to 2013 monthly frequency trend. In order to detrend the monthly regime frequencies, the regimes were replaced with respect to the observed

sequence of regimes between 1957 and 2013. Keeping a reasonable sequence of regimes is fundamental because the atmospheric variability is continuous over time and the sequence of regimes that naturally occurs follows a specific order (Table 2-4). The construction of the detrended sequence of regimes is described in detail in the supplementary material (Section S4).

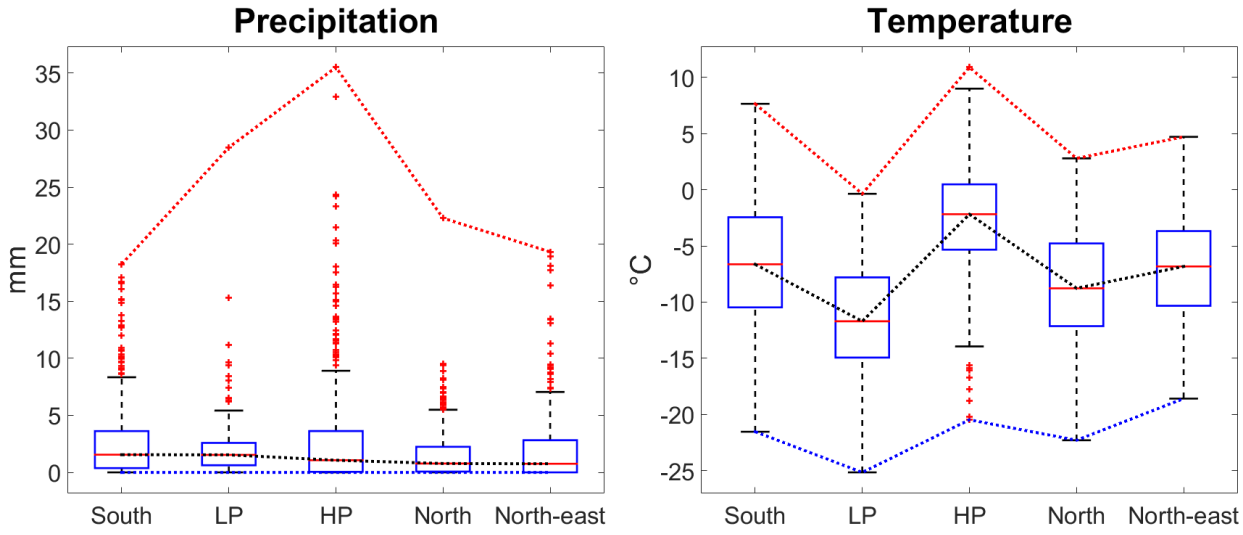

Figure 2-2 Regimes Distribution of daily temperature and precipitation averaged for the 4 watersheds between 1957 and 2012 in January. The dotted red line (blue line) is the maximum (minimum) value for each regime. The doted black line shows the median.

Following the construction of the new sequence of regime, temperature and precipitation conditions associated to the removed regimes were replaced by conditions associated to the new regime. New temperature and precipitation conditions were taken from daily observations in each grid point over the 1957 to 2013 period. For each month, the daily temperature and precipitation conditions for all grid points in the watersheds were averaged. These mean daily conditions were ranked for each regime. The observation of the old regime was replaced by conditions situated in the same rank of the new regime. For example in January if the day to switch corresponded to the regime HP (High Pressure) and was associated to the highest intra-regime temperature (ranked

first), the new conditions will be from the day associated to the first rank of the new regime (5 degrees on average if regime North-east) (Figure 2-2). The same process was performed for the precipitation data.

Even though the algorithm used the observed sequence of regime to construct the experimental dataset, several possibilities in the switch of regime can be often made (Section S4). Therefore, it was important to repeat the algorithm several times to create different experimental dataset and consider the range of possible changes in weather regimes. In consideration of these different possibilities of new experimental datasets, we repeated the algorithm 100 times. This method produced an experimental dataset to identify climate variability associated with the large-scale atmospheric circulation and preserved climate variability from all other sources. It also kept the same statistical properties as the original data (Section S4) and can be used in hydrological models. The CTL and 100 EXP climate dataset were used as input in PRMS for each watershed.

2.4 Results

2.4.1 Weather regimes and local meteorological conditions

Five regimes were identified as the most robust and recurrent atmospheric configurations over northeast North America in the 1957-2013 period (Figure 2-3). Two of the regimes consisted of high geopotential (HP, High Pressure) or low geopotential (LP, Low Pressure) anomalies centered in the eastern Great Lakes region. The regime North-east was characterized by high geopotential in Northeastern Québec while low geopotential conditions occurred in the Atlantic Ocean. Northeasterly winds are more likely to occur in this configuration. The regime South was characterized by anticyclonic conditions anomalies over the Atlantic Ocean but cyclonic

conditions in northern Ontario and northern Manitoba causing southerly winds over the region. Regime North was characterized by low geopotential anomalies in the east with high geopotential conditions in the west causing northerly winds over the Great Lakes region (Figure 2-3).

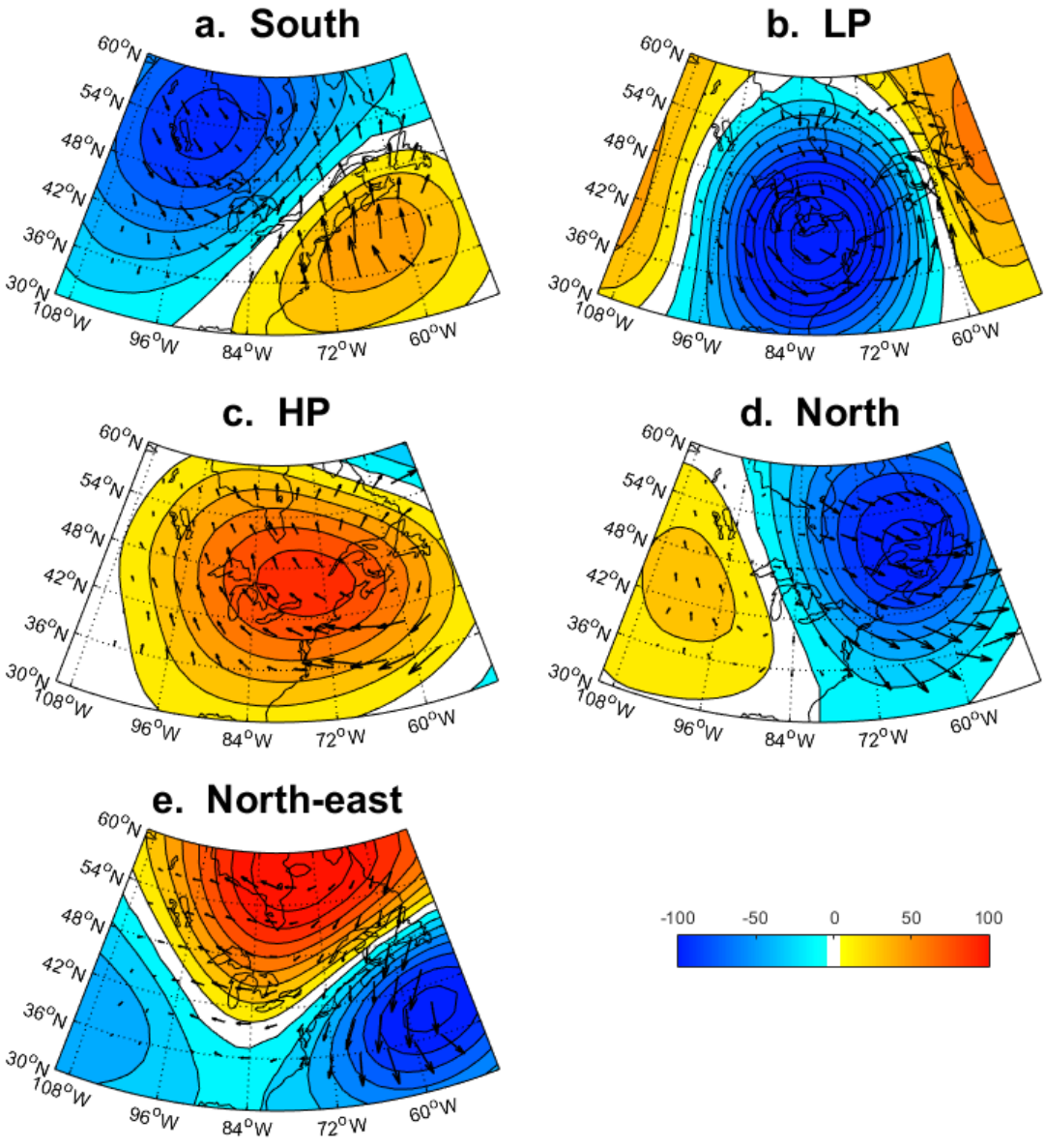

Figure 2-3 500 hPa level Geopotential height anomalies (Colors, interval 10m) and wind anomalies (vectors) for each weather regimes in the northeastern North America domain. All anomalies are significant at the 95% confidence level according to *t* test

The Regimes annual frequencies are depicted in Figure 2-4 and show a seasonal variability for the Regimes LP, North and North-east (Figure 2-4). The regime North was more frequent during summer while Regimes LP and North-east occurred more frequently in winter months. Inter-annual and decadal variability of weather regimes frequency was also observed over the 1957 to 2013 period (Figure 2-4). The regime HP increased every month except October when no trend was found. The most significant increasing trend for HP was between January and April, July and September and in November. Regime North also demonstrated significant increases in January and February, Regime North-east increased significantly during June and Regime South increased the most during October. Notable decreasing trends were also observed in the regime North-east and South between January and March. Regime North also declined during warm season (April through October) while Regime LP declined during the cold months (November to March). However, these negative trends were found to be non-significant.

Inter-annual occurrences of weather regimes were compared to PNA and NAO indices to identify if a significant correlation exists with the most influential indices over the region (Figure 2-5). Between January and March, the occurrence of regimes HP and North were positively correlated to a positive NAO (NAO^+) while regimes LP and North-east were correlated to negative NAO (NAO^-). Between October and June The regime LP was correlated to the positive phase of PNA (PNA^+) while regime South was correlated to negative PNA (PNA^-) (Figure 2-5).

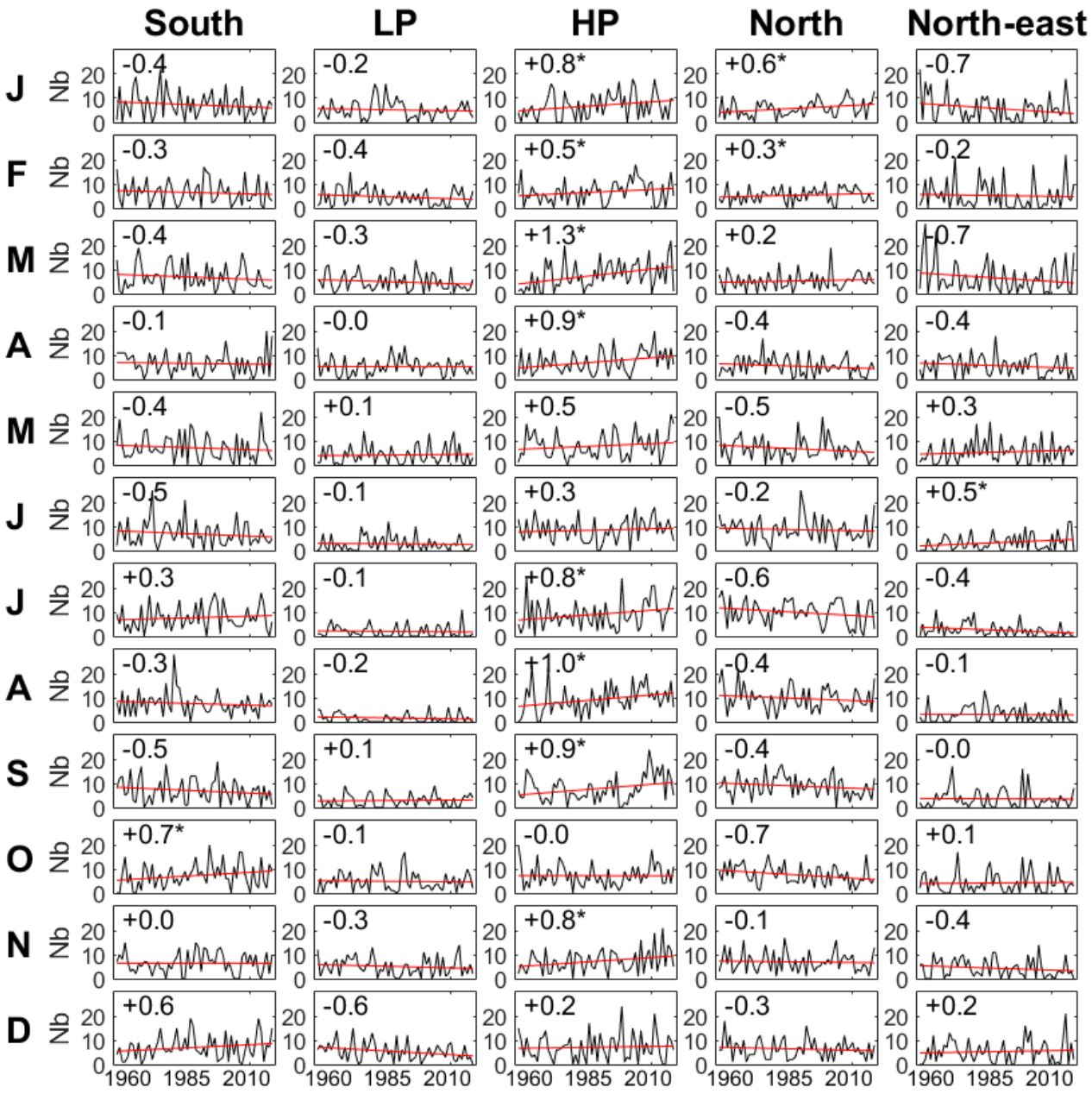

Figure 2-4 Monthly inter-annual frequency (black lines) and trend (red lines) of weather regimes. The numbers indicate the evolution of annual frequency per decades and the stars indicate a trend significant at 95% confidence according to the Spearman's rank order correlation test.

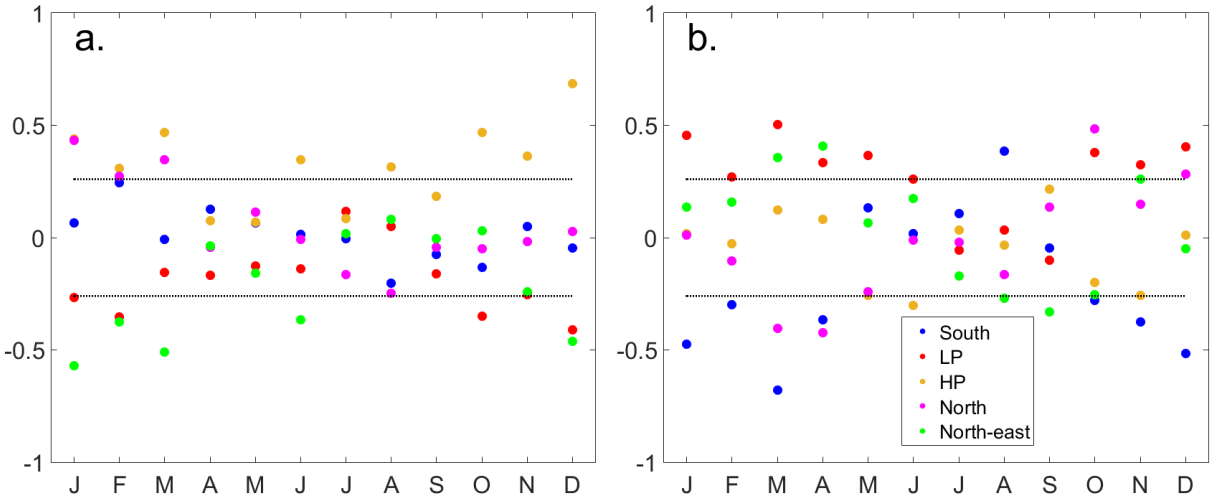

Figure 2-5 Monthly interannual correlations between regime occurrence and (a) NAO or (b) PNA.

Figure 2-6 shows monthly average temperature and precipitation conditions in all watersheds for each regime and season. The regime HP was the warmest during all months of the year while LP and North were the coldest. Regimes South and North-east were similar throughout the year except that North-east was warmer during summer. South was the wettest regime throughout the year but the inter-regime variability of precipitation was higher between months. During winter, HP was relatively wet from November to April and was the driest regime in August. The other three regimes produced less precipitation amount compared to HP between January and April, but were wetter during the warm season. While the regimes LP and North-east remained wet during the fall season, North was the driest regime after September. These results showed that the weather conditions were well discretized by the regimes in all four watersheds but does not quantify the impacts of trend in weather regimes occurrence on the change of temperature and precipitation in the region.

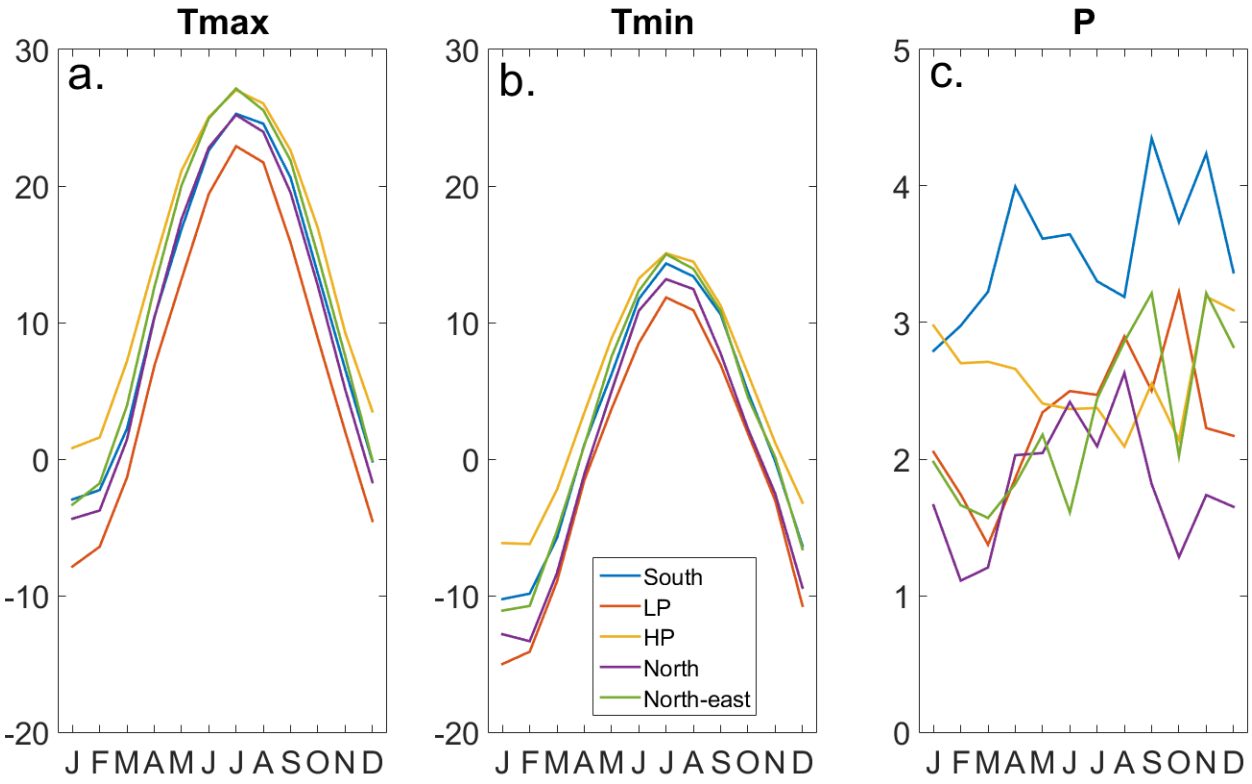

Figure 2-6 Monthly average maximum temperature, minimum temperature, and precipitation per regime for all watersheds grids altogether.

Temperature (Figure 2-7) and precipitation (Figure 2-8) trends for each month between 1957 and 2013 in southern Ontario are shown for the control dataset (CTL), the experiment dataset (EXP) and the contribution of weather regimes to the change of temperature or precipitation (CTL minus EXP). The CTL dataset showed a significant increase of temperature in the entire area during every month with the exception of October and November. The increasing trend of temperature was highest between December and March in areas further North from the Great Lakes. The warming was also higher in the eastern part of the study area during winter and in the Greater Toronto area during summer. The EXP data set showed less intense warming and was generally non-significant with more intense cooling during October as compared to CTL. The weather regime contribution

to temperature increases was higher in winter, particularly during March and December. During March, weather regimes showed more intense warming west of the Greatest Toronto area while in December the warming was higher in the eastern part of the area.

Spatially, CTL precipitation was found to vary on a monthly basis (Figure 2-8). Precipitation was found to significantly increase in October in most of the study area. A trend toward wetter conditions also occurred in the eastern part of the area in June and September and in the northern part of the region in March. Dryer conditions were observed in the Greater Toronto region during August and in the east during February. The EXP dataset showed weaker increases of precipitation during October and March while during June and September the increase of precipitation was enhanced. The dryer conditions observed with the CTL data set were also detected by the EXP data, with drier conditions near Lake Huron in July. The weather regimes contributed to an increase of precipitation between October and December, and during March and April. In July, weather regimes contributed to the increase of precipitation near Lake Huron.

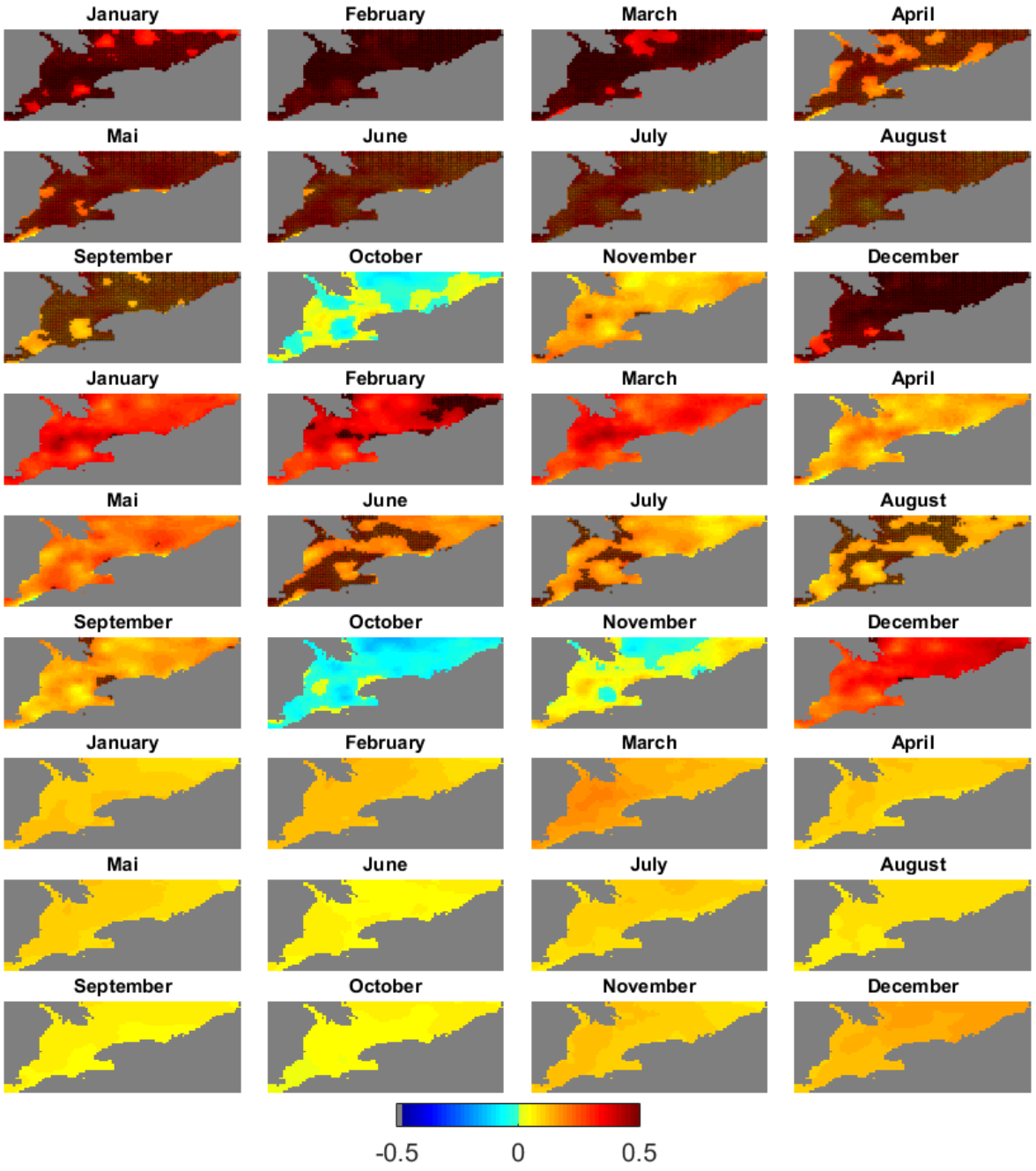

Figure 2-7 Temperature trend for the control dataset (CTL) (top 3 rows), the experiment dataset (EXP) (middle 3 rows) and CTL minus EXP (bottom 3 rows) between 1957 and 2013. The grids with a trend significant at 95% confidence level with the Spearman's rank-order correlation are shown by black dots.

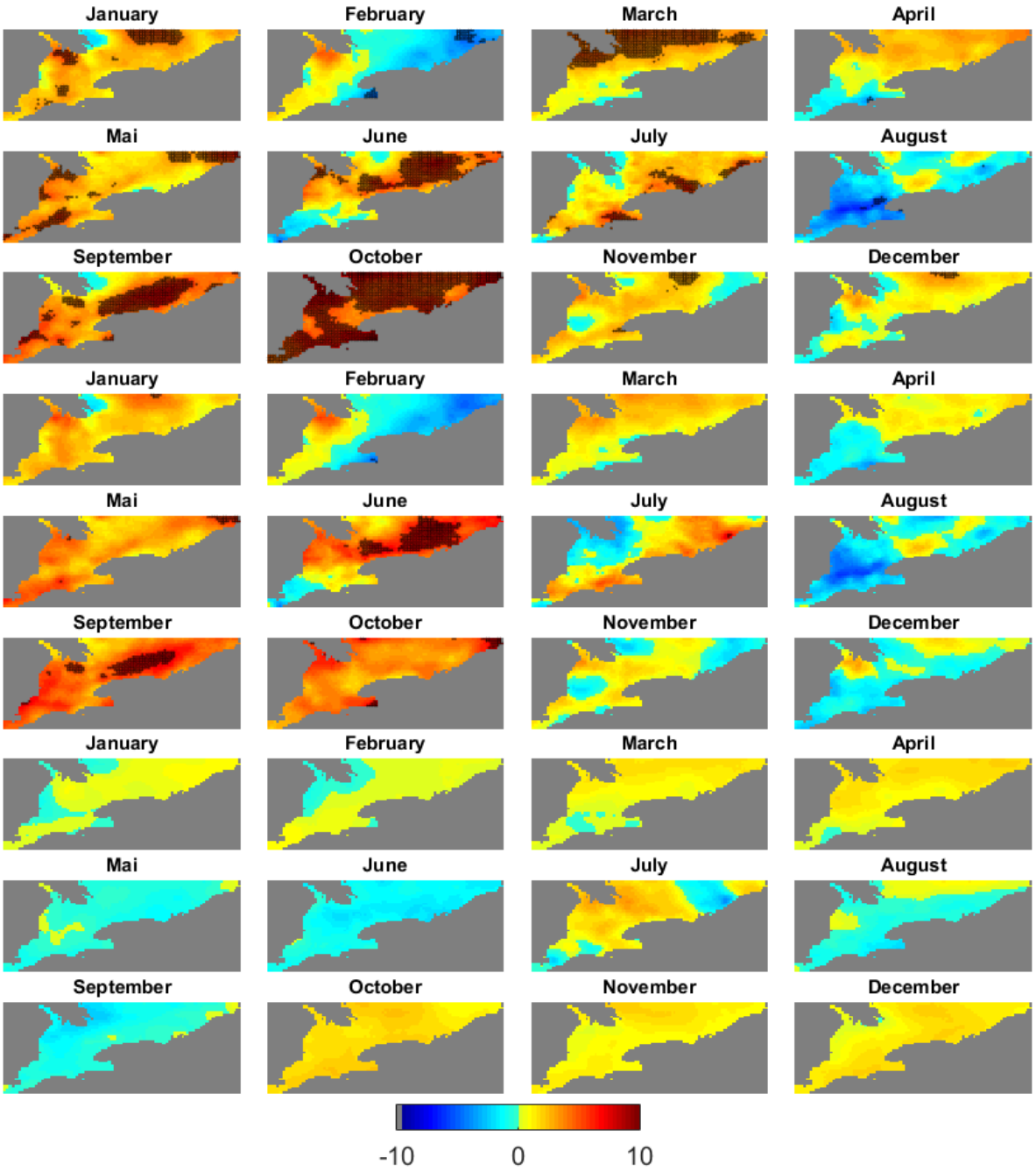

Figure 2-8 precipitation trend for the control dataset (CTL) (top 3 rows), the experiment dataset (EXP) (middle 3 rows) and CTL minus EXP (bottom 3 rows) between 1957 and 2013. The grids with a trend significant at 95% confidence level with the Spearman's rank-order correlation are shown by black dots.

2.4.2 Contribution of weather regimes to the change in streamflow

Streamflow in the four watersheds have been calculated between 1951 and 2013 with PRMS using the best set of parameters retained after calibration (Table 2-2). The Nash Sutcliff Efficency (NSE) values were higher than 0.65 for both calibration and validation periods (Table 2-2). The percent bias (PBIAS) was between -15% and +15% with the exception of Credit River during the validation period and Big Creek during the calibration period in winter. A NSE higher than 0.65 and a PBIAS lower than 15% is generally considered a good quantitative fit (Moriasi et al., 2007). Figure 2-9 shows the simulation and the observation of the daily streamflow in all four watersheds and confirms visually the goodness of simulation fit. The observed peak at the beginning of the validation period is not well captured by PRMS (Figure 2-9) but similar results were found with the model Mike-She in another watershed located in the same region (Sultana and Coulibaly, 2011). Snowpack and Snow water equivalent are also reasonably well simulated by PRMS (section S2).

Table 2-2 Efficiency of PRMS model to simulate daily streamflow

	Calibration				Validation			
	NSE		PBIAS		NSE		PBIAS	
	Annual	Winter	Annual	Winter	Annual	Winter	Annual	Winter
Thames River	0.72	0.70	-10.8	-16.3	0.72	0.70	-5.3	-10.6
Big Creek	0.75	0.70	1.8	9.8	0.74	0.69	6.7	3.1
Grand River	0.71	0.69	-5	-4.3	0.69	0.68	1.7	-3.2
Credit River	0.71	0.67	-0.1	1.4	0.65	0.68	18	4

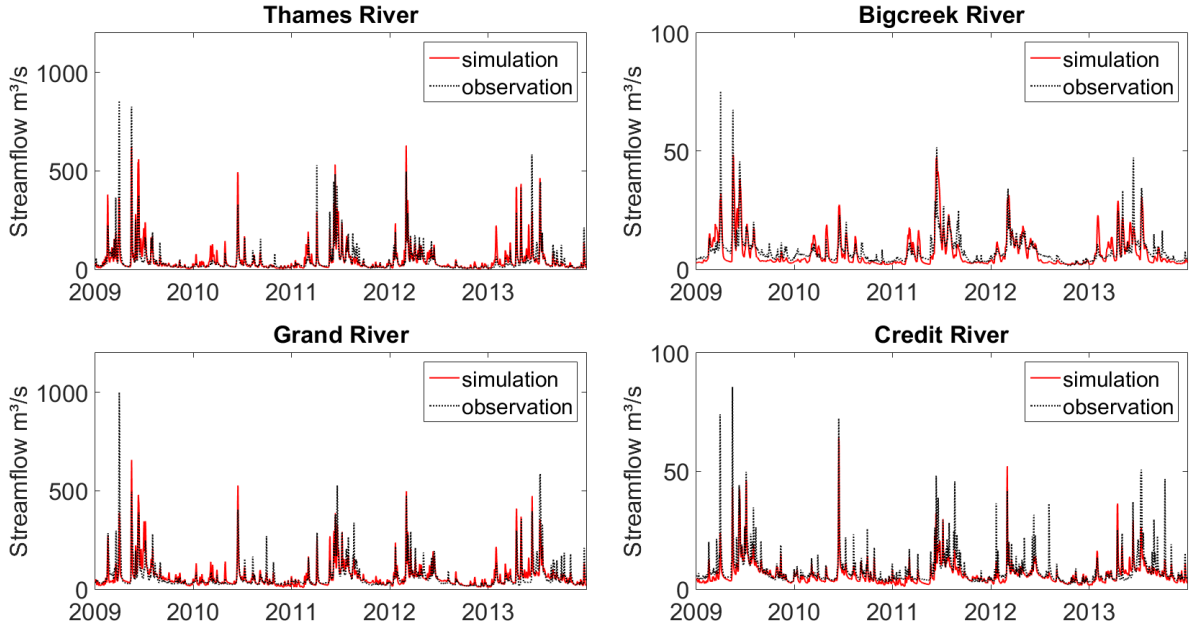

Figure 2-9 Simulated and observed streamflow during the validation period (2009-2013)

The monthly trend of streamflow simulated by the CTL and EXP dataset between 1957 and 2013 are shown for all four watersheds in Figure 2-10. In CTL, streamflow was increasing between December and March and was decreasing in April. The increase of streamflow was significant for all four watersheds in January but only for Grand River and Credit River in February and March. Between May and December, the evolution of streamflow was lower and non-significant. Removing the trend in the occurrence of weather regimes had a clear impact on streamflow with lower increases of streamflow between December and March and lower decreases during April (Figure 2-10). The ratio of the 100 EXP average to CTL, calculated for each month, showed that between December and March, 40 to 50% of the increase of streamflow was due to the shift in weather regimes. In April, 45% of the decrease of streamflow was due to the shift in weather regimes in Thames and Big Creek and 30% in Credit and Grand River. Figure 2-10 shows the temporal evolution of the number of high flow counts in all months between 1957 and 2013 for

the CTL and the EXP datasets. The high flow counts were determined by peak over threshold approach where the threshold was defined as the average streamflow plus 3SD (standard deviation) for each watershed. High flow counts increased in all four watersheds during January. Increasing high flow counts were highest in Thames River and continued into February while the trend declined for the three other watersheds. In March, the trend was increasing again for Grand and Credit River watersheds and was decreasing for Thames and Big Creek. In April, a decrease of number of high flows was observed in Grand and Credit Rivers. Removing the trend of weather regimes attenuated the increase of high flows but amplified the decrease of high flows in April for Grand and Credit watersheds.

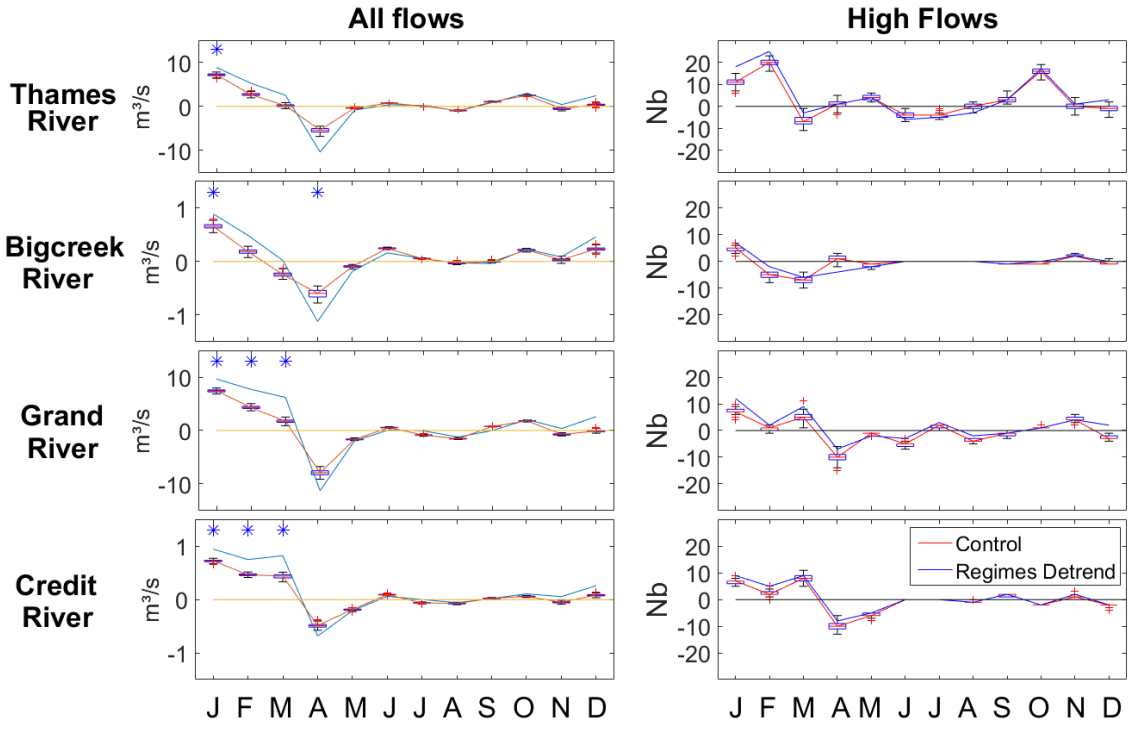

Figure 2-10 Monthly decadal trends of mean streamflow (left column) and the number of high flows (right column) between 1957 and 2013 for the control (CTL, blue line) and the experimental (EXP, red line) datasets. The blue stars indicate a trend significant at 95% confidence level.

To examine processes driving the shift of streamflow, Figure 2-11 shows the change of rain and snowmelt values between two equal periods 1957 to 1984 and 1985 to 2012 for both CTL and EXP simulations. The CTL simulation (Figure 2-11, red and purple or purple without blue) showed rain and snowmelt increased for all four watersheds in January. The increase of snowmelt was also observed in February with the exception of the Big Creek River watershed. In March, only Credit River showed an increase of snowmelt. In April, a large decrease of snowmelt was simulated in all four watersheds with the Big Creek watershed demonstrating the smallest decrease. Changes due to rain remain low between February and April. In the EXP simulation (purple and blue or purple without red), weather regimes contributed to both rain and snowmelt. The weather regimes contributed to increase snowmelt and rain during January. In February and March, weather regimes contributed to increase or attenuate the decrease of snowmelt and rain. In April, weather regimes contributed to decrease the snowmelt, but at the same time, attenuate the decrease of rain.

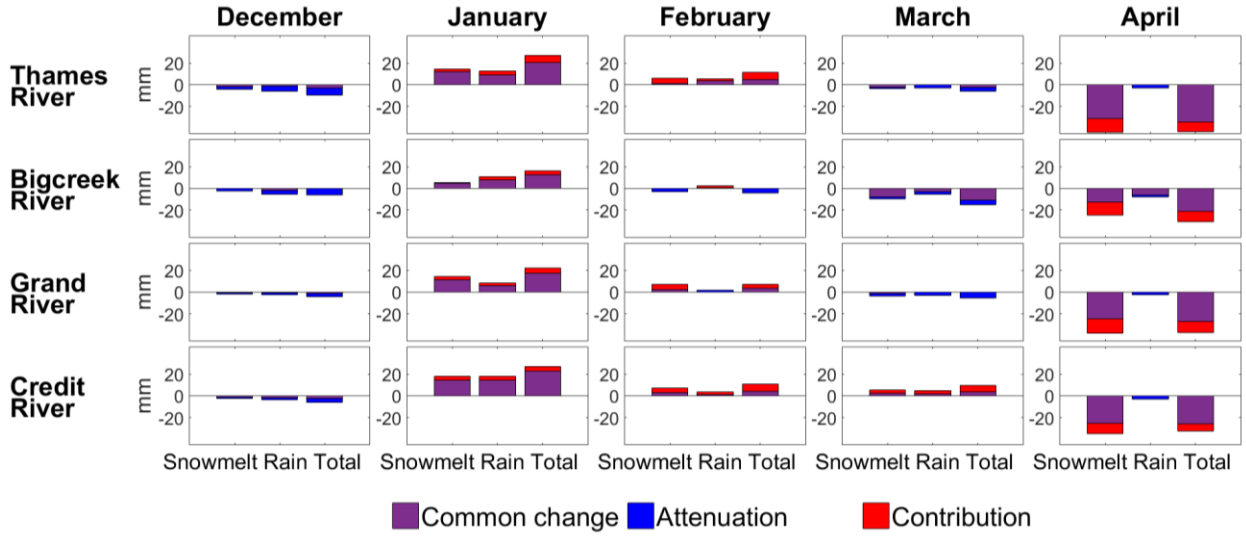

Figure 2-11 Contribution or attenuation of weather regimes to the change of monthly snowmelt and rain between 1957-1984 and 1985-2013 for the months of December through April.

2.5 Discussion

2.5.1 Temperature and precipitation drivers on seasonal and spatial variability of streamflow

The results of this study suggest an increase of streamflow between December and March and decline in April. This shift was also observed by previous studies and was attributed to reduction of snow as a fraction of total precipitation and a reduction of spring snowpack; both caused by recent warming (Burn et al., 2010; Burn and Whitfield, 2016; Cunderlik and Ouarda, 2009). Monthly streamflow analyses in these four watersheds in southern Ontario showed that processes differ among months and among watersheds. Significant streamflow increases during January in all watersheds (Figure 2-10) may have occurred because both temperature and precipitation have increased to enhance the snowmelt and rain (Figure 2-7 and 2-8). The temperature was also increasing in February and March (Figure 2-7), but snowmelt increases were diminished (Figure 2-11) probably because of thinner snowpack available. A seasonal approach was often used by previous studies to describe the past change of precipitation and temperature which oversimplify the results. Change of temperature and precipitation will not have a similar impact of streamflow for all the months of the same season. For example, considering the spring (March to Mai), snow is still an important component of the streamflow in March while it completely disappeared in May. Previous studies that analyzed monthly projections of streamflow in southern Ontario showed a shift to early winter clearly due to a shift in snowmelt but also due to increase in precipitation in January (Grillakis et al., 2011; Rahman et al., 2012; Sultana and Coulibaly, 2011).

Variability in streamflow change between watersheds is likely due to differences in latitude, elevation, or proximity of the Great Lakes. In lower latitude, lower elevation, and lakeshore

watersheds such as Big Creek, the snowpack was thinner and the increase of temperature in winter depletes completely the snowpack as soon as January, causing a lack of melting later in the winter season (Figure 2-11). Snowmelt contribution to streamflow started to decrease later in the other watersheds; in March for Thames and Grand River and in April for the Credit River; probably because the conditions are colder and the increase of temperature were not sufficient to deplete completely the snowpack or to significantly reduce snowfall amounts. Therefore, streamflow increase is enhanced by snowmelt earlier in Big creek watershed and later in Credit river. In April, the streamflow decreases in all four watersheds (Figure 2-10) is likely due to reduced snowpack availability for snowmelt in recent decades. Previous studies projecting the near future evolution of streamflow in southern Ontario suggests a similar spatial variability. In the Canard watershed situated near lake Erie, streamflow is projected to increase in January but decrease in February and March (Rahman et al., 2012). Further North, the shift is expected to occur later between February and March near lake Ontario (Grillakis et al., 2011; Sultana and Coulibaly, 2011) or lake Simcoe (Kuo et al., 2017; Oni et al., 2014).

2.5.2 Atmospheric circulation drivers on hydrological processes

The shift in streamflow can be attributed to global warming as changes in streamflow were driven by changes in snowmelt volume (Figure 2-11) and warming between December and March (Figure 2-7). However the shift in atmospheric circulation contributed for a part to the warming (Figure 2-7) and to the increase in snowmelt and rain early in the winter (Figure 2-11). The part of the warming due to atmospheric circulation between December and April can be associated to the increase of frequency of regime HP (Figure 2-4) which is associated with warmer and wetter conditions than average over the region (Figure 2-6). The regime HP was characterized by high

geopotential anomalies in the east side of North-east North America (Figure 2-3). These conditions were classically associated to a northern shift of the Rossby wave in Northeastern North America and a southern shift of the waves in western North America (Ahrens, 1994). This distortion of the Rossby waves coincided with the development of extratropical cyclones (Ahrens, 1994). These cyclones were associated with frontal systems bringing significant amount of rain in their east side where the air masses were warm and charged with humidity. The regime South was also characterized by a poleward shift of the Rossby waves but the waves were shifted to the east (Figure 2-3). In this situation the region would have been closer to the center of the depressions making the warm periods shorter than for a regime HP. The regime North, characterized by negative geopotential anomalies centered on the Saint Lawrence estuary (Figure 2-3) was also increasing in January and February (Figure 2-4) and was associated with cold and dry conditions on great lakes (Figure 2-6). The increase of frequency of this regime probably offset a part of the warming due to the regime HP in January and February. This was why the largest warming from atmospheric circulation occurred in March (Figure 2-7) when the regime HP was the only regime increasing significantly (Figure 2-4).

Previous studies have presented correlations of local climate and hydrological processes to the large-scale atmospheric indices in the Great Lakes region and found conclusive links with NAO and PNA. NAO^- is known for being associated with the southward migration of the polar front in eastern North America and therefore negative Z500 anomalies over southern Ontario and the east coast (Zhao et al., 2013). This situation corresponds well to the regime LP or the regime North-East (Figure 2-3) which were correlated to NAO^- (Figure 2-5). Regimes HP and North, on the

contrary, were characterized by high pressure anomalies in southern Canada and low anomalies close to the Arctic (Figure 2-3), conditions typically associated with NAO^+ in winter (Ning and Bradley, 2015a). Evidence of warmer temperature corresponding to winter NAO^+ had been found in a large region surrounding the Great Lakes (Ning and Bradley, 2015a). NAO^+ occurrences have been shown to reduce the maximum snowpack (Zhao et al. 2013) and increase the winter streamflow (Bradbury et al., 2002). NAO^+ has occurred more frequently since the end of the 1980s (Ning and Bradley, 2015a; Vincent et al., 2015), but a low contribution of NAO^+ was found to the recent warming (Vincent et al., 2015). In our study, that focused on southern Ontario, higher geopotential anomalies around the Great Lakes in winter which are characteristic of NAO^+, were able to explain 25 to 30% of the observed warming in winter (Figure 2-7) and 40% of the increase of streamflow between December and March (Figure 2-10).

The PNA index has also been shown to impact local conditions with PNA^- correlated to more precipitation extremes and peak flows (Mallakpour and Villarini, 2016; Thiombiano et al., 2017). Mallakpour & Villarini (2016) found that winter PNA^- is associated with positive Z500 anomalies in the east coast of United States while negative anomalies occur in the west, bringing high moisture transport, heavy precipitation and flooding events in the Ohio Valley region . The Z500 anomalies that correspond to the regime South (Figure 2-3) are similar to the situation associated with PNA^- defined by Mallakpour and Villarini (2016). Long-term trends in the PNA index shows a positive trend between 1950 and 2000 which could explain the negative trend in the occurrence of the regime South in winter (Figure 2-4). Regime LP also follows a negative trend correlated to PNA^-, however this relationship is complicated as this regime is also correlated to NAO^+ (Figure

2-5). The long-term trends of regimes South or LP were not significant (Figure 2-4) so their role in the evolution of climate variables and streamflow may be limited. These results emphasize the advantage of weather regimes analyses over large-scale mode of variability to study the impact of atmospheric circulation on streamflow. The weather regimes showed more directly the different variable sources of temperature and precipitation by composing the different modes of variability in a single series of recurrent weather patterns.

During the warm season, changes in weather regimes had a less clear impact on streamflow. This may be due to the dominance of precipitation variability as a driver of streamflow while temperature played a larger role in winter by changing the snow ratio and the snowmelt period. Summer precipitation are also largely derived from local convective systems and not from large frontal systems associated with the changes in atmospheric circulation.

2.5.3 Calibration method

In this study, a trial and error approach has been used to calibrate PRMS. This manual calibration approach directs the parameters search toward local improvements and may be unable to find a global optimal solution (Sorooshian, 2008). The main drawback in these local improvements approaches is that Satisfactory results in term of streamflow does not mean that all hydrological processes are well simulated (Mendoza et al., 2016). Despite this shortcoming, the simulation shows satisfactory results in term of streamflow (Figure 2-9 and Table 2-2) and snow processes (Section S2). Moreover, the purpose of this study was not to investigate the different hydrological processes but to focus on the contribution of atmospheric circulation to the trend of streamflow. For future works focusing on the different components of the water balance or on PRMS coupled

with the MODFLOW groundwater model, a global search algorithm should be used. The Shuffle complex evolution (SCE-UE), a global search calibration method previously used for PRMS (Markstrom et al., 2015) could be considered.

2.5.4 Non stationarity of weather data and land use

For the purpose of this study, the PRMS model was used at a daily time step. Therefore, the change in intensity of precipitation at a higher timescale (i.e. hourly) was not taken into consideration. A study to characterize extreme precipitation in southern Ontario have shown an increase of precipitation intensity between 1960 and 2012 at a sub-daily timescale (Soulis et al., 2016). The increase of sub-daily intensity of precipitation may have an impact on streamflow through the enhancement of surface runoff. A higher hourly intensity of precipitation supports an increase in streamflow due to a reduction of the infiltration rate. This is particularly true for summer streamflow affected by convective storms. In winter, precipitation is primarily derived from extratropical cyclonic systems which has a large temporal and spatial extension, and therefore captured by the daily time-step. The aim of our study was to assess the impact of atmospheric circulation on the shift of streamflow during winter and spring. The hourly time-step would therefore have not significantly improved the results of this study, but could be considered in future studies focusing on summer streamflow.

The evolution of land use was not taken into consideration in PRMS. Geospatial data showed that forest and urban land cover have been increasing during the 20th century (Lake Erie Source Protection Region Technical Team, 2008). Shifts in land use may have implication on the streamflow through a change in evapotranspiration. Land use in the watersheds is dominated by

agriculture and evapotranspiration values varied considerably depending on crop types, stage of the crops and irrigation practices (Irmak, 2017). The shape and size of the plants modulate interception/evaporation and plants have different water needs for the photosynthesis process (Irmak, 2017). Agricultural techniques and especially in their drainage systems would have also impacted streamflow (King et al., 2014) even though it appeared low in southern Ontario (Spaling, 1995). The advantage of not taking into consideration land use change in our study was that the relative change of streamflow due to atmospheric circulation or global warming were better assessed and not affected by an eventual change in land use.

2.6 Conclusion

This study investigated the role played by atmospheric circulation on the shift of observed streamflow in southern Ontario from 1957 to 2013. Five recurrent and robust weather regimes were computed for northeastern North America. The trend of occurrence of weather regimes was removed to create experimental climate dataset used as input in the Precipitation Runoff modelling system (PRMS) hydrological model.

The results showed that 40% of the increase of streamflow between December and March and 45% decrease of streamflow in April was due to more frequent Z500 positive anomalies in the Great Lakes region associated with the northern shift of the polar vortex. This shift in atmospheric circulation was also contributing to increase the number of high flows by 25 to 50% in early winter and especially in January.

This study will help to highlight the significance of atmospheric circulation for local hydrologic conditions and streamflow in a highly populated region of southern Ontario. It also encourages

future studies to consider the internal variability of climate in streamflow projections. Climate data from multi-members ensemble may be used as input in hydrological models to assess the hydrological processes projections uncertainties due to internal variability of climate. This will help planers to improve the management of the watersheds and evaluate the risks associated with floods.

2.7 Acknowledgement

Financial support for this study was provided by the Natural Sciences and Engineering Research Council (NSERC) of Canada through the FloodNet Project. We also acknowledge support and contributions from Global Water Future Program, Environment and Climate Change Canada, Natural Resources Canada and Long Point Region Conservation Authority. The anonymous reviewers are also acknowledged for their comments that helped to improve this manuscript.

2.8 References

Adamowski, J., Adamowski, K., Prokoph, A., 2013. Quantifying the spatial temporal variability of annual streamflow and meteorological changes in eastern Ontario and southwestern Quebec using wavelet analysis and GIS. Journal of Hydrology 499, 27–40. https://doi.org/10.1016/j.jhydrol.2013.06.029

Ahrens, C.D., 1994. Meteorology today: an introduction to weather, climate, and the environment, 5th ed. ed. West Pub, Minneapolis/St. Paul.

Barnett, T.P., Adam, J.C., Lettenmaier, D.P., 2005. Potential impacts of a warming climate on water availability in snow-dominated regions. Nature 438, 303–309. https://doi.org/10.1038/nature04141

Barnston, A.G., Livezey, R.E., 1987. Classification, Seasonality and Persistence of Low-Frequency Atmospheric Circulation Patterns. Monthly Weather Review 115, 1083–1126. https://doi.org/10.1175/1520-0493(1987)115<1083:CSAPOL>2.0.CO;2

Beauchamp, M., Assani, A.A., Landry, R., Massicotte, P., 2015. Temporal variability of the magnitude and timing of winter maximum daily flows in southern Quebec (Canada). Journal of Hydrology 529, 410–417. https://doi.org/10.1016/j.jhydrol.2015.07.053

Bliss, A., Hock, R., Radić, V., 2014. Global response of glacier runoff to twenty-first century climate change. Journal of Geophysical Research: Earth Surface 119, 717–730. https://doi.org/10.1002/2013JF002931

Bradbury, J.A., Dingman, S.L., Keim, B.D., 2002. New England drought and relations with large scale atmospheric circulation patterns. Journal of the American Water Resources Association 38, 1287–1299. https://doi.org/10.1111/j.1752-1688.2002.tb04348.x

Burn, D.H., Sharif, M., Zhang, K., 2010. Detection of trends in hydrological extremes for Canadian watersheds. Hydrological Processes 24, 1781–1790. https://doi.org/10.1002/hyp.7625

Burn, D.H., Whitfield, P.H., 2016. Changes in floods and flood regimes in Canada. Canadian Water Resources Journal / Revue canadienne des ressources hydriques 41, 139–150. https://doi.org/10.1080/07011784.2015.1026844

Buttle, J.M., Allen, D.M., Caissie, D., Davison, B., Hayashi, M., Peters, D.L., Pomeroy, J.W., Simonovic, S., St-Hilaire, A., Whitfield, P.H., 2016. Flood processes in Canada: Regional and special aspects. Canadian Water Resources Journal / Revue canadienne des ressources hydriques 1–24. https://doi.org/10.1080/07011784.2015.1131629

Cassou, C., Terray, L., Phillips, A.S., 2005. Tropical Atlantic influence on European heat waves. Journal of climate 18, 2805–2811. https://doi.org/10.1175/JCLI3506.1

Chen, Y., Todd, A.S., Murphy, M.H., Lomnicky, G., 2016. Anticipated Water Quality Changes in Response to Climate Change and Potential Consequences for Inland Fishes. Fisheries 41, 413–416. https://doi.org/10.1080/03632415.2016.1182509

Collins, M.J., Kirk, J.P., Pettit, J., DeGaetano, A.T., McCown, M.S., Peterson, T.C., Means, T.N., Zhang, X., 2014. Annual floods in New England (USA) and Atlantic Canada: synoptic climatology and generating mechanisms. Physical Geography 35, 195–219. https://doi.org/10.1080/02723646.2014.888510

Compo, G.P., Whitaker, J.S., Sardeshmukh, P.D., Matsui, N., Allan, R.J., Yin, X., Gleason, B.E., Vose, R.S., Rutledge, G., Bessemoulin, P., others, 2011. The twentieth century reanalysis project. Quarterly Journal of the Royal Meteorological Society 137, 1–28. https://doi.org/10.1002/qj.776

Coulibaly, P., Burn, D.H., 2005. Spatial and temporal variability of Canadian seasonal streamflows. Journal of Climate 18, 191–210.

Cunderlik, J.M., Ouarda, T.B.M.J., 2009. Trends in the timing and magnitude of floods in Canada. Journal of Hydrology 375, 471–480. https://doi.org/10.1016/j.jhydrol.2009.06.050

Djebbar, R., Morris, R., Thevenard, D., Perez, R., Schlemmer, J., 2012. Assessment of SUNY Version 3 Global Horizontal and Direct Normal Solar Irradiance in Canada. Energy Procedia 30, 1274–1283. https://doi.org/10.1016/j.egypro.2012.11.140

Dressler, K.A., Leavesley, G.H., Bales, R.C., Fassnacht, S.R., 2006. Evaluation of gridded snow water equivalent and satellite snow cover products for mountain basins in a hydrologic model. Hydrological Processes 20, 673–688. https://doi.org/10.1002/hyp.6130

Fernández-Montes, S., Rodrigo, F.S., Seubert, S., Sousa, P.M., 2013. Spring and summer extreme temperatures in Iberia during last century in relation to circulation types. Atmospheric Research 127, 154–177. https://doi.org/10.1016/j.atmosres.2012.07.013

Fleig, A.K., Tallaksen, L.M., James, P., Hisdal, H., Stahl, K., 2015. Attribution of European precipitation and temperature trends to changes in synoptic circulation. Hydrology and Earth System Sciences 19, 3093–3107. https://doi.org/10.5194/hess-19-3093-2015

Gardner, M.A., Morton, C.G., Huntington, J.L., Niswonger, R.G., Henson, W.R., 2018. Input data processing tools for the integrated hydrologic model GSFLOW. Environmental Modelling & Software 109, 41–53. https://doi.org/10.1016/j.envsoft.2018.07.020

Grillakis, M.G., Koutroulis, A.G., Tsanis, I.K., 2011. Climate change impact on the hydrology of Spencer Creek watershed in Southern Ontario, Canada. Journal of Hydrology 409, 1–19. https://doi.org/10.1016/j.jhydrol.2011.06.018

Hamlet, A.F., Lettenmaier, D.P., 2007. Effects of 20th century warming and climate variability on flood risk in the western U.S. Water Resources Research 43. https://doi.org/10.1029/2006WR005099

Irmak, S., 2017. Evapotranspiration Basics and Estimating Actual Crop Evapotranspiration from Reference Evapotranspiration and Crop--Specific Coefficients 9.

Jones, P.D., 1994. Synoptic climatology in environmental analysis: A primer, Brent Yarnal, Belhaven Press (London), 1993. No. of pages: xv + 195. Price: £37.50. ISBN 185293 1175. International Journal of Climatology 14, 115–115. https://doi.org/10.1002/joc.3370140116

King, K.W., Fausey, N.R., Williams, M.R., 2014. Effect of subsurface drainage on streamflow in an agricultural headwater watershed. Journal of Hydrology 519, 438–445. https://doi.org/10.1016/j.jhydrol.2014.07.035

Kuo, C.C., Gan, T.Y., Higuchi, K., 2017. Evaluation of Future Streamflow Patterns in Lake Simcoe Subbasins Based on Ensembles of Statistical Downscaling. Journal of Hydrologic Engineering 22, 04017028. https://doi.org/10.1061/(ASCE)HE.1943-5584.0001548

Lake Erie Source Protection Region Technical Team, 2008. Long Point Region Watershed Characerisation Report.

Leathers, D.J., Ellis, A.W., 1996. SYNOPTIC MECHANISMS ASSOCIATED WITH SNOWFALL INCREASES TO THE LEE OF LAKES ERIE AND ONTARIO. International Journal of Climatology 16, 1117–1135. https://doi.org/10.1002/(SICI)1097-0088(199610)16:10<1117::AID-JOC80>3.0.CO;2-4

Liao, C., Zhuang, Q., 2017. Quantifying the Role of Snowmelt in Stream Discharge in an Alaskan Watershed: An Analysis Using a Spatially Distributed Surface Hydrology Model: ROLE OF SNOWMELT IN STREAMFLOW IN ALASKA. Journal of Geophysical Research: Earth Surface 122, 2183–2195. https://doi.org/10.1002/2017JF004214

Mallakpour, I., Villarini, G., 2016. Investigating the relationship between the frequency of flooding over the central United States and large-scale climate. Advances in Water Resources 92, 159–171. https://doi.org/10.1016/j.advwatres.2016.04.008

Markstrom, S.L., Regan, R.S., Hay, L.E., Viger, R.J., Payn, R.A., LaFontaine, J.H., 2015. precipitation-runoff modeling system, version 4: U.S. Geological Survey Techniques and Methods (No. Book 6, chapter B7).

Mastin, M.C., Chase, K.J., Dudley, R.W., 2011. Changes in Spring Snowpack for Selected Basins in the United States for Different Climate-Change Scenarios. Earth Interactions 15, 1–18. https://doi.org/10.1175/2010EI368.1

McKenney, D.W., Hutchinson, M.F., Papadopol, P., Lawrence, K., Pedlar, J., Campbell, K., Milewska, E., Hopkinson, R.F., Price, D., Owen, T., 2011. Customized Spatial Climate Models for North America. Bulletin of the American Meteorological Society 92, 1611–1622. https://doi.org/10.1175/2011BAMS3132.1

Mendoza, P.A., Clark, M.P., Mizukami, N., Gutmann, E.D., Arnold, J.R., Brekke, L.D., Rajagopalan, B., 2016. How do hydrologic modeling decisions affect the portrayal of climate change impacts?: Subjective Hydrologic Modelling Decisions in Climate Change Impacts. Hydrological Processes 30, 1071–1095. https://doi.org/10.1002/hyp.10684

Michelangeli, P.-A., Vautard, R., Legras, B., 1995. Weather Regimes: Recurrence and Quasi Stationarity. Journal of the Atmospheric Sciences 52, 1237–1256. https://doi.org/10.1175/1520-0469(1995)052<1237:WRRAQS>2.0.CO;2

Moriasi, D.N., Arnold, J.G., Van Liew, M.W., Bingner, R.L., Harmel, R.D., Veith, T.L., 2007. Model evaluation guidelines for systematic quantification of accuracy in watershed simulations. Transactions of the ASABE 50, 885–900.

Nalley, D., Adamowski, J., Khalil, B., Biswas, A., 2016. Inter-annual to inter-decadal streamflow variability in Quebec and Ontario in relation to dominant large-scale climate indices. Journal of Hydrology 536, 426–446. https://doi.org/10.1016/j.jhydrol.2016.02.049

Nilsen, I.B., Stagge, J.H., Tallaksen, L.M., 2017. A probabilistic approach for attributing temperature changes to synoptic type frequency: Probabilistic approach to attribute temperature changes. International Journal of Climatology 37, 2990–3002. https://doi.org/10.1002/joc.4894

Ning, L., Bradley, R.S., 2015. Winter climate extremes over the northeastern United States and southeastern Canada and teleconnections with large-scale modes of climate variability*. Journal of Climate 28, 2475–2493.

Oni, S.K., Futter, M.N., Molot, L.A., Dillon, P.J., Crossman, J., 2014. Uncertainty assessments and hydrological implications of climate change in two adjacent agricultural catchments of a rapidly urbanizing watershed. Science of The Total Environment 473–474, 326–337. https://doi.org/10.1016/j.scitotenv.2013.12.032

Pfahl, S., 2014. Characterising the relationship between weather extremes in Europe and synoptic circulation features. Natural Hazards and Earth System Science 14, 1461–1475. https://doi.org/10.5194/nhess-14-1461-2014

Pim, L.R., Ornoy, J., Federation of Ontario Naturalists, 2005. A smart future for Ontario: how to create greenways and curb urban sprawl in your community. Federation of Ontario Naturalists, Toronto.

Rahman, M., Bolisetti, T., Balachandar, R., 2012. Hydrologic modelling to assess the climate change impacts in a Southern Ontario watershed. Canadian Journal of Civil Engineering 39, 91–103. https://doi.org/10.1139/l11-112

Rohli, R.V., Vega, A.J., Binkley, M.R., Britton, S.D., Heckman, H.E., Jenkins, J.M., Ono, Y., Sheeler, D.E., 2001. Synoptic circulation and stream discharge in the Great Lakes basin, USA. Applied Geography 21, 369–385. https://doi.org/10.1016/S0143-6228(01)00011-X

Santos, M., Santos, J.A., Fragoso, M., 2015. Historical damaging flood records for 1871–2011 in Northern Portugal and underlying atmospheric forcings. Journal of Hydrology 530, 591–603. https://doi.org/10.1016/j.jhydrol.2015.10.011

Sorooshian, S. (Ed.), 2008. Hydrological modelling and the water cycle: coupling the atmospheric and hydrological models, Water science and technology library. Springer, Berlin ; London.

Soulis, E.D., Sarhadi, A., Tinel, M., Suthar, M., 2016. Extreme precipitation time trends in Ontario, 1960-2010: Hydrological Processes. Hydrological Processes 30, 4090–4100. https://doi.org/10.1002/hyp.10969

Spaling, H., 1995. Analyzing cumulative environmental effects of agricultural land drainage in southern Ontario, Canada. Agriculture, Ecosystems and Environment 53, 279–292.

Sultana, Z., Coulibaly, P., 2011. Distributed modelling of future changes in hydrological processes of Spencer Creek watershed. Hydrological Processes 25, 1254–1270. https://doi.org/10.1002/hyp.7891

Surfleet, C.G., Tullos, D., Chang, H., Jung, I.-W., 2012. Selection of hydrologic modeling approaches for climate change assessment: A comparison of model scale and structures. Journal of Hydrology 464–465, 233–248. https://doi.org/10.1016/j.jhydrol.2012.07.012

Tan, X., Gan, T.Y., 2015. Nonstationary Analysis of Annual Maximum Streamflow of Canada. Journal of Climate 28, 1788–1805. https://doi.org/10.1175/JCLI-D-14-00538.1

Teng, F., Huang, W., Cai, Y., Zheng, C., Zou, S., 2017. Application of Hydrological Model PRMS to Simulate Daily Rainfall Runoff in Zamask-Yingluoxia Subbasin of the Heihe River Basin. Water 9, 769. https://doi.org/10.3390/w9100769

Teng, F., Huang, W., Ginis, I., 2018. Hydrological modeling of storm runoff and snowmelt in Taunton River Basin by applications of HEC-HMS and PRMS models. Natural Hazards 91, 179–199. https://doi.org/10.1007/s11069-017-3121-y

Thiombiano, A.N., El Adlouni, S., St-Hilaire, A., Ouarda, T.B.M.J., El-Jabi, N., 2017. Nonstationary frequency analysis of extreme daily precipitation amounts in Southeastern Canada using a peaks-over-threshold approach. Theoretical and Applied Climatology 129, 413–426. https://doi.org/10.1007/s00704-016-1789-7

Thornthwaite, C.W., 1948. An Approach toward a Rational Classification of Climate. Geographical Review 38, 55. https://doi.org/10.2307/210739

Ullmann, A., Fontaine, B., Roucou, P., 2014. Euro-Atlantic weather regimes and Mediterranean rainfall patterns: present-day variability and expected changes under CMIP5 projections: EURO-ATLANTIC WEATHER REGIMES AND MEDITERRANEAN RAINFALL PATTERNS. International Journal of Climatology 34, 2634–2650. https://doi.org/10.1002/joc.3864

Vincent, L.A., Zhang, X., Brown, R.D., Feng, Y., Mekis, E., Milewska, E.J., Wan, H., Wang, X.L., 2015. Observed Trends in Canada's Climate and Influence of Low-Frequency Variability Modes. Journal of Climate 28, 4545–4560. https://doi.org/10.1175/JCLI-D-14-00697.1

Wu, W.-Y., Lan, C.-W., Lo, M.-H., Reager, J.T., Famiglietti, J.S., 2015. Increases in the annual range of soil water storage at northern middle and high latitudes under global warming: SOIL WATER CHANGES UNDER GLOBAL WARMING. Geophysical Research Letters 42, 3903–3910. https://doi.org/10.1002/2015GL064110

Yarnal, B., Frakes, B., 1997. Using synoptic climatology to define representative discharge events. International Journal of Climatology 17, 323–341.

Zhang, X., Wang, J., Zwiers, F.W., Groisman, P.Y., 2010. The Influence of Large-Scale Climate Variability on Winter Maximum Daily Precipitation over North America. Journal of Climate 23, 2902–2915. https://doi.org/10.1175/2010JCLI3249.1

Zhao, H., Higuchi, K., Waller, J., Auld, H., Mote, T., 2013. The impacts of the PNA and NAO on annual maximum snowpack over southern Canada during 1979-2009. International Journal of Climatology 33, 388–395. https://doi.org/10.1002/joc.3431

2.9 Supplementary materials

2.9.1 Modules and parameters used in PRMS

PRMS allows the user to choose among different modules in each step of the computation. In our study the distribution of precipitations and temperatures across the watershed was computed with the precip_1sta and temp_1sta modules. In these modules, each HRU is assigned to the closest meteorological station or grid point. Temperature and precipitation were adjusted in each HRU according to the elevation and monthly lapse rates calculated for each watershed. The potential evapotranspiration was computed according to the Jensen Haise formulation using air temperature, solar radiation and elevation of each HRU. The shortwave solar radiation was estimated using a degree day method. The Snow module separates precipitation in rain or snow according to the threshold Tmax_allrain that has to be calibrated. The Snowpack is considered as a two-layers system and the melting process follows an energy balance approach computed over day and night (12 hours intervals). A comprehensive explanation of the snow module can be found in Leavesley et al., (1983). The surface runoff was estimated from infiltration and saturation excesses water in soil column. Routing of flow from upstream to downstream was computing using the Muskingum flow routing method. The different parameters used by these modules are referenced in Table 2-3.

The reader is referred to Markstrom et al., (2015) for more details on the different modules available in PRMS.

Table 2-3 Parameter values after calibration for all for watersheds (C= Calibrated, GIS= estimated by arcpy_GSFLOW)

Parameter	Unit	Thames River	Big Creek River	Grand River	Credit River	Spatial and temporal	Source
dday_intcp	Degrees days	-26 – -11	-27 – -10	-26 – -9	-26 – -9	monthly	C
dday_slope	Degrees days / °F	0.38 – 0.42	0.38 – 0.41	0.38 – 0.42	0.38 – 0.42	monthly	C
tmax_index	°F	29.3 – 80	29.3 – 80	31.2 – 78	26.5 – 78.3	monthly	C
jh_coef	per °F	0.005 – 0.021	0.005 – 0.021	0.005 – 0.02	0.003 – 0.02	monthly	C
Jh_coef_hru	per °F	20.75 – 21.35	21.97 – 22.91	20.4 – 21.4	20.4 – 21.5	HRU	GIS
Adjmix_rain	Decimal fraction	1	0	0	0	One	C
Cecn_coef	Calories per °C > 0	10	20	15	0	One	C
emis_noppt	Decimal fraction	0.757	0.757	0.757	0.757	One	C
Fastcoef_lin	Fraction / day	0.1	0.001	0.2	0.2	One	C
Fastcoef_sq	none	0.4	0.005	0.1	0.5	One	C
Freeh2o_cap	inches	0.01	0.07	0.01	0.01	One	C
Gwflow_coef	Fraction / day	0.06	0.01	0.05	0.03	One	C
Potet_sublim	Decimal fraction	0.1	0.1	0.75	0.6	One	C
Smidx_coef	Decimal fraction	0.04	0.0001	0.05	0.001	One	C
Smidx_exp	1 / inch	0.2	0.2	0.2	0.3	One	C
Soil_rechr_max	inches	0.2 – 1.9	0.24 – 1.81	0.24 – 1.84	0.71– 5.5	HRU	GIS+C
Soil_moist_max	inches	0.8 – 6.3	1.2 – 9.1	0.79 – 6.12	0.79 – 6.1	HRU	GIS
Tmax_allrain	°F	33	34	35	36	One	C
hru_percent_imperv	Decimal fraction	0.1 – 0.6	0.1 – 0.6	0.1 – 0.6	0.1 – 0.6	HRU	GIS
Carea_max	Decimal fraction	0.4 – 0.9	0.4 – 0.9	0.4 – 0.9	0.4 – 0.9	HRU	GIS
Ssr2gw_exp	none	1.5	3	1	3	One	C

Ssr2gw_rate	Fraction / day	0.01 – 0.26	0.30 – 0.95	0.02 – 0.66	0.02 – 0.47	HRU	GIS+C
Slowcoef_sq	none	0.002 – 1.97	0.0004 – 7.6	0 – 133	0 – 11.9	HRU	GIS+C
Slowcoef_lin	Fraction / day	0.004 –0.71	0.02 – 12.3	0 – 0.07	0 – 0.33	HRU	GIS+C
K_coef	hours	1.78 – 3.56	2.8 – 8.4	1.6 – 3.2	1.35 – 2.68	Segments	GIS+C
Pref_flow_den	Decimal Fraction	0.1	0.1	0.1	0.2	One	C
Rain_adj	Decimal Fraction	0.92 – 1.04	0.77 – 0.86	0.69 – 1.12	0.87 – 0.94	HRU Monthly	GIS
Snow_adj	Decimal Fraction	0.92 – 1.04	0.96 – 1.06	0.69 – 1.12	0.72 – 0.76	HRU Monthly	GIS

2.9.2 Ability of PRMS to simulate snow processes

The ability of PRMS model to simulate snow processes has been evaluated in this section. Observed snow depth has been measured in a 80 years old pine forest area at Turkey-Point in the vicinity of Big Creek watershed, (Peichl et al., 2010). Observed Snow Water Equivalent has been measured biweekly by the Long Point Region conservation authority (LPRCA) at Little-Lake, situated in the Big Creek watershed. The daily simulation of snowpack from all forested HRU's have been averaged and compared to the observation at Turkey point (Figure 2-12). The ability of PRMS to simulate snowpack in forested area is satisfactory. The simulation of Snow Water Equivalent has been taken from the HRU situated at Little lake's measurement. The comparison between observations and simulations are generally satisfactory as well (Figure 2-13).

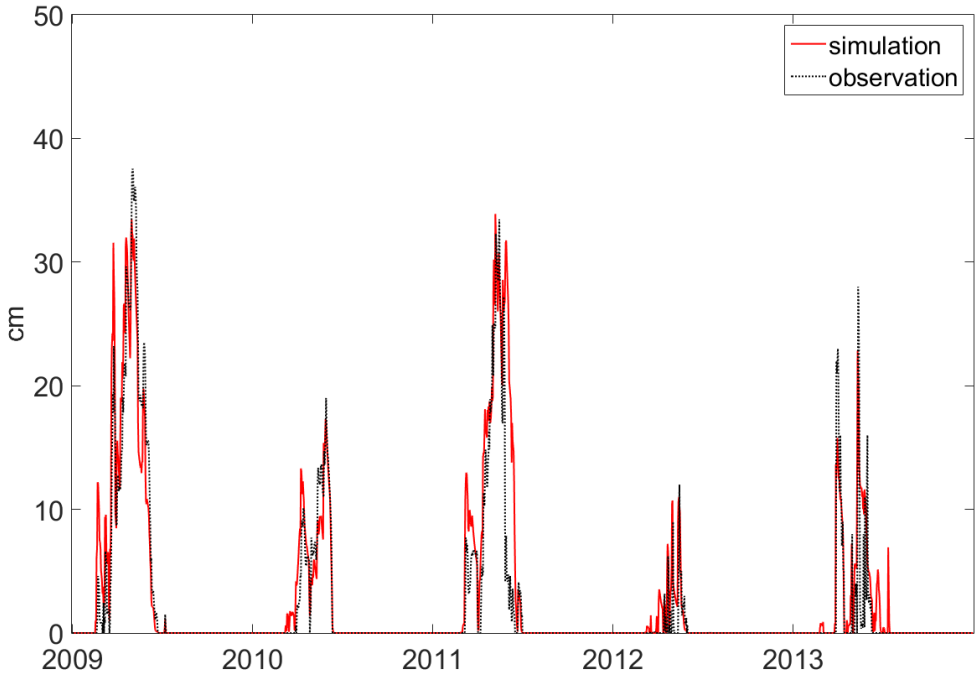

Figure 2-12 Comparison between daily observed and simulated Snow Depth in Big Creek watershed.

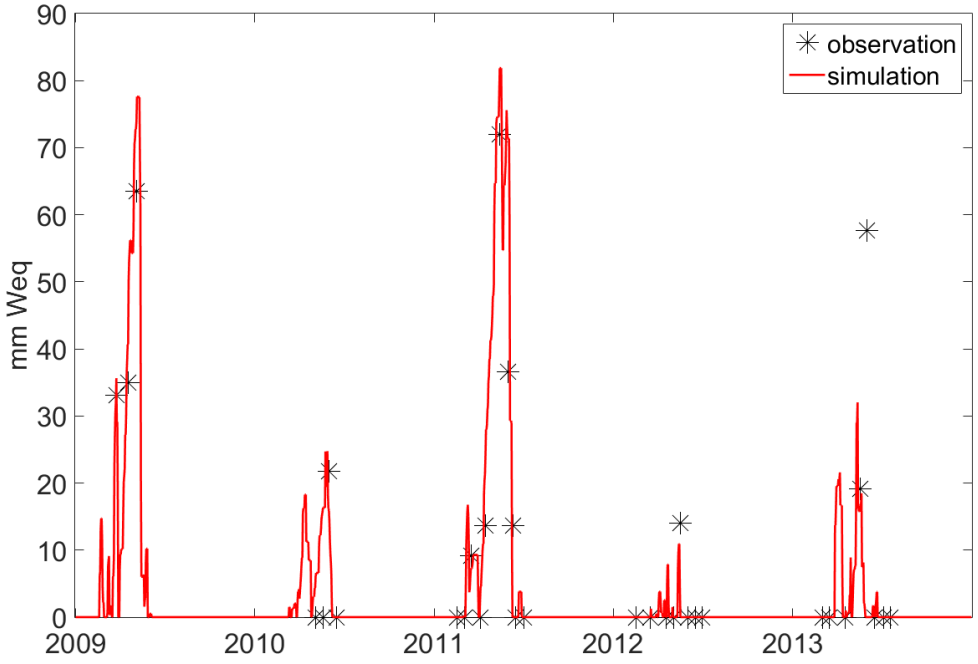

Figure 2-13 Comparison between bi-weekly observed and daily simulated Snow Water Equivalent in Big Creek watershed.

2.9.3 Number of weather regimes

The number of weather regimes was determined by a red-noise test. This test consists in the comparison of the maps from the 100 k-means partitions calculated with the observed atmosphere maps and with a numerically generated atmosphere that has the same statistical properties (e.g. serial correlation) as the observations to be classified. 5 regimes appear to be the most robust choice (Figure 2-14).

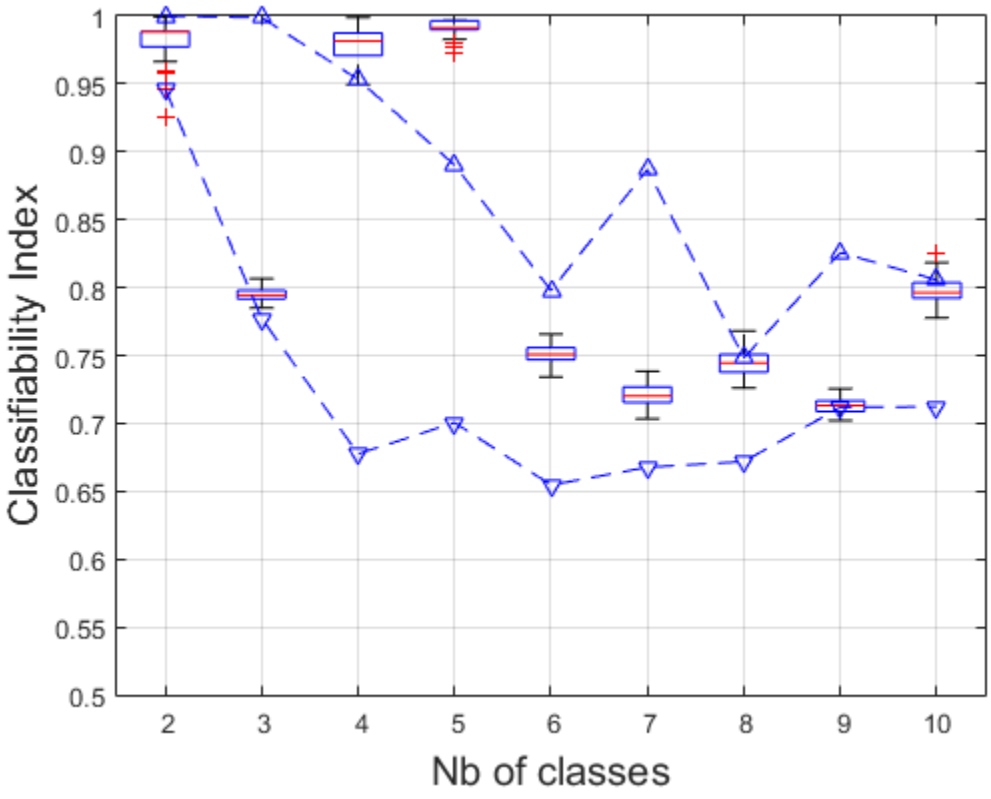

Figure 2-14 Classifiability index of 20thCR Z_{500} fields, period 1957–2012, represented as a function of the number of classes *k*. Dashed lines with up (down) triangles represent the 5% (95%) confidence levels according to the red-noise test. Box-and-whisker diagrams show the classifiability index of Z_{500} data for the 100 *k*-means partitions. Boxes extend from the 25th to the 75th percentile, with a horizontal red bar showing the median value. The whiskers are lines extending from each end of the box to the 1.5 interquartile range. Plus signs correspond to outliers.

2.9.4 Hypothetical dataset construction

A new algorithm was created in our study to remove the impact of regional atmospheric circulation trends on precipitations and temperature trends. For each month of each year, our algorithm selected first which regime has the highest number of occurrences to add to the sequence in order to remove the overall trend. The algorithm then looked at all the days of the month of a given year that precede (follow) a regime coming statistically the most after (before) the regime to add (Table 2-4). Only the positions occupied by a regime that must be removed were considered. If only one position is in this situation, the corresponding regime is replaced by the regime that must be added. If more than one position were in this situation, a position was randomly chosen, and the regime was replaced. If no position in this situation was found, the algorithm looked at all the positions that were before (after) the regime coming statistically the second most after (before) the regime to add. If again no regime can be replaced the procedure is apply to the third regime the most occurring after or before the regime to add. This process was repeated until the entire Table 2-4 was investigated. When a regime successfully replaced another regime, the algorithm looked at the next regimes to be replaced following the same procedure. If at the end of this procedure, the regimes cannot be switched, the procedure was delayed to the next year. This condition happened only if a regime to remove was not existent in a given year. This delay in the regime replacement will broadly affect the trend calculated in a long period of times. This algorithm was repeated for the yearly regime series of each month and is summarized in Figure 2-15.

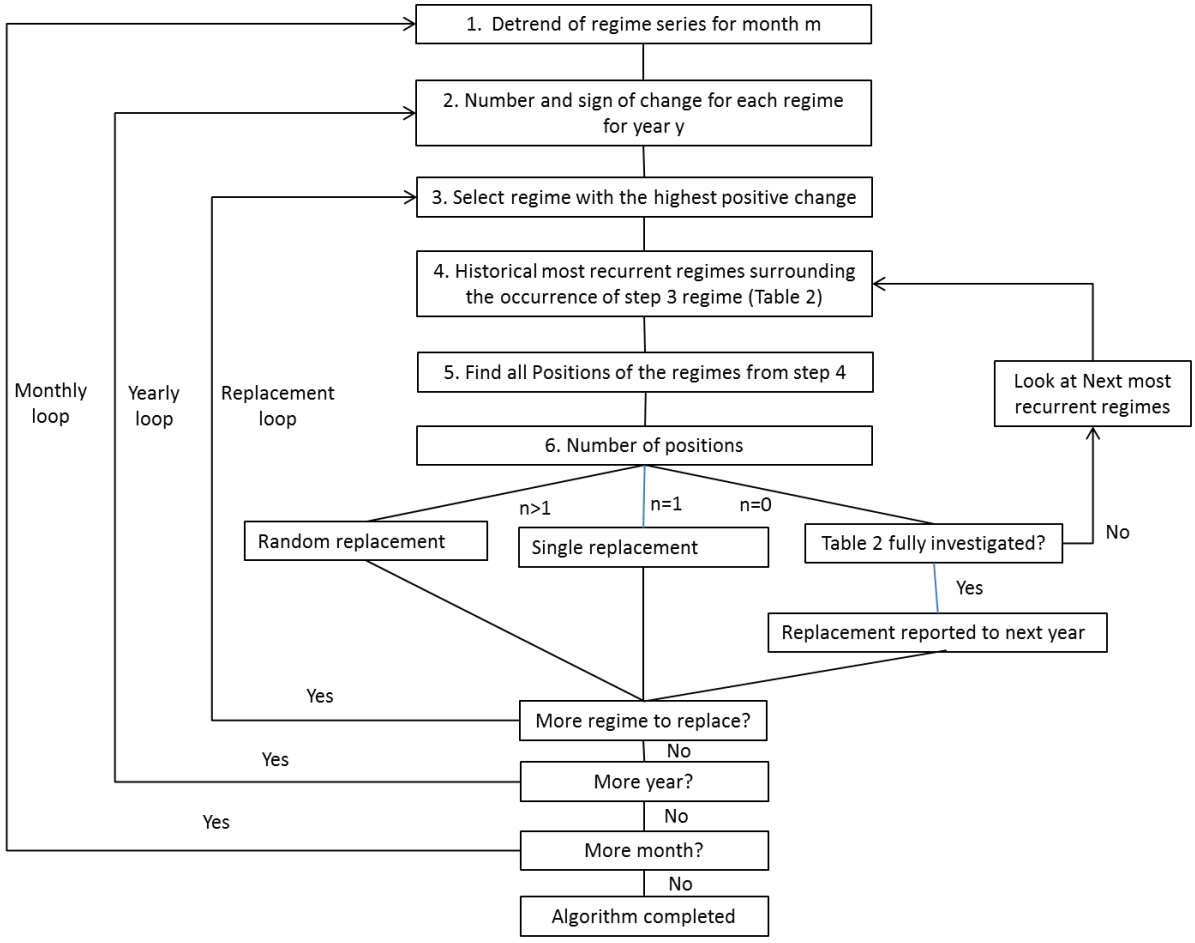

Figure 2-15 Diagram of the algorithm used to replace the daily occurrences of regimes for one EXP dataset.

An example of weather regime switches is given for January 1957. The step numbers are following the steps introduced in Figure 2-15:

- Step 1: The time series of occurrence of each weather regimes are detrended for each month. The number of occurrences of each regime that have to be added or removed for each year and each month is defined.

- Step 2: Number and sign of regimes to switch: 4 switches to make in January 1957: Two regimes HP and North have to be added; two regimes LPs, 1 regime North-West and 1 regime South have to be removed (table 2-5, column 1).

- Switch 1:

  - Step 3: The regime HP (#3) have the highest number (in Table 2-5 rounded number are presented and Regimes #3 and #4 are both equal to 2. In reality this number is not rounded and the highest number _here #3_ is chosen)

  - Step 4: according to Table 2-4 the regime #3 is historically preceding or following the most with another regime #3 (Row 3 and column 3 shows 285 cases in total in January).

  - Step 5: Among the positions following or preceding a regime #3, the 4th,5th,7th, 28th or 30th days of the month (Table 2-6 column 1) correspond to regimes that can be removed (Minus signs in Table 2-5 column 1).

  - Step 6: more than one position can be switched (n=5). Day #30 is chosen randomly.

- Switch 2:

  - Step 3: Regime North (#4) is the highest on Table 2-5 column 2.

  - Step 4: according to Table 2-4 the regime #4 is historically preceding or following the most with another regime #4.

  - Step 5: The regimes before or after a regime #4 (1st,2nd or 3th of January 1957) are not regimes that can be removed (Minus signs in Table 2-5 column 2).

  - Step 6: n=0 and the next highest historical occurrence before or after a regime #4 has to be investigated (back to Step 4).

  - Step 4: The next most occurrent regimes before and after a regime #4 are respectively #2 and #3 (Table 2-4).

  - Step 5: the 5th of January 1957 (following a #2) and 28th of January 1957 (preceding a #3) belong to regimes #2 and #5 and are candidates to be removed.

  - Step 6: n=2, the choice of the regime to switch has to be random. The 5th is chosen randomly.

- Switch 3:

  - Step 3: The regime #3 has the highest number in Table 2-5 column 3

  - Step 4: according to Table 2-4 the regime #3 is historically preceding or following the most with another regime #3.

  - Step 5: Among the positions following or preceding a regime #3, the 4th, 7th and 28th days of the month (Table 2-6, column 3) correspond to regimes that can be removed (Table 2-5).

  - Step 6: n=3. more than one position can be switched. Day 4th is chosen randomly.

- Switch 4:

  - Step 3: Regime #4 is the highest on Table 2-5 column 4.

  - Step 4: according to Table 2-4 the regime #4 is historically preceding or following the most with another regime #4.

  - Step 5: The regimes before or after a regime #4 (1th,2nd or 3th of January 1957) are not regimes that can be removed.

  - Step 6: n=0 and the next highest historical occurrence before or after a regime #4 has to be investigated (back to Step 4).

  - Step 4: The next most occurrent regimes before and after a regime #4 as it appearing in the Table 2-4 are respectively #2 and #3.

  - Step 5: The 28th of January 1957 (preceding a #3) belong to regimes #5 and is the only candidate to be removed.

  - Step 6: n=1, regime #5 is replaced by regime #4 in January 28th 1957.

This procedure is repeated for each month of each year and 100 times to create the 100 new sequences of regimes.

Table 2-4 Recurences of weather regimes in January. The rows represent the total number of occurrences in the entire period (1957-2012) following the regime indicated in the left column.

	South	LP	HP	North	North-east
South	290	47	28	42	3
LP	16	169	9	65	33
HP	36	15	285	30	23
North	42	28	47	183	27
North-east	26	32	19	9	236

Table 2-5 number of days to remove for each regime and each switch step (Sw). Positive (negative) values indicate that an occurrence has to be added (removed). Numbers in read represent the regimes switched at each switch step.

	Sw1	**Sw2**	**Sw3**	**Sw4**	
1 (South)	-1	0	0	0	0
2 (LP)	-2	-2	-1	0	0
3 (HP)	+2	+1	+1	0	0
4 (North)	+2	+2	+1	+1	0
5 (North-west)	-1	-1	-1	-1	0

Table 2-6 Example of the replacement of regimes made in January 1957. Red numbers indicate the possible days that can be switched for each Switch Step (Sw). Red columns are the days with a switch performed at the end of the algorithm applied to January 1957.

Day	Sw1	Sw2	Sw3	Sw4	
1	4	4	4	4	4
2	4	4	4	4	4
3	3	3	3	3	3
4	2	2	**2**	**3**	**3**
5	2	**2**	**4**	**4**	**4**
6	3	3	3	3	3
7	5	5	5	5	5
8	5	5	5	5	5
9	5	5	5	5	5
10	5	5	5	5	5
11	5	5	5	5	5
12	5	5	5	5	5
13	5	5	5	5	5
14	5	5	5	5	5
15	5	5	5	5	5
16	5	5	5	5	5
17	5	5	5	5	5
18	5	5	5	5	5
19	5	5	5	5	5
20	5	5	5	5	5
21	5	5	5	5	5
22	5	5	5	5	5
23	5	5	5	5	5
24	5	5	5	5	5
25	5	5	5	5	5
26	5	5	5	5	5
27	5	5	5	5	5
28	5	5	5	5	**4**
29	3	3	3	3	3
30	**1**	**3**	**3**	**3**	**3**
31	3	3	3	3	3

After the 100 new sequences of weather regimes are created, the data themselves are replaced. Table 2-7 shows the 4 replacements performed in January 1957 with the sequence of regimes previously created. For example, on January 4th 1957 corresponding to a regime LP (regime #2), the temperature was -2 which corresponds to the 419th coldest value ever recorded for this regime. The 419th coldest value for regime #3 is 5.7 and corresponded to January 23rd 1967. The minimal and maximal temperature observed on January 23rd 1967 are used for January 4th 1957 in the EXP dataset. The same process is performed for precipitations for each switch and for the 100 EXP dataset.

Table 2-7 original and experimental data for the switched days in January 1957

Day	Regime CTL	T CTL and rank	P CTL and rank	Regime EXP	T EXP (°C) and date	P (mm) EXP and date
4/1/1957	2	-2 (419st)	2.1 (318st)	3	5.7 (23/1/1967)	3.8 (4/1/1992)
5/1/1957	2	-3 (415st)	0.1 (19st)	4	1 (11/1/2001)	0 (6/1/2012)
28/1/1957	5	-7.5 (295st)	1.5 (300st)	4	-8.4 (8/1/1972)	1.7 (6/1/1985)
30/1/1957	1	-1.3 (274st)	10 (405st)	3	-1.4 (19/1/1969)	11.1 (31/1/2002)

The experimental temperature and precipitation dataset have the same statistical properties as the CTL dataset because the data are replaced by other data from the same dataset. However, new precipitation and temperature conditions in EXP dataset are not from the same days (Table 2-7) and the physical relationships between precipitation and temperature may not be preserved. A large discrepancy between our algorithm and what the physical daily relationships between temperature and precipitation allows is partially avoided because the algorithm keeps the same rank of temperature or precipitation for a given regime. To test the physical feasibility of our algorithm,

the scatter plot of daily temperature in respect to daily precipitation have been graphed for the CTL and EXP data (Figure 2-16). For 10 experimental datasets taken randomly, there are no days showing unreasonable precipitation amounts in respect to temperature. This result suggests that EXP preserves a reasonable relationship between temperature and precipitation.

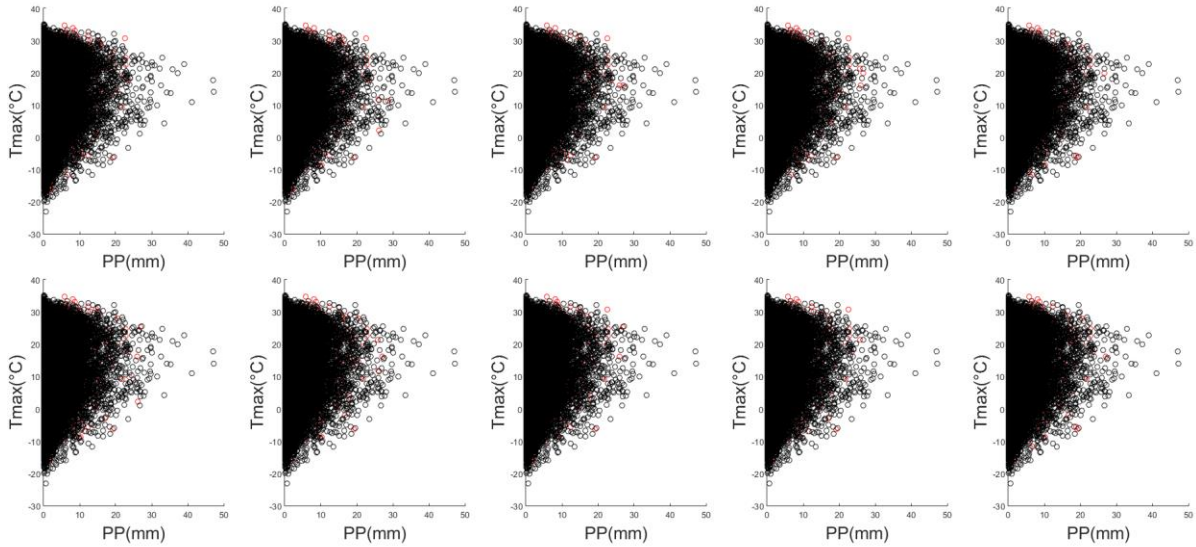

Figure 2-16 4 watersheds average daily observed temperature in respect to daily observed precipitation for the CTL dataset (Black) and 10 EXP dataset (each plot) taken randomly (Red). The points shared by the experimental and the control data are shown in black.

2.9.5 Supplementary materials references

Leavesley, G.H., Lichty, R.W., Troutman, B.M., Saindon, L.G., 1983. Precipitation-runoff modeling system; user's manual. https://doi.org/10.3133/wri834238

Markstrom, S.L., Regan, R.S., Hay, L.E., Viger, R.J., Payn, R.A., LaFontaine, J.H., 2015. precipitation-runoff modeling system, version 4: U.S. Geological Survey Techniques and Methods (No. Book 6, chapter B7).

Peichl, M., Arain, M.A., Brodeur, J.J., 2010. Age effects on carbon fluxes in temperate pine forests. Agricultural and Forest Meteorology 150, 1090–1101. https://doi.org/10.1016/j.agrformet.2010.04.008

Chapter 3. Future shift in winter streamflow modulated by internal variability of climate in southern Ontario

Champagne Olivier, Arain M.Altaf, Leduc Martin, Coulibaly Paulin, McKenzie Shawn. 2019. Future shift in winter streamflow modulated by internal variability of climate in southern Ontario. *Hydrology and Earth System Sciences Discussions*, 1–30. https://doi.org/10.5194/hess-2019-204 In review.

3.1 Abstract

Fluvial systems in southern Ontario is regularly affected by widespread early-spring flood events primarily caused by rain-on-snow events. Recent studies have shown an increase in winter floods in this region due to increasing winter temperature and precipitation. Streamflow simulations are associated with uncertainties tied to the internal variability of climate. These uncertainties can be assessed using hydrological models fed by downscaled Global Climate Model Large Ensemble (GCM-LE) data. The Canadian Regional Climate Model Large Ensemble (CRCM5-LE), a was developed to simulate climate and internal climate variability over northeastern North America under the RCP8.5 scenario. In this study, CRCM5-LE temperature and precipitation projections were used as input in the Precipitation Runoff Modelling System (PRMS) to simulate near future (2040s) streamflow for four watersheds in southern Ontario. Model simulations show a 14% (16%) probability of high (low) increase in the January-February streamflow volume. Streamflow increases may be driven by rain and snowmelt modulation caused by the development of high (low) pressure anomalies in North America's East Coast. Additionally, the streamflow may be enhanced by an increase in snowmelt and an increasing rainfall/snowfall ratio caused by high pressure circulation patterns over the Great Lakes region (16%). These results are important to

assess the internal variability of the hydrological projections and to inform society of increased winter flooding events.

3.2 Introduction

Increasing atmospheric greenhouse gases (GHG) concentration is projected to increase air temperatures globally and modify the regional precipitation regimes (Hoegh-Guldberg et al., 2018). GHG-driven climate change is projected to impact watershed fluvial hydrological regimes especially in snow dominated regions (Barnett et al., 2005) with serious implications for flood management and water resources (Hamlet and Lettenmaier, 2007; Wu et al., 2015).

The quantification of streamflow and other hydrological processes using hydrological models is becoming an active area of research in various regions of the world. However, the use of hydrological models is subject to a number of choices such as the Global Climate Model (GCM) and GHG emission scenario (Kour et al., 2016; Stephens et al., 2010), climate data downscaling method (Fowler et al., 2007; Schoof, 2013) hydrological model (Boorman et al., 2007; Devia et al., 2015) and model calibration technique (Khakbaz et al., 2012; Moriasi et al., 2007). In addition, the future temporal evolution of temperature and precipitation patterns will be modulated by the internal variability of climate due to the inherently chaotic characteristic of the atmosphere (Deser et al., 2014; Lorenz, 1963) and will also impact hydrological processes and streamflow (Lafaysse et al., 2014). Therefore, the uncertainties associated with future projections of streamflow and hydrological processes are very high (Clark et al., 2016) and have recently been the subject of intense research (Leng et al., 2016).

The uncertainties due to the internal climate variability is one of the biggest source of uncertainty for the early 21st century hydrological projections (Harding et al., 2012; Hawkins and Sutton, 2009; Lafaysse et al., 2014). The internal variability of climate is a cause of the hiatus observed in global warming in the 2000s (Dai et al., 2015) and is expected to mask the impact of human-induced climate change on precipitation (Rowell, 2012) and streamflow (Zhuan et al., 2018). Single-GCM Large Ensembles (GCM-LE) are based on small initial condition variations between members of the ensemble and have been used recently to assess the contribution of internal variability on the overall uncertainty of climate-change projections (Deser et al., 2014; Kay et al., 2015; Kumar et al., 2015) and hydrological processes in large watersheds (Gelfan et al., 2015).

Due to GCM's coarse spatial resolution, future climate data should not be used directly for small watersheds hydrological modelling and downscaling techniques must be applied to climate data (Fowler et al., 2007). Statistical downscaling methods are generally preferred as Regional Climate Model Large Ensembles (RCM-LEs) are computationally costly (Lafaysse et al., 2014; Thompson et al., 2015). However, RCM-LEs offer the possibility to relate each member of a Regional Climate Model (RCM) to large scale variability from GCM-LEs. Furthermore, RCM-LEs avoid additional and ambiguous sources of uncertainty from the statistical methods (Gelfan et al., 2015).

The Canadian Regional Climate Model Large Ensemble (CRCM5-LE) is a 50-member regional model ensemble at a 12km resolution produced over northeastern North America in the scope of the Québec-Bavaria international collaboration on climate change (ClimEx project; (Leduc et al., 2019)). For the purposes of this study, precipitation and temperature data from CRCM5-LE were used as input in the Precipitation Runoff Modelling System (PRMS), which was applied to four

watersheds in southern Ontario. The 50-members were then grouped into classes of similar weather and streamflow projections to assess the impact of internal climate variability on future hydrological processes in southern Ontario. Few members ensembles have been previously used as input in multiple hydrological models in a Québec catchment (Seiller and Anctil,2014) and in the Grand River watershed in southern Ontario (Erler et al., 2018). However, using more members is beneficial to assess the entire range of internal variability and to adopt a probabilistic approach in the projections of the future hydrological processes. This analysis, therefore, is very relevant to understand the contribution of anthropogenic and natural forcing on the temporal evolution of runoff in southern Ontario and better predict future streamflow for these watersheds.

This paper is organized as follows: Section 2 presents the PRMS hydrological model, the CRCM5-LE dataset and the classification procedure. Section 3 examines the impact of atmospheric circulation on streamflow projections. Section 4 is dedicated to the discussion of results and the concluding remarks are presented in Section 5.

3.3 Data and methods

3.3.1 Study area

Four watersheds in southern Ontario were selected for their long hydrometric time series archives and represent well the diversity of scale, soil type, and land use in this region (Figure 3-1 and Table 3-1). Land use in all four watersheds are dominated by agricultural activity. Two major cities, Brantford along the Grand River, and London along the Thames River are present in the study area and additional urban areas are located in the Credit river watershed. The Big Creek watershed contains the lowest proportion of urbanization (2%). The watersheds also vary in soil type: sand

predominates in Big Creek (79%) and Credit River (43%), but a large area of Credit is also covered by loamy soil (49%). Grand River has almost an equal proportion of sand (30%), loam (32%) and clay (38%) while Thames River contains more clay (39%). The elevation is also highly variable with the highest altitudes in the North parts of Grand River (531 m) and Credit River (521 m) while the lowest areas are located in the sandplains further south in Grand River (178 m) and Big Creek (179 m).

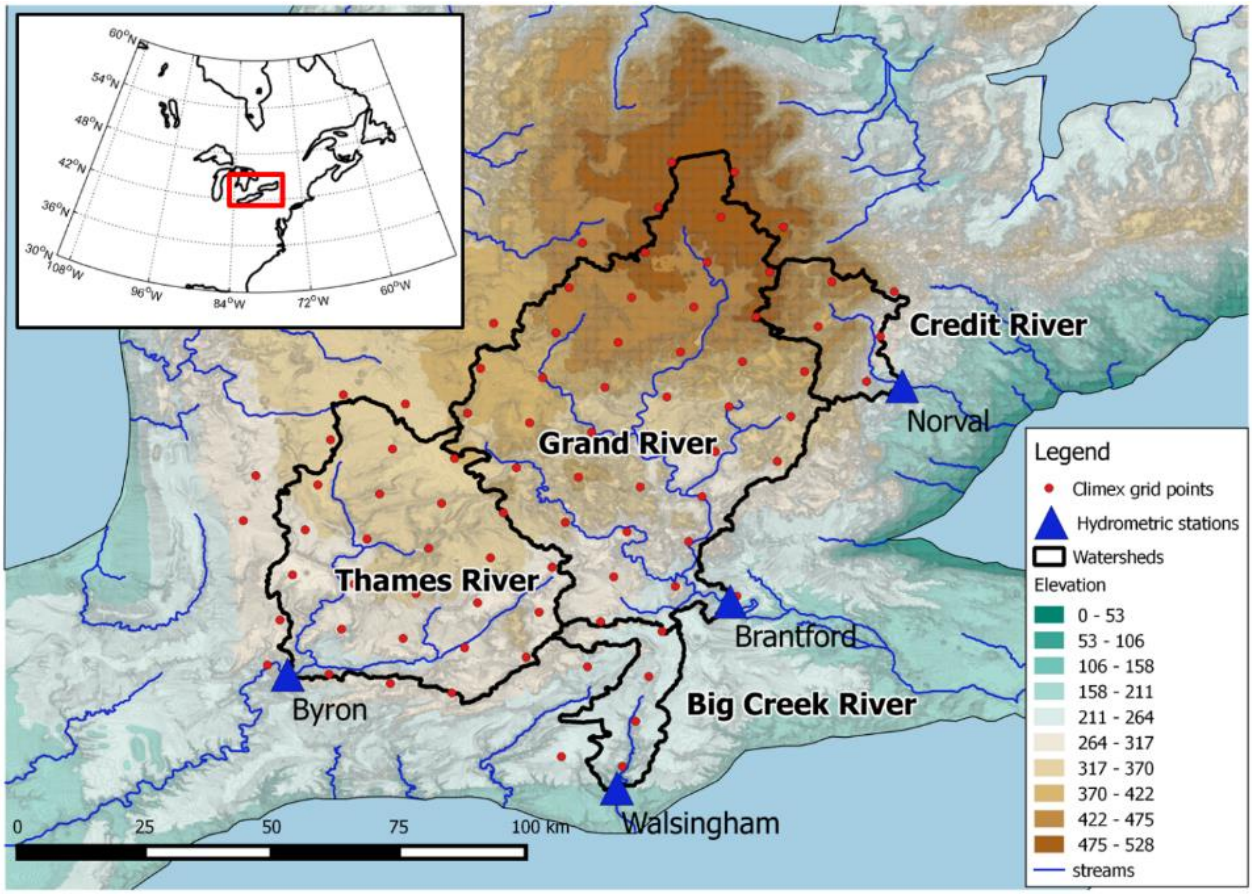

Figure 3-1 Location map of the four studied watersheds in Southern Ontario.

Table 3-1 Geomorphic, land use, and soil characteristics of the four watersheds examined in this study

	Size (km^2)	Elevation (m)	Land use (%)				Soil type (%)		
			Barren	Forest	Shrub	Crops/Grass	Sand	Loam	Clay
Big Creek at Walsingham (02GC007)	571	179-336	1.9	17	0	81.1	78.6	6.4	15
Grand River at Brantford (02GB001)	5091	178-531	7.1	11.9	0	80.9	30.4	31.6	38
Thames River at Byron (02GE002)	3061	215-423	6.9	5.4	0	87.7	14	46.7	39.4
Credit River at Norval (02HB025)	646	190-521	6.6	31.7	0	61.8	42.5	49.1	8.4

3.3.2 PRMS hydrological model

The Precipitation Runoff Modelling System (PRMS), a semi-distributed conceptual hydrological model developed by Leavesley et al. (1983), was applied to all four watersheds to simulate the future evolution of streamflow for each member of a large climate ensemble. PRMS needs only minimal temperature, maximal temperature and precipitation as forcing variables and has been widely used in watersheds affected by periodic snow (Dressler et al., 2006; Liao and Zhuang, 2017; Mastin et al., 2011; Surfleet et al., 2012; Teng et al., 2017, 2018). The hydrological calculations in PRMS are based on physical laws and empirical relations between measured and estimated quantities. A series of hydrologic reservoirs are used (plant canopy interception, snowpack, soil zone, subsurface) and the water flowing between the reservoirs are computed for each hydrological

response units (HRU). For more information about the structure of a more recent version of PRMS, refer to Markstrom et al., (2015). One of the main advantages of this model for a climate change impact study is the snowmelt algorithm using the concepts of the energy balance approach. This approach uses temperature and precipitation data projections and is a better physical conceptualization of snow processes than a temperature index approach. PRMS already proved its ability to satisfactory simulate the snow processes in the Big Creek watershed (Champagne et al., 2019).

In this study the model was set up for each watershed using Arcpy-GSFLOW, a series of ARCGIS scripts (Gardner et al., 2018). Arcpy-GSFLOW constructed the HRUs as surface grid cells of 200m² for Big Creek and Credit River watersheds and 400m² for Grand River and Thames River. These latter two watersheds have coarser HRU's to reduce the parametrization calculation time. The modules choose to compute the hydrological processes in these four watersheds have been described by Champagne et al., (2019). Parameter values associated to these modules were found in the literature and were spatialized for each HRU's using Arcpy-GSFLOW (Table 2-3) according to land use, elevation, aspect, slope and soil type. Elevation, slope and aspect were derived from the High-Resolution Digital Elevation Model (HRDEM) and the Land Use data from the Canadian Land Cover CIRCA 2000. Both datasets were furnished by Natural Resources Canada. Soil type was from the surficial geology of Southern Ontario furnished by The Ontario Ministry of Northern development, Mines and Forestry. For each HRU the percentage of each land use type and soil type was calculated by Arcpy-GSFLOW and used to estimate the value of some parameters. Other PRMS parameters are based on the single dominant land-use (bare soil, grass, shrubs, coniferous

trees or deciduous trees) and a single dominant soil type (sand, loam or clay) determined by the most dominant type. Arcpy-GSFLOW was also used to define the stream network from the HRDEM. The threshold used for accumulation flow was determined empirically by matching the created streams with the aerial photographs. We then estimated the water cascade between the HRU's and the river segments. The control dams were not taken into consideration in this study because of their limited impact on the 30-year streamflow average used in this study. The lakes represent a very small areas of the watersheds and were also neglected in this study.

Some of the parameters used in PRMS were modified during calibration while keeping their relative spatial variability (Table 2-3). The calibration was performed with a trial and error approach by comparing the daily streamflow simulated by PRMS and daily mean streamflow measured at each watershed outlet (Figure 3-1, Table 3-1). These observed hydrometric data were extracted from the Environment and Climate Change Canada Historical Hydrometric Data web site. The simulated streamflow was computed using precipitation, minimal temperature and maximal temperature from NRCANmet, the most commonly used dataset in Canada (Werner et al., 2019). The dataset was produced using stational observations from Environment and Climate Change Canada and Natural Resources Canada and the gridding at 10 km spatial resolution was accomplished with the Australian National University Spline (ANUSPLIN, McKenney et al., 2011, Hutchinson et al., 2009). 186 data points were needed to cover the area of the four watersheds (red markers on Figure 3-1). For model calculations, each HRU used climate data from the closest NRCANmet grid point. Five years were used as the warm-up period (Oct 1984-Sept 1989) to remove the error due to initial conditions. Different simulations with a varying

initialization period length were tested in the Big Creek watershed and showed that five years were necessary for the hydrological model to forget the initial conditions of the reservoirs. The calibration period was between Oct 1989 and Sept 2008 and the years 2009 to 2013 were used as the validation period. The steps involved in this calibration are described in Champagne et al. (2019).

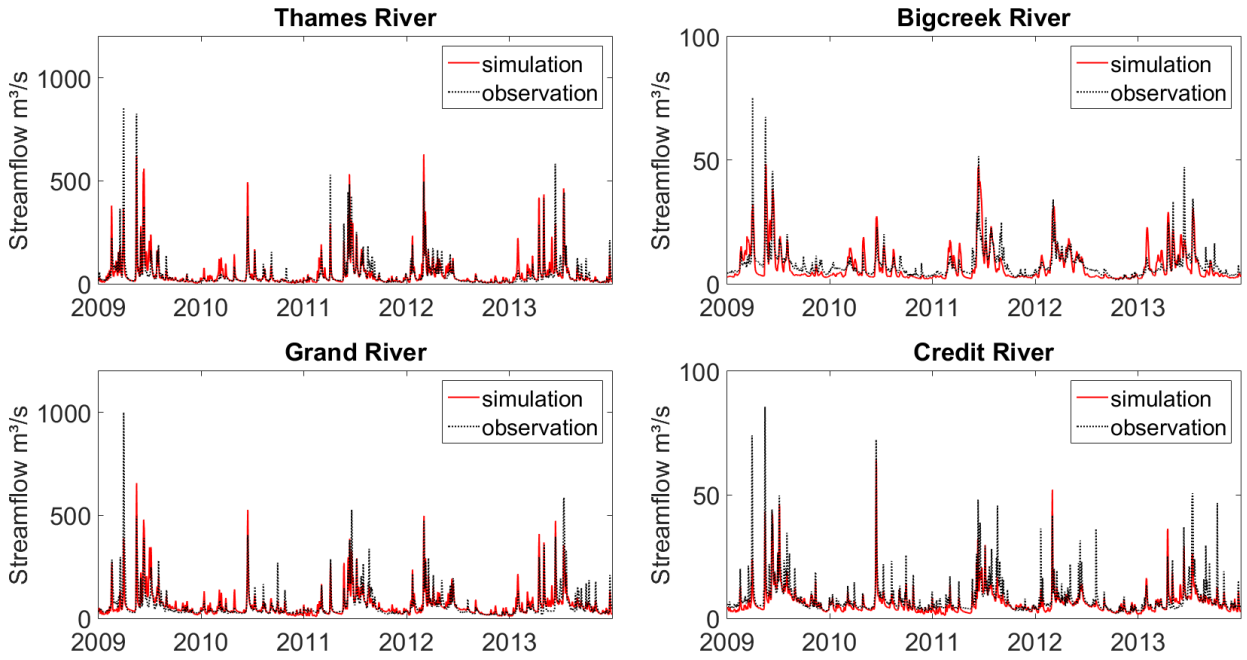

Figure 3-2 Simulated and observed streamflow during the validation period (2009-2013)

The best set of parameters retained after calibration is shown in Table 3-2. The Nash Sutcliff Efficiency (NSE) values are always higher than 0.65 for both calibration and validation periods (Table 3-2). The percent bias (PBIAS) is between -15% and +15% except for Credit River during the validation period. A NSE higher than 0.65 and a PBIAS lower than 15% is generally considered a good quantitative fit (Moriasi et al., 2007). Figure 3-2 shows the simulation and the observation

of the daily streamflow in all four watersheds and confirms visually the goodness of simulation fit.

Table 3-2 Efficiency of PRMS model for best fit parameters

	Calibration		Validation	
	NSE	PBIAS	NSE	PBIAS
Big Creek	0.75	1.8	0.74	6.7
Grand River	0.71	-5	0.69	1.7
Thames River	0.72	-10.8	0.72	-5.3
Credit River	0.71	-0.1	0.65	18

3.3.3 Climate data projections

The set of parameters identified for each watershed during the calibration were used to simulate the future evolution of streamflow for each member of the Canadian Regional Climate Model Large Ensemble (CRCM5-LE). CRCM5-LE is a 50-member ensemble of climate change projections at 0.11° (~12-km) resolution available at 5-minute time steps over Northeastern North-America (Leduc et al., 2019). Each member of CRCM5-LE was driven by 6-hourly atmospheric and oceanic fields from each member of the Canadian Earth System Model version 2 Large Ensemble (CanESM2-LE) at a 2.8° (~310 km) resolution (Fyfe et al., 2017; Sigmond et al., 2018). The downscaling from CanESM2-LE was performed using the Canadian Regional Climate Model (CRCM5 v3.3.3.1; Martynov et al., 2010; Šeparović et al., 2013) developed by the ESCER Centre at UQAM (Université du Québec à Montréal) with the collaboration of Environment and Climate Change Canada. The ensemble extends from the historical (1954-2005) to the projected (2006-2099) period forced with the RCP8.5 scenario (Meinshausen et al., 2011). The CRCM5-LE Data grid-points the closest to NRCANmet data points were used in this study. Before their use in PRMS, temperature and precipitation from CRCM5-LE were bias-corrected against NRCANmet over the historical period (1954-2005) using the method developed by Ines and Hansen (2006). A

gamma distribution was used for both observed and modelled precipitation intensities while a normal distribution was used for the temperature bias correction. These bias-correction calculated from the historical period were then applied to the CRCM5-LE grid points for the entire period 1954-2099.

3.3.4 Ascending hierarchical classification

An ascending hierarchical classification (AHC) was used to classify all 50 members into classes of similar change of forcing CRCM5-LE meteorological conditions and streamflow simulated by PRMS. The classification was used to simplify the study of the connections between the future change in large scale atmospheric circulation, local meteorological conditions and streamflow. The AHC calculates first the Euclidean distance between each pair of members. The pair with the closest Euclidean distance are merged into a single class. The Euclidean distance of this class is then calculated by averaging the Euclidean distance between each member of this class and all other members. The next pair of classes or members with the smallest Euclidean distance is merged and averaged similarly. This process is repeated 49 times, until all classes of members have been merged into a single class. The AHC was applied first to the 4-watersheds January-February normalized change of streamflow and then to the 4 watersheds average change of temperature and precipitation between the historical (1961-1990) and 2040's periods (2026-2055). The AHC was performed using January-February data because these months correspond to a large change of streamflow during the period. For precipitation and temperature, the period from 25 December to 22 February was used to account for the delay between weather conditions and streamflow at the outlet. A delay of 6 days showed the best correlation between the increase in temperature and precipitation and the increase of streamflow for all 4 watersheds. The number of classes to retain

for change of streamflow and number of classes for change of weather conditions corresponds to the highest interclass Euclidean distance variance.

The future projection of atmospheric circulation for each class was analyzed using climate variables from CanESM2-LE with a geographical domain from 30°N to 60°N latitude and 100°W to 50°W longitude. Climate variables used for analysis included air temperature at 850hPa level (850T), precipitation (PP), sea level pressure (SLP), geopotential height at 500hPa (Z500) and surface winds. These climate variables were separated into internal and forcing contributors. The forcing contribution of the climate variables corresponds to the average change of all ensemble members between the historical period and 2040s. The internal contribution associated to each member was calculated by subtracting the original member data from the forcing contribution. This method was previously used by Deser et al. (2014) to assess the internal contribution of future change in temperature and precipitations in North America.

3.4 Results

3.4.1 Streamflow projections

Figure 3-3 shows the average daily streamflow volume and the number of high flows for all members for the historical (HIST) and future (2040s) periods. Observational streamflow measured at each watershed outlet (OBS) and the streamflow simulated by PRMS using temperature and precipitation from NRCANmet (CTL for control) are also shown for the historical period.

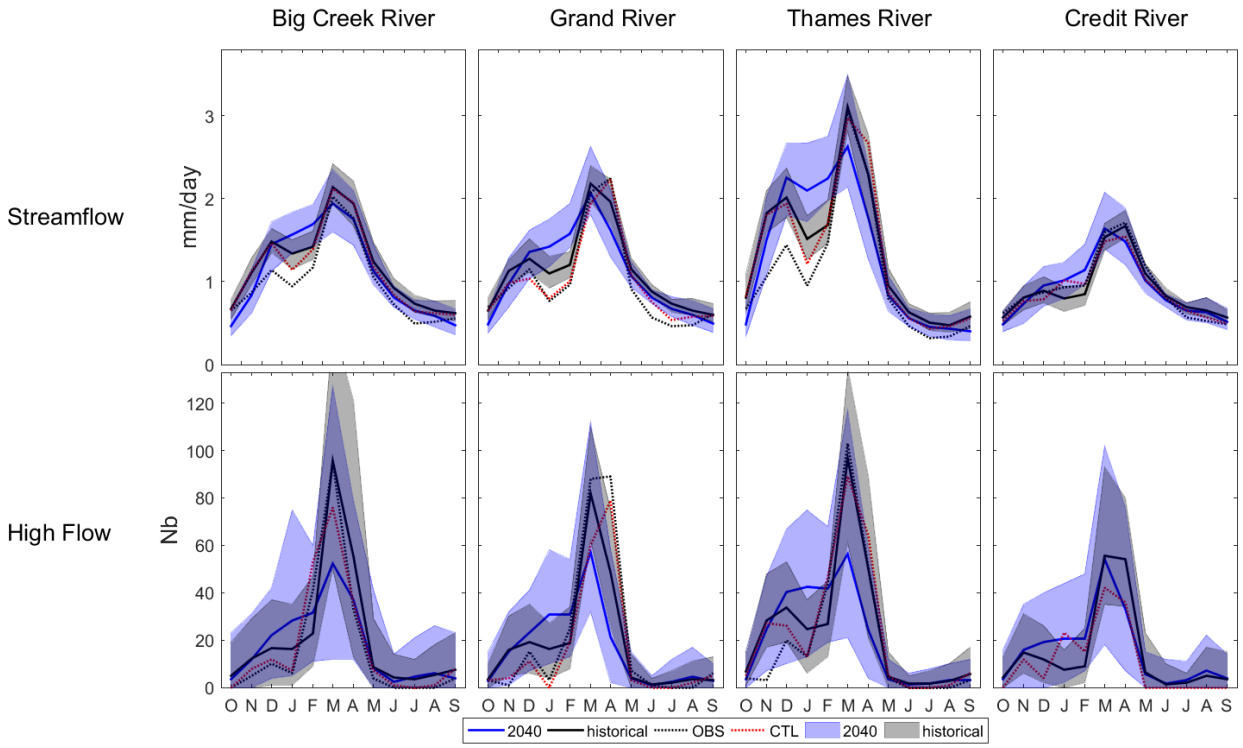

Figure 3-3 50-members range and average streamflow and number of high-flows for the historical and the 2040s period.

In the historical period, average streamflow from OBS, CTL and the 50-member data sets followed similar annual cycles with the first peak of the hydrological year occurring in November-December and the highest peak in March-April. By 2040, a clear peak in streamflow and the number of high-flow events are still modelled in March but streamflow is more evenly distributed among winter months. This result suggests a shift from two maximal peaks to one winter peak by the mid-21st Century. Lastly, the simulated range of streamflow volume and number of high flows is wide among the 50 different members in winter.

Daily rainfall, snowmelt, and actual ET are also expected to change by 2040s (Figure 3-4). The amount of rain is simulated to consistently increase among the 50-member average in winter and early spring in all four watersheds. In summer, PRMS simulates future average rainfall to decline, but the direction of change is inconsistent between individual members. The amount of snowmelt is expected to shift from high melt volume in March to a volume consistent throughout the winter. In November and in March-April, snowmelt is expected to decline while in January-February, snowmelt is expected to increase. Future ET will slightly increase in winter following by dramatic increases in spring period (March and April). In summer ET is simulated to slightly decrease on average but the difference between the member with the highest and the member with the lowest ET amount is larger as compared to winter ET values.

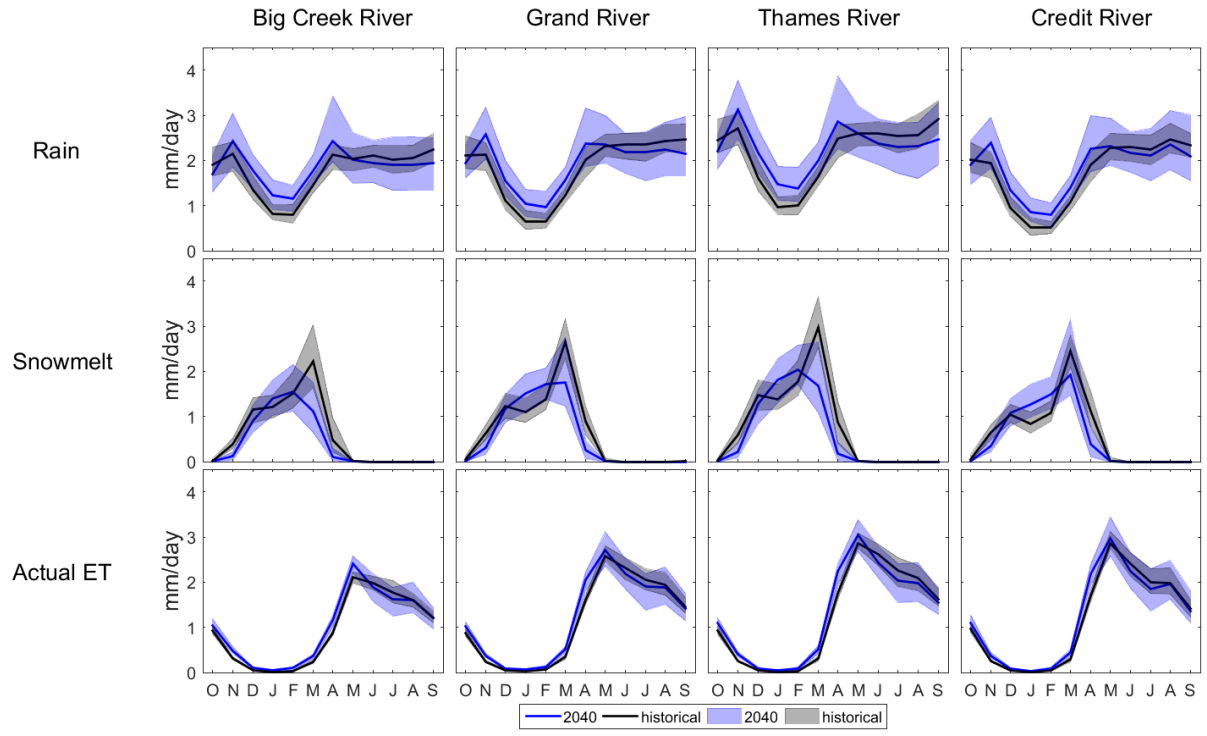

Figure 3-4 50-members range and average rain, snowmelt and actual ET amounts for the historical and the 2040s period.

Figure 3-5 shows the 50-member historical and projected bias-corrected temperature and precipitation for all four watersheds. Air temperature is shown to consistently increase for all months while the range of precipitation amounts projected by the 50 members is higher. On average, simulated precipitation increases in November-April and decreases in June-September.

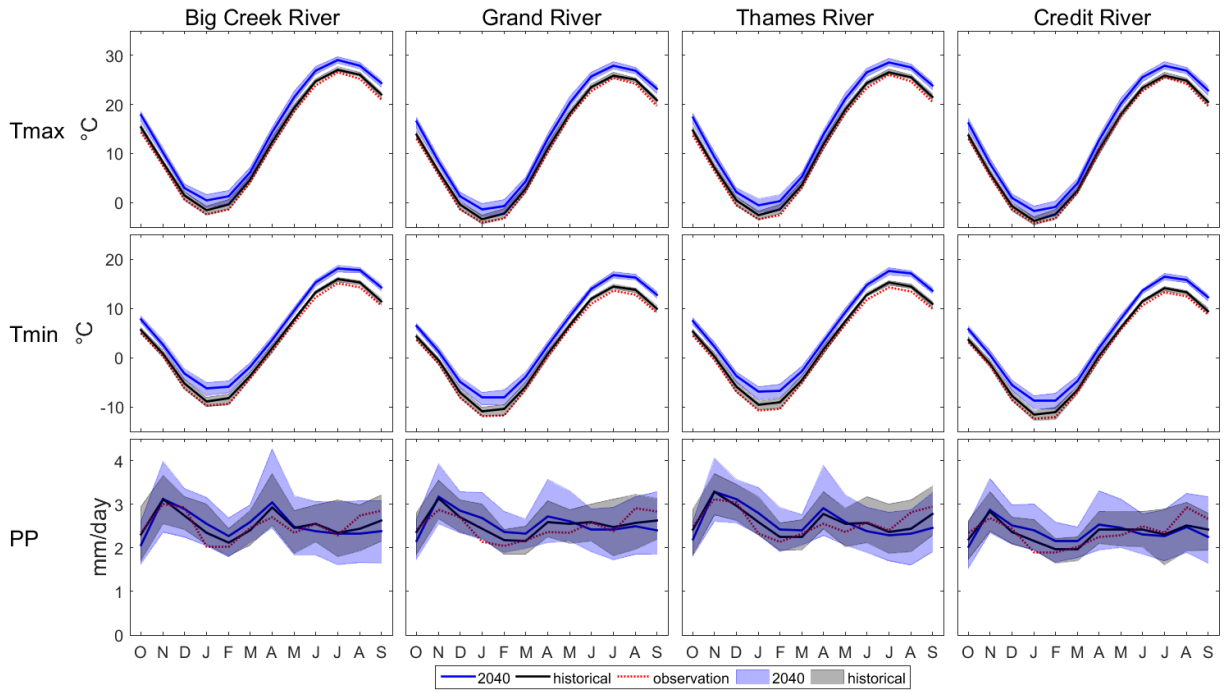

Figure 3-5 CRCM5-LE 50-members range and average bias-corrected temperature and precipitation amounts for the historical and the 2040s period, together with NRCANmet temperature and precipitation in the historical period.

3.4.2 January-February streamflow projections variability

The 50 members of the ensemble were classified first in classes of similar streamflow change between the historical period and 2040s using the AHC described in the method section. The number of classes to retain was determined using a dendrogram (Figure 3-6). The dendrogram shows the variance of Euclidean distance for the successive merging, from the first merging that uses all members (bottom) to the last merging creating a single class (top). The highest vertical

distance between two successive merging in the Y axis corresponds to the number of classes with the highest interclass variance. The number of weather classes was identified using the same method (Figure 3-6). Three streamflow classes (HiQ, MoQ and LoQ for high, medium and low increase of streamflow) and four weather classes (HiPT, MoPT, LoPT and HiT) correspond to the number of classes with the lowest interclass Euclidean distance variance (Figure 3-6). Three of the weather classes (HiPT, MoPT and LoPT) show a gradient from high to low increase for both precipitation and temperature while one weather class show a high increase in temperature but low increase in precipitation (HiT) (Figure 3-6, right panel). The labels High and Low are not refering to absolute values but correspond to higher or lower increase in streamflow, temperature or precipitation relative to the other members.

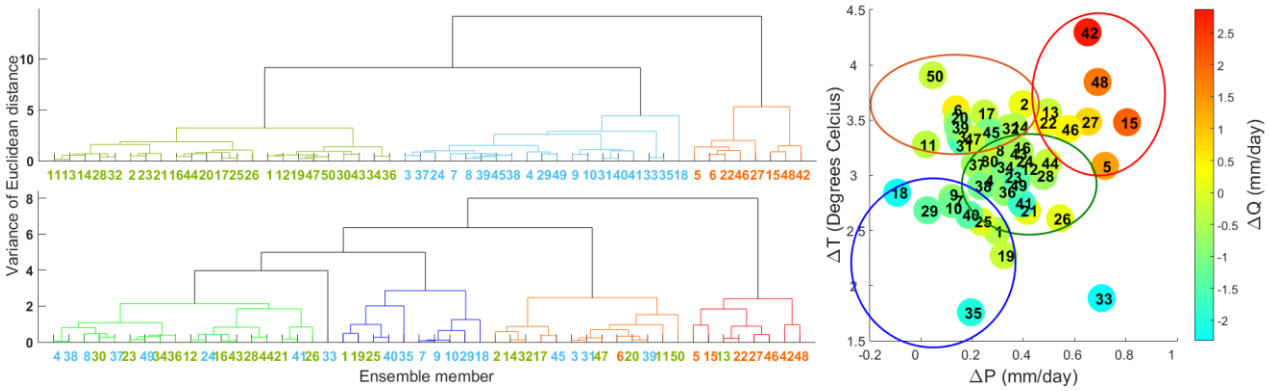

Figure 3-6 Left: Results of the Ascending Hierarchical Classification (AHC) for the normalized change of streamflow (Q) (above) and normalized change of average Temperature (T) and Precipitation (P) (below). Colored numbers represent Q classes. Right: 4-watersheds average change of streamflow (Q) (Colors) with respect to average change of P and T. Large hollow circles represent the 4 weather classes.

The streamflow and weather classes were then aggregated, grouping the members that are in the same streamflow and weather groups, giving a total of nine classes (Table 3-3).

Table 3-3 Classes members, number of members in the class (in % of the ensemble) and average January-February increase of streamflow between historical and 2040's period.

Name	Members	%	ΔQ (mm/day)			
			Big Creek	Grand River	Thames River	Credit River
HiQHiPT	5,15,22,27, 42,46,48	14%	0.43 (0.09)	0.55 (0.10)	0.73 (0.11)	0.43 (0.09)
HiQHiT	6	2%	0.32	0.46	0.57	0.35
MoQHiPT	13	2%	0.33	0.40	0.56	0.29
MoQHiT	2,11,14,17, 20,32,47,50	16%	0.29 (0.05)	0.37 (0.03)	0.49 (0.08)	0.27 (0.02)
MoQMoPT	12,16,21,23,26,28, 30,34,36,43,46	22%	0.25 (0.05)	0.36 (0.04)	0.49 (0.06)	0.26 (0.04)
MoQLoPT	1,19,25	6%	0.25 (0.02)	0.36 (0.02)	0.44 (0.02)	0.28 (0.02)
LoQHiT	3,31,39,45	8%	0.15 (0.03)	0.29 (0.02)	0.38 (0.02)	0.19 (0.04)
LoQMoPT	4,8,24,33, 37, 38,41,49	16%	0.19 (0.06)	0.25 (0.04)	0.36 (0.05)	0.17 (0.06)
LoQLoPT	7,9,10,18, 29,35,40	14%	0.12 (0.11)	0.23 (0.06)	0.30 (0.10)	0.16 (0.05)

Seven out of the eight members associated with high increase in precipitation and temperature (HiPT) show a large increase in streamflow (HiQHiPT) while one member show a moderate streamflow increase (MoQHiPT). Eight of the thirteen members associated with a large increase in temperature only (HiT) generate a moderate increase in streamflow (MoQHiT) while four have a low increase (LoQHiT) and one has a high increase in streamflow (HiQHiT). The members associated with a moderate increase in precipitation and temperature (MoPT) majoritarly produce a moderate increase in streamflow (MoQMoPT) but eight out of nineteen members demonstrate low increases in streamflow (LoQMoPT). Lastly, the class LoPT consists of members with the lowest change in precipitation and temperature with eight members showing a low increase

(LoQLoPT) and three members that show moderate increases in streamflow (MoQLoPT). The interclass variability is generally consistent between watersheds with the exception of Big Creek. The classes HiQHiT and LoQHiT show relatively low streamflow increases as compared to the other three watersheds (Table 3-3).

Figure 3-7 shows scatter plots of averaged change in streamflow to average change in precipitation, temperature, snowmelt and rain between the historical period and the 2040s period for all nine classes shown in Table 3-3. HiQHiPT and LoQLoPT classes are associated with the highest (lowest) increases in streamflow due to high (low) increases of snowmelt and rain (Figure 3-7). The larger increase in rain and snowmelt for HiQHiPT members are likely due a larger warming and increase in precipitation. MoQLoPT demonstrates a larger increase in simulated streamflow compared to LoQLoPT, which is likely due to a larger increase in precipitation amounts despite lower warming. MoQLoPT is especially larger than LoQLoPT in term of snowmelt suggesting more snowfall for MoQLoPT members. The three weather classes associated with a large increase in temperature only (HiT) depict a moderate increase in rain and snowmelt suggesting that these members increase the rain to snow ratio and accelerate the snowmelt. LoQHiT shows also a strong warming but a low increase in snowmelt explaing the low increase in streamflow (Figure 3-7). Lastly, MoQMoPT has a higher increase in both rainfall and snowmelt compared to LoQMoPT but both classes demonstrate similar change in precipitation and temperature. These results suggest that alternative factors than average change in temperature and precipitation could explain the change in rainfall, snowmelt and streamflow in january-february. These factors will be described

in part 3.4 and discuss in section 4.4. Lastly, the main visual difference between watersheds was a lower increase in snowmelt expected in Big Creek.

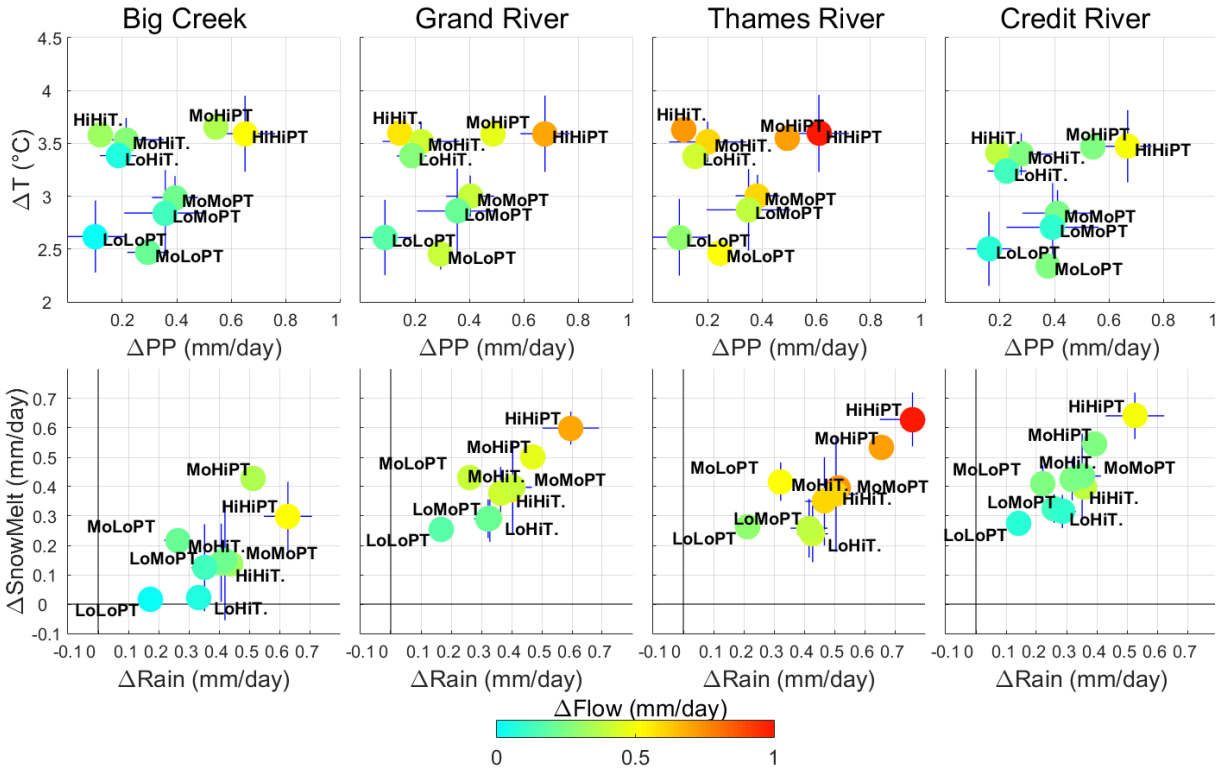

Figure 3-7 Change of streamflow (Colors) with respect to changes of daily temperature and precipitation amount (above) and snowmelt and rain amounts (below) between the historical and the 2040's future periods in January-February.

3.4.3 Atmospheric circulation and streamflow projections

The 50 members average change in temperature and precipitation between the historical period and the 2040's is shown in figure 3-8. An increase in air temperature at 850hPa (T850) and geopotential height at 500hPa (Z500) is expected to occur within the entire domain with a stronger gradient closer to the Arctic (Figure 3-8c). Precipitation was also simulated to increase by the 2040s throughout the domain while SLP was shown to decrease (Figure 3-8d). In the region close to the Great Lakes, the magnitude of warming and variability between members is higher on the

northern shorelines as compared to the open water and shorelines south of the Lakes (Figure 3-8a). Precipitation increases were also shown to be higher on land and on the east side of the Great Lakes and toward the Atlantic coast (Figure 3-8b and 3-8d).

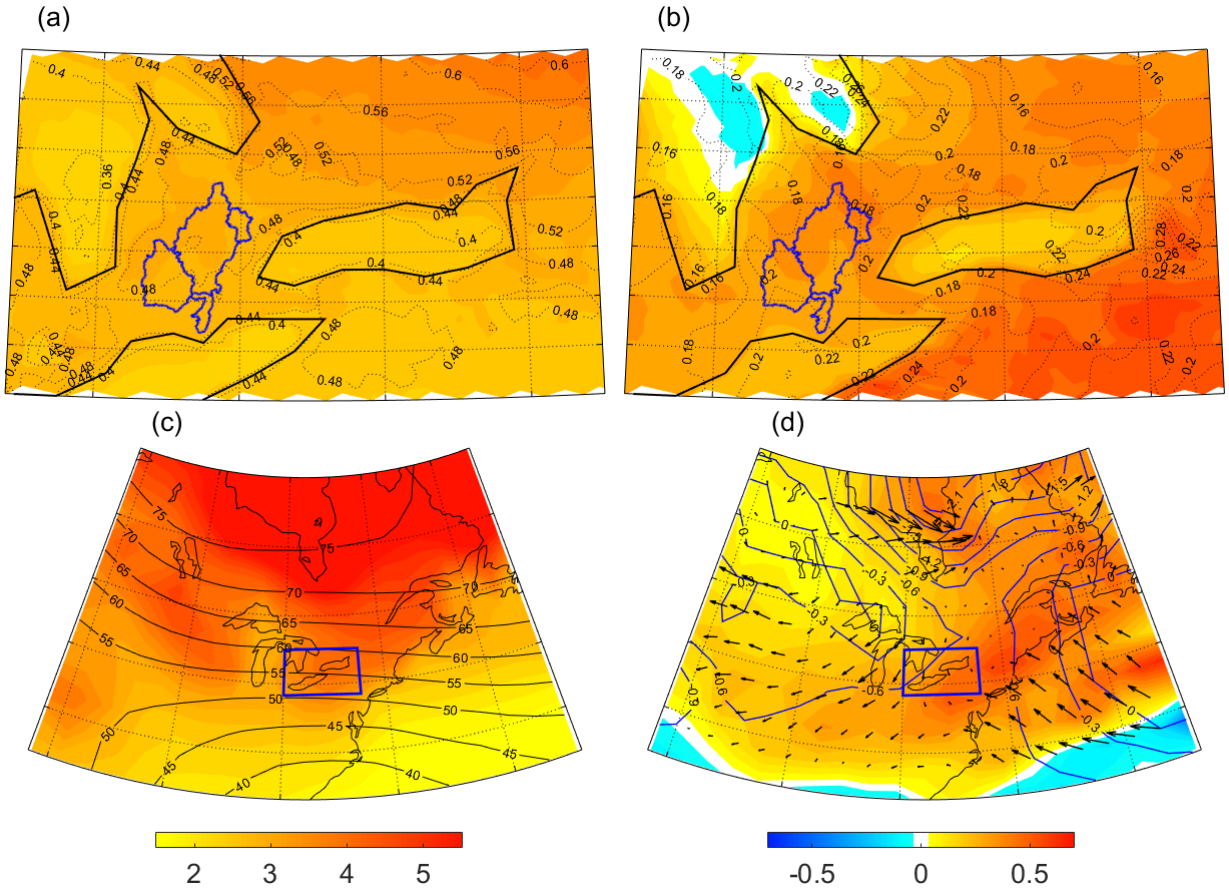

Figure 3-8 50-members ensemble average change of atmospheric conditions between the historical and the 2040's period in January-February for a. CRCM5-LE average temperature (shade) and standard deviation (black lines), b. CRCM5-LE average precipitation (shade) and standard deviation (black lines), c. CanESM2-LE T850 (shade) and Z500 (black lines) and d. CanESM2-LE precipitation (shade), SLP (blue lines) and wind (vectors).

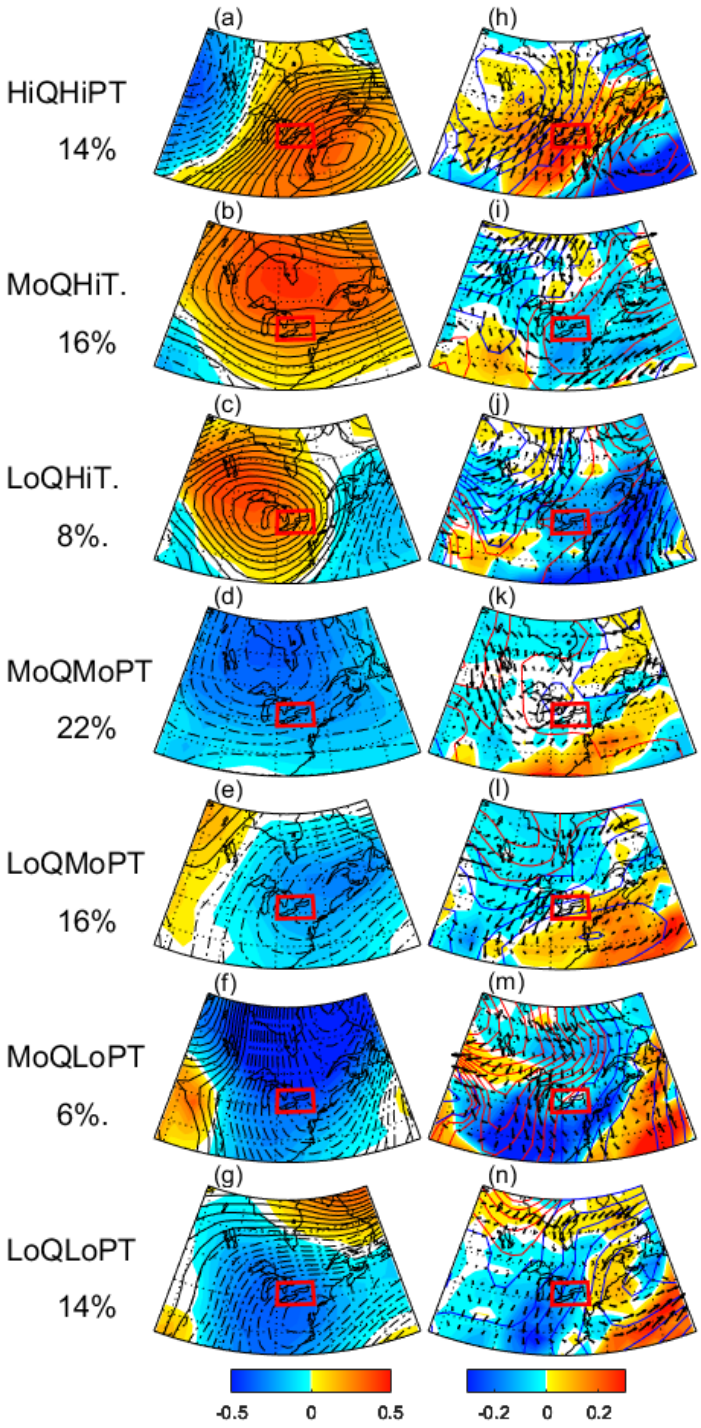

Figure 3-9 a-g: Classes averaged internal contribution of a-g T850 (shade) and Z500 (black lines, in intervals of 1m) and h-n: Precipitations (shade), SLP (lines, in intervals of 0.1hPa) and wind (vectors) of the 50-members average change between the historical and the 2040's period in January-February.

The internal contribution of each member of CanESM2-LE to the change of climate variables was averaged for each class (Figure 3-9). The class HiQHiPT is projected to be associated with positive temperature, precipitation, and southwesterly winds change anomalies between high pressure anomalies in the east and low pressure anomalies in west side of the domain (Figure 3-9a and 3-9h). LoQLoPT has opposite pressure gradient anomalies and is the only class that show negative increase of precipitation and temperature anomalies occurring simultaneously (Figure 3-9g and 3-9n). LoQMoPT demonstrates a similar pattern to LoQLoPT, but the negative pressure anomalies are attenuated, and precipitation increase is higher (Figure 3-9e and 3-9l). MoQHiT and LoQHiT are characterized by positive temperature and pressure change anomalies over southern Ontario, while MoQMoPT and MoQLoPT have an opposite pattern.

3.4.4 Antecedent conditions and streamflow

Alternative factors than January-February atmospheric conditions are examined that may help to explain the January-February evolution in streamflow between the historical and the future period. Figure 3-10 shows the change in precipitation amount in November-December, groundwater flow in January-February and amount of snowpack water equivalent for the first and the last day of the January-February period.

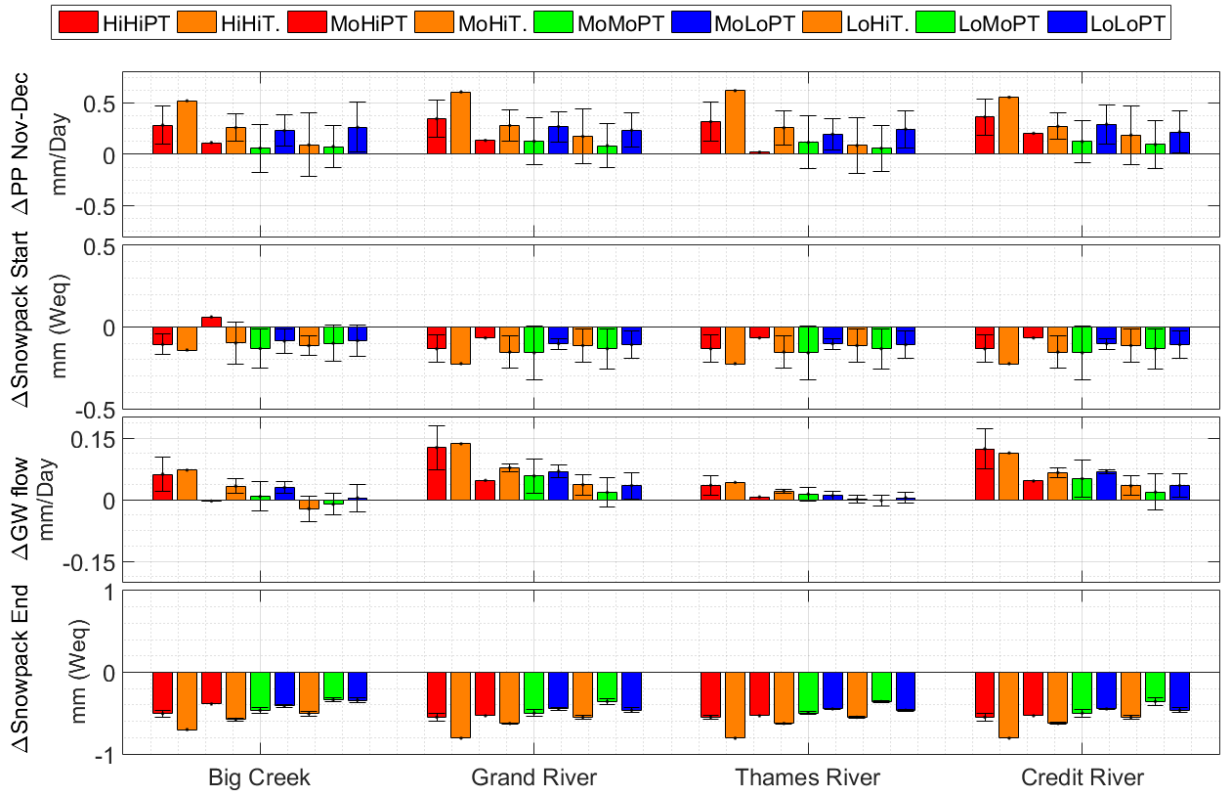

Figure 3-10 Evolution between the historical and 2040's period for first row: precipitation amount (mm) in November-December, second row: snowpack amount (mm water-equivalent) in December 25th, third row: Groundwater flow in January-February and fourth row: snowpack amount (mm water-equivalent) in February 23th.

November-December precipitation are expecting to increase for all classes but a large intraclass and interclass variability is shown. The classes HiHiPT, HiHiT, MoHiT and the two LoPT weather classes show visually a higher increase of November-December precipitation as compared to the other classes. The amount of snowpack water equivalent at the beginning of the January-February period is expected to decrease with low variability between the classes but a large intra-class variability (Figure 3-10). The snowpack at the end of January-February is expected to decrease significantly for all classes with a low intraclass variability. The groundwater flow shows visually

a large difference between watersheds with a higher increase in Credit River and Grand River compared to Big Creek and Thames River.

3.5 Discussion

3.5.1 Historical simulations

The observed seasonal cycle of streamflow was visually well reproduced by the simulated CTL and ensemble data for the historical period (1961-1990) (Figure 3-3). However, the simulated streamflow from CTL and the ensemble overestimated streamflow between November and February in the Thames and Big Creek watersheds. The overestimation is stronger in January for the ensemble which can be attributed to an overestimation of precipitation (Figure 3-5). Winter overestimation was previously reported for the Grand River watershed (Erler et al., 2018) and was attributed to the monthly resolution and the representation of the winter processes .The version of PRMS used in our study is for example not representing the frozen soil. However, a comparison of the observed streamflow during frozen and non-frozen soil in the Big creek watershed have shown a small difference (Not shown) suggesting a low impact of frozen soil to the streamflow in this region. Moreover, the streamflow simulations using NRCANmet data performed very well in Grand River (Figure 3-3). These results suggest that the hydrological model structure is not responsible for the discrepancies. The quality of NRCANmet could be incriminated. The ANNUSPLIN method, used by NRCANmet to interpolate the station-based observations, generally overestimates precipitation in this region (Newlands et al., 2011). Despites these biases, NRCANmet is the most widely used gridded dataset in Canada (Werner et al., 2019) and NRCANmet can be used with confidence, awaiting further improvements. The observed streamflow itself can also be affected by wrong measurements during ice conditions and especially

an overestimation of the discharge. The validation of simulations using other variables such as evapotranspiration or soil moisture would be beneficial to improve the confidence in the results. Evapotranspiration from CRCM5-LE was not available for this work but could be investigated in future works.

3.5.2 Increase in streamflow amplified or attenuated by Z500 anomalies

Despite the discrepancies highlighted in the last section, the results show a clear increase in streamflow in January-February (Figure 3-3) which has been previously simulated for other watersheds in the Great Lakes region (Byun et al., 2019; Erler et al., 2018; Grillakis et al., 2011; Kuo et al., 2017). January-February streamflow increases are likely caused by temperature and precipitation increases (Figure 3-5 and 3-8) that causes rain and snowmelt amounts to rise (Figure 3-4). Grillakis et al. (2011) used several hydrological models in a small catchment close to Lake Ontario and reported that streamflow increases are due to rainfall increases in January and snowmelt increases in February. In our study we found an increase in rain and snowmelt for both months (Figure 3-4). The future increase in January-February rain and snowmelt is due to a warming (Figure 3-8) that has a global feature (Hoegh-Guldberg et al., 2018). Warming amplitudes projected for southern Ontario with CanESM2-LE are conformed to the CMIP5 multi-model projections with the same RCP8.5 scenario (Zhang et al., 2019). January-February precipitation increases are likely to occur in a large part of the domain (Figure 3-8) which is conform to other climate models (Zhang et al., 2019). Precipitation increase between Lake Ontario/Erie and the East coast (Figure 3-8) is not expected by the multi-model projections and is likely inherent to CanESM2-LE. This precipitation pattern is probably associated to stronger winds from the east coast (Atlantic Ocean) due to a higher pressure decrease on land (Figure 3-8).

The 50 members produce a variable increase in streamflow (Figure 3-3) which is likely due to the variability in atmospheric circulation (Figure 3-9). 14% of the ensemble shows a high increase in streamflow simultaneously with high geopotential height anomalies near the east coast and southerly winds through the Great Lakes region (Table 3-3 and Figure 3-9a and 3-9h). High geopotential height anomalies located in the eastern United States has been previously found to be responsible for more precipitation and higher temperature in the Great Lakes region in winter due to southerly winds (Mallakpour and Villarini, 2016; Thiombiano et al., 2017), thereby increasing the streamflow and high flow events (Bradbury et al., 2002; Mallakpour and Villarini, 2016). 14% of the ensemble corresponds to the opposite pattern with low geopotential height anomalies in the east coast and northern winds anomalies (Figure 3-9g and 3-9n). These atmospheric conditions attenuate the warming and precipitation amounts and are therefore associate to a lower increase in streamflow (Table 3-3 and Figure 3-7). 6% of the ensemble (Class MoQLoPT) shows a low warming but a moderate increase in precipitation and snowmelt (Figure 3-7 and 3-9f and 3-9m) suggesting snowfall enhance. The north-west wind anomalies associated to this class (Figure 3-9f and 3-9m) could enhance snowfall in this region through lake effect snow (Suriano and Leathers, 2017). Another 16% of the ensemble shows a moderate increase in streamflow associated to a strong warming (MoQHiT) which may be driven by high-geopotential height anomalies on the Great Lakes (Figure 3-9b and 3-9i). This pattern drives moderate increases in snowmelt and rain-to-snow ratio associated with strong warming (Figure 3-7, 3-9b and 3-9i). Correspondence between high geopotential height and high temperature on the Great Lakes in winter have been previously reported (Ning and Bradley, 2015b). Ning and Bradley (2015) suggest that the high

geopotential anomalies on the great Lakes prevent the polar jet-stream and the cold air masses from entering the region.

3.5.3 Consistency in the weather classes

The weather classes are associated to specific trends in atmospheric conditions (Figure 3-9) but are composed from an average of members that have their own signature. Changes in Z500 anomalies and T850 for each member are depicted in Figure 3-11 to investigate the variability between members. The members that comprise classes HiPT show high Z500 anomalies enhance in the east coast consistently for six members while for two members (#13 and #48) the high increase in Z500 anomalies is centered north from the Great Lakes. Eight members of the class LoPT show strong Z500 decrease in the east coast but in two members (#1 and #10) the decline is rather centered in the northern side of the Great Lakes. HiT show generally Z500 increase centered on the Great Lakes but four of the thirteen members depict a different pattern (#2, #20, #31 and #47). Finally, members from MoPT show generally a decrease in Z500 but we observe a high diversity in the change in circulation patterns. Members from MoPT depict a lower Z500 gradient compared to other classes suggesting a lower contribution of internal variability of climate to the total change in atmospheric conditions (Figure 3-11). Despite the atmospheric anomalies differences between members predicting similar local weather, this study gives a good probabilistic overview on how the change in regional atmospheric anomalies will impact local weather.

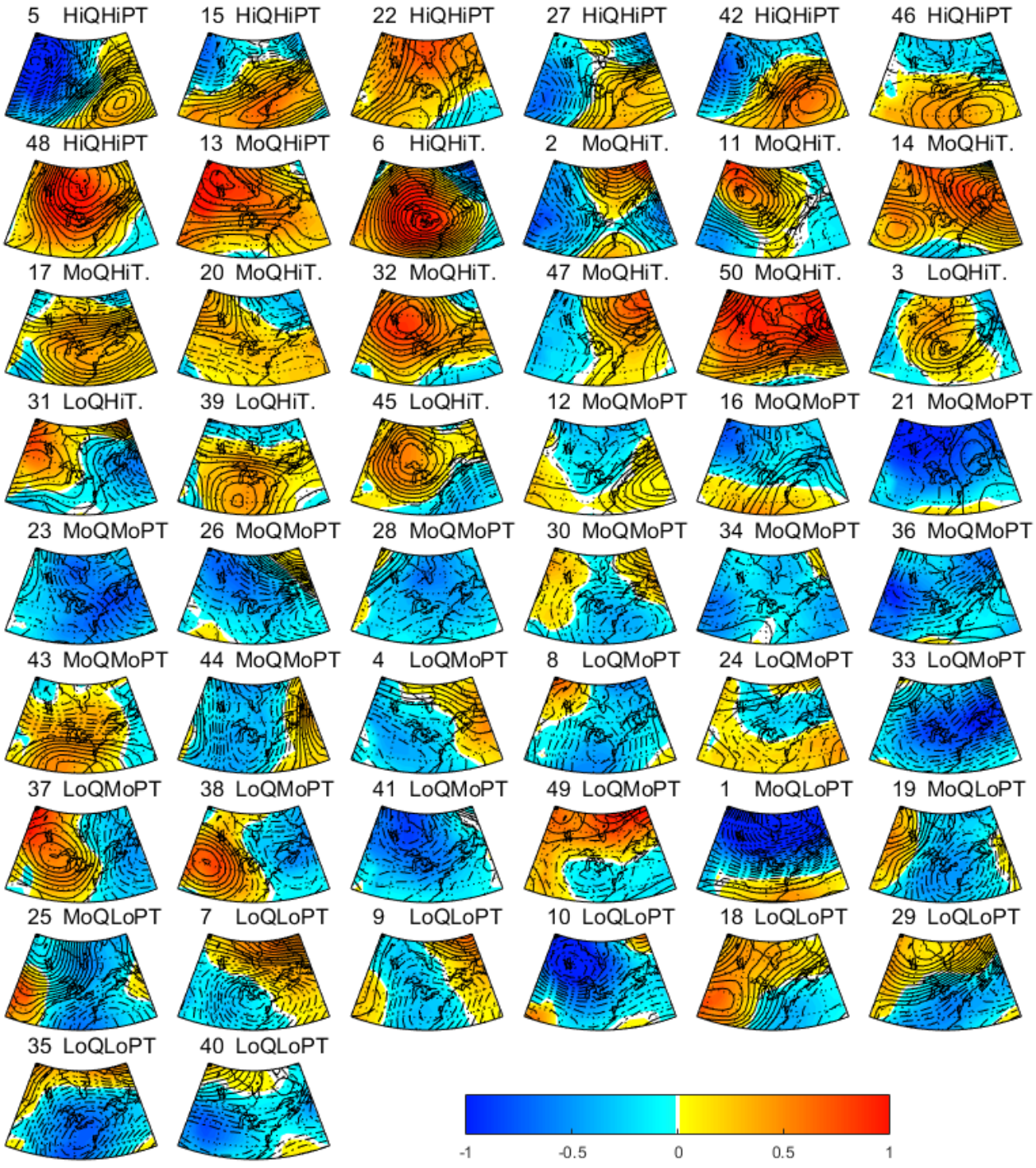

Figure 3-11 Internal change of T850 (shade) and Z500 (black lines, interval 2m) between the historical and the 2040's period in January-February for each member.

3.5.4 Lag between atmospheric circulation shifts, local climate conditions and streamflow

Results show that interclass variability in the increase in January-February streamflow is mostly due to temperature and precipitation variability. The members with the highest increase in precipitation and temperature (HiPT) are the members associated with the highest streamflow increases, except for MoQHiPT (Table 3-3). The members associated with the lowest increase in precipitation and temperature (LoPT) show the lowest streamflow increase (LoQLoPT). Three other members of LoPT are associated with higher streamflow increase (MoQLoPT) which can be due to more precipitation and snowfall despite a lower warming (Figure 3-7).

Within the other two weather classes, HiT and MoPT, a similar change in January-February weather conditions translates to a large range in streamflow projections. These discrepancies between the evolution of weather conditions and streamflow volume in January-February can be associated to a delay between weather conditions and streamflow. To account for the routing delay between rain/snowmelt events and streamflow observed at the outlet, our analyses use a lag-time of 6 days between the precipitation/temperature and the streamflow. Any remaining delay between weather conditions and streamflow could occur due to snowpack remaining from the previous months. Figure 3-10 shows a low variability between all MoPT members and all HiT members in term of change in starting snowpack volume suggesting a low impact of snowpack remaining at the end of December on change in January-February streamflow. In the meanwhile, snowpack remaining at the end of January-February is decreasing at a higher rate for MoQMoPT members as compared to LoQMoPT members and for MoQHiT members compared to LoQHiT members (Figure 3-10) which may be associated with a higher increase in snowmelt (Figure 3-7). However, these two classes show very similar change in temperature and precipitation (Figure 3-7)

suggesting that average weather change obscures intra-seasonal variability change. For example, if more snow fall in the second half of February and temperature stays below the freezing point, this snow is likely to melt in March and is therefore not counted in the January-February streamflow.

The discrepancy between change in weather conditions and streamflow can also be due to groundwater recharge/discharge variability. The lower streamflow increase in LoQHiT is for example associated simultaneously with a lower increase in groundwater flow and a lower increase in November-December precipitation amount (Figure 3-10). A correlation close to 0.7 between the 50 members November-December change in precipitation amount and the January-February change in groundwater flow confirms the connexion between fall precipitation and winter groundwater flow. These results emphasize the role of processes delaying the streamflow (i.e. Snowpack, Groundwater) and the need to study the succession of different atmospheric patterns leading to the modulation of streamflow.

3.5.5 Spatial variability of streamflow change modulation

The changes in the amount of rain and snowmelt between the historical period and the 2040's are visually similar for three of the watersheds (Figure 3-7). The Big Creek watershed is distinctly different as it shows a lower snowmelt contribution to streamflow (Figure 3-7). This suggests that there will be less snow available to be melted in this watershed as it is situated in the southern part of the study area near Lake Erie and experiences the mildest winters (Figure 3-5). In this watershed, the snowmelt volume is expected to increase only slightly in January (Figure 3-4). The increase in snowmelt is also expected to occur only in January for Thames River while the increase will be

stronger in February for Grand and Credit River. A similar South-North pattern is observed in previous studies. A high increase in streamflow in December and January followed by a decrease in streamflow in February was simulated for the Canard watershed near Lake Erie (Rahman et al., 2012) while this shift is expected to occur between February and March further north near Lake Ontario (Grillakis et al., 2011; Sultana and Coulibaly, 2011) or Lake Simcoe (Kuo et al., 2017; Oni et al., 2014). These results suggest that the winter increase in streamflow is expected to be lower in the warmest watersheds classically situated further south, in lowlands and close to the Great Lakes. In these watersheds the snowpack was already reduced in the historical period and the further warming is not expected to increase the snowmelt contribution to the streamflow. However, similar to previous studies in southern Ontario, the reduced snowpack is not projected to decrease the streamflow in winter because the winter precipitation are also projected to increase as suggested in the majority of the climate models (Zhang et al., 2019).

3.6 Conclusion

This study used a 50-member ensemble of regional climate data, forced with the IPCC RCP8.5 scenario, as input in the PRMS hydrological model to show how the internal variability of climate is transferred to the near future winter (January-February) projections of streamflow in four diverse watersheds in southern Ontario. An ascending hierarchical classification was used to construct classes of similar change in temperatures/precipitations/streamflow and define streamflow change probabilities and associated regional atmospheric drivers. First, the results showed that all members of the ensemble are associated with a January-February increase in streamflow due to a strong warming trend and an increase in precipitation projected by the RCP8.5 scenario. Second, the results suggested that the future increase in temperature and precipitation in January-February

will be modulated by the internal variability of climate with implication for hydrological processes. We projected:

(i) 14% of the ensemble showing a large (small) increase in the near future streamflow due to the modulation of rain and snowmelt associated with the development of high (low) pressure anomalies in the east coast of North America.

(ii) 16% of the ensemble showing a moderate streamflow enhancement due to an increase in the rainfall to snowfall ratio associated with warmer conditions driven by high pressure over the Great Lakes region.

(iii) 38% of the ensemble showing a change in temperature and precipitations close to the 50-members average with a small contribution of internal variability of climate to the long-term trends in temperature and precipitation in southern Ontario.

The evolution of streamflow in January-February will be also modulated by inter-member variability of groundwater recharge from November-December precipitation and by the evolution of snow accumulation/melting due to the timing in the increase of temperature and precipitation.

This study focussed on average change while the intra-seasonal variability of atmospheric circulation may greatly impact the streamflow and especial high-flows due to day to day variability. The use of the same regional ensemble together with a classification of daily atmospheric fields would be useful to assess the future projections of high flows in the region. Despite a large number of regional climate simulations used here to drive a hydrological model, the results are derived from a single model chain (CanESM2, CRCM5 and PRMS). As a result,

this ensemble does not consider other important sources of uncertainty from emission scenario and model structure. Future studies could use other global climate models and different scenarios and can be extended to the end of the 21st century. Other hydrological models could also be used to increase the confidence regarding the projections of hydrological processes. This work is important to assess the natural variability of the hydrological projections and help the society to be prepared for large range of possible changes in flooding regimes in future.

3.7 Acknowledgments

Financial support for this study was provided by the Natural Sciences and Engineering Research Council (NSERC) of Canada through the FloodNet Project. The production of ClimEx was funded within the ClimEx project by the Bavarian State Ministry for the Environment and Consumer Protection. The CRCM5 was developed by the ESCER centre of Université du Québec à Montréal (UQAM; www.escer.uqam.ca) in collaboration with Environment and Climate Change Canada. We acknowledge Environment and Climate Change Canada's Canadian Centre for Climate Modelling and Analysis for executing and making available the CanESM2 Large Ensemble simulations used in this study, and the Canadian Sea Ice and Snow Evolution Network for proposing the simulations. Computations with the CRCM5 for the ClimEx project were made on the SuperMUC supercomputer at Leibniz Supercomputing Centre (LRZ) of the Bavarian Academy of Sciences and Humanities. The operation of this supercomputer is funded via the Gauss Centre for Supercomputing (GCS) by the German Federal Ministry of Education and Research and the Bavarian State Ministry of Education, Science and the Arts. We also acknowledge Natural Resources Canada for their contribution in providing climate data sets, Global Water Future Program for their support and the reviewers for their constructive comments on the paper.

3.8 References

Barnett, T. P., Adam, J. C. and Lettenmaier, D. P.: Potential impacts of a warming climate on water availability in snow-dominated regions, Nature, 438(7066), 303–309, doi:10.1038/nature04141, 2005.

Boorman, D. B., Williams, R. J., Hutchins, M. G., Penning, E., Groot, S. and Icke, J.: A model selection protocol to support the use of models for water management, Hydrol. Earth Syst. Sci., 11(1), 634–646, 2007.

Bradbury, J. A., Dingman, S. L. and Keim, B. D.: New England drought and relations with large scale atmospheric circulation patterns, J. Am. Water Resour. Assoc., 38(5), 1287–1299, doi:10.1111/j.1752-1688.2002.tb04348.x, 2002.

Byun, K., Chiu, C.-M. and Hamlet, A. F.: Effects of 21st century climate change on seasonal flow regimes and hydrologic extremes over the Midwest and Great Lakes region of the US, Sci. Total Environ., 650, 1261–1277, doi:10.1016/j.scitotenv.2018.09.063, 2019.

Champagne, O., Arain, M. A. and Coulibaly, P.: Atmospheric circulation amplifies shift of winter streamflow in Southern Ontario, J. Hydrol., 124051, doi:10.1016/j.jhydrol.2019.124051, 2019.

Clark, M. P., Wilby, R. L., Gutmann, E. D., Vano, J. A., Gangopadhyay, S., Wood, A. W., Fowler, H. J., Prudhomme, C., Arnold, J. R. and Brekke, L. D.: Characterizing Uncertainty of the Hydrologic Impacts of Climate Change, Curr. Clim. Change Rep., 2(2), 55–64, doi:10.1007/s40641-016-0034-x, 2016.

Dai, A., Fyfe, J. C., Xie, S.-P. and Dai, X.: Decadal modulation of global surface temperature by internal climate variability, Nat. Clim. Change, 5(6), 555–559, doi:10.1038/nclimate2605, 2015.

Deser, C., Phillips, A. S., Alexander, M. A. and Smoliak, B. V.: Projecting North American climate over the next 50 years: uncertainty due to internal variability*, J. Clim., 27(6), 2271–2296, 2014.

Devia, G. K., Ganasri, B. P. and Dwarakish, G. S.: A Review on Hydrological Models, Aquat. Procedia, 4, 1001–1007, doi:10.1016/j.aqpro.2015.02.126, 2015.

Dressler, K. A., Leavesley, G. H., Bales, R. C. and Fassnacht, S. R.: Evaluation of gridded snow water equivalent and satellite snow cover products for mountain basins in a hydrologic model, Hydrol. Process., 20(4), 673–688, doi:10.1002/hyp.6130, 2006.

Erler, A. R., Frey, S. K., Khader, O., d'Orgeville, M., Park, Y.-J., Hwang, H.-T., Lapen, D., Peltier, W. R. and Sudicky, E. A.: Simulating Climate Change Impacts on Surface Water Resources within a Lake Affected Region using Regional Climate Projections, Water Resour. Res., doi:10.1029/2018WR024381, 2018.

Fowler, H. J., Blenkinsop, S. and Tebaldi, C.: Linking climate change modelling to impacts studies: recent advances in downscaling techniques for hydrological modelling, Int. J. Climatol., 27(12), 1547–1578, doi:10.1002/joc.1556, 2007.

Fyfe, J. C., Derksen, C., Mudryk, L., Flato, G. M., Santer, B. D., Swart, N. C., Molotch, N. P., Zhang, X., Wan, H., Arora, V. K., Scinocca, J. and Jiao, Y.: Large near-term projected snowpack loss over the western United States, Nat. Commun., 8(1), doi:10.1038/ncomms14996, 2017.

Gardner, M. A., Morton, C. G., Huntington, J. L., Niswonger, R. G. and Henson, W. R.: Input data processing tools for the integrated hydrologic model GSFLOW, Environ. Model. Softw., 109, 41–53, doi:10.1016/j.envsoft.2018.07.020, 2018.

Gelfan, A., Semenov, V. A., Gusev, E., Motovilov, Y., Nasonova, O., Krylenko, I. and Kovalev, E.: Large-basin hydrological response to climate model outputs: uncertainty caused by internal atmospheric variability, Hydrol. Earth Syst. Sci., 19(6), 2737–2754, doi:10.5194/hess-19-2737-2015, 2015.

Grillakis, M. G., Koutroulis, A. G. and Tsanis, I. K.: Climate change impact on the hydrology of Spencer Creek watershed in Southern Ontario, Canada, J. Hydrol., 409(1–2), 1–19, doi:10.1016/j.jhydrol.2011.06.018, 2011.

Hamlet, A. F. and Lettenmaier, D. P.: Effects of 20th century warming and climate variability on flood risk in the western U.S., Water Resour. Res., 43(6), doi:10.1029/2006WR005099, 2007.

Harding, B. L., Wood, A. W. and Prairie, J. R.: The implications of climate change scenario selection for future streamflow projection in the Upper Colorado River Basin, Hydrol. Earth Syst. Sci., 16(11), 3989–4007, doi:10.5194/hess-16-3989-2012, 2012.

Hawkins, E. and Sutton, R.: The Potential to Narrow Uncertainty in Regional Climate Predictions, Bull. Am. Meteorol. Soc., 90(8), 1095–1108, doi:10.1175/2009BAMS2607.1, 2009.

Hoegh-Guldberg, O., Jacob, D., Taylor, M., Bindi, M., Brown, S., Camilloni, I., Diedhiou, A., Djalante, R., Ebi, K. L., Engelbrecht, F., Guiot, J., Hijioka, Y., Mehrotra, S., Seneviratne, S. I., Thomas, A., Warren, R., Halim, S. A., Achlatis, M., Alexander, L. V., Berry, P., Boyer, C., Byers, E., Brilli, L., Buckeridge, M., Cheung, W., Craig, M., Evans, J., Fischer, H., Fraedrich, K., Ganase, A., Gattuso, J. P., Bolaños, T. G., Hanasaki, N., Hayes, K., Hirsch, A., Jones, C., Jung, T., Kanninen, M., Krinner, G., Lawrence, D., Ley, D., Liverman, D., Mahowald, N., Meissner, K. J., Millar, R., Mintenbeck, K., Mix, A. C., Notz, D., Nurse, L., Okem, A., Olsson, L., Oppenheimer, M., Paz, S., Petersen, J., Petzold, J., Preuschmann, S., Rahman, M. F., Scheuffele, H., Schleussner, C.-F., Séférian, R., Sillmann, J., Singh, C., Slade, R., Stephenson, K., Stephenson, T., Tebboth, M., Tschakert, P., Vautard, R., Wehner, M., Weyer, N. M., Whyte, F., Yohe, G., Zhang, X., Zougmoré, R. B., Marengo, J. A., Pereira, J. and Sherstyukov, B.: Impacts of 1.5°C of Global Warming on Natural and Human Systems, , 138, 2018.

Ines, A. V. M. and Hansen, J. W.: Bias correction of daily GCM rainfall for crop simulation studies, Agric. For. Meteorol., 138(1–4), 44–53, doi:10.1016/j.agrformet.2006.03.009, 2006.

Kay, J. E., Deser, C., Phillips, A., Mai, A., Hannay, C., Strand, G., Arblaster, J. M., Bates, S. C., Danabasoglu, G., Edwards, J., Holland, M., Kushner, P., Lamarque, J.-F., Lawrence, D., Lindsay, K., Middleton, A., Munoz, E., Neale, R., Oleson, K., Polvani, L. and Vertenstein, M.: The Community Earth System Model (CESM) Large Ensemble Project: A Community Resource for Studying Climate Change in the Presence of Internal Climate Variability, Bull. Am. Meteorol. Soc., 96(8), 1333–1349, doi:10.1175/BAMS-D-13-00255.1, 2015.

Khakbaz, B., Imam, B., Hsu, K. and Sorooshian, S.: From lumped to distributed via semi-distributed: Calibration strategies for semi-distributed hydrologic models, J. Hydrol., 418–419, 61–77, doi:10.1016/j.jhydrol.2009.02.021, 2012.

Kour, R., Patel, N. and Krishna, A. P.: Climate and hydrological models to assess the impact of climate change on hydrological regime: a review, Arab. J. Geosci., 9(9), doi:10.1007/s12517-016-2561-0, 2016.

Kumar, S., Allan, R. P., Zwiers, F., Lawrence, D. M. and Dirmeyer, P. A.: Revisiting trends in wetness and dryness in the presence of internal climate variability and water limitations over land: WETNESS AND DRYNESS TRENDS OVER LAND, Geophys. Res. Lett., 42(24), 10,867-10,875, doi:10.1002/2015GL066858, 2015.

Kuo, C. C., Gan, T. Y. and Higuchi, K.: Evaluation of Future Streamflow Patterns in Lake Simcoe Subbasins Based on Ensembles of Statistical Downscaling, J. Hydrol. Eng., 22(9), 04017028, doi:10.1061/(ASCE)HE.1943-5584.0001548, 2017.

Lafaysse, M., Hingray, B., Mezghani, A., Gailhard, J. and Terray, L.: Internal variability and model uncertainty components in future hydrometeorological projections: The Alpine Durance basin, Water Resour. Res., 50(4), 3317–3341, doi:10.1002/2013WR014897, 2014.

Leavesley, G. H., Lichty, R. W., Troutman, B. M. and Saindon, L. G.: Precipitation-runoff modeling system; user's manual., 1983.

Leduc, M., Mailhot, A., Frigon, A., Martel, J.-L., Ludwig, R., Brietzke, G. B., Giguère, M., Brissette, F., Turcotte, R., Braun, M. and Scinocca, J.: The ClimEx Project: A 50-Member Ensemble of Climate Change Projections at 12-km Resolution over Europe and Northeastern North America with the Canadian Regional Climate Model (CRCM5), J. Appl. Meteorol. Climatol., 58(4), 663–693, doi:10.1175/JAMC-D-18-0021.1, 2019.

Leng, G., Huang, M., Voisin, N., Zhang, X., Asrar, G. R. and Leung, L. R.: Emergence of new hydrologic regimes of surface water resources in the conterminous United States under future warming, Environ. Res. Lett., 11(11), 114003, doi:10.1088/1748-9326/11/11/114003, 2016.

Liao, C. and Zhuang, Q.: Quantifying the Role of Snowmelt in Stream Discharge in an Alaskan Watershed: An Analysis Using a Spatially Distributed Surface Hydrology Model: ROLE OF SNOWMELT IN STREAMFLOW IN ALASKA, J. Geophys. Res. Earth Surf., 122(11), 2183–2195, doi:10.1002/2017JF004214, 2017.

Lorenz, E. N.: Deterministic Nonperiodic Flow, J. Atmospheric Sci., 20(2), 130–141, doi:10.1175/1520-0469(1963)020<0130:DNF>2.0.CO;2, 1963.

Mallakpour, I. and Villarini, G.: Investigating the relationship between the frequency of flooding over the central United States and large-scale climate, Adv. Water Resour., 92, 159–171, doi:10.1016/j.advwatres.2016.04.008, 2016.

Markstrom, S. L., Regan, R. S., Hay, L. E., Viger, R. J., Payn, R. A. and LaFontaine, J. H.: precipitation-runoff modeling system, version 4: U.S. Geological Survey Techniques and Methods., 2015.

Martynov, A., Sushama, L. and Laprise, R.: Simulation of temperate freezing lakes by one-dimensional lake models: Performance assessment for interactive coupling with regional climate models, Boreal Environ. Res., 15(2), 143–164, 2010.

Mastin, M. C., Chase, K. J. and Dudley, R. W.: Changes in Spring Snowpack for Selected Basins in the United States for Different Climate-Change Scenarios, Earth Interact., 15(23), 1–18, doi:10.1175/2010EI368.1, 2011.

McKenney, D. W., Hutchinson, M. F., Papadopol, P., Lawrence, K., Pedlar, J., Campbell, K., Milewska, E., Hopkinson, R. F., Price, D. and Owen, T.: Customized Spatial Climate Models for North America, Bull. Am. Meteorol. Soc., 92(12), 1611–1622, doi:10.1175/2011BAMS3132.1, 2011.

Meinshausen, M., Smith, S. J., Calvin, K., Daniel, J. S., Kainuma, M. L. T., Lamarque, J.-F., Matsumoto, K., Montzka, S. A., Raper, S. C. B., Riahi, K., Thomson, A., Velders, G. J. M. and van Vuuren, D. P. P.: The RCP greenhouse gas concentrations and their extensions from 1765 to 2300, Clim. Change, 109(1–2), 213–241, doi:10.1007/s10584-011-0156-z, 2011.

Moriasi, D. N., Arnold, J. G., Van Liew, M. W., Bingner, R. L., Harmel, R. D. and Veith, T. L.: Model evaluation guidelines for systematic quantification of accuracy in watershed simulations, Trans. ASABE, 50(3), 885–900, 2007.

Newlands, N. K., Davidson, A., Howard, A. and Hill, H.: Validation and inter-comparison of three methodologies for interpolating daily precipitation and temperature across Canada, Environmetrics, 22(2), 205–223, doi:10.1002/env.1044, 2011.

Ning, L. and Bradley, R. S.: Winter climate extremes over the northeastern United States and southeastern Canada and teleconnections with large-scale modes of climate variability*, J. Clim., 28(6), 2475–2493, 2015.

Oni, S. K., Futter, M. N., Molot, L. A., Dillon, P. J. and Crossman, J.: Uncertainty assessments and hydrological implications of climate change in two adjacent agricultural catchments of a rapidly urbanizing watershed, Sci. Total Environ., 473–474, 326–337, doi:10.1016/j.scitotenv.2013.12.032, 2014.

Rahman, M., Bolisetti, T. and Balachandar, R.: Hydrologic modelling to assess the climate change impacts in a Southern Ontario watershed, Can. J. Civ. Eng., 39(1), 91–103, doi:10.1139/l11-112, 2012.

Rowell, D. P.: Sources of uncertainty in future changes in local precipitation, Clim. Dyn., 39(7–8), 1929–1950, doi:10.1007/s00382-011-1210-2, 2012.

Schoof, J. T.: Statistical Downscaling in Climatology: Statistical Downscaling, Geogr. Compass, 7(4), 249–265, doi:10.1111/gec3.12036, 2013.

Seiller, G. and Anctil, F.: Climate change impacts on the hydrologic regime of a Canadian river: comparing uncertainties arising from climate natural variability and lumped hydrological model structures, Hydrol. Earth Syst. Sci., 18(6), 2033–2047, doi:10.5194/hess-18-2033-2014, 2014.

Šeparović, L., Alexandru, A., Laprise, R., Martynov, A., Sushama, L., Winger, K., Tete, K. and Valin, M.: Present climate and climate change over North America as simulated by the fifth-generation Canadian regional climate model, Clim. Dyn., 41(11–12), 3167–3201, doi:10.1007/s00382-013-1737-5, 2013.

Sigmond, M., Fyfe, J. C. and Swart, N. C.: Ice-free Arctic projections under the Paris Agreement, Nat. Clim. Change, 8(5), 404–408, doi:10.1038/s41558-018-0124-y, 2018.

Stephens, G. L., L'Ecuyer, T., Forbes, R., Gettelmen, A., Golaz, J.-C., Bodas-Salcedo, A., Suzuki, K., Gabriel, P. and Haynes, J.: Dreary state of precipitation in global models: MODEL AND OBSERVED PRECIPITATION, J. Geophys. Res. Atmospheres, 115(D24), doi:10.1029/2010JD014532, 2010.

Sultana, Z. and Coulibaly, P.: Distributed modelling of future changes in hydrological processes of Spencer Creek watershed, Hydrol. Process., 25(8), 1254–1270, doi:10.1002/hyp.7891, 2011.

Surfleet, C. G., Tullos, D., Chang, H. and Jung, I.-W.: Selection of hydrologic modeling approaches for climate change assessment: A comparison of model scale and structures, J. Hydrol., 464–465, 233–248, doi:10.1016/j.jhydrol.2012.07.012, 2012.

Suriano, Z. J. and Leathers, D. J.: Synoptic climatology of lake-effect snowfall conditions in the eastern Great Lakes region: SYNOPTIC CLIMATOLOGY OF LAKE-EFFECT SNOWFALL CONDITIONS, Int. J. Climatol., 37(12), 4377–4389, doi:10.1002/joc.5093, 2017.

Teng, F., Huang, W., Cai, Y., Zheng, C. and Zou, S.: Application of Hydrological Model PRMS to Simulate Daily Rainfall Runoff in Zamask-Yingluoxia Subbasin of the Heihe River Basin, Water, 9(10), 769, doi:10.3390/w9100769, 2017.

Teng, F., Huang, W. and Ginis, I.: Hydrological modeling of storm runoff and snowmelt in Taunton River Basin by applications of HEC-HMS and PRMS models, Nat. Hazards, 91(1), 179–199, doi:10.1007/s11069-017-3121-y, 2018.

Thiombiano, A. N., El Adlouni, S., St-Hilaire, A., Ouarda, T. B. M. J. and El-Jabi, N.: Nonstationary frequency analysis of extreme daily precipitation amounts in Southeastern Canada using a peaks-over-threshold approach, Theor. Appl. Climatol., 129(1–2), 413–426, doi:10.1007/s00704-016-1789-7, 2017.

Thompson, D. W. J., Barnes, E. A., Deser, C., Foust, W. E. and Phillips, A. S.: Quantifying the Role of Internal Climate Variability in Future Climate Trends, J. Clim., 28(16), 6443–6456, doi:10.1175/JCLI-D-14-00830.1, 2015.

Werner, A. T., Schnorbus, M. A., Shrestha, R. R., Cannon, A. J., Zwiers, F. W., Dayon, G. and Anslow, F.: A long-term, temporally consistent, gridded daily meteorological dataset for northwestern North America, Sci. Data, 6(1), doi:10.1038/sdata.2018.299, 2019.

Wu, W.-Y., Lan, C.-W., Lo, M.-H., Reager, J. T. and Famiglietti, J. S.: Increases in the annual range of soil water storage at northern middle and high latitudes under global warming, Geophys. Res. Lett., 42, 3903–3910, doi:10.1002/2015gl064110, 2015.

Zhang, Flato, G., Wan, H., Wang, X., Rong, R., Fyfe, J., Li, G., Kharin, V.V., Kirchmeier-Young, M, Vincent, L, Wan, H., Wang, X, Rong, R., Fyfe, J., Li, G. and Kharin, V.V.: Canada's Changing Climate Report, Government of Canada, Ottawa, Ontario., 2019.

Zhuan, M.-J., Chen, J., Shen, M.-X., Xu, C.-Y., Chen, H. and Xiong, L.-H.: Timing of human-induced climate change emergence from internal climate variability for hydrological impact studies, Hydrol. Res., 49(2), 421–437, doi:10.2166/nh.2018.059, 2018.

Chapter 4. Winter hydrometeorological extreme events modulated by large scale atmospheric circulation in southern Ontario.

Champagne Olivier, Leduc Martin, Coulibaly Paulin, Arain M.Altaf., 2019. Winter hydrometeorological extreme events modulated by large scale atmospheric circulation in southern Ontario. *Earth System Dynamics Discussions* https://doi.org/10.5194/esd-2019-56 Accepted for publication.

4.1 Abstract

Extreme events are widely studied across the world because of their major implications for many aspects of society and especially floods. These events are generally studied in terms of precipitation or temperature extreme indices that are often not adapted for regions affected by floods caused by snowmelt. Rain on Snow index has been widely used, but it neglects rain only events which are expected to be more frequent in the future. In this study, we identified a new winter compound index and assessed how large-scale atmospheric circulation controls the past and future evolution of these events in the Great Lakes region. The future evolution of this index was projected using temperature and precipitation from the Canadian Regional Climate Model Large Ensemble (CRCM5-LE). These climate data were used as input in PRMS hydrological model to simulate the future evolution of high flows in three watersheds in Southern Ontario. We also used five recurrent large-scale atmospheric circulation patterns in north-eastern North America and identified how they control the past and future variability of the newly created index and high flows. The results show that daily precipitation higher than 10mm and temperature higher than 5°C were necessary historical conditions to produce high flows in these three watersheds. In the historical period, the occurrences of these heavy rain and warm events as well as high flows were

associated with two main patterns characterized by high Z500 anomalies centered on eastern Great Lakes (regime HP) and the Atlantic Ocean (regime South). These hydrometeorological extreme events will still be associated with the same atmospheric patterns in the near future. The future evolution of the index will be modulated by the internal variability of the climate system as higher Z500 in the east coast will amplify the increase in the number of events, especially the warm events. The relationship between the extreme weather index and high flows will be modified in the future as the snowpack reduces and rain becomes the main component of high flows generation. This study shows the value of the CRCM5-LE dataset to simulate hydrometeorological extreme events in Eastern Canada and to better understand the uncertainties associated with internal variability of climate.

4.2 Introduction

According to the actual pathway of greenhouse gases emissions, temperature will continue to rise in the future with serious implications for society (Hoegh-Guldberg et al., 2018). The amount of precipitation, especially for extreme events, is also projected to increase globally (Kharin et al., 2013), due to the acceleration of the hydrological cycle (Trenberth, 1999). Because extreme precipitation has a great societal impact across the world, internationally coordinated climate indices, built from precipitation and temperature data, are widely used to assess the evolution of different weather extremes (Zhang et al., 2011). Some of these indices such as monthly or annual maximum of precipitation can be used to improve flood management. However, in catchments that receive snowfall, a large number of floods may occur due to a combination of temperature and precipitation extreme events such as Rain on Snow (ROS) (Merz and Blöschl, 2003). The impact of ROS on floods generation has been widely studied in different regions of the world, including

Central Europe (Freudiger et al., 2014), the Alps (Würzer et al., 2016), the Rocky mountains (Musselman et al., 2018) or the New York State (Pradhanang et al., 2013). The projections of these events can be a challenge because they depend on the ability of the climate model to project the precipitation extremes and the aerial extent of snowmelt (McCabe et al., 2007). The climate models improvements allowed recent studies to project the future evolution of ROS (Jeong and Sushama, 2018; Musselman et al., 2018; Surfleet and Tullos, 2013). However strong uncertainties in the projections of such events remain, especially due to the internal variability of climate (Lafaysse et al., 2014). These uncertainties, even with the perfect climate model, will never be eradicated due to the inherently chaotic characteristic of the atmosphere (Lorenz, 1963; Deser et al., 2014). ROS are clearly controlled by large scale atmospheric circulation (Cohen et al., 2015) emphasizing the need to include internal climate variability uncertainties in the future evolution of ROS studies.

The Great Lakes region is one of the areas of the world highly impacted by ROS events in winter (Buttle et al., 2016; Cohen et al., 2015). In this region, previous studies found correlations between precipitation (rain and snow) and temperature extremes and large-scale circulation indices: The negative phase of the Pacific North America oscillation (PNA-) brings more heavy precipitation events in the region south of the Great Lakes (Mallakpour and Villarini, 2016; Thiombiano et al., 2017) and more snowfall in the region North of the Great Lakes (Zhao et al., 2013), due to high moisture transport over the region (Mallakpour and Villarini, 2016). Another study showed a negative phase of PNA and positive phase of North Atlantic Oscillation (NAO) associated with warm days (Ning and Bradley, 2015). Temperature and precipitation uncertainties associated with climate internal variability have also been assessed in North America using a global climate model

large ensemble (GCM-LE) (Deser et al., 2014). These studies generally separate precipitation and temperature while studying compound events, such as ROS, has been recommended recently to improve our understanding of extreme impacts (Leonard et al., 2014). However, the definition of ROS index is also subjected to high uncertainties (Kudo et al., 2017) and this index may not be relevant in regions affected by significant rain only events (Jeong and Sushama, 2018). The goal of this study is to understand the impact of atmospheric circulation on winter hydrometeorological extreme events in the Great Lakes region. We will be using the Canadian Regional Climate Model Large Ensemble (CRCM5-LE), a 50-member regional model ensemble at a 12km resolution produced over north-eastern North America with the following objectives:

(1) Define a regional precipitation and temperature compound index that explains the variability of winter high flows in Southern Ontario, which is the most populated area in the Great Lakes region.

(2) Assess the relationship between this index and the recent large-scale atmospheric circulation.

(3) Investigate the pertinence of the index to explain the future evolution of projected high flows and

(4) Demonstrate how internal variability of climate will modulate the future evolution of atmospheric circulation and number of hydrometeorological extreme events in the region.

4.3 Data and methods

4.3.1 Climate data

Observations of precipitation, minimum temperature and maximum temperature for the winter months (DJF) in the 1957-2012 period were taken from NRCANmet produced by McKenney et al., (2011). These data were generated from an interpolation of Natural Resources Canada and Environment and Climate Change Canada data (ECCC) archives at 10 km spatial resolution. The simulated evolution of precipitation and temperature are from the Canadian Regional Climate Model Large Ensemble (CRCM5-LE). CRCM5-LE is a 50-member regional model ensemble at 12km resolution produced over north-eastern North America in the scope of the Québec-Bavaria international collaboration on climate change (ClimEx project; Leduc et al., 2019). CRCM5-LE is the downscaled version of the 310km resolution global Canadian model large ensemble (CanESM2-LE, Fyfe et al., 2017; Sigmond et al., 2018). The advantage of using a fine resolution large ensemble is that the processes at a local scale are better represented than a global ensemble and the local climate from each member of CRCM5-LE can be related to atmospheric circulation from CanESM2-LE. Temperature and precipitation from each member of CRCM5-LE have been bias corrected following the method of Ines and Hansen (2006) and using the observations and CRCM5-LE in the 1957-2012 period. For each month of the year, the intensity distribution of temperature was corrected using a normal distribution. For the bias correction of precipitation, the frequency and the daily intensity were bias corrected separately: The precipitation frequency was first corrected by truncating the modelled frequency distribution in order to match the observed distribution. The truncated distribution of precipitation intensity was then corrected with a gamma distribution (Ines and Hansen, 2006). Each CRCM5-LE grid point has been bias-corrected in the

1957-2055 period using the closest NRCANmet point. Using a unique NRCANmet point for each CRCM5-LE point is permitted in our study because of low elevation gradients between points, the spatial variability of temperature and precipitation being more dependent on the proximity of the lakes than the elevation (Scott and Huff, 1996). The bias corrected CRCM5-LE data are reported at each NRCANmet point.

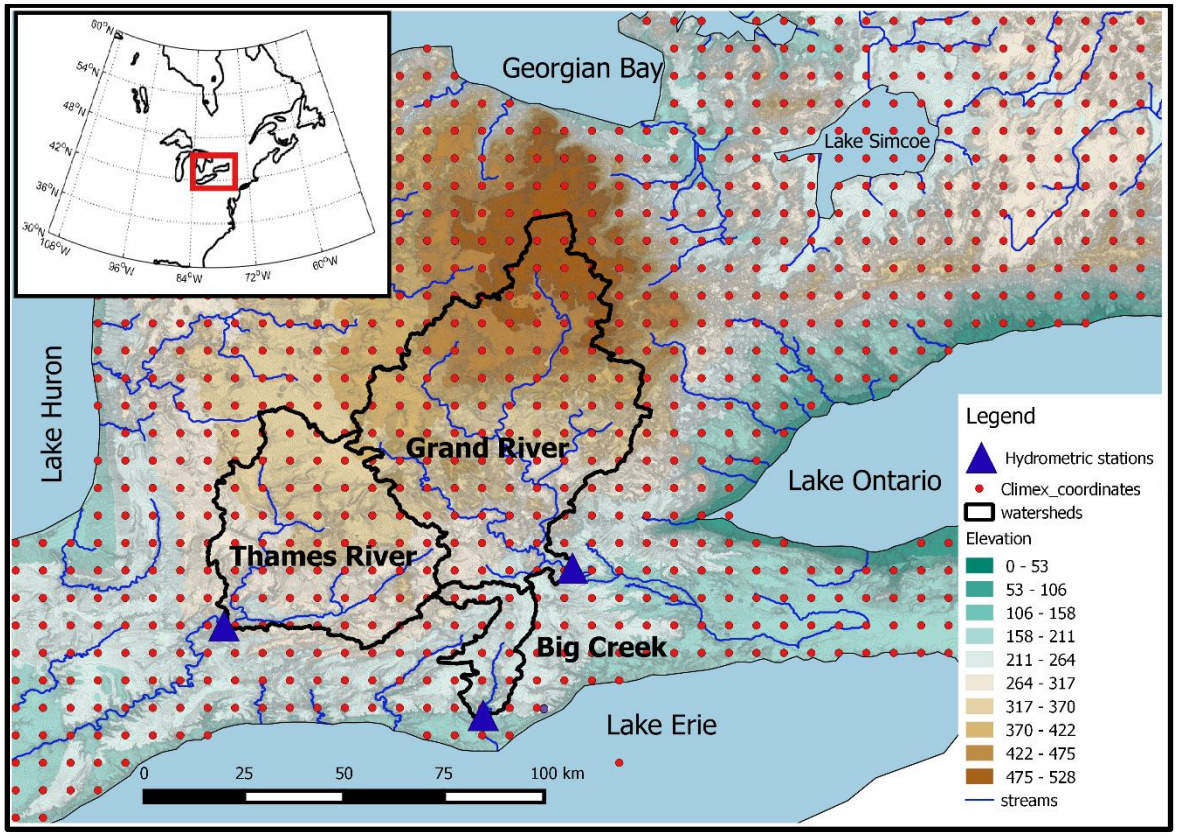

Figure 4-1 Location of the three watersheds and the ClimEx grid points used in this study and situation in the northeastern North American domain (Inset)

4.3.2 Heavy rain and warm index

Streamflow observations from three watersheds in southern Ontario (Figure 4-1) were used to define the daily temperature and precipitation thresholds needed to generate high flows in winter. A high flow event was defined for each watershed as streamflow higher than the 99th percentile.

When more than two days in a row were selected, the events were considered as a single event and only the day with the highest high flow was considered. Figure 4-2 shows for each high flow event the distribution of daily temperature and precipitation amounts from all grids of the watersheds. Only events that produced high flows at least in 2 of the 3 watersheds are shown in Figure 4-2. The precipitation and temperature data are from the day situated three days before the high flow event for Big Creek watershed and two days before the high flow event for Thames and Grand rivers. This lag corresponds to the delay between a rainfall and/or warm event and the peak flow at the outlet

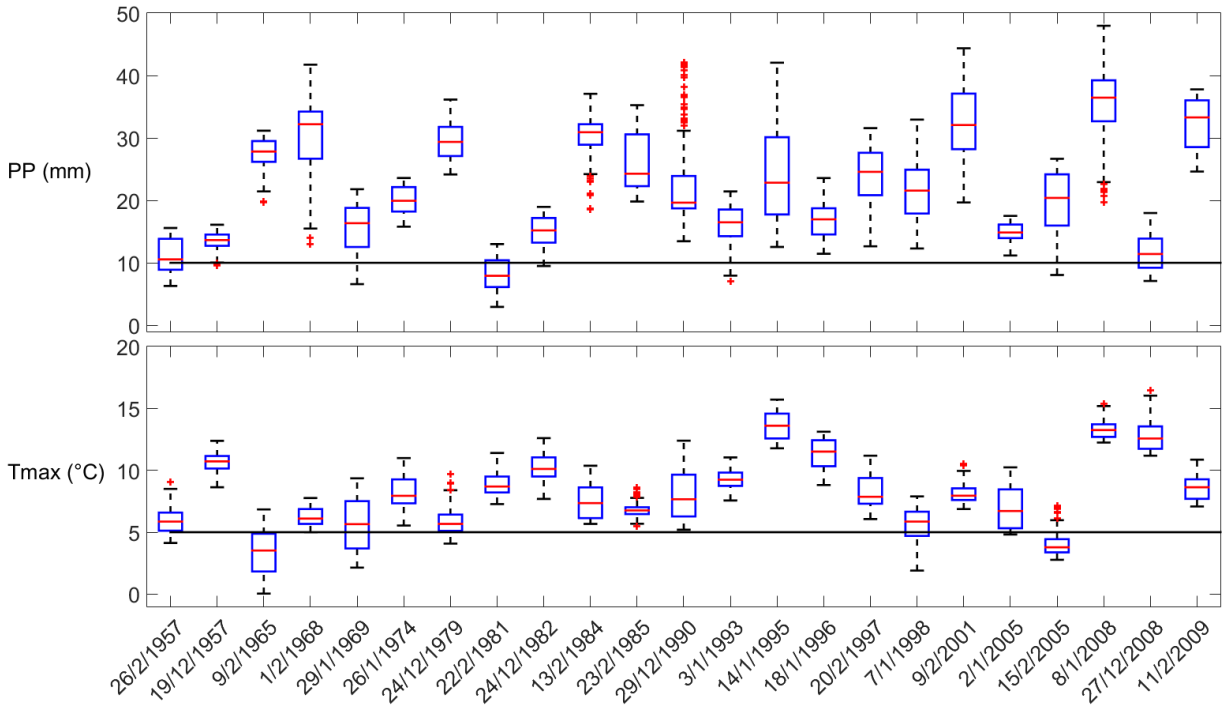

Figure 4-2 Distribution of NRCANmet temperature and precipitation from all 3 watersheds grid-points corresponding to each DJF high-flow event. Boxes extend from the 25th to the 75th percentile, with a horizontal red bar showing the median value. The whiskers are lines extending from each end of the box to the 1.5 interquartile range. Plus signs correspond to outliers. The horizontal black lines correspond to the thresholds used to define DJF weather extreme events.

Figure 4-2 shows a maximum temperature higher than 5°C and precipitation higher than 10mm for most grid points during the high flow events. The index is therefore defined by the number of days with a temperature higher than 5°C and precipitation higher than 10mm. This index defines days with a significant rain and warm event that has the potential to generate a high flow event. The 5°C threshold gives a strong indication that precipitation is in a form of rain, and that the eventual snow in the ground is melting. This index is similar to the Rain on Snow index (ROS) defined by previous studies. The threshold of 10 mm was previously used to define ROS events with floods potential (Cohen et al., 2015; Musselman et al., 2018). Our newly created index can be defined rather as a heavy rain and warm index because snowpack is not integrated in the calculation.

4.3.3 Atmospheric circulation patterns

The recurrent atmospheric patterns in north-eastern North-America were identified by a weather regimes technique computed by a k-means algorithm (Michelangeli et al., 1995). The algorithm used daily geopotential height anomalies at 500hPa level (Z500) from the 20th century reanalyses (20thCR, Compo et al., 2011) and was applied in the 1957-2012 period to the north-eastern part of North America (30 N-60 N/110 W-50 W). Prior to the k-means calculations, we identified the principal components of the Z500 maps that explain 80% of the spatial variance. These principal components have been decomposed in weather regimes thanks to the k-means algorithm. k-means identifies classes centroids using an iteration method that minimizes intra-regime Euclidean distance and maximizes inter-regime Euclidean distance between the principal components of each day. The algorithm is repeated 100 times for each number of class between 2 and 10. The choice of the final class number is decided by a red noise test. This test consists in assessing the

significance of the decomposition against weather regimes calculated from 100 randomly generated theoretical datasets that have the same statistical properties than the original dataset. The weather regimes have been previously calculated for the same domain and the red noise test showed five classes as the most robust choice (Champagne et al., 2019a).

The eigenvectors of the principal components calculated with 20thCR have been used to calculate the daily principal components for each member of CanESM2-LE. This transformation was applied to the daily Z500 normalized anomalies calculated for periods of 30 years between 1950 and 2099. By calculating the anomalies for periods of 30 years we minimized the low frequency variability. Therefore, the internal variability of climate through the 50-members can be fully investigated. Each day of the principal component dataset was then placed to the closest class centroid among the 5 classes previously identified using the historical 20thCR Z500 anomalies. This process was done for each member of CanESM2-LE.

4.3.4 Hydrological modelling

The future evolution of high flows in the three watersheds have been simulated using the Precipitation Runoff Modelling System (PRMS). PRMS is a semi distributed conceptual hydrological model widely used in snow dominated regions (Dressler et al., 2006; Liao and Zhuang, 2017; Mastin et al., 2011; Surfleet et al., 2012; Teng et al., 2017, 2018). PRMS computes the water flowing between hydrological reservoirs (plan canopy interception, snowpack, soil zone, subsurface) for each hydrological response unit (HRU). For a general description of PRMS the reader is referred to Markstrom et al. (2015). Champagne et al. (2019a) previously applied PRMS to these three watersheds and extensively described the parametrization process. PRMS has been

calibrated in the 1989-2009 period using Precipitation, minimum temperature and maximum temperature from NRCANmet. The three steps trial-and-error calibration approach applied to each watershed showed satisfactory results (Champagne et al., 2019a). The streamflow was simulated for each member of the ensemble in the 1957-2055 period using CRCM5-LE bias corrected data described in the section 2.1.

To quantify the winter change in number of high flows due to a change in number of weather extreme events, the theoretical high flows frequency change due to the occurrence change in number of heavy rain and warm events (OCC) have been calculated. For each member of the ensemble, the simulated historical number of high flows events (99th percentile) associated with each weather regime has been multiplied by the change factor between number of rain and warm events in the historical period (1961-1990) and in the future period (2026-2055). The difference between this calculated number of high flows and the historical number of high flows corresponds to OCC. The total change in number of high flows simulated by PRMS (TOT) corresponding to each weather regimes is finally subtracted by OCC for each ensemble member to account for a change in number of high flows not due to a change in number of heavy rain and warm events (DIF).

4.4 Results

4.4.1 Weather regimes in northeastern North America

Five weather regimes have been identified in north-eastern North America according to the red noise test and show distinct weather patterns (Figure 4-3).

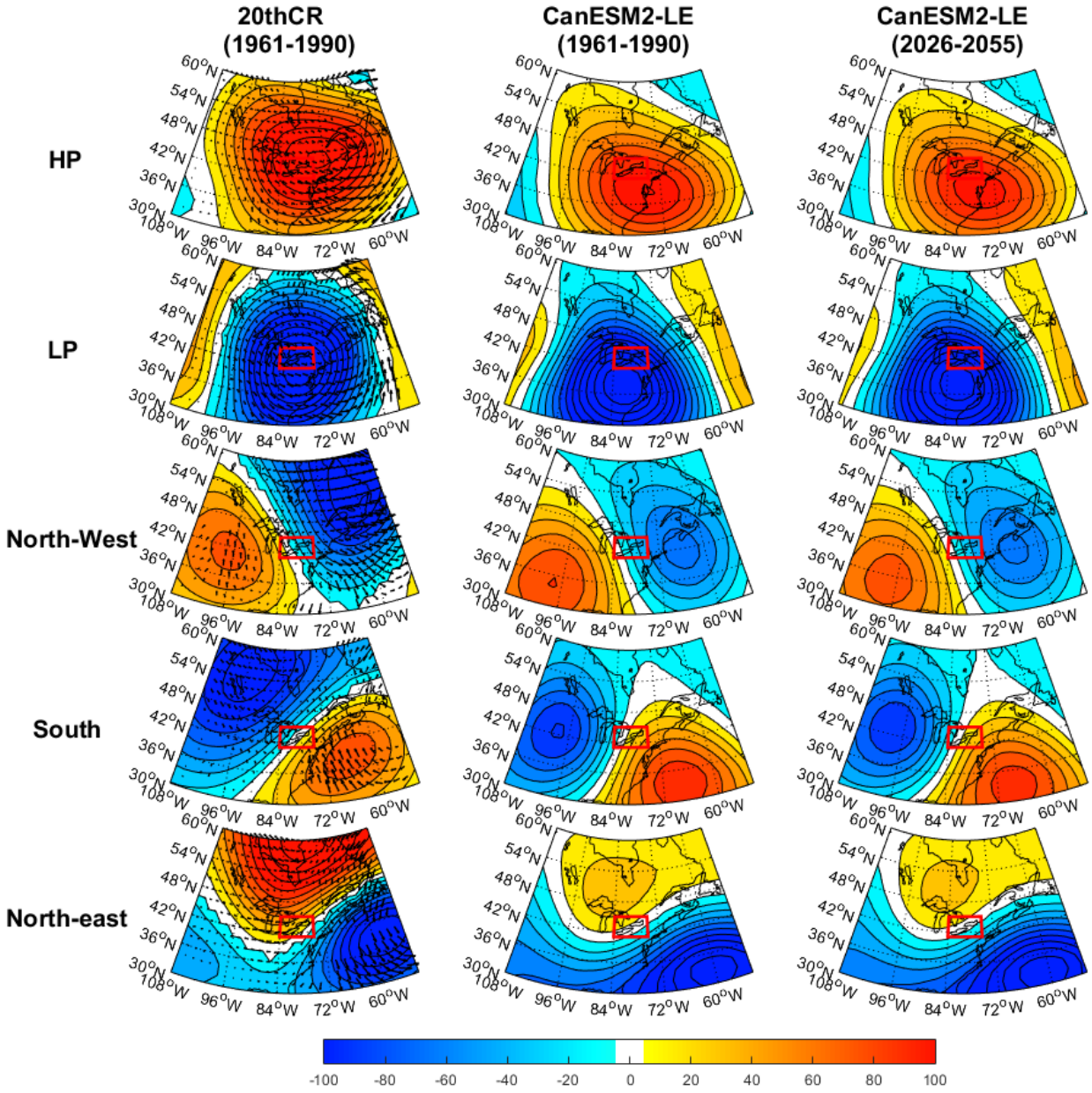

Figure 4-3 Left panels: DJF Z500 anomalies (colours) and winds (vectors) corresponding to Weather regimes calculated with 20thCR in the 1961-1990 period. Mid panels: DJF 50 members average Z500 anomalies calculated with CanESM2-LE in the 1961-1990 period. Right panels: DJF 50 members average Z500 anomalies calculated with CanESM2-LE in the 2026-2055 period.

The weather regimes computed with 20thCR data show two clear opposite patterns characterized by positive (HP) and negative (LP) geopotential height anomalies on the Great Lakes. The regime South was characterized by positive Z500 anomalies in the Atlantic Ocean and negative anomalies in the north-west part of the domain and was associated with southerly winds. The regime North-West had low geopotential height on the Gulf of Saint-Lawrence together with winds from the northwest over the Great Lakes region. Finally, the regime North-East was associated with low geopotential height in the Atlantic Ocean but high geopotential height close to the Arctic that drove north-eastern winds over the Great Lakes

The weather regimes calculated with CanESM2-LE data, using the k-means centroids identified with 20thCR anomalies, have very similar patterns in the historical period (1961-1990) (Figure 4-3). CanESM2 50 members average Z500 anomalies were generally less strong than the 20thCR weather regimes and the anomalies were slightly shifted to the south. Over the Great Lakes, 20thCR and CanESM2-LE Z500 anomalies were similar for most of the regimes excepted for regime South showing higher Z500 anomalies with CanESM2-LE. In the 2026-2055 period the weather regimes show meteorological systems in similar locations, but the anomalies are clearly weaker (Figure 4-3).

4.4.2 Validation of heavy rain and warm index and high flows simulated by CRCM5-LE

The ability of the bias corrected CRCM5-LE data to recreate the number of heavy rain and warm events relative to the number of occurrences of each weather regime is assessed in this section. For the heavy precipitation events the observations show higher number of events during the

occurrence of regime HP (10% of all HP days) compared to other regimes, especially in the southern parts of the region (13% of all HP days) (Figure 4-4).

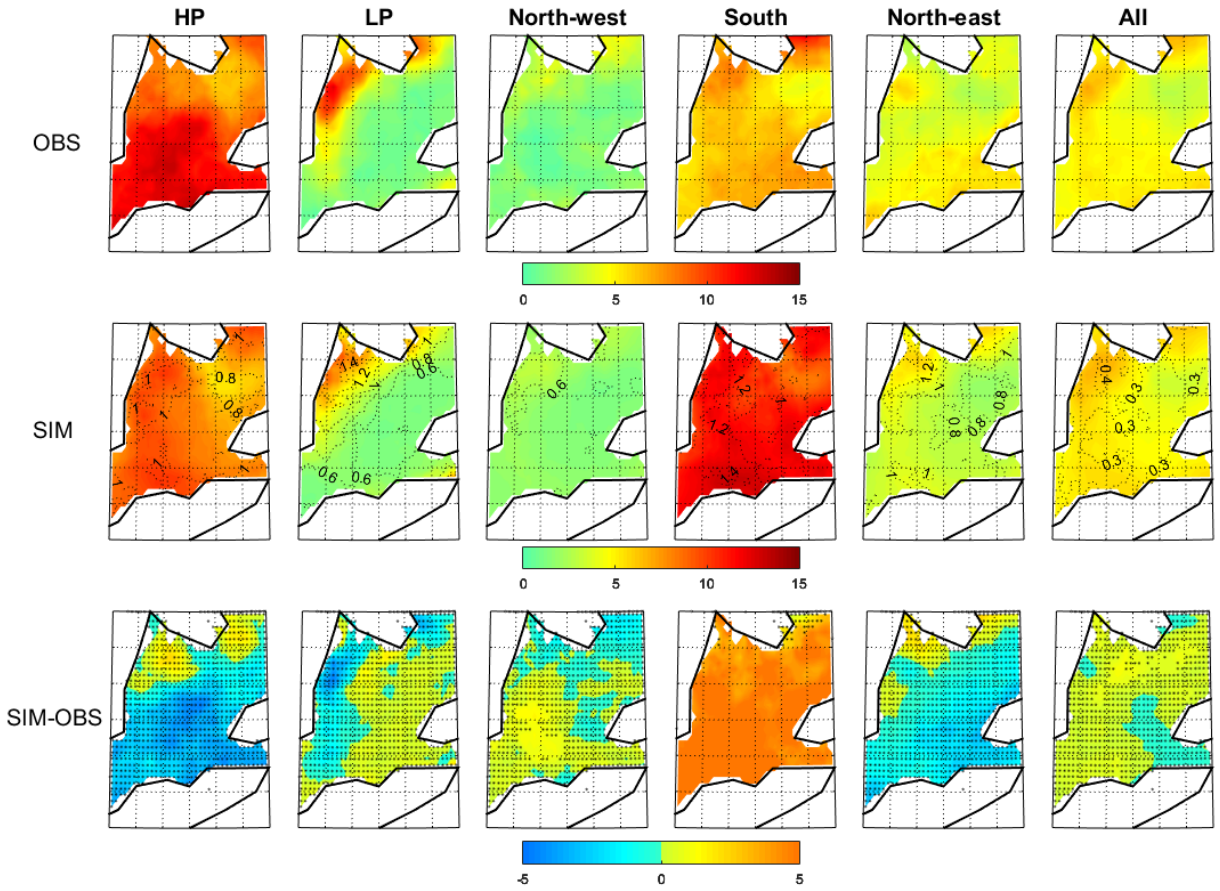

Figure 4-4 Percentage of DJF number of precipitation events relative to DJF occurrence of weather regimes in the historical period (1961-1990) for NRCANmet (OBS, upper panels), simulations from CRCM5-LE 50 members average (SIM, mid panels) and SIM minus OBS (lower panels). The dotted lines in the mid panels represent the standard deviation of the 50-members CRCM5-LE simulated percentage. Stippled regions in the lower panels indicate where the observations lie within the CRCM5-LE ensemble spread.

The regime South shows the second largest occurrence of heavy precipitation events (7% of all South days) while the regime North-West was associated with the least number of observed heavy precipitation events (2% of all North-West days). The number of precipitation events associated with a regime LP is spatially variable with a large number of events limited to the Lake Huron

shoreline (12% of all LP days). The number of heavy precipitation events per winter was generally well recreated by the regional ensemble in the historical period (Figure 4-4). The regime South is the exception with much more events with the 50 members average (11% of all South days) compared to the observations (7% of all South days). In southern areas the simulations were also slightly overestimating the number of heavy precipitation events during regime North-West while underestimating during regime HP (Figure 4-4).

Figure 4-5 shows that the observed number of warm events (7.5% of all days) were overall more frequent than the number of heavy precipitation events (5% of all days, Figure 4-4). The number of warm events occurred more frequently in southern areas, particularly in the Niagara peninsula between Lake Erie and Lake Ontario, where 12-14% of all days were considered as warm days (Figure 4-5). The observed warm events occurred mostly during regime HP (23% of all HP days) while they were non-existent during regime LP (Figure 4-5). The number of warm events was similar between regimes North-West, North-East and South in a large part of the area. In the Niagara peninsula more events were occurring during a regime South (15% of all South days). The simulated number of warm events averaged for all members overestimated the observations and represented 11% of all days (Figure 4-5). This discrepancy was due to an overestimation during regimes North-West and South (Figure 4-5). Specifically, the number of events per occurrence of regime South for the 50 members average (19% of all South days) was twice the number of events calculated with the observations (9%).

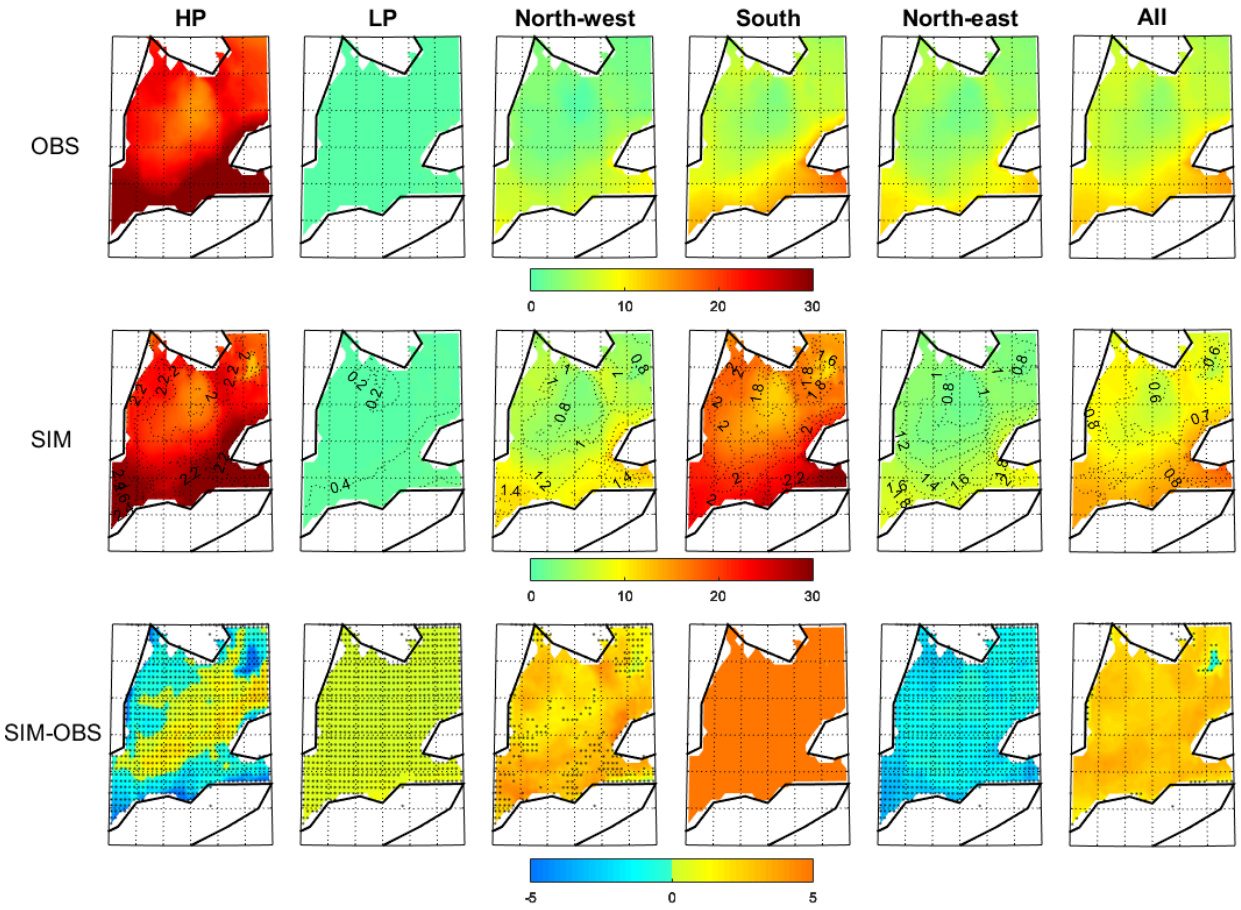

Figure 4-5 Percentage of DJF number of warm events relative to DJF occurrence of weather regime in the historical period (1961-1990) for NRCANmet (OBS, upper panels), simulations from CRCM5-LE 50 members average (SIM, mid panels) and SIM minus OBS (lower panels)). The dotted lines in the mid panels represent the standard deviation of the 50-members CRCM5-LE simulated percentage. Stippled regions in the lower panels indicate where the observations lie within the CRCM5-LE ensemble spread.

The number of compound events, heavy rain and warm temperature was more frequent in the area close to Lake Erie in both observations and simulations if we consider all weather regimes together (Figure 4-6). The number of events was overestimated by the ensemble mean in the northern parts of the region. In this region, many grid points show all members of the ensemble overestimating the number of events. Close to Lake Erie the overestimation was lower and even non-existent in

the Niagara peninsula. These compound index heavy rain and warm events were more frequent during a regime HP in both observations and simulations (4.5% of all HP days). The simulations show a similar number of events during a regime South (4.5% of all South days) but the results largely overestimated the observations (1.5% of all Souths days). Finally, the occurrences of events were very low for LP and North-West (Figure 4-6).

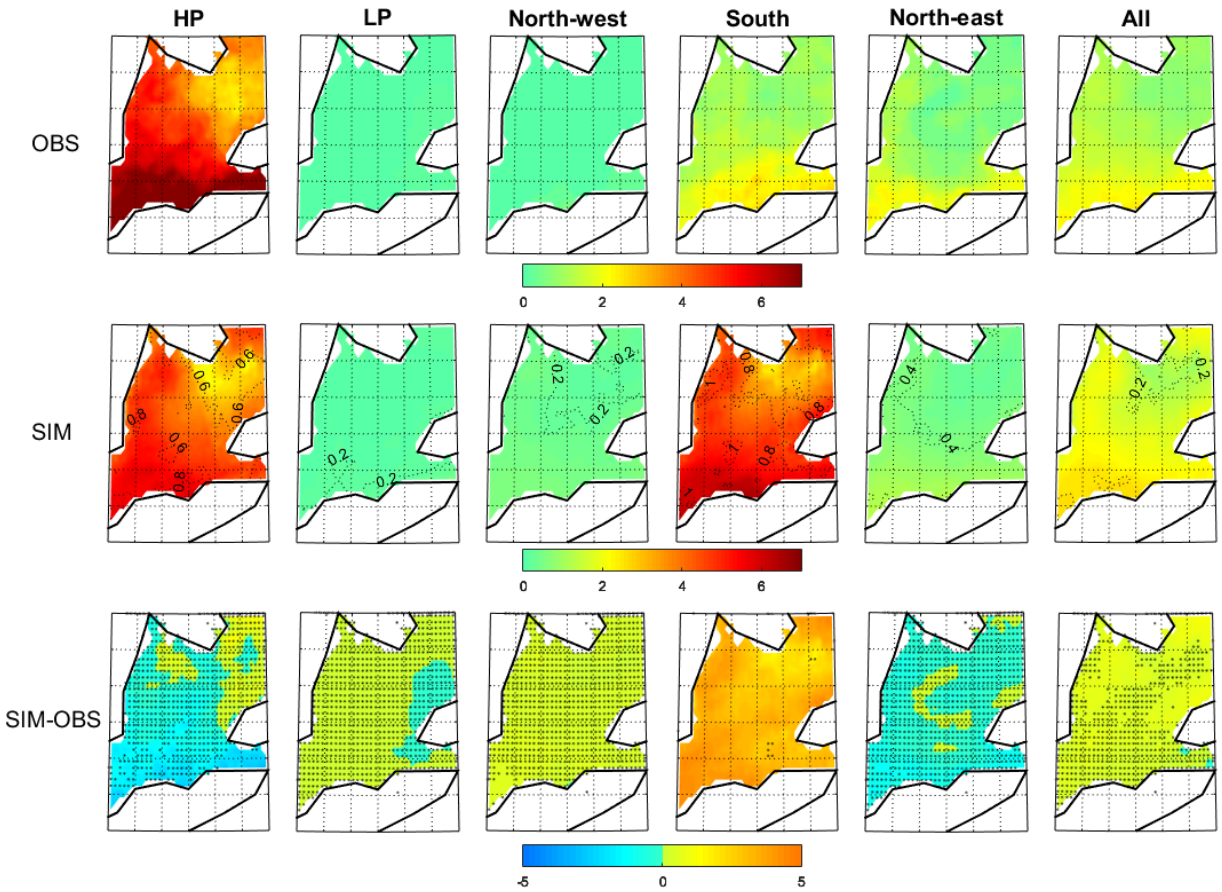

Figure 4-6 Percentage of DJF number of heavy rain and warm events relative to DJF occurrence of weather regimes in the historical period (1961-1990) for NRCANmet (OBS, upper panels), simulations from CRCM5-LE 50 members average (SIM, mid panels) and SIM minus OBS (lower panels). The dotted lines in the mid panels represent the standard deviation of the 50-members CRCM5-LE simulated percentage. Stippled regions in the lower panels indicate where the observations lie within the CRCM5-LE ensemble spread.

The historical distribution of streamflow associated with heavy rain and warm events for the observed streamflow (OBS), streamflow simulated with NRCANmet (CTL) and streamflow simulated for all CRCM5-LE members (ENS) are depicted in Figure 4-7.

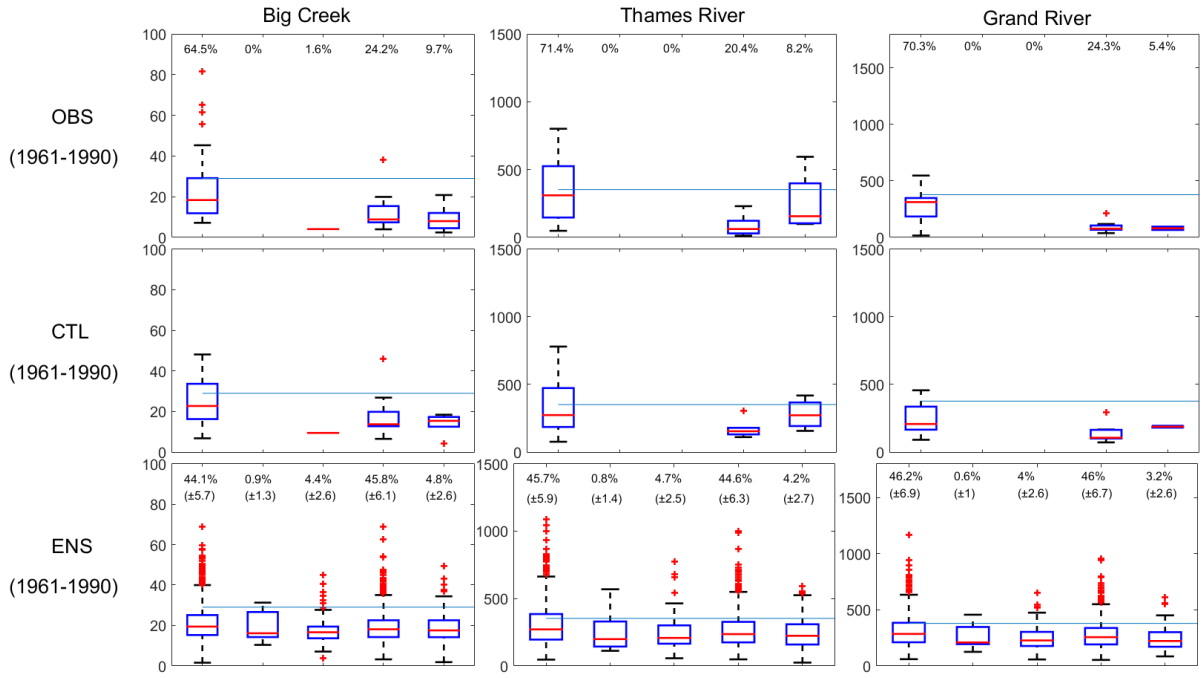

Figure 4-7 First and second rows: Distribution of observed (OBS) and simulated (CTL) daily streamflow corresponding to all heavy rain and warm events calculated from NRCANmet. Lower row: Distribution of simulated streamflow corresponding to all simulated heavy rain and warm events pooled from the entire ensemble pooled for all members (ENS). Boxes extend from the 25th to the 75th percentile, with a horizontal red bar showing the median value. The whiskers are lines extending from each end of the box to the 1.5 interquartile range. Plus signs correspond to outliers. The horizontal blue lines correspond to high flows (99% percentile).

The results show an observed streamflow frequently higher than the high flows threshold when the heavy rain and warm events occurred during a regime HP. The streamflow simulated with NRCANmet weather data (CTL) is underestimated but show a similar inter-regime variability with higher streamflow during HP heavy rain and warm events compared to events associated with

other weather regimes. The 50 simulations from CRCM5-LE show a less strong variability between weather regimes but again higher streamflow when heavy rain and warm events correspond to regimes HP. High flows are also occurring for other weather regimes especially regime South (Figure 4-7).

4.4.3 Future evolution in the number of hydrometeorological extreme events

The number of heavy precipitation events simulated by CRCM5-LE is expected to increase between 1961-1990 and 2026-2055, with a maximum increase between 1 and 2 events per winter expected close to the Georgian Bay (Figure 4-8). The increase in the number of events is mainly expected during the regime South but also for the regime LP near Lake Huron. The increased frequency of warm events is expected to be even higher reaching a total increase of about 10 events per winter close to Lake Erie. The highest increase is expected for HP and South regimes and at a lower rate for regimes North-East and North-West. The number of compound events is expected to increase by 1 or 2 events per winter with a maximal increase between Lake Erie and Huron. The increase in the number of heavy rain and warm events is expected to concern mainly the regime South and HP (Figure 4-8).

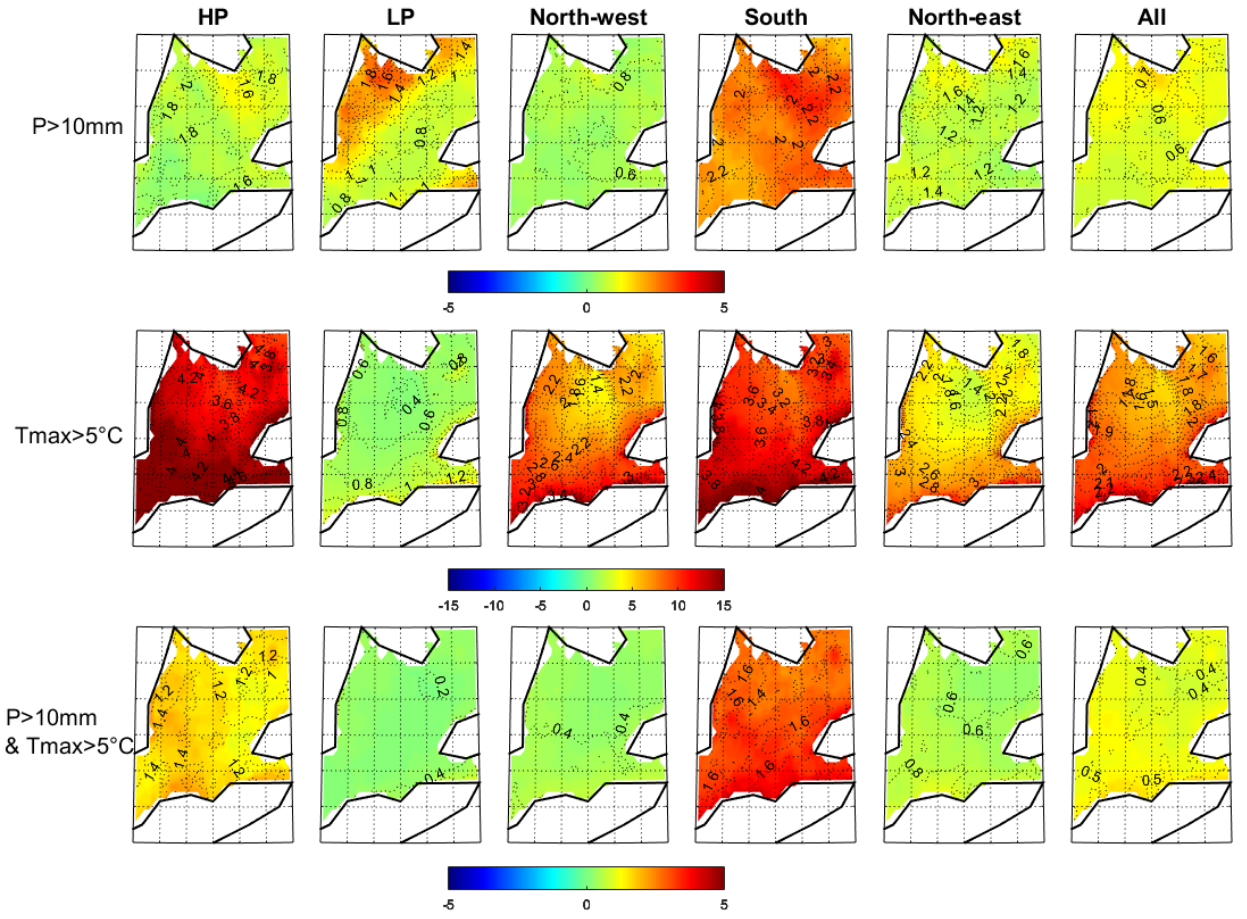

Figure 4-8 DJF change in 50-members CRCM5-LE average percentage of DJF number of precipitation and warm events relative to DJF occurrence of weather regimes between the historical (1961-1990) and the future period (2026-2055) for the 50 members CRCM5-LE average. The dotted lines represent the standard deviation of the 50-members CRCM5-LE simulated change.

The contribution of the trend in heavy rain and warm events to the trend in number of high flows has been investigated (Figure 4-9). Taking all weather regimes events together, the total change in number of high flows simulated by PRMS (TOT) is expected to increase in the future. The theoretical high flows frequency change due to the occurrence change in number of heavy rain and warm events (OCC) is slightly lower than the increase in TOT for most of the weather regimes

(DIF positive, Figure 4-9). Regime HP shows an opposite result with higher OCC compared to TOT on average (DIF negative, Figure 4-9).

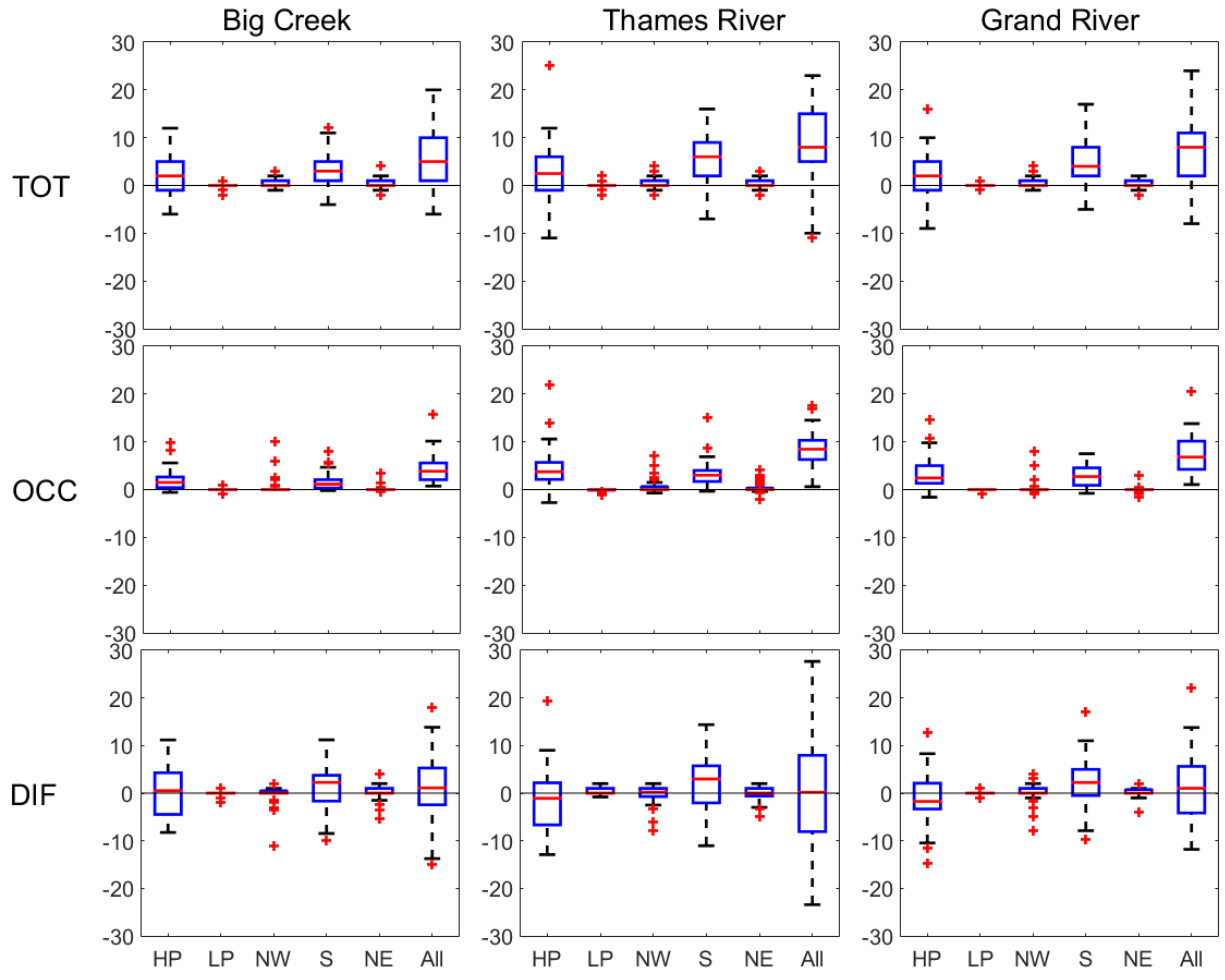

Figure 4-9 Upper panels: Distribution of change in number of high flows between 1961-1990 and 2026-2055 simulated from the 50 members of the ensemble (TOT). Mid panels: Distribution of theoretical change in number of high flows using the factor of change in number of heavy rain and warm events between 1961-1990 and 2026-2055 (OCC). Lower panels: TOT minus OCC (DIF). Boxes extend from the 25th to the 75th percentile, with a horizontal red bar showing the median value. The whiskers are lines extending from each end of the box to the 1.5 interquartile range. Plus signs correspond to outliers.

The 50-members distribution change in rainfall and snowfall amounts corresponding to all compound events simulated by PRMS at each watershed outlet have been investigated (Figure 4-10). The amount of snowmelt and rainfall taken together is generally decreasing but a large difference between members was simulated. Many members show an increase in amount of rain and snowmelt especially during regime LP. The change in amount of snowmelt follows a similar decreasing trend for most of the cases but an increase in snowmelt during LP extreme days is expected, especially in Grand River. The amount of rainfall slightly increases for most of the members especially for LP in Thames river and Big Creek river.

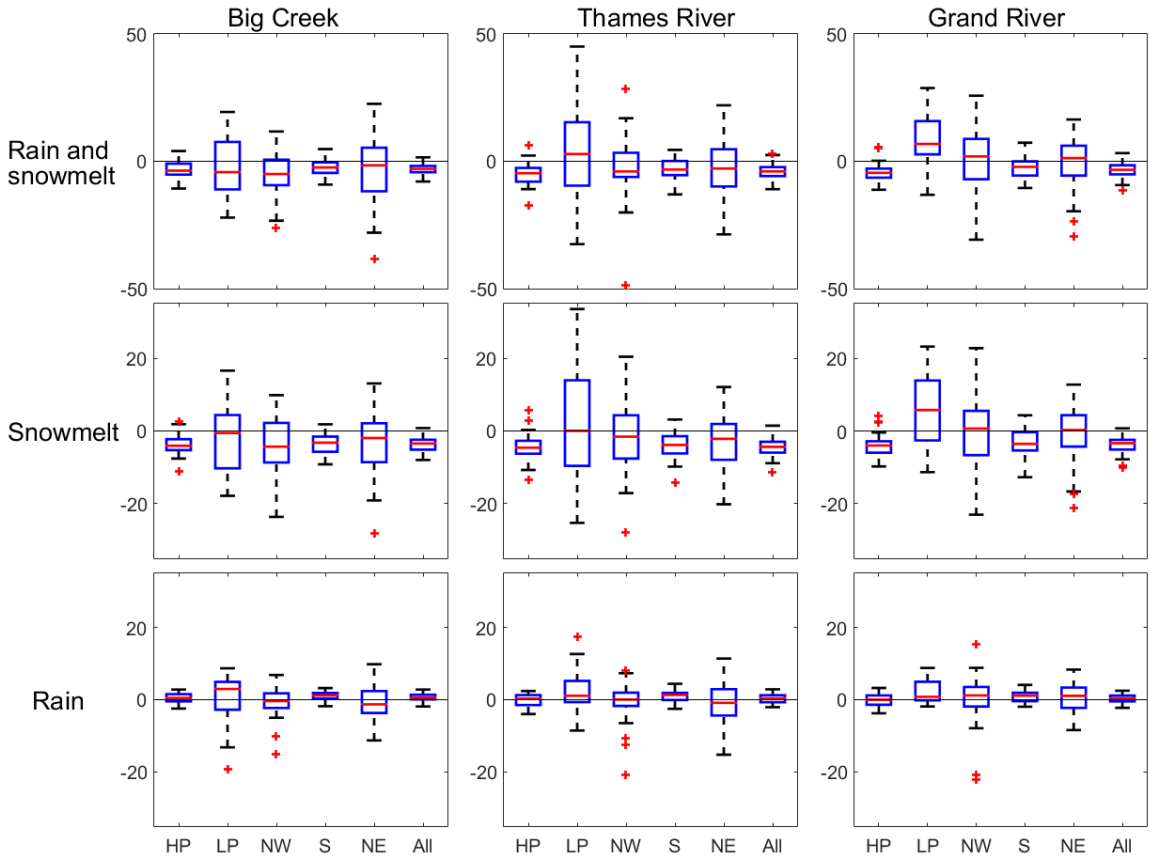

Figure 4-10 Distribution of change in simulated rainfall (mm) and snowmelt amounts (mm Weq) for all compound's extreme events between 1961-1990 and 2026-2055 from the 50 members of the ensemble.

4.4.4 Relationship between change in occurrence of weather regimes and extreme events

Correlations between change in occurrence of weather regimes and change in number of Rain and Warm events between 1961-1990 and 2026-2055 for the 50 members have been calculated for each grid point (Figure 4-11).

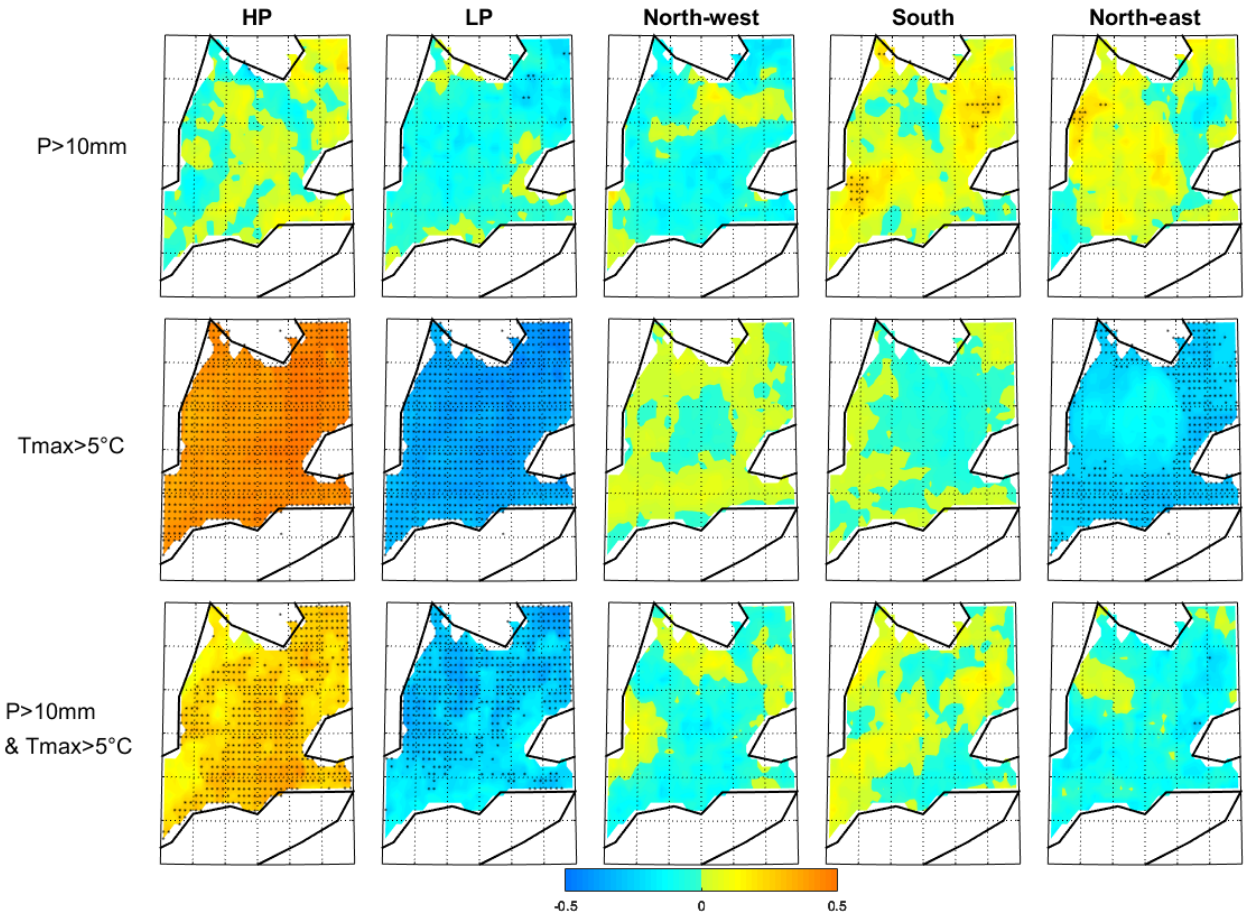

Figure 4-11 DJF inter-members correlations between change in occurrence of weather regimes and change in number of events between 1961-1990 and 2026-2055. Black points indicate a correlation significant at 95% according to the Pearson's correlation table.

The magnitude of the correlations between occurrence of weather regimes and warm events is higher compared to correlations with heavy precipitation events. The results show significant positive correlations (95% confidence) between warm events and the change in occurrence of

regime HP and negative correlations (95% confidence) between warm events and the change in occurrence of regime LP/North-east. For the precipitation events the results varied spatially with few areas showing positive correlations for regime South (Figure 4-11). The compound index shows positive correlations between the number of events and regime HP close to Lake Erie and negative correlations between the number of events and regime LP near Lake Huron.

Inter-member correlations between the change in the frequency of a combination of weather regimes and the change in the frequency of heavy Rain and warm events, averaged over the entire region, have also been investigated (Table 4-1). The goal is to identify the impact of a combination of two weather patterns on the hydrometeorological events. The weather regimes are a discretization of a continuous process and the combination of weather regimes aim to show the impact of weather regimes interactions on local climate. The combinations of weather regimes have been done by summing the change of occurrence from the two regimes of each combination. The correlation between change of any weather regimes combinations and change in number of heavy precipitation events are not significant. The correlations between change in number of warm events and change in occurrence of weather regimes is increased when regime South is calculated with regime HP and when regime LP is calculated with regime North-East compared to correlations with regimes HP or LP only (Table 4-1). Concerning the compound index, the number of heavy rain and warm events is positively correlated with a combination of regime South-HP (significant at 95% confidence interval) and negatively correlated with a combination of North-East-LP and North-East-LP (significant at 90% confidence interval).

Table 4-1 inter-members correlations between DJF change in occurrence of weather regimes and DJF change in number of events between 1961-1990 and 2026-2055. Bold show correlations significant at 90% confidence level, a single underline significant at 95% and double underline significant at 99% according to the Pearson's correlation table.

	P>10mm					Tmax>5°C					P>10mm & Tmax>5°C				
	HP	**LP**	**NW**	**S**	**NE**	**HP**	**LP**	**NW**	**S**	**NE**	**HP**	**LP**	**NW**	**S**	**NE**
HP	0.02	-0.04	-0.05	0.10	0.06	**0.45**	0.20	**0.38**	**0.48**	0.20	**0.30**	0.10	0.21	**0.35**	0.18
LP		-0.08	-0.14	0.02	-0.01		**-0.38**	**-0.23**	**-0.25**	**-0.45**		**-0.29**	**-0.23**	-0.17	**-0.27**
NW			-0.08	-0.01	-0.04			0.02	0.01	-0.20			-0.04	-0.02	-0.13
S				0.10	0.12				-0.01	-0.21				0.03	-0.06
NE					0.06					**-0.25**					-0.10

The correlations with the change in number of high flows in each watershed have also been investigated (Table 4-2) and shows significance in the Big Creek and Grand River watersheds. In both watersheds, LP and a combination LP-North-West are negatively correlated with high flows while a combination North-West-South is positively correlated with high flows. In Grand River the number of high flows is also negatively correlated with a combination of regime HP-LP.

Table 4-2 inter-members correlations between DJF change in occurrence of weather regimes and DJF change in number of high flows events between 1961-1990 and 2026-2055. Bold show correlations significant at 90% according to the Pearson's correlation table.

	Big Creek					Thames River					Grand River				
	HP	**LP**	**NW**	**S**	**NE**	**HP**	**LP**	**NW**	**S**	**NE**	**HP**	**LP**	**NW**	**S**	**NE**
HP	0.00	-0.18	0.18	0.04	-0.08	0.06	-0.02	0.11	0.04	0.04	-0.05	**-0.27**	0.13	0.10	-0.10
LP		**-0.24**	0.05	-0.12	**-0.25**		-0.12	-0.02	-0.11	-0.10		-0.31	-0.01	-0.07	**-0.28**
NW			0.22	**0.23**	0.14			0.07	0.03	0.06			0.20	**0.29**	0.14
S				0.05	-0.05				-0.04	-0.05				0.18	0.06
NE					-0.11					-0.02					-0.09

The change of heavy precipitation, warm and compound events frequency in respect to change in occurrence of regimes South, HP, LP and North-East for each member of the ensemble is shown in Figure 4-12. The correspondence between change in number of heavy precipitations events and change in number of occurrences of weather regimes is not clear, confirming the low correlations in Figure 4-11 and Table 4-1. Regarding the warm events, the large increase in occurrence of regime HP-South or large decrease in regimes LP-North-East are generally associated with a large increase in number of warm events confirming the results from Figure 4-11 and Table 4-1. Concerning the compound index, a high increase of HP and South occurrences does not systematically lead to a large increase in number of events (Figure 4-12).

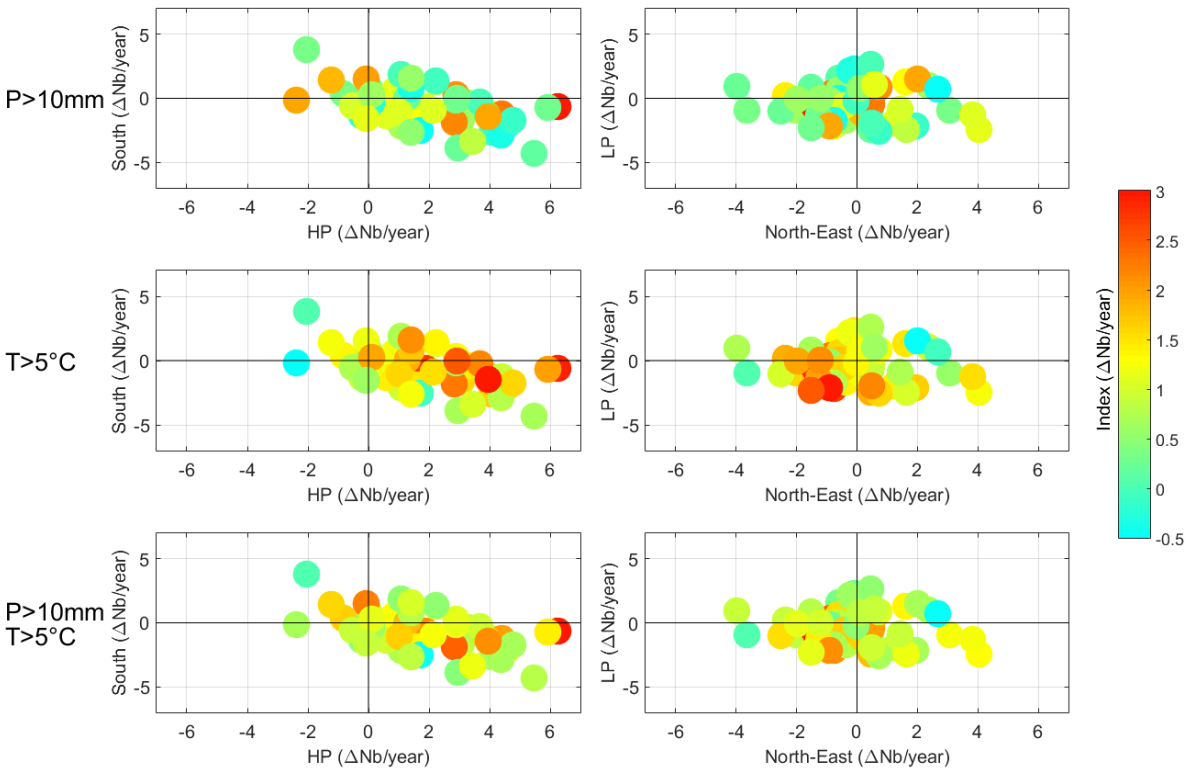

Figure 4-12 DJF change in occurrences of regimes HP-South (left) and LP-north-East (right) in respect to change in number of precipitation and warm events (Coloured) for each member of CRCM5-LE between 1961-1990 and 2026-2055.

4.5 Discussion

4.5.1 Atmospheric circulation and extreme weather events

The extreme weather events investigated in this study were identified from data that have been bias corrected by an univariate method (Ines and Hansen, 2006) that can potentially increase the simulation bias for variables depending equally strongly on more than one climatic driver (Zscheischler et al., 2019). In our study, the number of warm events was clearly overestimated in a large area of the domain (Figure 4-5), but the bias corrected data satisfactory recreated the number of heavy precipitation and number of compound events (Figure 4-4 et 4-6). Despite remaining biases in the simulated data, the bias correction improved the results compared to analysis using raw data (Supplementary material Figure 4-13 and 4-14). This univariate bias correction method has been chosen in this study because was satisfactory used in previous works in the region (Champagne et al., 2019b; Wazneh et al., 2017). Future studies should consider using multivariate bias corrected methods to further improve the simulation of compound indices.

The occurrence of heavy rain and warm events calculated from bias corrected temperature and precipitation data are modulated by specific atmospheric patterns in winter which corroborates previous studies in the Great Lakes region. These studies found that heavy precipitation and flooding events are associated with high geopotential height anomalies in the east coast of North America similarly to regimes HP or South (Mallakpour and Villarini, 2016; Zhang and Villarini, 2019; Farnham et al., 2018). Our results found differences between observations and simulations with more heavy precipitation events during regime HP in the observations while the simulations with CRCM5-LE show more precipitation events during regime South (Figure 4-4). The overestimation of the number of precipitation events for regime South can be associated with the

difference in pattern between regimes calculated with 20thCR and CanESM2-LE (Figure 4-3). Regime South calculated with CanESM2-LE shows Z500 anomalies shifted to the west and likely a more meridional flux compared to the regime South from 20thCR. The weather regimes associated with heavy precipitations in the Mid-west defined by Zhang and Villarini (2019) show high pressure anomalies on the east and low pressure on the west sides of the Great lakes similarly to regime South calculated with CanESM2-LE. The regime South calculated with 20thCR shows negative Z500 anomalies with a northern position compared to CanESM2-LE and therefore a stronger zonal flux while the regime South calculated with CanESM2-LE has likely a more meridional flux driving humidity from the Gulf of Mexico (Figure 4-3). This pattern also brings warm temperature events even though the regime HP brings even more warm events in both the observations and the ensemble average (Figure 4-5). Regime HP has similarities with the positive phase of the NAO, previously associated with warm winter temperature in the Great Lakes region (Ning and Bradley, 2015). The other weather regimes bring generally fewer heavy precipitation or warm events apart from regime LP bringing heavy precipitation close to Lake Huron (Figure 4-4). LP is not associated with warm events (Figure 4-5) suggesting that these extreme precipitations are in form of snow and likely from lake effect snow. Suriano and Leathers (2017) show that low pressure anomalies north-east from Great lakes bring major lake effects snow in the eastern shores of Lake Huron due to less zonal wind and cold outbreaks from the Arctic. The regime LP shows low geopotential height anomalies right on the Great lakes and the associated north-west winds on the Lake Huron are likely to bring lake effect snowfall in this area.

4.5.2 Future evolution of rain and warm events

The future increase in winter heavy precipitation events in Southern Ontario was already described in Deng et al., (2016). Compound events such as Rain on Snow (ROS) events have also been investigated by Jeong and Sushama (2018). These authors defined ROS events as liquid precipitation and snow cover higher than 1mm and found no significant trend of ROS events in the Great Lakes region, in continuity to what was observed in the past (Wachowicz et al., 2019). These studies show that the Great Lakes region is located between a region of increase ROS events due to increase of rainfall in the north and a decrease in ROS events due to decrease of snowpack in southern regions. Increase of rainfall and decrease of snowpack are both expected to occur in Southern Ontario (Figure 4-10) and are likely to cancel each other in term of ROS events. Our heavy rain and warm index does not consider snowpack and is expecting to be more frequent in the future (Figure 4-8). The increase of heavy rain and warm events is likely driven by warmer temperature shown by the increase of the compound events and warm events both occurring at a higher extent close to Lake Erie (Figure 4-8). The increase in extreme precipitation events is less significant than the increase in warm events and is occurring mostly in the Northern parts of the area (Figure 4-8).

The future evolution of ROS or heavy rain and warm events corresponding to different weather patterns have not been yet investigated in previous literature. It is interesting to note that the future increase in the number of heavy rain and warm events are expected to occur only for the regimes HP and South, the number of events remaining very low for the other regimes (Figure 4-8). This result suggests that the global increase of mean temperature and precipitation is not sufficient to reach the 10 mm and 5°C threshold for LP, North-West and North-East regimes. More

precipitation events are expected during regime LP but the temperature stays too low to increase the numbers of heavy rain and warm events (Figure 4-8). Regime North-West and North-East show an increase of warm events but not an increase in precipitation events and therefore the number of rain and warm events is not expected to increase.

4.5.3 Change in frequency of heavy rain and warm events partially modulated by the occurrence of weather regimes

Despite clear association between regimes HP/South and occurrences of rain and warm events, the uncertainties linked to internal variability of climate are not fully driven by the frequency of weather regimes. Members of the ensemble associated with a simultaneous high increase of regime HP and South frequencies are generally associated with higher increase in rainfall and warm events (Table 4-1), but the association is less straightforward than suggested by the correlation values (Figure 4-12) probably due to poor association between precipitation extremes and occurrence of weather regimes (Table 4-1 and Figure 4-11). Similar change in the occurrence of South-HP weather regimes can lead to variable change in number of heavy rain and warm events (Figure 4-12). This suggests that other scales than the weather regimes calculated in the northeastern North American domain are likely to play a role in weather extreme events and especially the change of heavy rain and warm events and precipitation events. The presence of the Great lakes has a large role in the variability of precipitation at a local scale (Martynov et al., 2012) suggesting that variability of precipitation events depend not so much on the atmospheric circulation over the Great Lakes at the day of the events. The temperature of the lakes and the amount of ice covering the lakes plays for example a great role in the variability of precipitation (Martynov et al., 2012).

4.5.4 Non stationarity in the relationship between weather extreme events and high flows

The projections show that the increase in number of high flows associated with a regime HP is expected to be lower than the increase in number of heavy rain and warm events (negative DIF in Figure 4-9). This result suggests that the conditions that produce high flows may change in the future. As the temperature increases, snowmelt is expected to be a less important component in the generation of high flows in the region (Figure 4-10). In the historical period regimes HP and South produce approximately the same number of high flows in the simulations (Figure 4-7), but are driving mostly by heavy precipitation for the regime South and warm events for the regime HP (Figure 4-4 and 4-5). More importantly, HP shows a further increase of warm events in the future while South show rather an increase of precipitation (Figure 4-8). In the context of less snow, the importance of precipitation to drive high flows will be higher in the future because warmer conditions do not increase snowmelt in case of a snowpack reduction (Figure 4-10). Therefore, the increase of weather extreme events associated with the regime South will generate an increase of high flows more strenuously than the increase of events associated with regime HP (Figure 4-9).

The future change in number of high flows is associated with a large inter-member uncertainty (Figure 4-9). The weather extreme events inter-member uncertainty was partly associated with the change in occurrence of weather regimes especially for the warm component (Figure 4-11, 4-12 and Table 4-1). The association between occurrence of weather regimes and high flows is less clear and shows opposite results (Table 4-1 and 4-2). Especially, change of occurrence of regime North-West is positively correlated with the change in number of high flows in Big Creek and Grand river watersheds (Table 4-2) while it is negatively correlated with the change in number of weather extreme events in this area (Figure 4-11). The correlation is even significant when regimes

North-west and South are associated (Table 4-2). This result could be due to the preferential sequence of weather regimes and more snow generated by patterns similar to the regime North-West (Champagne et al., 2019b). The pattern associated with regime North-west shows anticyclonic systems in the west part of the domain (Figure 4-3). The meteorological systems have a tendency to move eastward and this anticyclonic system is likely to become a regime South or HP (Champagne et al., 2019a, Supplementary material, Table S2). In addition, as already stated in the previous paragraph, regime HP will be less likely to produce a heavy rain event than a regime South in the future. Therefore, members projecting an increase in the combination of the snowy regime North-West and wetter and warmer regime South are more likely to project more high flow events. These results emphasize the need to study not only each hydrometeorological extreme events and relationship with atmospheric circulation independently, but to also focus on the sequence of weather patterns preceding the high flows events.

4.5.5 Relevance of rain and warm events to explain future evolution of high flows

Our method that uses an index based on daily temperature and precipitation to study the future evolution of high flows is questionable. Even if a heavy rain and warm event is a necessary condition to create a high flow event (Figure 4-2), such event is not systematically followed by a high flow event (Figure 4-7). The previous section suggests that snow falling days before the high flow event has an important role in the generation of high flows. Other factors such as multi-days rain events could also contribute to increase the streamflow. This study focused on single day events to introduce first results in the ability of CRCM5-LE to recreate extreme events in southern Ontario, but future studies should investigate multi-day events.

Moreover, as stated in the previous section, the relationship between the extreme weather events index and high flows is affected by non-stationarity. Applied in the past, the Rain and warm index works well to define the high flows risk in Southern Ontario (Figure 4-2), the warm component of this index being a condition to trigger snowmelt. In a warming climate, snowpack is reduced, and the rain to snow ratio is increasing (Jeong and Sushama, 2018), changing the relationship between extreme weather events and high flows.

To integrate snow processes and reduce the uncertainties from non-stationarity of temperature, Rain on snow index could be used in lieu of our heavy rain and warm index. However, this index is not projected to be more frequent in the future in the Great Lakes region, precisely because of less snow in the ground (Jeong and Sushama, 2018). Moreover, ROS index integrates events with a very small contribution of snowmelt to the high flows while neglecting rainfall only events (Cohen et al., 2015; Jeong and Sushama, 2018; Pradhanang et al., 2013). The definition of ROS also introduces more uncertainties as it depends on the combination of simulated precipitation and temperature for several days (Kudo et al., 2017). Our heavy rain and warm index minimizes this uncertainty and take into consideration heavy rainfall whatever the amount of snow covering the ground. It is therefore a good tool to assess the potential risk of high flows in Southern Ontario from all ranges of rain events, even though it is important to keep in mind that the flood risk diminished as snowpack decreases. A rain only index could also be used but the impact of snowpack on streamflow would be completely eradicated while snow will still play a role in the future hydrology. ROS events, liquid precipitation events and our heavy rain and warm events,

ideally with multi-day events integrated, should be investigated together to fully understand the future evolution of the flood risk due to a shift in weather extreme events.

4.6 Conclusion

The aim of this study was to assess the ability of the Canadian Regional Climate Model Large Ensemble (CRCM5-LE), a downscaled version of the 50-members global Canadian model Large Ensemble (CanESM2-LE), to simulate winter hydrometeorological extreme events in Southern Ontario and to investigate how the internal variability of climate will modulate the future evolution of these extremes. The winter composite index heavy rain and warm temperature was identified in the past with gridded observation data (NRCANmet) by investigating what conditions of temperature and precipitation are necessary to produce a high flow in three watersheds in Southern Ontario. PRMS model was used to simulate the future evolution of high flows for each member of CRCM5-LE in these three watersheds. The large-scale circulation patterns corresponding to these events were assessed by identifying past recurrent weather regimes based on daily Z500 from the 20th century reanalyses and estimating the evolution of the same weather regimes in the future for each member of CanESM2-LE. The results of this study show that CRCM5-LE was able to:

(1) Recreate the historical larger number of events close to Lake Erie despite an overestimation of warm events.
(2) Simulate more heavy rain and warm events as well as high flows during the regimes associated with high pressure anomalies on the Great Lakes (HP) and the Atlantic-Ocean (South).
(3) Project an increase in the future number of heavy rain and warm events and associated high flows especially during the regimes HP and South and in the vicinity of Lake Erie.

These results suggest that depending on the future evolution of natural variability of climate, the increase in the number of events will be amplified or attenuated by the favoured positions of the pressure systems. The natural variability of climate is not expected to greatly modulate the number of high flows due to an increase of the importance of precipitation in generating high flows. The role of more localized processes such as impact of the lakes on precipitation events needs to be further evaluated to improve the ability of the next versions of regional climate models to recreate the precipitation events. The newly created weather index did not integrate snowpack because the uncertainties in the ability of CRCM5-LE to recreate precipitation and temperature extremes at a daily basis would be further increased in snowmelt estimates. However, snowpack variability will have a large impact in the modulation of high flows in the region and future studies should investigate snow processes by taking advantage of rapid improvements in climate regional modelling. Other regional climate models and different scenarios should also be used to improve our understanding of the future evolution of hydrometeorological extreme events in Southern Ontario. Despite these future possible improvements, our study gives a good estimation of what to expect in term of change in number of hydrometeorological events in Southern Ontario and will serve to better estimate the future flood risk in this populated region.

4.7 Acknowledgement

Financial support for this study was provided by the Natural Sciences and Engineering Research Council (NSERC) of Canada through the FloodNet Project. We also acknowledge support and contributions from Global Water Future Program, Environment and Climate Change Canada, Natural Resources Canada and Water Survey of Canada. The production of ClimEx was funded within the ClimEx project by the Bavarian State Ministry for the Environment and Consumer

Protection.The CRCM5 was developed by the ESCER centre of Université du Québec à Montréal (UQAM; www.escer.uqam.ca) in collaboration with Environment and Climate Change Canada. We acknowledge Environment and Climate Change Canada's Canadian Centre for Climate Modelling and Analysis for executing and making available the CanESM2 Large Ensemble simulations used in this study, and the Canadian Sea Ice and Snow Evolution Network for proposing the simulations. Computations with the CRCM5 for the ClimEx project were made on the SuperMUC supercomputer at Leibniz Supercomputing Centre (LRZ) of the Bavarian Academy of Sciences and Humanities. The operation of this supercomputer is funded via the Gauss Centre for Supercomputing (GCS) by the German Federal Ministry of Education and Research and the Bavarian State Ministry of Education, Science and the Arts.

4.8 References

Buttle, J. M., Allen, D. M., Caissie, D., Davison, B., Hayashi, M., Peters, D. L., Pomeroy, J. W., Simonovic, S., St-Hilaire, A. and Whitfield, P. H.: Flood processes in Canada: Regional and special aspects, Canadian Water Resources Journal / Revue canadienne des ressources hydriques, 1–24, doi:10.1080/07011784.2015.1131629, 2016.

Champagne, O., Arain, M. A. and Coulibaly, P.: Atmospheric circulation amplifies shift of winter streamflow in Southern Ontario, Journal of Hydrology, 124051, doi:10.1016/j.jhydrol.2019.124051, 2019a.

Champagne, O., Arain, A., Leduc, M., Coulibaly, P. and McKenzie, S.: Future shift in winter streamflow modulated by internal variability of climate in southern Ontario, Hydrology and Earth System Sciences Discussions, 1–30, doi:10.5194/hess-2019-204, 2019b.

Cohen, J., Ye, H. and Jones, J.: Trends and variability in rain-on-snow events: RAIN-ON-SNOW, Geophysical Research Letters, 42(17), 7115–7122, doi:10.1002/2015GL065320, 2015.

Compo, G. P., Whitaker, J. S., Sardeshmukh, P. D., Matsui, N., Allan, R. J., Yin, X., Gleason, B. E., Vose, R. S., Rutledge, G., Bessemoulin, P. and others: The twentieth century reanalysis project, Quarterly Journal of the Royal Meteorological Society, 137(654), 1–28, doi:10.1002/qj.776, 2011.

Deng, Z., Qiu, X., Liu, J., Madras, N., Wang, X. and Zhu, H.: Trend in frequency of extreme precipitation events over Ontario from ensembles of multiple GCMs, Climate Dynamics, 46(9–10), 2909–2921, doi:10.1007/s00382-015-2740-9, 2016.

Deser, C., Phillips, A. S., Alexander, M. A. and Smoliak, B. V.: Projecting North American climate over the next 50 years: uncertainty due to internal variability*, Journal of Climate, 27(6), 2271–2296, 2014.

Dressler, K. A., Leavesley, G. H., Bales, R. C. and Fassnacht, S. R.: Evaluation of gridded snow water equivalent and satellite snow cover products for mountain basins in a hydrologic model, Hydrological Processes, 20(4), 673–688, doi:10.1002/hyp.6130, 2006.

Farnham, D. J., Doss-Gollin, J. and Lall, U.: Regional Extreme Precipitation Events: Robust Inference From Credibly Simulated GCM Variables, Water Resources Research, 54(6), 3809–3824, doi:10.1002/2017WR021318, 2018.

Freudiger, D., Kohn, I., Stahl, K. and Weiler, M.: Large-scale analysis of changing frequencies of rain-on-snow events with flood-generation potential, Hydrology and Earth System Sciences, 18(7), 2695–2709, doi:10.5194/hess-18-2695-2014, 2014.

Fyfe, J. C., Derksen, C., Mudryk, L., Flato, G. M., Santer, B. D., Swart, N. C., Molotch, N. P., Zhang, X., Wan, H., Arora, V. K., Scinocca, J. and Jiao, Y.: Large near-term projected snowpack loss over the western United States, Nature Communications, 8(1), doi:10.1038/ncomms14996, 2017.

Hoegh-Guldberg, O., Jacob, D., Taylor, M., Bindi, M., Brown, S., Camilloni, I., Diedhiou, A., Djalante, R., Ebi, K. L., Engelbrecht, F., Guiot, J., Hijioka, Y., Mehrotra, S., Seneviratne, S. I., Thomas, A., Warren, R., Halim, S. A., Achlatis, M., Alexander, L. V., Berry, P., Boyer, C., Byers, E., Brilli, L., Buckeridge, M., Cheung, W., Craig, M., Evans, J., Fischer, H., Fraedrich, K., Ganase, A., Gattuso, J. P., Bolaños, T. G., Hanasaki, N., Hayes, K., Hirsch, A., Jones, C., Jung, T., Kanninen, M., Krinner, G., Lawrence, D., Ley, D., Liverman, D., Mahowald, N., Meissner, K. J., Millar, R., Mintenbeck, K., Mix, A. C., Notz, D., Nurse, L., Okem, A., Olsson, L., Oppenheimer, M., Paz, S., Petersen, J., Petzold, J., Preuschmann, S., Rahman, M. F., Scheuffele, H., Schleussner, C.-F., Séférian, R., Sillmann, J., Singh, C., Slade, R., Stephenson, K., Stephenson, T., Tebboth, M., Tschakert, P., Vautard, R., Wehner, M., Weyer, N. M., Whyte, F., Yohe, G., Zhang, X., Zougmoré, R. B., Marengo, J. A., Pereira, J. and Sherstyukov, B.: Impacts of 1.5°C of Global Warming on Natural and Human Systems, , 138, 2018.

Ines, A. V. M. and Hansen, J. W.: Bias correction of daily GCM rainfall for crop simulation studies, Agricultural and Forest Meteorology, 138(1–4), 44–53, doi:10.1016/j.agrformet.2006.03.009, 2006.

Jeong, D. and Sushama, L.: Rain-on-snow events over North America based on two Canadian regional climate models, Climate Dynamics, 50(1–2), 303–316, doi:10.1007/s00382-017-3609-x, 2018.

Kharin, V. V., Zwiers, F. W., Zhang, X. and Wehner, M.: Changes in temperature and precipitation extremes in the CMIP5 ensemble, Climatic Change, 119(2), 345–357, doi:10.1007/s10584-013-0705-8, 2013.

Kudo, R., Yoshida, T. and Masumoto, T.: Uncertainty analysis of impacts of climate change on snow processes: Case study of interactions of GCM uncertainty and an impact model, Journal of Hydrology, 548, 196–207, doi:10.1016/j.jhydrol.2017.03.007, 2017.

Lafaysse, M., Hingray, B., Mezghani, A., Gailhard, J. and Terray, L.: Internal variability and model uncertainty components in future hydrometeorological projections: The Alpine Durance basin, Water Resources Research, 50(4), 3317–3341, doi:10.1002/2013WR014897, 2014.

Leduc, M., Mailhot, A., Frigon, A., Martel, J.-L., Ludwig, R., Brietzke, G. B., Giguère, M., Brissette, F., Turcotte, R., Braun, M. and Scinocca, J.: The ClimEx Project: A 50-Member Ensemble of Climate Change Projections at 12-km Resolution over Europe and Northeastern North America with the Canadian Regional Climate Model (CRCM5), Journal of Applied Meteorology and Climatology, 58(4), 663–693, doi:10.1175/JAMC-D-18-0021.1, 2019.

Leonard, M., Westra, S., Phatak, A., Lambert, M., van den Hurk, B., McInnes, K., Risbey, J., Schuster, S., Jakob, D. and Stafford-Smith, M.: A compound event framework for understanding extreme impacts: A compound event framework, Wiley Interdisciplinary Reviews: Climate Change, 5(1), 113–128, doi:10.1002/wcc.252, 2014.

Liao, C. and Zhuang, Q.: Quantifying the Role of Snowmelt in Stream Discharge in an Alaskan Watershed: An Analysis Using a Spatially Distributed Surface Hydrology Model: ROLE OF SNOWMELT IN STREAMFLOW IN ALASKA, Journal of Geophysical Research: Earth Surface, 122(11), 2183–2195, doi:10.1002/2017JF004214, 2017.

Lorenz, E. N.: Deterministic Nonperiodic Flow, Journal of the Atmospheric Sciences, 20(2), 130–141, doi:10.1175/1520-0469(1963)020<0130:DNF>2.0.CO;2, 1963.

Mallakpour, I. and Villarini, G.: Investigating the relationship between the frequency of flooding over the central United States and large-scale climate, Advances in Water Resources, 92, 159–171, doi:10.1016/j.advwatres.2016.04.008, 2016.

Markstrom, S. L., Regan, R. S., Hay, L. E., Viger, R. J., Payn, R. A. and LaFontaine, J. H.: precipitation-runoff modeling system, version 4: U.S. Geological Survey Techniques and Methods., 2015.

Martynov, A., Sushama, L., Laprise, R., Winger, K. and Dugas, B.: Interactive lakes in the Canadian Regional Climate Model, version 5: the role of lakes in the regional climate of North America, Tellus A: Dynamic Meteorology and Oceanography, 64(1), 16226, doi:10.3402/tellusa.v64i0.16226, 2012.

Mastin, M. C., Chase, K. J. and Dudley, R. W.: Changes in Spring Snowpack for Selected Basins in the United States for Different Climate-Change Scenarios, Earth Interactions, 15(23), 1–18, doi:10.1175/2010EI368.1, 2011.

McCabe, G. J., Clark, M. P. and Hay, L. E.: Rain-on-Snow Events in the Western United States, Bulletin of the American Meteorological Society, 88(3), 319–328, doi:10.1175/BAMS-88-3-319, 2007.

McKenney, D. W., Hutchinson, M. F., Papadopol, P., Lawrence, K., Pedlar, J., Campbell, K., Milewska, E., Hopkinson, R. F., Price, D. and Owen, T.: Customized Spatial Climate Models for North America, Bulletin of the American Meteorological Society, 92(12), 1611–1622, doi:10.1175/2011BAMS3132.1, 2011.

Merz, R. and Blöschl, G.: A process typology of regional floods: PROCESS TYPOLOGY OF REGIONAL FLOODS, Water Resources Research, 39(12), doi:10.1029/2002WR001952, 2003.

Michelangeli, P.-A., Vautard, R. and Legras, B.: Weather Regimes: Recurrence and Quasi Stationarity, Journal of the Atmospheric Sciences, 52(8), 1237–1256, doi:10.1175/1520-0469(1995)052<1237:WRRAQS>2.0.CO;2, 1995.

Musselman, K. N., Lehner, F., Ikeda, K., Clark, M. P., Prein, A. F., Liu, C., Barlage, M. and Rasmussen, R.: Projected increases and shifts in rain-on-snow flood risk over western North America, Nature Climate Change, 8(9), 808–812, doi:10.1038/s41558-018-0236-4, 2018.

Ning, L. and Bradley, R. S.: Winter climate extremes over the northeastern United States and southeastern Canada and teleconnections with large-scale modes of climate variability*, Journal of Climate, 28(6), 2475–2493, 2015.

Pradhanang, S. M., Frei, A., Zion, M., Schneiderman, E. M., Steenhuis, T. S. and Pierson, D.: Rain-on-snow runoff events in New York: RAIN-ON-SNOW EVENTS IN NEW YORK, Hydrological Processes, 27(21), 3035–3049, doi:10.1002/hyp.9864, 2013.

Scott, R. W. and Huff, F. A.: Impacts of the Great Lakes on regional climate conditions, Journal of Great Lakes Research, 22(4), 845–863, 1996.

Sigmond, M., Fyfe, J. C. and Swart, N. C.: Ice-free Arctic projections under the Paris Agreement, Nature Climate Change, 8(5), 404–408, doi:10.1038/s41558-018-0124-y, 2018.

Surfleet, C. G. and Tullos, D.: Variability in effect of climate change on rain-on-snow peak flow events in a temperate climate, Journal of Hydrology, 479, 24–34, doi:10.1016/j.jhydrol.2012.11.021, 2013.

Surfleet, C. G., Tullos, D., Chang, H. and Jung, I.-W.: Selection of hydrologic modeling approaches for climate change assessment: A comparison of model scale and structures, Journal of Hydrology, 464–465, 233–248, doi:10.1016/j.jhydrol.2012.07.012, 2012.

Suriano, Z. J. and Leathers, D. J.: Synoptic climatology of lake-effect snowfall conditions in the eastern Great Lakes region: SYNOPTIC CLIMATOLOGY OF LAKE-EFFECT SNOWFALL CONDITIONS, International Journal of Climatology, 37(12), 4377–4389, doi:10.1002/joc.5093, 2017.

Teng, F., Huang, W., Cai, Y., Zheng, C. and Zou, S.: Application of Hydrological Model PRMS to Simulate Daily Rainfall Runoff in Zamask-Yingluoxia Subbasin of the Heihe River Basin, Water, 9(10), 769, doi:10.3390/w9100769, 2017.

Teng, F., Huang, W. and Ginis, I.: Hydrological modeling of storm runoff and snowmelt in Taunton River Basin by applications of HEC-HMS and PRMS models, Natural Hazards, 91(1), 179–199, doi:10.1007/s11069-017-3121-y, 2018.

Thiombiano, A. N., El Adlouni, S., St-Hilaire, A., Ouarda, T. B. M. J. and El-Jabi, N.: Nonstationary frequency analysis of extreme daily precipitation amounts in Southeastern Canada using a peaks-over-threshold approach, Theoretical and Applied Climatology, 129(1–2), 413–426, doi:10.1007/s00704-016-1789-7, 2017.

Trenberth, K. E.: Conceptual Framework for Changes of Extremes of the Hydrological Cycle with Climate Change, Climatic Change, 42(1), 327–339, doi:10.1023/A:1005488920935, 1999.

Wachowicz, L. J., Mote, T. L. and Henderson, G. R.: A rain on snow climatology and temporal analysis for the eastern United States, Physical Geography, 1–16, doi:10.1080/02723646.2019.1629796, 2019.

Wazneh, H., Arain, M. A. and Coulibaly, P.: Historical Spatial and Temporal Climate Trends in Southern Ontario, Canada, Journal of Applied Meteorology and Climatology, 56(10), 2767–2787, doi:10.1175/JAMC-D-16-0290.1, 2017.

Würzer, S., Jonas, T., Wever, N. and Lehning, M.: Influence of Initial Snowpack Properties on Runoff Formation during Rain-on-Snow Events, Journal of Hydrometeorology, 17(6), 1801–1815, doi:10.1175/JHM-D-15-0181.1, 2016.

Zhang, W. and Villarini, G.: On the weather types that shape the precipitation patterns across the U.S. Midwest, Climate Dynamics, doi:10.1007/s00382-019-04783-4, 2019.

Zhang, X., Alexander, L., Hegerl, G. C., Jones, P., Tank, A. K., Peterson, T. C., Trewin, B. and Zwiers, F. W.: Indices for monitoring changes in extremes based on daily temperature and precipitation data, Wiley Interdisciplinary Reviews: Climate Change, 2(6), 851–870, doi:10.1002/wcc.147, 2011.

Zhao, H., Higuchi, K., Waller, J., Auld, H. and Mote, T.: The impacts of the PNA and NAO on annual maximum snowpack over southern Canada during 1979-2009, International Journal of Climatology, 33(2), 388–395, doi:10.1002/joc.3431, 2013.

Zscheischler, J., Fischer, E. M. and Lange, S.: The effect of univariate bias adjustment on multivariate hazard estimates, Earth System Dynamics, 10(1), 31–43, doi:10.5194/esd-10-31-2019, 2019.

4.9 Supplementary materials

The two figures in this supplementary material aim to compare the weather extreme events calculated from the bias-corrected CRCM5-LE data (Figure 4-13) and from the CRCM5-LE raw data (Figure 4-14). The weather extreme events calculated from the bias-corrected data show a better representation of NRCANmet and are therefore used in the article.

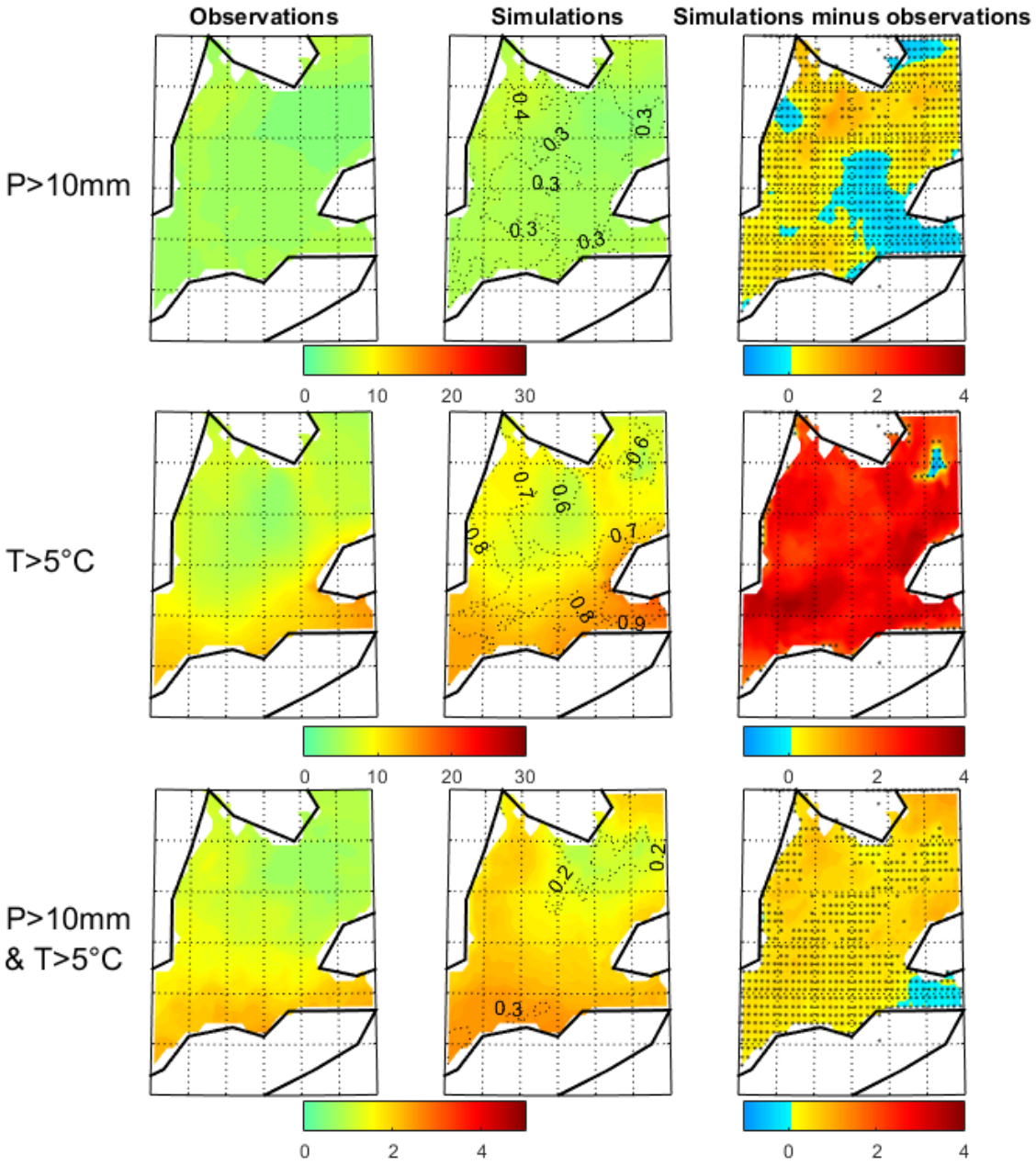

Figure 4-13 DJF number of precipitation and warm extreme events in the historical period (1961-1990) for NRCANmet (observations, left panels), bias corrected CRCM5-LE 50 members average (simulations, mid panels) and NRCANmet minus bias corrected CRCM5-LE (right panels). The dotted lines in the mid panels represent the standard deviation of the 50-members bias-corrected CRCM5-LE simulated number of events. Stippled regions in the right panels indicate where NRCANmet lie within the CRCM5-LE ensemble spread.

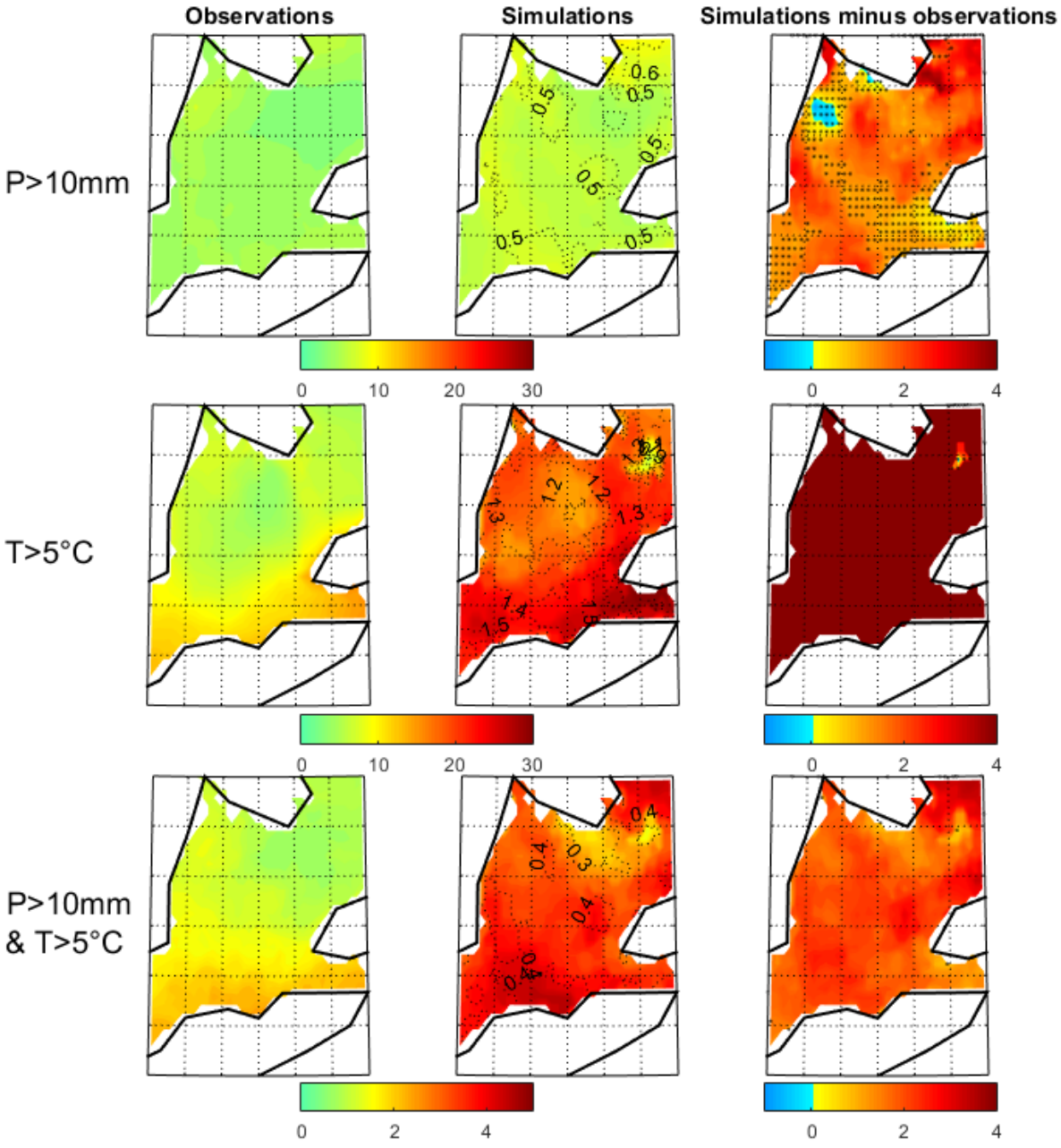

Figure 4-14 DJF number of precipitation and warm extreme events in the historical period (1961-1990) for NRCANmet (observations, left panels), raw CRCM5-LE 50 members average (simulations, mid panels) and NRCANmet minus raw CRCM5-LE (right panels). The dotted lines in the mid panels represent the standard deviation of the 50-members raw CRCM5-LE simulated number of events. Stippled regions in the right panels indicate where NRCANmet lie within the CRCM5-LE ensemble spread.

Chapter 5. Sources of uncertainties in the projection of streamflow in a small Great Lakes watershed

Champagne Olivier, Leduc Martin, Coulibaly Paulin, Arain, M. Altaf, 2019. Sources of uncertainties in the projections of streamflow in a small Great Lakes watershed. *Journal of hydrology: Regional studies.* EJRH_2019_371. In Review.

5.1 Abstract

Study region: Big Creek watershed, Ontario (ON), Canada.

Study focus: Using an analysis of variance, this study quantifies the different sources of uncertainty in the simulated winter-spring evolution of streamflow and number of high flows in a watershed of the Great Lakes basin. The Precipitation Runoff modeling system (PRMS) is forced with temperature and precipitation from 50 members of the Canadian Regional Climate Model Large Ensemble (CRCM5-LE) and 11 downscaled CMIP5 Global climate models (GCMs) using two RCP scenarios. Each of these climate simulations is used with 7 PRMS sets of parameters, given a total of 504 simulations in the 1960-2099 period. The sets of parameters were determined using different combinations of local hydrometeorological data in the objective function of the Dynamical Dimension Search calibration algorithm (DDS).

New hydrological insights for the region: The uncertainties in the future evolution of streamflow will be dominated by scenarios in winter and GCMs in spring. The increase in precipitation amount while the snow to rain ratio decreases will attenuate the impact of future climate scenarios on the modulation of streamflow and amplify the impact of GCMs and internal variability. This study

highlighted the need for improving the simulation of precipitation by GCMs to reduce the uncertainties in the future evolution of streamflow in the Great Lakes region.

5.2 Introduction

The hydrological regimes are changing in many areas of the world in the context of climate change. The warming is impacting snowmelt timing (Barnett et al., 2005) and is enhancing precipitation extremes due to an increase of water holding capacity of the air (Pall et al., 2007; Trenberth et al., 2003). As the temperature continues to rise, future hydrological regimes are expecting to continue their shift. To study the impact of climate change on hydrological processes, driving hydrological models with future climate scenarios have become widely used around the world. The simulation of streamflow using this method is subjected to uncertainties because the modelers have a myriad of methodological choices (Clark et al., 2016; Giuntoli et al., 2015) such as: (i) the scenarios of greenhouse gases emission; (ii) the general circulation models (GCMs), producing different climate projections because of a wide range of parametrizations and resolutions (Kour et al., 2016); (iii) the downscaling methods, dynamical (physical) or statistical, that need to be applied to the climate data because of GCMs low spatial resolution for watershed scale hydrological studies (Fowler et al., 2007; Schoof, 2013); (iv) the choice of the hydrological model between a large panel of physical, conceptual or statistical based models (Boorman et al., 2007; Devia et al., 2015); and (v) the calibration of the hydrological model that need to be in balance between complexity of processes and computational cost (Khakbaz et al., 2012; Moriasi et al., 2007). The uncertainties may also come from the inherently chaotic characteristic of the climate (Deser et al., 2012; Lorenz, 1963) also known as internal variability of climate. Internal variability of climate can be separated into large scale and local scale internal variability (Lafaysse

et al., 2014). Large scale internal variability is due to different possible atmospheric circulation trajectories produced by a single GCM and is assessed by running the GCM several time with slightly different initial conditions. There is also a local component to internal variability that emerges from the interactions between atmosphere, land surface and water bodies, which can be derived from regional climate models (RCM) (Lafaysse et al., 2014). Dynamical downscaling using a RCM allows to refine, in a physically consistent way, the coarse resolution atmospheric conditions from a GCM to a few kilometers spatial resolution (Laprise, 2008). In the statistical downscaling method, this uncertainty is derived from the different realization of the stochastic process used to replicate the large-scale climate data from the GCM (Schoof, 2013). These multiple uncertainties have been quantified by number of studies using a combination of simulations from the different methods. Some studies compared the simulations produced by a single hydrological model forced by different scenarios, GCMs, GCM runs and RCMs (Sulis et al., 2012; Harding et al., 2012). Other studies used several hydrological models forced similarly with different climate data sources and used the spread between the different simulations to determine the sources of uncertainties (Dobler et al., 2012; Chen et al., 2011). These methods have limitations for a large number of simulations and a new method developed by Hawkins and Sutton (2009) using variance between simulations of temperature and precipitation was used to partition uncertainties of streamflow in large watersheds (Eisner et al., 2017). The analysis of variance (ANOVA) was also recently applied to quantify the sources of uncertainties in annual cycle of runoff and runoff quantiles projections (Bosshard et al., 2013), seasonal change in runoff (Hattermann et al., 2018), peak discharge (Su et al., 2017) or an ensemble of climate and hydrological processes (Lafaysse et al., 2014). Generally these studies found that the largest

uncertainties are from GCM but the results are highly dependent on the method used to quantify the uncertainties (Lee et al., 2017), the region of the world (Giuntoli et al., 2015) and the season (Ashraf Vaghefi et al., 2019). The source of uncertainty that dominates the overall uncertainty also depends on the metric used (Chegwidden et al., 2019; Her et al., 2019). The uncertainty due to the parametrization of hydrological models is important for soil moisture and groundwater (Her et al., 2019), the GCMs are mostly important for high flows related to rainfall, the scenarios have more impact on snowpack while uncertainties from hydrological models are more relevant for low flows (Chegwidden et al., 2019). These studies generally focused on the average streamflow (Lafaysse et al., 2014, Chegwidden et al., 2019; Chen et al., 2011; Harding et al., 2012) or on the annual high flows (Chen et al., 2011; Dobler et al., 2012; Hattermann et al., 2018; Lafaysse et al., 2014) but rarely on the seasonal high flows. Southern Ontario is a highly populated region in the Great Lakes and is affected by a strong change in the seasonality of high flows from spring to winter (Burn and Whitfield, 2015; Cunderlik and Ouarda, 2009). The aim of this research is to assess the contribution of different sources of uncertainties in the projections of winter-spring high flows in a small watershed in southern Ontario.

5.3 Data and methods

5.3.1 Study area and local data measurements

This study was conducted in the Big Creek watershed, covering 571 km^2 in the northern shore of Lake Erie upstream from Walsingham hydrometric station (Figure 5-1). This watershed is at 80% constituted by sandy soils and is covered mainly by crops (81%) while a small proportion is covered by forest (17%). The elevation varies from 179m at the stream outlet to 336 meters in the northern part of the watershed. This watershed was chosen because of long Water Survey of

Canada hydrometric records at Kelvin (02GC011), Delhi (02GC006) and Walsingham (02GC007). The watershed is also located close to the Turkey point observatory Flux tower where half-hourly observations of key hydrological variables such as evapotranspiration, soil moisture and snowpack has been made since 2003 (Peichl et al., 2010; Skubel et al., 2017). These variables were calculated at daily timestep and were used in the calibration and validation of the hydrological model described below.

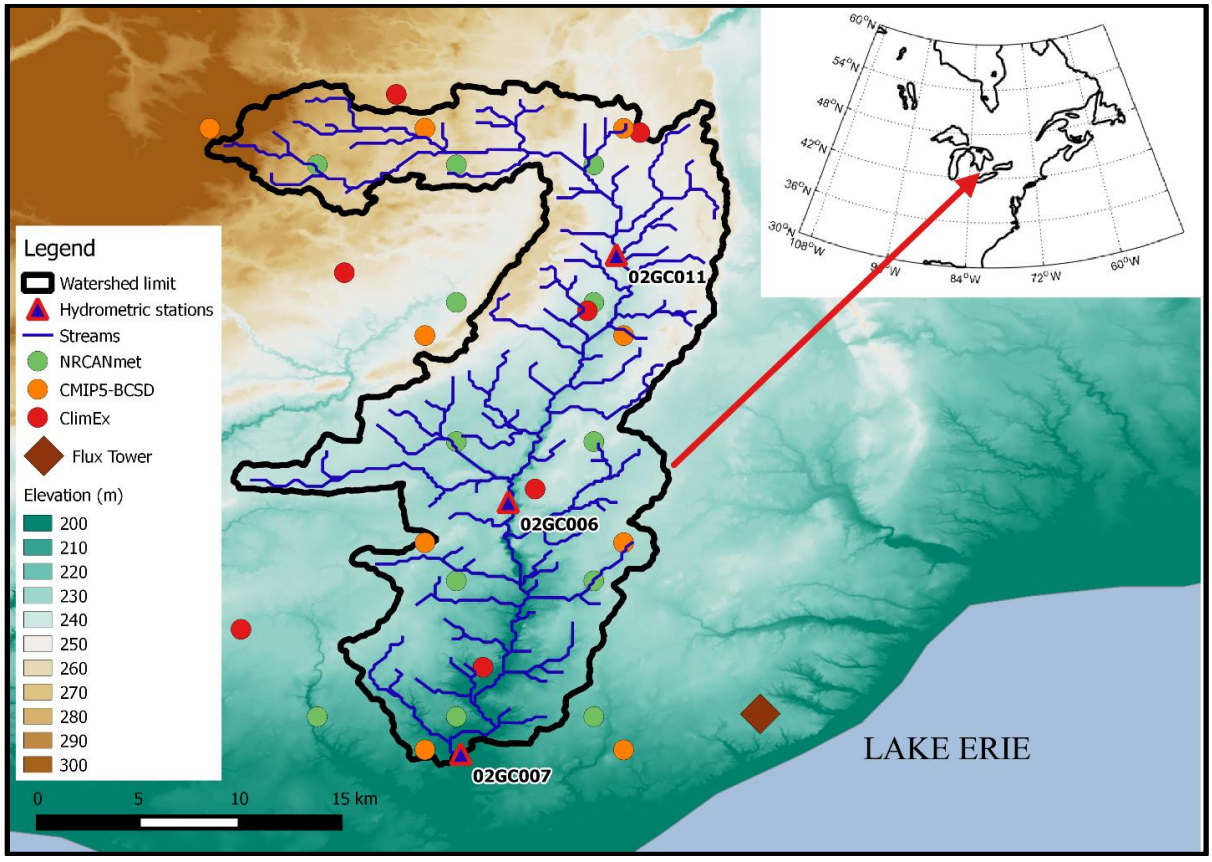

Figure 5-1 Location of Big Creek watershed in Southern Ontario

5.3.2 Hydrological model and calibration

The hydrological model used to simulate streamflow in the Big Creek watershed was the Precipitation and Runoff Modelling system (PRMS), a semi-distributed hydrological model.

PRMS computes the water flowing between hydrological reservoirs (i.e. plant canopy interception, snowpack, soil zone and subsurface) for each hydrological response unit (HRU) using conceptualized equations (Leavesley et al., 1983). A recent version of PRMS used in this study is described in Markstrom et al., (2015). The set up and parametrization of the model in Big Creek watershed was previously described in (Champagne et al., 2019a) and showed that seventeen parameters were needed to calibrate the model.

In this study the calibration of these parameters was done using the Dynamically Dimensioned Search (DDS) automatic calibration (Tolson & Shoemaker, 2007) using the *Optimization Software Toolkit for Research Involving Computational Heuristics* (OSTRICH, Mattot, 2016). The objective function used by DDS was the weighted sum of squared error applied to the observations and the simulations of local hydrological processes. To assess the impact of the objective function choice on the projections of streamflow, the calibration was done using seven different objective functions metrics. The first calibration was done using the daily streamflow in the 1989-2008 period, also called long period ("Long"). Two other methods aimed to assess the impact of using a higher weight on high streamflow and were also applied to 1989-2008 streamflow data. The first method doubled the weights on high streamflow ("Long HF2") and the second method tripled the weight on high streamflow ("Long HF3"). High flows were defined as streamflow higher than the mean streamflow plus three times the standard deviation. The weight was applied to all the days surrounding the high-flow from the day of starting rise to the last day of decrease in streamflow. The last day of the decrease was considered when the daily decrease started to be lower than $1 m^3 s^{-1}$. The four other methods were applied to 2003-2011 observations and simulations and served to

test the multi-process calibration. A short period (2003-2011) was chosen because the measurements of soil moisture and evapotranspiration were available for that period. The first method used only the streamflow ("Short"), the second method used daily streamflow, soil moisture and evapotranspiration together in the objective function and is referred as the Multi-Parameter calibration ("Short MP"). Soil moisture and evapotranspiration were measured at a flux tower site in a coniferous forest planted in 1939 (known as CATP4 or TP39 in global Fluxnet literature, Peichl et al., 2010) located close to the Big Creek watershed (Figure 5-1). The simulated soil moisture and evapotranspiration were taken from an HRU having a similar environment as the tower site in term of latitude, elevation, slope, aspect, land use, and soil. The third method used a combination of the multi-processes calibration and a weight doubled for high flows ("Short MP-HF2"). Finally, the last method was similar to Long-HF2 but for the 2003-2011 period ("Short HF2").

5.3.3 Climate data

The calibration of PRMS described in the previous section has been done using NRCANmet minimum Temperature (Tmin), maximum temperature (Tmax) and precipitation (P) as forcing data. NRCANmet is a 10km^2 resolution gridded dataset made from the interpolation of Environment and Climate Change Canada and Natural Resources Canada weather stations (McKenney et al., 2011). To simulate the future evolution of streamflow, two climate products were used. The first product is the bias-correction spatial disaggregation (BCSD) of temperature and precipitation from 11 models of the Climate Model Intercomparison Project version 5 (CMIP5) available in 1950-2099 period (Reclamation, 2013). Each of the 11 CMIP5-BCSD models listed in Table 5-1 were forced with two Intergovernmental Panel on Climate Change

(IPCC) scenarios of climate change (i.e. RCP 4.5 and RCP 8.5) applied in the 2006-2099 period. The other climate dataset used in this study is the Canadian Regional Climate Model Large Ensemble (CRCM5-LE). CRCM5-LE is a 50-member regional model ensemble produced over northeastern North America in the scope of the Québec-Bavaria international collaboration on climate change (ClimEx project; Leduc et al., 2019). CRCM5-LE is the downscaled version of the global Canadian model large ensemble (CanESM2-LE) at 310km^2 grid resolution forced with RCP8.5 scenario. CMIP5-BCSD and CRCM5-LE have a similar spatial resolution of about 12km^2 (Figure 5-1). Temperature and precipitation data from each member of these datasets have been bias corrected following Ines and Hansen (2006) using the NRCANmet data as observations in the 1957-2005 period. For each month of the year, the intensity distribution of temperature was corrected using a normal distribution. The precipitation frequency was first corrected by truncating the modelled rainfall distribution in order to reproduce the observed distribution of precipitation. The truncated intensity distribution was then corrected with a gamma distribution (Ines and Hansen, 2006). Each modelled grid point was bias corrected using the closest NRCANmet point. Using a unique NRCANmet point for each CRCM5-LE or CMIP5-BCSD point was permitted in this study because of low elevation gradients between points, the spatial variability of temperature and precipitation being more dependent on the proximity of the Lakes than the elevation (Scott and Huff, 1996). Even though the grid points do not match between CRCM5, CMIP5-BCSD and NRCANmet, the resolution is similar and close to 10-12km^2 on average (Figure 5-1). Each of these bias corrected datasets have been used as forcing data in PRMS with each of the seven calibrated set of parameters, giving a total of 504 simulations of multiple hydrological variables in the 1960-2099 period.

Table 5-1 CMIP5-BCSD GCMs used in the study

Modelling center	Institute ID	Model Name
Institut Pierre-Simon Laplace	IPSL	IPSL-CM5A-LR
Institut for Numerical Mathematics	INM	INM-CM4
Atmosphere and Ocean Research Institute (The University of Tokyo), National Institute for environmental Studies, and Japan Agency for Marine-Earth Science and Technology	MIROC	MIROC5
NOAA Global Modeling and Assimilation Office	NOAA GFDL	GFDLESM2M
		GFDLESM2G
Commonwealth Scientific and Industrial Research Organization in collaboration with Queensland Climate Change Centre of Excellence	CSIRO-QCCCE	CSIRO-Mk3.6.0
Centre National de Recherches Météorologiques / Centre Européen de Recherche et Formation Avancée en Calcul Scientifique	CNRM-CERFACS	CNRM-CM5
National Center for Atmospheric Research	NCAR	CCSM4
Canadian Centre for Climate Modelling and Analysis	CCCMA	CANESM2
Beijing Climate Center, China Meteorological Administration	BCC	BCC-CSM1.1
Commonwealth Scientific and Industrial Research Organization (CSIRO) and Bureau of Meteorology (BOM), Australia	CSIRO-BOM	ACCESS1.0

5.3.4 Uncertainty analysis

The uncertainties in the hydrological metrics caused by the choice of the greenhouse gases emissions scenarios (SCE), the GCMs, the internal variability (INT) and the calibration technique (CAL) were quantified using a method derived from Hawkins and Sutton (2009) and previously applied in watershed hydrology (Eisner et al., 2017). The method was applied to different streamflow metrics such as the daily average streamflow and number of high flows. The number of high flows was defined as number of days with streamflow higher than the observed average streamflow plus three times the standard deviation (24 m^3/s in this watershed). The method was also applied to Tmax, Tmin and P and daily average processes such as rainfall, snowfall, snowmelt

and evapotranspiration. Other metrics representing extreme events were investigated (i.e. seasonal maximal daily rainfall, seasonal maximal daily snowmelt and Heavy rain and warm events). The heavy Rain and warm events index, applied only in winter, was previously identified as necessary conditions to generate high flows in southern Ontario (Champagne et al., 2019c). Each of these metrics was calculated for a 30years moving average period every 5 years between 1961 and 2095. The first time period was therefore 1961-1990, the second 1966-1995, the third 1971-2000 and the last was 2066-2095 (Noted as 1975, 1980, 1985 and 2080 respectively in the Figures). This gave a total of twenty-two timesteps from 1961-1990 to 2066-2095 for which the variance was calculated for each source of uncertainty. The uncertainty from the scenarios was obtained by averaging the variance calculated between the two scenarios of each CAL-GCM simulation. For calibration uncertainties we averaged the variance calculated between the simulations from the seven calibration methods of each SCE-GCM and the variance between the seven calibration methods of each CRCM5-LE member. For the GCM uncertainties the variance between the simulations from the eleven GCM's of each CAL-SCE have been averaged. Finally, the uncertainty from internal variability was obtained by averaging the variance of the 50 members of CRCM5-LE for each calibration method. Because only CRCM5-LE ensemble was available for this study we assume that the variance obtained from the CRCM5-LE 50 members is representative of other ensembles calculated from different GCM-RCM chains. The relative part of the variance due to each source of uncertainty was determine for each metric by calculating the ratio of each source of uncertainty to the sum of the variance from each sources of uncertainty at each timestep. All simulations mean ($\sigma(t)$) was also calculated for each metric at each timestep. Assuming normal distributions, the upper (lower) limit of the 95 % confidence interval around the mean was obtained

by adding (subtracting) 1.645 x std(t) to σ(t), with std(t) the standard deviation of all simulations for each time step. The total range between the upper and the lower limits was split into the different sources of uncertainties according to their relative part previously calculated (Second and fourth rows in Figures 5-4 to 5-7 and second row in Figure 5-8). The reader must be aware that the sum of the variance from each sources of uncertainty was slightly higher than the variance calculated for all simulations. Therefore, the share in sources of uncertainties in the Second and fourth rows in Figures 5-4 to 5-7 and second row in Figure 8 should be read as relative uncertainties compare to one another.

5.4 Results

5.4.1 Validation of hydrological processes simulated by PRMS

The simulations of hydrological processes using PRMS forced with Tmax, Tmin and precipitation from NRCANmet were compared with the observed streamflow. The Nash Sutcliffe efficiency (NSE, Nash and Sutcliffe, 1970) and the percentage bias (Pbias, Moriasi et al., 2007) were used to assess the efficiency of the streamflow simulations (Table 5-2, 5-3 and 5-4).

Table 5-2 Efficiency of PRMS to simulate daily streamflow

	Calibration		Validation	
	NSE	PBias	NSE	PBias
Long	0.76	-2.2	0.74	3.1
Long HF2	0.72	-10.5	0.77	-4.7
Long HF3	0.79	-2.8	0.78	2.4
Short	0.73	-11.2	0.78	-6
Short MP	0.70	-3.4	0.71	1.7
Short HF2	0.67	-6.6	0.77	-0.6
Short MP-HF2	0.71	-1.8	0.72	3.5

Table 5-3 Efficiency of PRMS to simulate daily streamflow at three hydrometric stations

	Kelvin [02GC011]		Delhi [02GC006]		Walsingham [02GC007]	
	NSE	PBias	NSE	PBias	NSE	PBias
Long	0.55	-17.3	0.70	-4.9	0.74	3.1
Long HF2	0.55	-27.1	0.70	-13.3	0.77	-4.7
Long HF3	0.55	-18.2	0.75	-5.9	0.78	2.4
Short	0.53	-28.1	0.72	-14.6	0.78	-6
Short MP	0.44	-19.6	0.64	-6.3	0.71	1.7
Short HF2	0.65	-22.4	0.74	-8.8	0.77	-0.6
Short MP-HF2	0.50	-17.1	0.68	-4.4	0.72	3.5

Table 5-4 Efficiency of PRMS to simulate daily streamflow in winter (DJF) and spring (MAM)Table

	MAM				DJF			
	Calibration		Validation		Calibration		Validation	
	NSE	PBias	NSE	PBias	NSE	PBias	NSE	PBias
Long	0.70	-7.8	0.68	-2.7	0.74	-5.8	0.74	-1.3
Long HF2	0.62	-13	0.71	-10.5	0.70	-12.7	0.78	-9.4
Long HF3	0.74	-2.7	0.72	-2.5	0.71	-12.5	0.77	-2.2
Short	0.68	-6.9	0.71	-10.5	0.69	-13.9	0.78	-10.1
Short MP	0.58	-4.4	0.69	-3.3	0.72	5.1	0.67	-1.6
Short HF2	0.57	-14.3	0.72	-7	0.58	-16.7	0.80	-6.1
Short MP-HF2	0.65	-11.1	0.72	-2.6	0.69	-8.4	0.71	-1.3

Figure 5-2 shows the hydrographs of the simulated and observed streamflow for three hydrographs in the watershed. The results were satisfactory whatever the calibration method employed (Figure 5-2 and Table 5-2) even though the efficiency was lower in the northern part of the watershed, upstream from the Kelvin hydrometric station (Table 5-3). The model performed better when considering all seasons and performed generally better in winter compared to spring (Table 5-3 and 5-4). The long and short calibrations using only streamflow gave similar good results. The calibration with a factor 3 applied to the high flows (Long HF3) show the best result and improved the calibration applied only to streamflow (Long), while using the factor 2 (Long HF2) improved the results only for the validation period. The difference between calibration and validation are

lower when considering the entire year (Table 5-2), while better results generally appeared for validation when considering winter or spring (Table 5-3). The bias was negative for most of the calibration methods and was stronger for the high flows factor 2 in winter and spring. The bias was also strongly negative when using the short calibration. Even though significant differences were observed in the NSE and Pbias, the difference between simulations was not significantly large (Figure 5-2 and 5-3).

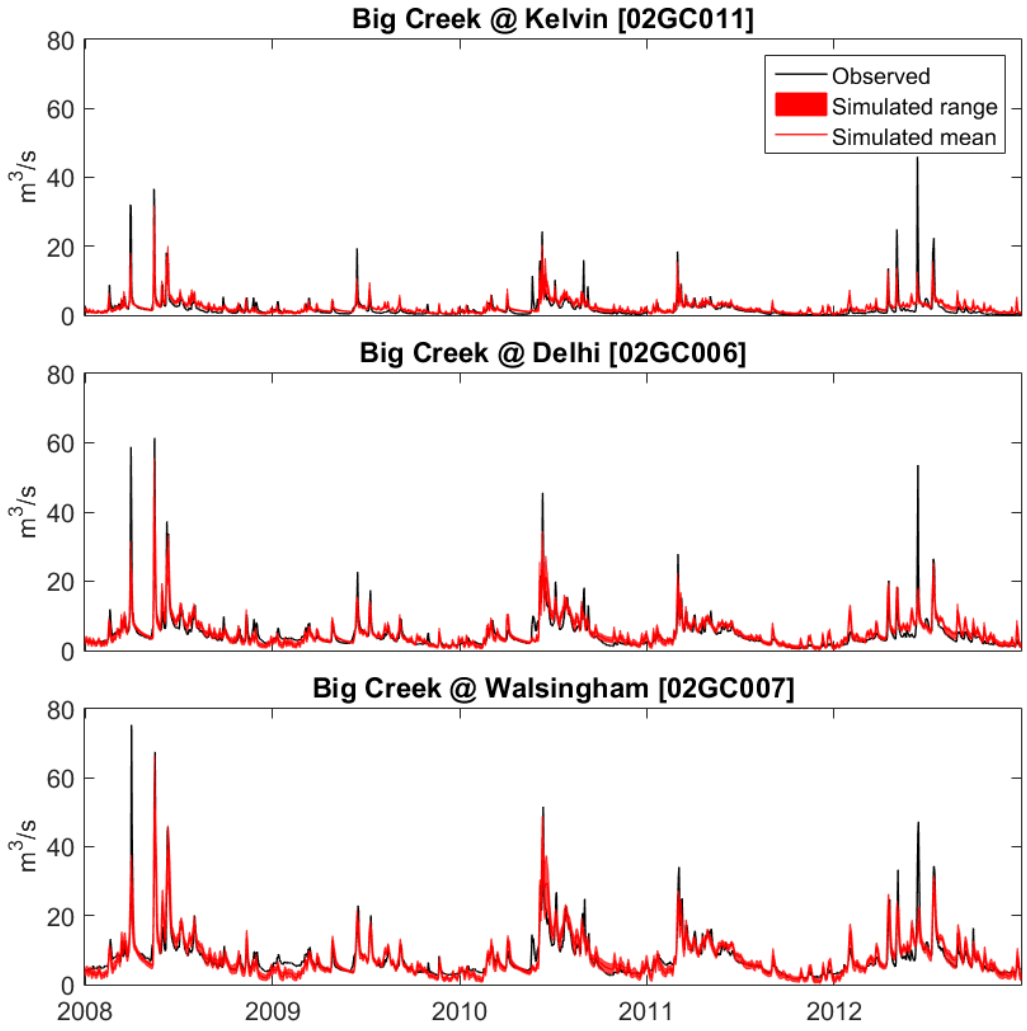

Figure 5-2 Comparison between the seven calibration methods range and mean daily simulated streamflow and daily observed streamflow for three hydrometric stations.

Soil moisture, evapotranspiration and snow-depth measured and calculated by PRMS were compared visually and in term of the normal root mean square error (NRMSE, Figure 5-3 and Table 5-5).

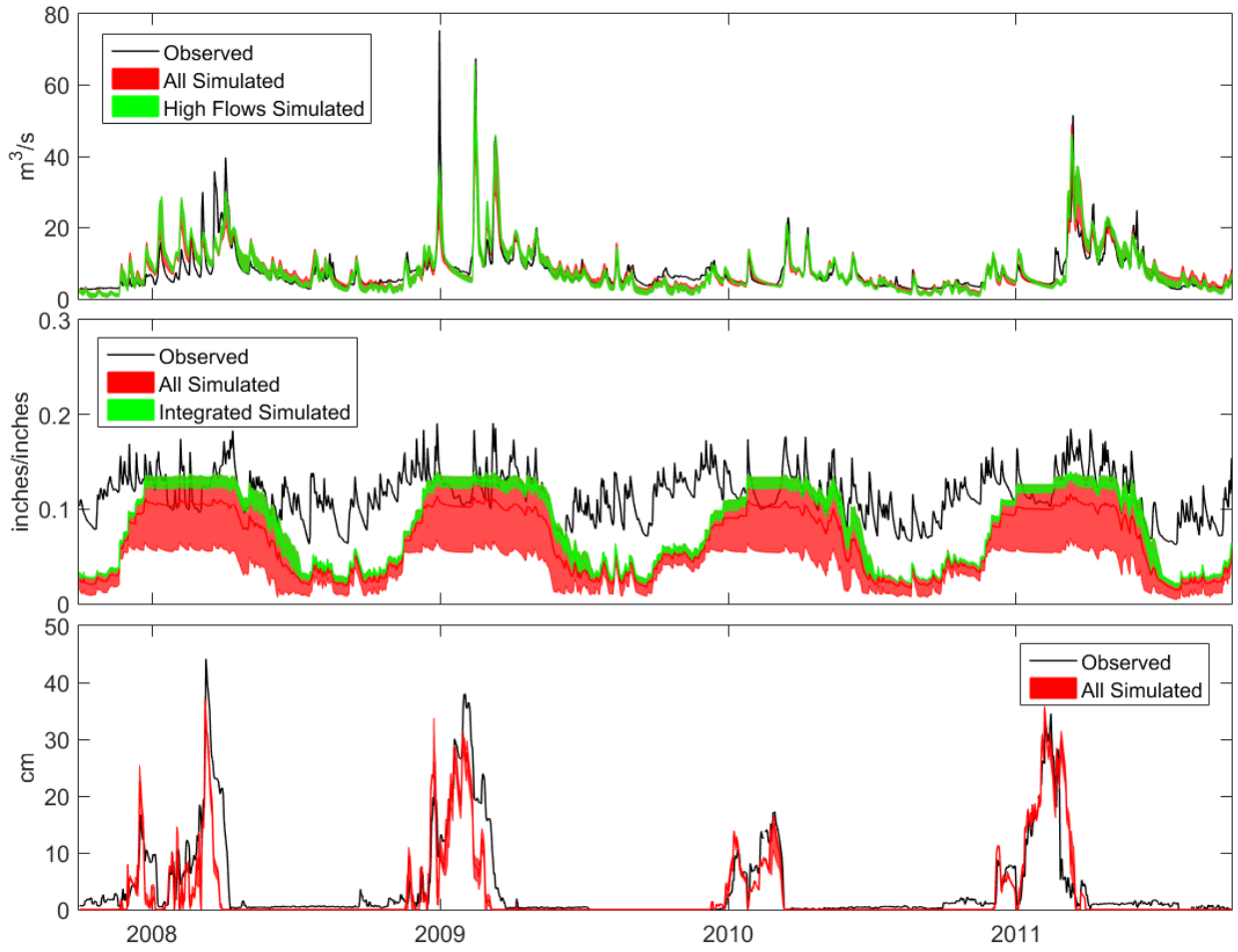

Figure 5-3 Comparison between simulation and observations in the validation period for streamflow (upper row), soil moisture (mid row) and snowpack (lower row).

The NRMSE of evapotranspiration did not varied between the different calibration methods in both seasons. Snow depth was generally well simulated by PRMS (Figure 5-3) but was slightly less satisfactory with the multi-processes calibration (Short MP). Regarding the soil moisture it was clearly underestimated (Figure 5-3) but varied greatly from one calibration method to another.

The calibration using streamflow only and no weight in high flows (Long) showed the greatest underestimation. The long calibration with a factor 2 applied on high flows was also largely underestimated. The effect of using soil moisture in the calibration process did not improve the results compared to the streamflow-only calibration in winter while using multi-parameters calibration improved the results in spring especially when associated with the high flows factor.

Table 5-5 NRMSE between simulations and observations of hydrological processes

	Soil moisture		Evapotranspiration		Snow-depth	
	DJF	MAM	DJF	MAM	DJF	MAM
Long	1.48	1.17	1.54	0.97	0.58	0.71
Long HF2	2.76	2.86	1.54	0.97	0.57	0.70
Long HF3	1.48	1.33	1.55	0.97	0.59	0.70
Short	3.80	3.69	1.53	0.97	0.60	0.72
Short MP	1.56	1.09	1.54	0.97	0.66	0.74
Short HF	1.73	1.74	1.53	0.97	0.56	0.71
Short MP-HF	1.46	0.72	1.55	0.97	0.61	0.73

5.4.2 Future evolution of CRCM5-LE and CMIP5 forcing data.

Figure 5-4 shows the 30 years running average of bias corrected Tmin, Tmax and P from each member of CRCM5-LE and each emission scenario of CMIP5 in winter and spring. Tmin and Tmax are increasing and CRCM5-LE and the two scenarios of CMIP5 show a similar trend until 2040's. After the mid-21st-century the warming is expected to accelerate in CRCM5-LE and CMIP5 forced by RCP 8.5 while a low trend is expected in CMIP5 forced by RCP4.5. Precipitation is also expected to increase but the trend is less consistent throughout the period. In winter, precipitation from CMIP5 forced by RCP 8.5 starts to be higher than RCP 4.5 in beginning of the 21st century and the difference between the two scenarios will slowly increase through the 21st century. CRCM5-LE winter precipitation followed CMIP5 forced by RCP4.5 in the historical period and will slowly catch up to CMIP5-RCP8.5 at the end of the century. In spring the two

CMIP5 scenarios are expecting to separate only at the end of the century and CRCM5-LE is expecting to stay much lower than both CMIP5 scenarios.

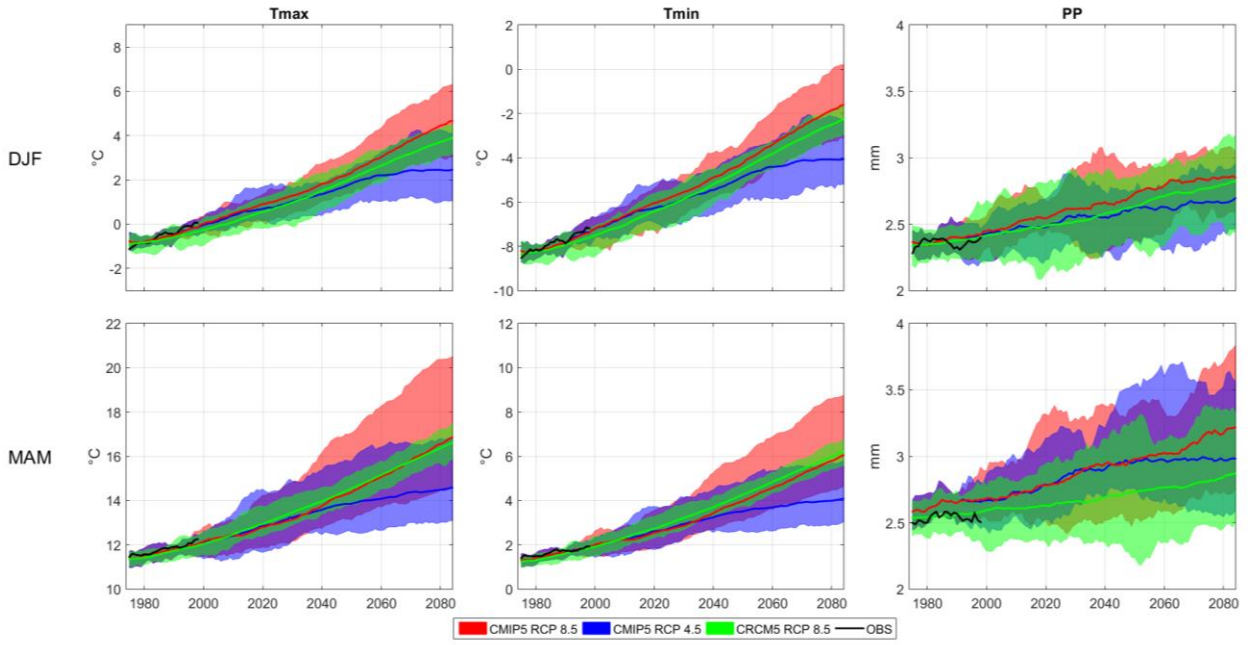

Figure 5-4 30-years running average and range of bias corrected temperature and precipitation in Big Creek watershed

The total spread of all 11 CMIP5 simulations of temperature from RCP4.5 or RCP8.5 is similar to the 50-members CRCM5-LE spread in the historical period. The CMIP5 spread will consistently increase throughout the 21st century to become much larger than CRCM5-LE at the end of the century. The spread in precipitation is similar for CMIP5 and CRCM5 and is larger in spring.

Figure 5-5 shows the partition of the uncertainties in the projection of temperature and precipitation. Overall, GCM is the highest source of uncertainties for the projections of temperature especially in spring while the uncertainties from scenarios and internal variability is higher in winter. At the end of the 21st century the part of uncertainties due to the scenarios is

expecting to increase significantly for both seasons while uncertainties from internal variability will become very low. The partition of the uncertainties in the projections of precipitation shows higher uncertainties from scenarios in winter while in spring GCM dominates the uncertainties.

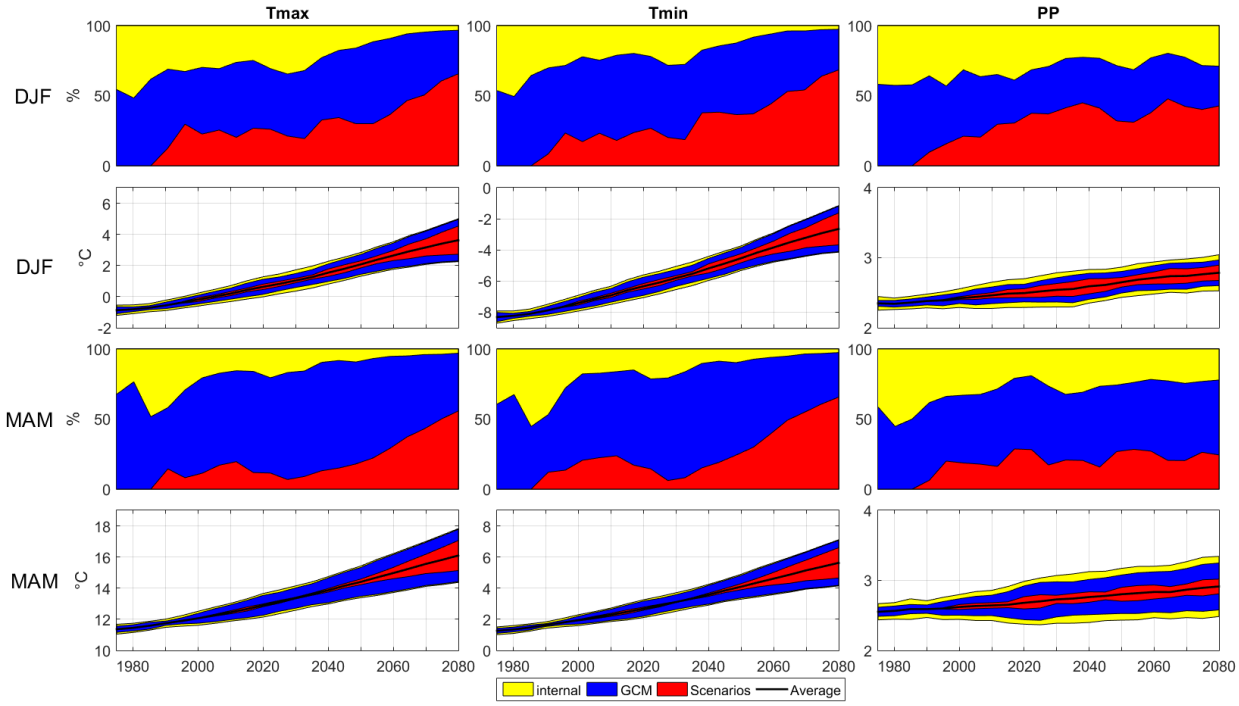

Figure 5-5 Distribution of temperature and precipitation variance between sources of uncertainty in december-january-february (top two rows) and march-april-may (bottom two rows). Rows 1 and 3: Part of different sources of uncertainty relative to the total variance (in %) for a 30 years running average. Rows 2 and 4: All simulations average (Black line) with 95% confidence interval (total colored).

5.4.3 Variance in the future evolution of hydrological processes

The simulated streamflow in Big Creek watershed is expected to increase in winter and decrease in spring (Figure 5-6). In 2000's, the daily average streamflow of all simulations was clearly higher in spring ($12 m^3 s^{-1}$) compared to winter ($9 m^3 s^{-1}$) and the number of high flows in spring (0.7 per year) was twice the number of high flows in winter (0.35 per year). By 2080's difference between both seasons is expected to be much lower with a daily average streamflow of $11 m^3 s^{-1}$ in spring

and $10 m^3 s^{-1}$ in winter and a number of high flows close to 0.6 per year in spring and 0.5 in winter. Figure 5-6 shows that this change in streamflow is affected by a strong spread similarly partitioned into different sources of uncertainties for daily average streamflow and seasonal number of high flow. In the historical period the calibration was the most important source of uncertainties in both winter and spring. The emission scenarios should become the highest source of uncertainty around 2030s in winter while in spring uncertainties from GCM are expected to become prevalent. The contribution of internal variability of climate to the total uncertainty is not greatly changing throughout the period whatever the season or the metrics used.

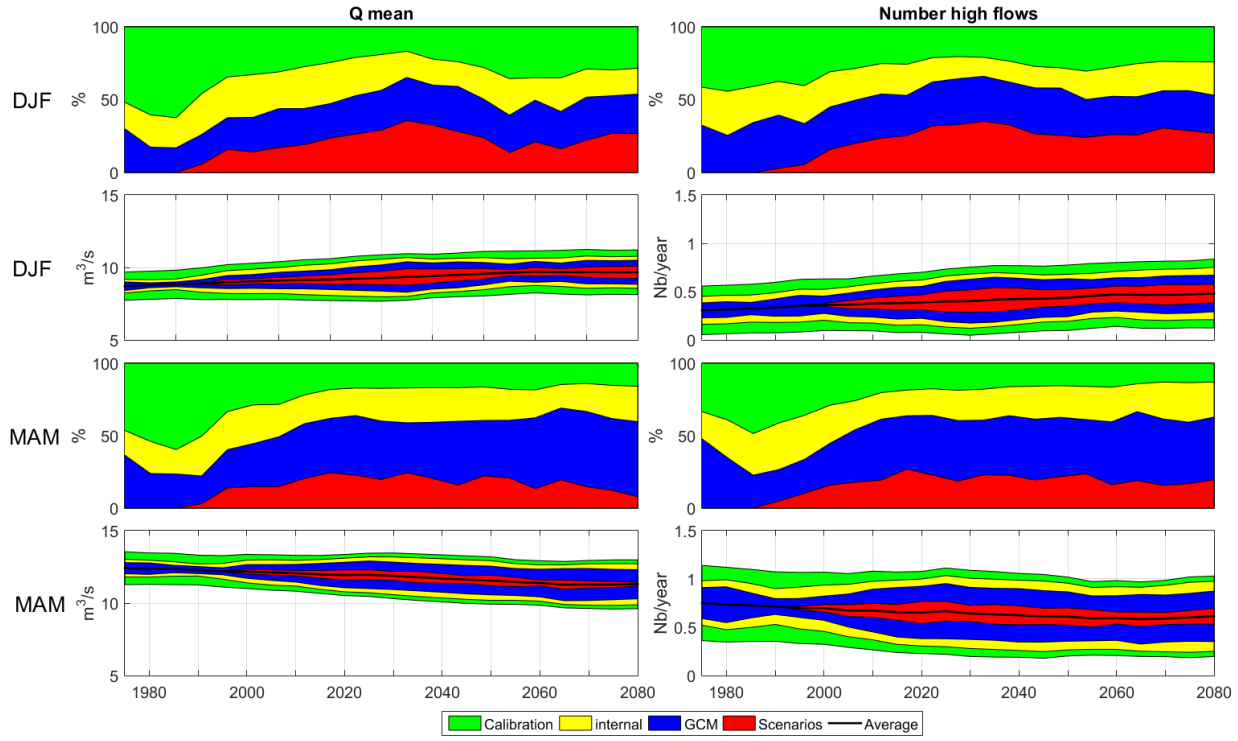

Figure 5-6 Distribution of variance between sources of uncertainty for the average daily streamflow (Left) and number of high flows (Right) in december-january-february (top two rows) and march-april-may (bottom two rows). Rows 1 and 3: Part of different sources of uncertainty relative to the total variance (in %) for a 30 years running average. Rows 2 and 4: All simulations average (Black line) with 95% confidence interval (total colored).

The change in the simulated amount of rainfall, snowfall, snowmelt and evapotranspiration were also investigated (Figure 5-7). In 2000s the simulated amount of rainfall (1.2 mm day^{-1}) and snowfall (1 mmWeq day^{-1}) are comparable in winter. By the end of the 21st century the amount of rainfall (1.8 mm day^{-1}) will increase by 50% and will be much higher than the amount of snowfall (0.55 mmWeq day^{-1}). Consequently, the amount of snowmelt is also expected to decrease by 32%. In spring, rainfall will increase by 20% from 2 mm day^{-1} in 2000s to 2.4 mm day^{-1} in 2080's and the snowmelt amount will decrease by two-third from 0.6 mmWeq day^{-1} to only 0.2 mmWeq day^{-1}. Evapotranspiration is very low in winter but is expected to increase dramatically in Spring from 1.16 mm day^{-1} in 2000s to 1.50 mm day^{-1} in 2080s.

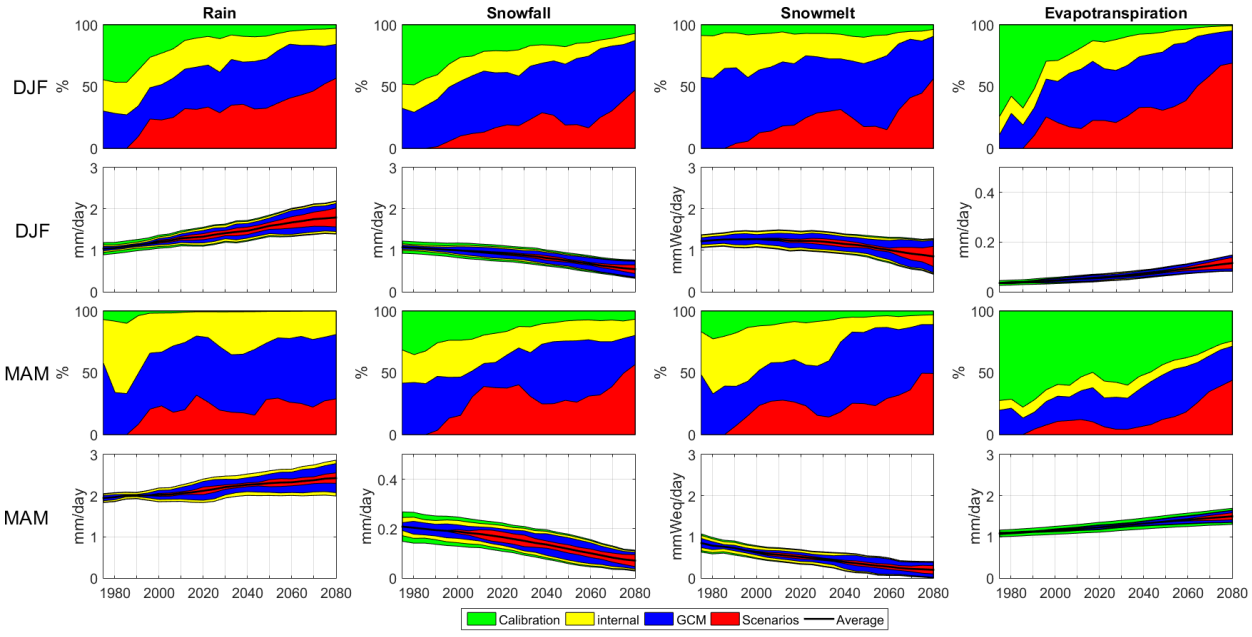

Figure 5-7 Distribution of variance between sources of uncertainty for simulated daily rainfall, snowfall, snowmelt and evapotranspiration in december-january-february (top two rows) and march-april-may (bottom two rows). Rows 1 and 3: Part of different sources of uncertainty relative to the total variance (in %) for a 30 years running average. Rows 2 and 4: All simulations average (Black line) with 95% confidence interval (total colored).

The uncertainty in the simulation of rainfall amount was mostly due to the calibration method in winter and to the internal variability in spring in the historical period (Figure 5-7). In the future, the scenarios are expected to become a large source of uncertainty in winter while GCM is expected to dominate in spring. Snow processes shows slightly different results with GCM dominating the uncertainties in most of the 21st century but scenarios becoming important at the end of the century in winter. In spring the internal variability of climate dominated for the historical period, GCM uncertainty is taking over in the near future and scenarios should become the most important source of uncertainty by the end of the century. Regarding evapotranspiration, calibration dominated the overall uncertainties in the historical period while at the end of the 21st century scenarios and GCM are expecting to become dominant.

To explain the evolution in number of high flows, the seasonal maximal amount of daily rainfall and snowmelt have been analyzed (Figure 5-8), They show similar trends compared to the mean conditions (Figure 5-7). In the historical period the winter average daily maximum amount of rain (19.7 mm) was lower than the winter average daily maximum amount of snowmelt (23.1 mmWeq) but is expecting to increase to reach 24mm by 2080, while snowmelt should decrease to 17.1mmWeq. The average daily maximum amount of rainfall is also expecting to increase in spring from 23.9mm to 28.4mm, while the amount of snowmelt will dramatically decrease from 16mmWeq to 6.7mmWeq. The distribution of the uncertainties from scenarios and GCM show similar results between extremes and average values (Figure 5-7 and 5-8) while calibration

uncertainties appear lower and internal uncertainties appear larger when focusing on the extremes (Figure 5-7 and 5-8).

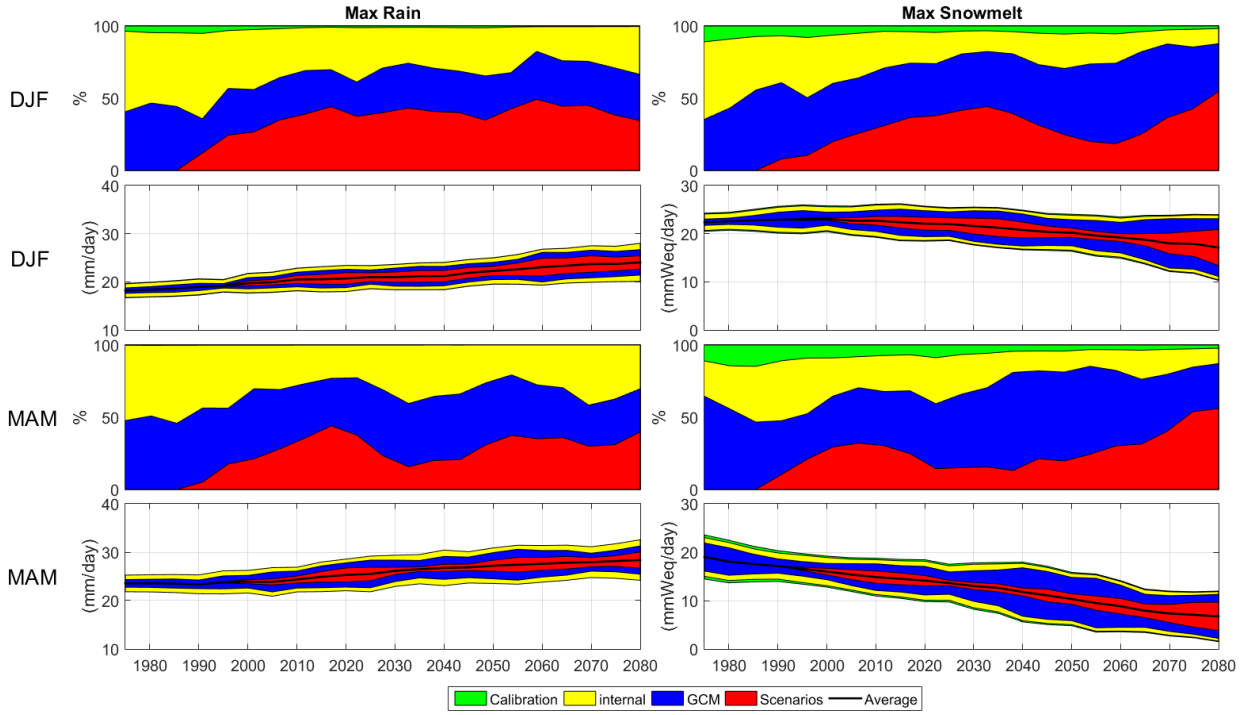

Figure 5-8 Distribution of variance between sources of uncertainty for daily maximum rainfall and snowmelt in december-january-february (top two rows) and march-april-may (bottom two rows). Rows 1 and 3: Part of different sources of uncertainty relative to the total variance (in %) for a 30 years running average. Rows 2 and 4: All simulations average (Black line) with 95% confidence interval (total colored).

The analyses also focused on winter heavy rain and warm index (Figure 5-8). The number of warm events was higher than the number of heavy rain events in the historical period but the increase in number of heavy rain events between 2000s and 2080s (23%) is expecting to be faster than the increase in number of warm events (12%). The compound index heavy rain and warm events should increase the most with about 75% share in increase. The partition of the sources of uncertainties are similar for the three kind of events and show an increase in the contribution of

scenarios but a decrease in the contribution of internal variability to the overall uncertainties (Figure 5-9).

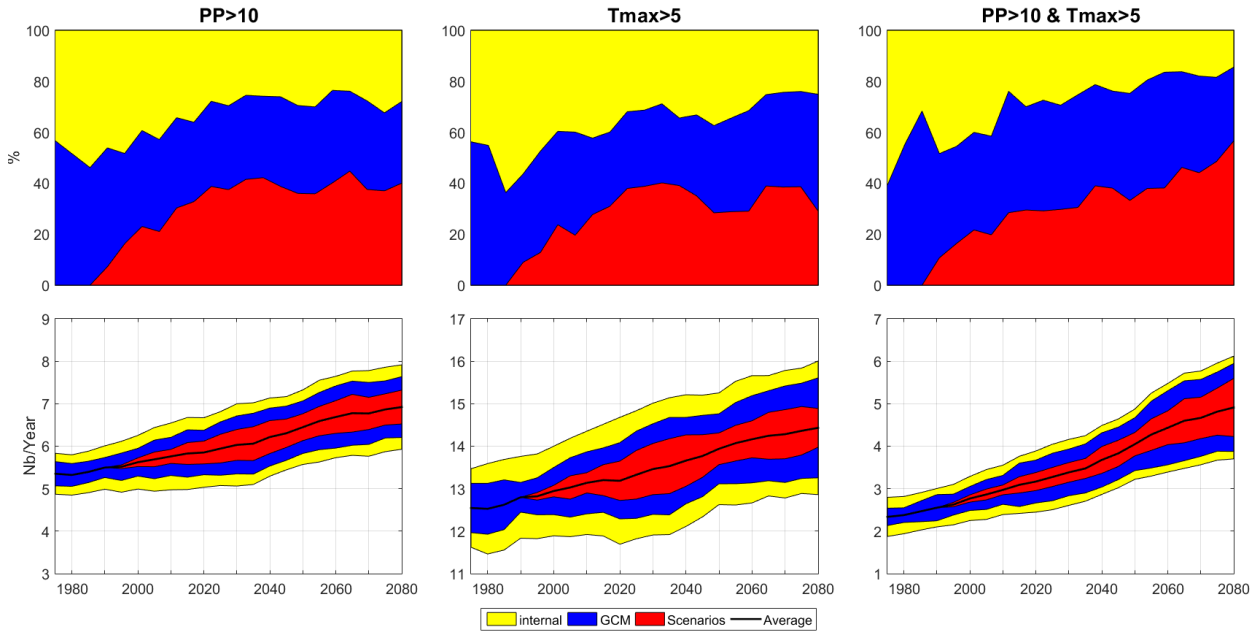

Figure 5-9 Distribution of variance between sources of uncertainties for DJF number of precipitation and temperature extremes. Rows 1 and 3: Part of different sources of uncertainties relative to the total variance (in %) for a 30 years running average of each 5 years timestep. Rows 2 and 4: All simulations average (Black line) with 95% confidence interval (total colored).

5.5 Discussion

5.5.1 Shift in number of high flows due to more winter weather extreme events

The results projecting an increase in streamflow in winter and a decrease in spring (Figure 5-6) are consistent with other watersheds in the Great Lakes region (Erler et al., 2018; Grillakis et al., 2011; Kuo et al., 2017; Rahman et al., 2012; Sultana and Coulibaly, 2011). The increase in winter streamflow will be mostly due to the increase in precipitation offset by a decrease in snowmelt (Figure 5-4 and 5-7). The decrease in snowfall will occur at a higher rate than the decrease in snowmelt in winter (Figure 5-7) suggesting that warming reduces the snow to rain ratio but

increases the snowmelt to snowpack ratio. The increase in winter streamflow due to precipitation enhancement was projected in the Canard watershed situated further west (Rahman et al., 2012). Grillakis et a1., (2011) studied the evolution of streamflow in a watershed located 80km north from our study area and showed that the increase in streamflow is due to an increase of rainfall in January while it is due to greater snowmelt in February. A previous study in the Big Creek watershed divided the winter season into specific months and showed a reduction in snowmelt in February (Champagne et al., 2019b). For watersheds situated further north or far from the lakes, snowmelt is expecting to increase especially in the first half of 21st century (Champagne et al., 2019b). In Big creek watershed, snowmelt was slightly increasing in the historical period and started to decline after 2000s (Figure 5-7). This suggests that due to warming the snowmelt to snowpack ratio was first dominant over the decrease in snow to rain ratio in the historical period, but later in the 21st century snow to rain ratio will become too small to increase the snowmelt, in particular in southern watersheds. In spring, despite an increase in precipitation, streamflow is expecting to decrease partly due to a dramatic decrease in snowmelt (Figure 5-7). Given that the spring reduction in snowfall will be very low as compared to the decrease in snowmelt, snowmelt decline is mostly due to less snowpack remaining from winter and not a reduction in snowfall. The decrease in streamflow can also be attributed to the increase in evapotranspiration.

The reduction in snowfall and snowmelt is also expected to have an impact on winter high flows. The number of heavy rain and warm events is expected to double by the end of the 21st century compare to the end of the 20th century (Figure 5-9) while the number of high flows is expected to occur only 1.5x times more frequently (Figure 5-6). The lower trend in the increase of

high flows compared to the increase in extreme weather events is associated for a part to the decrease in amount of annual maximum snowmelt (Figure 5-8). The decrease in the amount of winter maximum snowmelt is likely due to more frequent snowmelt periods associated to more warm extreme events. This suggest that the warm extreme events melt the snowpack more often and decrease the occurrence of thick snowpack that is more likely to produce high flows. This result also suggests that rain events will drive the generation of high flows in the future more than in the historical period. The decrease in spring maximum snowmelt is much larger and drives the reduction in number of high flows even though this reduction might be attenuated by the increase of rain events. The evapotranspiration likely plays a smaller role in the decline in number of high flows suggested by the lower decrease in number of high flows compared to the reduction in average streamflow.

5.5.2 Decomposition of the different sources of uncertainties

The shift from spring to winter in the streamflow volume and number of high flows is affected by a strong overall uncertainty (Figure 5-6). The decomposition of streamflow uncertainty showed contrasting results between winter and spring that can be explained by uncertainties from the forcing data. In winter the uncertainties in the average streamflow and number of high flows (Figure 5-6) is likely transferred from emission scenarios uncertainties in the projection of temperature and precipitation (Figure 5-5). The higher contribution of emission scenarios to the overall mean streamflow uncertainty in winter was also shown by Chen et al., (2011) in a catchment located in Quebec. In Spring, temperature and precipitation show a higher uncertainty caused by GCMs (Figure 5-5) and therefore a higher GCM uncertainty in the projections of average streamflow and number of high flows (Figure 5-6). These uncertainties are transferred

from precipitation volume and temperature that change the rain to snow ratio (Figure 5-7). Our results also suggest an increasing role of precipitation over temperature in the partitioning of the uncertainties due to decrease of snowfall amount (Figure 5-7). In winter, the 2030s peak in the emission scenarios uncertainties for the mean streamflow and number of high flows (Figure 5-6) corresponds to peaks in temperature and precipitation scenarios uncertainties (Figure 5-5). At the end of the 21st century the temperature uncertainties from scenarios clearly increase for both seasons (Figure 5-5) but this increase is not transferred to streamflow uncertainties (Figure 5-6) likely due to less snow availability (Figure 5-7). These results are in line with Hattermann et al., (2018) showing that the higher uncertainty from GCM occurs in seasons where streamflow is more affected by precipitation which is expecting to be increasingly the case in the future in southern Ontario. The increasing role of precipitation is also shown by the uncertainties from internal variability that is significantly reduced for temperature through the 21st century while it plays a consistent role in the overall uncertainties of precipitation (Figure 5-5) and streamflow (Figure 5-6). Lafaysse et al., (2014) similarly show that the large-scale internal variability uncertainties is expected to contribute less to the total snowmelt uncertainties in the future but will still contribute significantly to precipitation uncertainties. In a snow reduction context and increasing role of precipitation, the discharge uncertainty will still be greatly affected by internal variability of climate (Lafaysse et al., 2014). Chegwidden et al., (2019) showed that emission scenarios uncertainties are prevalent for metrics impacted by snowmelt while GCM and internal variability are more important for metrics affected by precipitation. We showed that streamflow could be more affected by precipitation in the future and therefore attenuating the uncertainties from emission scenarios but enhancing uncertainties from GCM and internal variability.

5.5.3 Other sources of uncertainties

In this study four main sources of uncertainties have been investigated using two emissions scenarios, 11 GCMs, 50 members of CRCM5-LE and seven objective functions in the DDS calibration algorithm. Other sources of uncertainties and a higher number of scenarios or models could be used to improve the uncertainty analysis. The scenario RCP 2.6 was not used in this study and therefore the complete range of emission scenarios was not investigated. However, the results are not expected to be very different using RCP2.6 because RCP 4.5 shows an evolution of greenhouse gases emissions and global temperature just slightly higher than RCP2.6 (Stocker, 2014). The number of GCM's used could also change the uncertainty range especially because of a high variability in inter-GCM amount of precipitation (Kay et al., 2009). In our study, only a portion of all CMIP5 models were used due to their availability and the exclusion of models showing suspicious values in our area. A systematic selection of the best GCMs could also be done to avoid using GCMs that don't recreate satisfactory local climates (Her et al., 2019). We also used only one bias corrected methods while the different methods can produce different results (Ehret et al., 2012). To represent the uncertainties from internal variability our study used the ensemble CRCM5-LE. It is likely that other ensembles made from other GCM-RCM chains could produce different results due to the interactions between GCMs and RCMs (Kay et al., 2009). However, the development of such large regional ensemble is recent and only available for few GCM-RCMs chain. Waiting for other products to be developed, it was relevant to show how such an ensemble can be integrated in the hydrological uncertainties studies and how it is positioned compare to other sources of uncertainties. The uncertainties due to the choice of the hydrological model were not investigated at all but can have a significant impact in snow dominated regions (Giuntoli et al.,

2015; Hattermann et al., 2018). Concerning the calibration, we assessed the uncertainties from the choice of the metrics used in the objective function. The Evapotranspiration and soil moisture data used in the objective function represent only one type of land use and soil type (Coniferous forest on sand) which is not representative of the entire watershed, covered mostly by crops. Measurements in areas more representative of the watershed would increase the confidence in the results. These variables have been calibrated using the DDS method, which is a widely used method (Tolson and Shoemaker, 2007), but other calibration techniques could change the uncertainty range. Despite possible improvements in the investigation of the sources of uncertainties, the number of simulations that can be handled by the hydrological model in a reasonable time is not infinite. Therefore, a compromise has to be found between the number of the simulations and the accurate representation of the different sources of uncertainties.

5.6 Conclusion

In this study we investigated different sources of uncertainties in the evolution of average streamflow and high flows in a small watershed located in the Great Lakes region. We used temperature and precipitation from 11 statistically downscaled CMIP5 global climate models forced with two scenarios of greenhouse gases emissions (i.e. RCP4.5 and RCP8.5) and 50 members of the regional climate model ensemble CRCM5-LE forced with RCP 8.5. Each of these datasets were used as input in the PRMS hydrological model for seven sets of parameters corresponding to different objective functions applied to the DDS calibration. An analysis of variance was performed for different hydrological processes using the 504 future simulations. The results show:

(i) An increase in projected average streamflow and number of high flows mostly due to an increase in precipitation in winter and a decrease in average streamflow and number of high flows due to an earlier snowmelt and increase in evapotranspiration in spring.

(ii) Uncertainties from scenarios higher in winter because the temperature plays a greater role in the variability of streamflow via the variability in snow processes while the uncertainties from GCMs are higher in spring due to high variability in the future evolution of precipitation.

(iii) The contribution of GCMs and internal variability to the total uncertainty is consistent through the 21st century while the calibration shows higher uncertainties in the historical period.

(iv) The uncertainties from scenarios peak in early-21st century and is decreasing at the end of the 21st century due to the disappearance of snow that decreases the importance of temperature in the streamflow variability.

These results emphasized the role of snow processes in the future evolution of streamflow and associated uncertainties in a watershed of the Great lakes region. This study focused on only one watershed while the snowpack is expected to vary greatly in short distance due to elevation, latitude and proximity with the Lakes. Other sources of uncertainties could be investigated by introducing other hydrological models, calibration methods or bias correction methods. The 50 members regional climate large ensemble to assess the uncertainties from internal variability of climate was the originality of this paper. However, by including more RCM ensembles in the

analysis, the uncertainties from internal variability of climate and the interactions GCM-RCM could be assessed with more accuracy. Despite the need of future improvement this study was able to quantify different sources of uncertainties in the future evolution of several hydrological processes, including high flows, in a small watershed of the Great Lakes basin. The study suggests that, in the context of decreasing snowfall due to a warming climate, the effort must be turned toward the GCMs that have a large room for improvements and constitute a large source of uncertainty in the Great Lakes basin.

5.7 Acknowledgment

Financial support for this study was provided by the Natural Sciences and Engineering Research Council (NSERC) of Canada through the FloodNet Project. The production of ClimEx was funded within the ClimEx project by the Bavarian State Ministry for the Environment and Consumer Protection. The CRCM5 was developed by the ESCER centre of Université du Québec à Montréal (UQAM; www.escer.uqam.ca) in collaboration with Environment and Climate Change Canada. We acknowledge Environment and Climate Change Canada's Canadian Centre for Climate Modelling and Analysis for executing and making available the CanESM2 Large Ensemble simulations used in this study, and the Canadian Sea Ice and Snow Evolution Network for proposing the simulations. Computations with the CRCM5 for the ClimEx project were made on the SuperMUC supercomputer at Leibniz Supercomputing Centre (LRZ) of the Bavarian Academy of Sciences and Humanities. The operation of this supercomputer is funded via the Gauss Centre for Supercomputing (GCS) by the German Federal Ministry of Education and Research and the Bavarian State Ministry of Education, Science and the Arts. We also acknowledge the World Climate Research Programme's Working Group on Coupled Modelling, which is responsible for

CMIP, and we thank the climate modeling groups (listed in Table 5-1 of this paper) for producing and making available their model output. For CMIP, the U.S. Department of Energy's Program for Climate Model Diagnosis and Intercomparison provides coordinating support and led development of software infrastructure in partnership with the Global Organization for Earth System Science Portals. We finally acknowledge support and contributions from Global Water Future Program, Environment and Climate Change Canada, Natural Resources Canada and Water Survey of Canada.

5.8 References

Ashraf Vaghefi, S., Iravani, M., Sauchyn, D., Andreichuk, Y., Goss, G., Faramarzi, M., 2019. Regionalization and parameterization of a hydrologic model significantly affect the cascade of uncertainty in climate-impact projections. Climate Dynamics. https://doi.org/10.1007/s00382-019-04664-w

Barnett, T.P., Adam, J.C., Lettenmaier, D.P., 2005. Potential impacts of a warming climate on water availability in snow-dominated regions. Nature 438, 303–309. https://doi.org/10.1038/nature04141

Boorman, D.B., Williams, R.J., Hutchins, M.G., Penning, E., Groot, S., Icke, J., 2007. A model selection protocol to support the use of models for water management. Hydrology and Earth System Sciences 11, 634–646.

Bosshard, T., Carambia, M., Goergen, K., Kotlarski, S., Krahe, P., Zappa, M., Schär, C., 2013. Quantifying uncertainty sources in an ensemble of hydrological climate-impact projections: UNCERTAINTY SOURCES IN CLIMATE-IMPACT PROJECTIONS. Water Resources Research 49, 1523–1536. https://doi.org/10.1029/2011WR011533

Burn, D.H., Whitfield, P.H., 2015. Changes in floods and flood regimes in Canada. Canadian Water Resources Journal / Revue canadienne des ressources hydriques 1–12. https://doi.org/10.1080/07011784.2015.1026844

Champagne, O., Arain, A., Leduc, M., Coulibaly, P., McKenzie, S., 2019a. Future shift in winter streamflow modulated by internal variability of climate in southern Ontario. Hydrology and Earth System Sciences Discussions 1–30. https://doi.org/10.5194/hess-2019-204

Champagne, O., Arain, M.A., Coulibaly, P., 2019b. Atmospheric circulation amplifies shift of winter streamflow in Southern Ontario. Journal of Hydrology 124051. https://doi.org/10.1016/j.jhydrol.2019.124051

Champagne, O., Leduc, M., Coulibaly, P., Arain, M.A., 2019c. Winter hydrometeorological extreme events modulated by large scale atmospheric circulation in southern Ontario. Earth System Dynamics Discussions. https://doi.org/10.5194/esd-2019-56

Chegwidden, O.S., Nijssen, B., Rupp, D.E., Arnold, J.R., Clark, M.P., Hamman, J.J., Kao, S., Mao, Y., Mizukami, N., Mote, P., Pan, M., Pytlak, E., Xiao, M., 2019. How do modeling decisions affect the spread among hydrologic climate change projections? Exploring a large ensemble of simulations across a diversity of hydroclimates. Earth's Future. https://doi.org/10.1029/2018EF001047

Chen, J., Brissette, F.P., Poulin, A., Leconte, R., 2011. Overall uncertainty study of the hydrological impacts of climate change for a Canadian watershed: OVERALL UNCERTAINTY OF CLIMATE CHANGE IMPACTS ON HYDROLOGY. Water Resources Research 47. https://doi.org/10.1029/2011WR010602

Clark, M.P., Wilby, R.L., Gutmann, E.D., Vano, J.A., Gangopadhyay, S., Wood, A.W., Fowler, H.J., Prudhomme, C., Arnold, J.R., Brekke, L.D., 2016. Characterizing Uncertainty of the Hydrologic Impacts of Climate Change. Current Climate Change Reports 2, 55–64. https://doi.org/10.1007/s40641-016-0034-x

Cunderlik, J.M., Ouarda, T.B.M.J., 2009. Trends in the timing and magnitude of floods in Canada. Journal of Hydrology 375, 471–480. https://doi.org/10.1016/j.jhydrol.2009.06.050

Deser, C., Knutti, R., Solomon, S., Phillips, A.S., 2012. Communication of the role of natural variability in future North American climate. Nature Climate Change 2, 775–779. https://doi.org/10.1038/nclimate1562

Devia, G.K., Ganasri, B.P., Dwarakish, G.S., 2015. A Review on Hydrological Models. Aquatic Procedia 4, 1001–1007. https://doi.org/10.1016/j.aqpro.2015.02.126

Dobler, C., Hagemann, S., Wilby, R.L., Stötter, J., 2012. Quantifying different sources of uncertainty in hydrological projections in an Alpine watershed. Hydrology and Earth System Sciences 16, 4343–4360. https://doi.org/10.5194/hess-16-4343-2012

Ehret, U., Zehe, E., Wulfmeyer, V., Warrach-Sagi, K., Liebert, J., 2012. HESS Opinions "Should we apply bias correction to global and regional climate model data?" Hydrology and Earth System Sciences 16, 3391–3404. https://doi.org/10.5194/hess-16-3391-2012

Eisner, S., Flörke, M., Chamorro, A., Daggupati, P., Donnelly, C., Huang, J., Hundecha, Y., Koch, H., Kalugin, A., Krylenko, I., Mishra, V., Piniewski, M., Samaniego, L., Seidou, O., Wallner, M., Krysanova, V., 2017. An ensemble analysis of climate change impacts on streamflow seasonality

across 11 large river basins. Climatic Change 141, 401–417. https://doi.org/10.1007/s10584-016-1844-5

Erler, A.R., Frey, S.K., Khader, O., d'Orgeville, M., Park, Y.-J., Hwang, H.-T., Lapen, D., Peltier, W.R., Sudicky, E.A., 2018. Simulating Climate Change Impacts on Surface Water Resources within a Lake Affected Region using Regional Climate Projections. Water Resources Research. https://doi.org/10.1029/2018WR024381

Fowler, H.J., Blenkinsop, S., Tebaldi, C., 2007. Linking climate change modelling to impacts studies: recent advances in downscaling techniques for hydrological modelling. International Journal of Climatology 27, 1547–1578. https://doi.org/10.1002/joc.1556

Giuntoli, I., Vidal, J.-P., Prudhomme, C., Hannah, D.M., 2015. Future hydrological extremes: the uncertainty from multiple global climate and global hydrological models. Earth System Dynamics 6, 267–285. https://doi.org/10.5194/esd-6-267-2015

Grillakis, M.G., Koutroulis, A.G., Tsanis, I.K., 2011. Climate change impact on the hydrology of Spencer Creek watershed in Southern Ontario, Canada. Journal of Hydrology 409, 1–19. https://doi.org/10.1016/j.jhydrol.2011.06.018

Harding, B.L., Wood, A.W., Prairie, J.R., 2012. The implications of climate change scenario selection for future streamflow projection in the Upper Colorado River Basin. Hydrology and Earth System Sciences 16, 3989–4007. https://doi.org/10.5194/hess-16-3989-2012

Hattermann, F.F., Vetter, T., Breuer, L., Su, B., Daggupati, P., Donnelly, C., Fekete, B., Flörke, F., Gosling, S.N., Hoffmann, P., Liersch, S., Masaki, Y., Motovilov, Y., Müller, C., Samaniego, L., Stacke, T., Wada, Y., Yang, T., Krysnaova, V., 2018. Sources of uncertainty in hydrological climate impact assessment: a cross-scale study. Environmental Research Letters 13, 015006. https://doi.org/10.1088/1748-9326/aa9938

Hawkins, E., Sutton, R., 2009. The Potential to Narrow Uncertainty in Regional Climate Predictions. Bulletin of the American Meteorological Society 90, 1095–1108. https://doi.org/10.1175/2009BAMS2607.1

Her, Y., Yoo, S.-H., Cho, J., Hwang, S., Jeong, J., Seong, C., 2019. Uncertainty in hydrological analysis of climate change: multi-parameter vs. multi-GCM ensemble predictions. Scientific Reports 9. https://doi.org/10.1038/s41598-019-41334-7

Ines, A.V.M., Hansen, J.W., 2006. Bias correction of daily GCM rainfall for crop simulation studies. Agricultural and Forest Meteorology 138, 44–53. https://doi.org/10.1016/j.agrformet.2006.03.009

Kay, A.L., Davies, H.N., Bell, V.A., Jones, R.G., 2009. Comparison of uncertainty sources for climate change impacts: flood frequency in England. Climatic Change 92, 41–63. https://doi.org/10.1007/s10584-008-9471-4

Khakbaz, B., Imam, B., Hsu, K., Sorooshian, S., 2012. From lumped to distributed via semi-distributed: Calibration strategies for semi-distributed hydrologic models. Journal of Hydrology 418–419, 61–77. https://doi.org/10.1016/j.jhydrol.2009.02.021

Kour, R., Patel, N., Krishna, A.P., 2016. Climate and hydrological models to assess the impact of climate change on hydrological regime: a review. Arabian Journal of Geosciences 9. https://doi.org/10.1007/s12517-016-2561-0

Kuo, C.C., Gan, T.Y., Higuchi, K., 2017. Evaluation of Future Streamflow Patterns in Lake Simcoe Subbasins Based on Ensembles of Statistical Downscaling. Journal of Hydrologic Engineering 22, 04017028. https://doi.org/10.1061/(ASCE)HE.1943-5584.0001548

Lafaysse, M., Hingray, B., Mezghani, A., Gailhard, J., Terray, L., 2014. Internal variability and model uncertainty components in future hydrometeorological projections: The Alpine Durance basin. Water Resources Research 50, 3317–3341. https://doi.org/10.1002/2013WR014897

Laprise, R., 2008. Regional climate modelling. Journal of Computational Physics 227, 3641–3666. https://doi.org/10.1016/j.jcp.2006.10.024

Leavesley, G.H., Lichty, R.W., Troutman, B.M., Saindon, L.G., 1983. Precipitation-runoff modeling system; user's manual. https://doi.org/10.3133/wri834238

Leduc, M., Mailhot, A., Frigon, A., Martel, J.-L., Ludwig, R., Brietzke, G.B., Giguère, M., Brissette, F., Turcotte, R., Braun, M., Scinocca, J., 2019. The ClimEx Project: A 50-Member Ensemble of Climate Change Projections at 12-km Resolution over Europe and Northeastern North America with the Canadian Regional Climate Model (CRCM5). Journal of Applied Meteorology and Climatology 58, 663–693. https://doi.org/10.1175/JAMC-D-18-0021.1

Lee, J.-K., Kim, Y.-O., Kim, Y., 2017. A new uncertainty analysis in the climate change impact assessment: UNCERTAINTY ANALYSIS IN CLIMATE CHANGE. International Journal of Climatology 37, 3837–3846. https://doi.org/10.1002/joc.4957

Lorenz, E.N., 1963. Deterministic Nonperiodic Flow. Journal of the Atmospheric Sciences 20, 130–141. https://doi.org/10.1175/1520-0469(1963)020<0130:DNF>2.0.CO;2

Markstrom, S.L., Regan, R.S., Hay, L.E., Viger, R.J., Payn, R.A., LaFontaine, J.H., 2015. precipitation-runoff modeling system, version 4: U.S. Geological Survey Techniques and Methods (No. Book 6, chapter B7).

Mattot, L.S., 2016. OSTRICH – An Optimization Software Toolkit for Research Involving Computational Heuristics.

McKenney, D.W., Hutchinson, M.F., Papadopol, P., Lawrence, K., Pedlar, J., Campbell, K., Milewska, E., Hopkinson, R.F., Price, D., Owen, T., 2011. Customized Spatial Climate Models

for North America. Bulletin of the American Meteorological Society 92, 1611–1622. https://doi.org/10.1175/2011BAMS3132.1

Moriasi, D.N., Arnold, J.G., Van Liew, M.W., Bingner, R.L., Harmel, R.D., Veith, T.L., 2007. Model evaluation guidelines for systematic quantification of accuracy in watershed simulations. Transactions of the ASABE 50, 885–900.

Nash, J.E., Sutcliffe, J.V., 1970. River flow forecasting through conceptual models part I — A discussion of principles. Journal of Hydrology 10, 282–290. https://doi.org/10.1016/0022-1694(70)90255-6

Pall, P., Allen, M.R., Stone, D.A., 2007. Testing the Clausius–Clapeyron constraint on changes in extreme precipitation under CO2 warming. Climate Dynamics 28, 351–363. https://doi.org/10.1007/s00382-006-0180-2

Peichl, M., Arain, M.A., Brodeur, J.J., 2010. Age effects on carbon fluxes in temperate pine forests. Agricultural and Forest Meteorology 150, 1090–1101. https://doi.org/10.1016/j.agrformet.2010.04.008

Rahman, M., Bolisetti, T., Balachandar, R., 2012. Hydrologic modelling to assess the climate change impacts in a Southern Ontario watershed. Canadian Journal of Civil Engineering 39, 91–103. https://doi.org/10.1139/l11-112

Reclamation, 2013. Downscaled CMIP3 and CMIP5 Climate Projections: Release of Downscaled CMIP5 Climate Projections, Comparison with Preceding Information, and Summary of User Needs.

Schoof, J.T., 2013. Statistical Downscaling in Climatology: Statistical Downscaling. Geography Compass 7, 249–265. https://doi.org/10.1111/gec3.12036

Scott, R.W., Huff, F.A., 1996. Impacts of the Great Lakes on regional climate conditions. Journal of Great Lakes Research 22, 845–863.

Skubel, R.A., Khomik, M., Brodeur, J.J., Thorne, R., Arain, M.A., 2017. Short-term selective thinning effects on hydraulic functionality of a temperate pine forest in eastern Canada. Ecohydrology 10, e1780. https://doi.org/10.1002/eco.1780

Stocker, T. (Ed.), 2014. Climate change 2013: the physical science basis: Working Group I contribution to the Fifth assessment report of the Intergovernmental Panel on Climate Change. Cambridge University Press, New York.

Su, B., Huang, J., Zeng, X., Gao, C., Jiang, T., 2017. Impacts of climate change on streamflow in the upper Yangtze River basin. Climatic Change 141, 533–546. https://doi.org/10.1007/s10584-016-1852-5

Sulis, M., Paniconi, C., Marrocu, M., Huard, D., Chaumont, D., 2012. Hydrologic response to multimodel climate output using a physically based model of groundwater/surface water interactions: MULTIMODEL CLIMATE CHANGE IMPACTS ON WATER RESOURCES. Water Resources Research 48. https://doi.org/10.1029/2012WR012304

Sultana, Z., Coulibaly, P., 2011. Distributed modelling of future changes in hydrological processes of Spencer Creek watershed. Hydrological Processes 25, 1254–1270. https://doi.org/10.1002/hyp.7891

Tolson, B.A., Shoemaker, C.A., 2007. Dynamically dimensioned search algorithm for computationally efficient watershed model calibration: DYNAMICALLY DIMENSIONED SEARCH ALGORITHM. Water Resources Research 43. https://doi.org/10.1029/2005WR004723

Trenberth, K.E., Dai, A., Rasmussen, R.M., Parsons, D.B., 2003. The Changing Character of Precipitation. Bulletin of the American Meteorological Society 84, 1205–1217. https://doi.org/10.1175/BAMS-84-9-1205

Chapter 6. Conclusions and recommendations

6.1 Conclusions

The goal of this research was to investigate the impact of internal variability of climate on the projections of hydrometeorological processes in southern Ontario, a populated area in the Great Lakes region. The PRMS conceptual semi-distributed model was used to study four main objectives. The first objective was to quantify the role of atmospheric circulation on the winter-spring streamflow shift observed in the region. The second objective was to investigate how the winter streamflow will be modulated by internal variability of climate in the future. The third component of this research focused on extreme events with an objective of understanding how large-scale atmospheric circulation will modulate the future evolution of winter hydrometeorological extremes. Finally, the uncertainties in the future evolution of the winter-spring hydrometeorological processes associated with internal variability of climate was compared to other sources of uncertainties. The main conclusions of each chapter are summarized below:

6.1.1 Impact of atmospheric circulation on past streamflow

- The recurrent weather patterns characterized by higher pressure anomalies located in the east side of the Great lakes region (HP) or in the east coast of North America (South) were associated with higher streamflow volume and number of high flows generated by the advection of wet and warm air masses from the south.
- HP weather pattern was correlated with NAO^+ and 'South' weather pattern was correlated with PNA^-. These large-scale modes of variability were previously identified as generators of warm and wet conditions in the Great Lakes region.

- The occurrence of HP increased in the 1957-2013 period, which significantly contributed to the winter warming, enhancing snowmelt and rain to snow ratio, especially in southern lowlands and close to the lakes.
- The decadal change in atmospheric circulation contributed as much as 40% to the spring to winter shift in streamflow volume and number of high flows.

6.1.2 Future streamflow modulated by internal variability of climate

- Despite a large variability in the projections of temperature and precipitation between the 50 members of the ensemble, the average streamflow was projected to increase by mid-21st century in January-February due to increase in rainfall and snowmelt because of warmer and wetter conditions.
- 16% of the members projected a simultaneously large increase in precipitation and temperature and 26% showed a large increase in temperature only.
- The enhancement of temperature and precipitation amounts were associated to higher pressure in the east coast of North America and stronger southerly winds in the Great Lakes region. The temperature-only amplification was associated to high pressure on top of the Great lakes.
- The modulation of the warming and wetting in January-February had a direct impact on the modulation of streamflow, but precipitation in fall and the timing in the change of temperature and precipitation also modulate the winter streamflow.

6.1.3 Winter hydrometeorological extremes modulated by atmospheric circulation

- The weather patterns identified in the past were accurately recreated by the 50-members regional climate model ensemble, except the weather pattern 'South' that depicted a more meridional flow pattern and an overestimation of rainfall and warm events.
- In the historical period, warm events were mainly generated by HP weather pattern, heavy precipitation were mainly generated by 'South' weather pattern and both patterns were associated with the generation of high flows.
- In the future, temperature will have a lower role in the generation of high flows due to the disappearance of snow, and the increase in number of weather extreme events during a HP pattern will not generate as much high flows.
- Internal variability of climate is expected to modulate the number of warm extremes through the modulation of the number of HP-South weather patterns but internal variability will not necessarily modulate the number of high flow events.

6.1.4 Sources of uncertainties in the projection of streamflow in Big Creek watershed

- Streamflow volume and number of high flows are expected to increase in winter due to precipitation amount enhancement and are expected to decrease in spring due to advance snowmelt and increase in evapotranspiration consecutive to the warming.
- The uncertainties in the projection of streamflow due to the greenhouse gas emission scenarios are higher in winter and are driven by temperature variability while the uncertainties associated to GCMs are higher in Spring and are driven by precipitation.

- The early-21st century winter peak in streamflow uncertainties was attributed to the snow uncertainties due to the temperature difference between RCP4.5 and RCP8.5.
- At the end of the 21st century high scenarios uncertainties in the evolution of temperature were not transferred to streamflow uncertainties because of disappearance of snow that may decrease the importance of temperature in the overall uncertainties.

6.2 Recommendations for future research

The four objectives investigated in this thesis, gave a good overview of the impact of climate internal variability on hydrometeorological processes in southern Ontario. However, improvements can be made in the methods used for the projections of these processes.

The climate variables observations used to calibrate or validate a hydrological model are often taken as an accurate representation of the reality but should be used with caution. In this study we used NRCANmet temperature and precipitation gridded data constructed from an interpolation of weather station observations using an ANNUSPLIN (McKenney et al., 2011). Despite good performance of ANNUSPLIN compared to other interpolation methods, this method overestimates precipitation (Newlands et al., 2011) and it would be important in the future studies to diversify the sources of observations used for calibration and validation of the hydrological model.

With a similar objective to diversify the data used in the analyses, other climate ensembles should be tested to project the future hydrological processes. The use of a 50 members regional climate model ensemble as input in a hydrological model was one of the originality of this study, but the ensemble overestimates the temperature and the precipitation in the study region (Leduc et al.,

2019) and testing other ensembles would increase the confidence in the results. The method used for the bias correction of the future climate data can also be critical for the projection of streamflow (Ehret et al., 2012). In this study the bias correction of precipitation has been done using a gamma distribution (Ines and Hansen, 2006) while other distribution methods may be selected to improve the accuracy of the bias-correction (Heo et al., 2019). Hydrological processes being driven by a combination of precipitation and temperature variability, a multivariate bias correction following the method of Zscheischler et al. (2019) should be considered for future analyses.

The temporal resolution of the regional climate model simulations are being continuously improved and PRMS or other hydrological models should take advantage of these improvements by using more systematically the hourly timesteps. Hourly-timestep is especially relevant for studies focusing on summer when flash floods are often generated by high intensity rainfall events. In winter and spring the intensity is less of a concern because floods are generally driven by snowmelt or long duration precipitation events from large scale frontal systems (Kunkel et al., 2012). However, some high flow events may not be taken into consideration when the maximal peak flow overlap two days. Hourly-timestep would overcome this issue and could also improve the separation between rainfall and snowfall that is subject to misrepresentation when calculated at a daily-timestep

Another hydrological model improvement to consider is a dynamical representation of land-use. In PRMS and most of other hydrological models the land-use is fixed to the historical maps and the parameters estimated from land-use cannot be variable with time. Some parameters will be outdated at the end of the 21st century due to urban sprawl and forests recovery. We also suggest

separating the urban land-use in function of their imperviousness because a single impervious value for all urban areas leads to misrepresentation of infiltration processes. The presence of frozen ground could also significantly alter the infiltration and the runoff processes. The version of PRMS used in this study has not considered frozen ground but could be upgraded using algorithms developed recently (Follum et al., 2018). The dams are another important features not taken into consideration in this study while they are widely used in the Grand River region to regulate streamflow (GRCA, 2016). However, it is unlikely that these dams significantly affected our results focusing on winter streamflow because the Lakes levels are kept constant in winter (GRCA, 2016). As the number of flood events are increasing in winter, the flood controls by the dam operators may be shifted from spring to winter. In this context, it will be relevant to include these dam operations in the hydrological modelling.

The validation of the hydrological simulations using not only observed streamflow, but also other processes is highly encouraged as it could avoid getting satisfactory streamflow simulations for the wrong reason. Validating snowpack, soil moisture or evapotranspiration could be systematically done in regions where measurements are available. In the meanwhile, we encourage more measurements in crops areas and not only in environments that are more often investigated such as forests or peatlands.

Results from this thesis also emphasized the possible links between the seasons in term of hydrological processes and encourage the use of coupled surface and groundwater models. PRMS has been especially coupled with the groundwater model MODFLOW for the purpose of a better understanding of these interactions (Model GS FLOW; Markstrom and regan, 2008). GS FLOW

was previously used in Oregon to link winter-spring change in snowmelt and runoff to summer streamflow (Huntington and Niswonger, 2012). The impact of summer recharge on winter streamflow was also investigated using another coupled model Grand River, Ontario (Erler et al., 2018). The use of GSFLOW in these watersheds is greatly encouraged to study the hydrological connections between groundwater and surface processes and between seasons. We also encourage an integrated modelling approach between climate, hydrology and vegetation.

Finally, the feedbacks between large scale atmospheric circulation and streamflow regimes should be investigated in the future. A recent study suggested that a streamflow shift in Siberian rivers modified the temperature of the Arctic ocean and influenced regional atmospheric circulation (Hudson and Thompson, 2019). Xiao et al., (2018) found similarly that temperature of the Great Lakes may have an impact on regional cyclonic activity. These studies suggest that the streamflow shift from spring to winter in southern Ontario may have implications for large-scale circulations which in turn could modulate the streamflow regimes.

6.3 References

Ehret, U., Zehe, E., Wulfmeyer, V., Warrach-Sagi, K. and Liebert, J.: HESS Opinions "Should we apply bias correction to global and regional climate model data?", Hydrology and Earth System Sciences, 16(9), 3391–3404, doi:10.5194/hess-16-3391-2012, 2012.

Erler, A. R., Frey, S. K., Khader, O., d'Orgeville, M., Park, Y.-J., Hwang, H.-T., Lapen, D., Peltier, W. R. and Sudicky, E. A.: Simulating Climate Change Impacts on Surface Water Resources within a Lake Affected Region using Regional Climate Projections, Water Resources Research, doi:10.1029/2018WR024381, 2018.

Follum, M. L., Niemann, J. D., Parno, J. T. and Downer, C. W.: A simple temperature-based method to estimate heterogeneous frozen ground within a distributed watershed model, Hydrology and Earth System Sciences, 22(5), 2669–2688, doi:10.5194/hess-22-2669-2018, 2018.

GRCA (Grand River Conservation Authority: Low Flow Reliabilities in Regulated River Reaches in the Grand River Watershed., 2016.

Heo, J.-H., Ahn, H., Shin, J.-Y., Kjeldsen, T. R. and Jeong, C.: Probability Distributions for a Quantile Mapping Technique for a Bias Correction of Precipitation Data: A Case Study to Precipitation Data Under Climate Change, Water, 11(7), 1475, doi:10.3390/w11071475, 2019.

Hudson, C. E. and Thompson, J. R.: Hydrological modelling of climate change impacts on river flows in Siberia's Lena River Basin and implications for the Atlantic Meridional Overturning Circulation, Hydrology Research, doi:10.2166/nh.2019.151, 2019.

Huntington, J. L. and Niswonger, R. G.: Role of surface-water and groundwater interactions on projected summertime streamflow in snow dominated regions: An integrated modeling approach: SW AND GW INTERACTIONS ON STREAMFLOW, Water Resources Research, 48(11), n/a-n/a, doi:10.1029/2012WR012319, 2012.

Ines, A. V. M. and Hansen, J. W.: Bias correction of daily GCM rainfall for crop simulation studies, Agricultural and Forest Meteorology, 138(1–4), 44–53, doi:10.1016/j.agrformet.2006.03.009, 2006.

Kunkel, K. E., Easterling, D. R., Kristovich, D. A. R., Gleason, B., Stoecker, L. and Smith, R.: Meteorological Causes of the Secular Variations in Observed Extreme Precipitation Events for the Conterminous United States, Journal of Hydrometeorology, 13(3), 1131–1141, doi:10.1175/JHM-D-11-0108.1, 2012.

Leduc, M., Mailhot, A., Frigon, A., Martel, J.-L., Ludwig, R., Brietzke, G. B., Giguère, M., Brissette, F., Turcotte, R., Braun, M. and Scinocca, J.: The ClimEx Project: A 50-Member Ensemble of Climate Change Projections at 12-km Resolution over Europe and Northeastern North America with the Canadian Regional Climate Model (CRCM5), Journal of Applied Meteorology and Climatology, 58(4), 663–693, doi:10.1175/JAMC-D-18-0021.1, 2019.

Markstrom, S. and regan, S.: GSFLOW—Coupled Ground-Water and Surface-Water Flow Model Based on the Integration of the Precipitation-Runoff Modeling System (PRMS) and the Modular Ground-Water Flow Model (MODFLOW-2005)., 2008.

McKenney, D. W., Hutchinson, M. F., Papadopol, P., Lawrence, K., Pedlar, J., Campbell, K., Milewska, E., Hopkinson, R. F., Price, D. and Owen, T.: Customized Spatial Climate Models for North America, Bulletin of the American Meteorological Society, 92(12), 1611–1622, doi:10.1175/2011BAMS3132.1, 2011.

Newlands, N. K., Davidson, A., Howard, A. and Hill, H.: Validation and inter-comparison of three methodologies for interpolating daily precipitation and temperature across Canada, Environmetrics, 22(2), 205–223, doi:10.1002/env.1044, 2011.

Xiao, C., Lofgren, B. M. and Wang, J.: WRF-based assessment of the Great Lakes' impact on cold season synoptic cyclones, Atmospheric Research, 214, 189–203, doi:10.1016/j.atmosres.2018.07.020, 2018.

Zscheischler, J., Fischer, E. M. and Lange, S.: The effect of univariate bias adjustment on multivariate hazard estimates, Earth System Dynamics, 10(1), 31–43, doi:10.5194/esd-10-31-2019, 2019.